DEPARTMENT OF NATIONAL DEVELOPMENT
BUREAU OF MINERAL RESOURCES, GEOLOGY AND GEOPHYSICS

BULLETIN 125

Geological Papers 1969

AUSTRALIAN GOVERNMENT PUBLISHING SERVICE
CANBERRA 1972

BUREAU OF MINERAL RESOURCES, GEOLOGY AND GEOPHYSICS

DIRECTOR: N. H. FISHER

ASSISTANT DIRECTOR, GEOLOGICAL BRANCH: J. N. CASEY

Published for the Minister for National Development, the
Hon. R. W. C. Swartz, M.B.E., E.D., M.P., by the
Australian Government Publishing Service

ISBN 0 642 00108 1

Printed by Graphic Services Pty. Ltd., 60 Wyatt Street, Adelaide, S.A. 5000

CONTENTS

Page

DE KEYSER, F.
Proterozoic tillite at Duchess, northwestern Queensland 1

COOK, P. J., and ARMSTRONG, K. A.
Clay mineralogy of the Middle Cambrian Beetle Creek Formation, Georgina Basin, northwest Queensland 7

WATTS, M. D.
Geological interpretation of a gravity survey over basement inliers near Millungera, north Queensland 17

SENIOR, B. R., and SENIOR, DANIELE A.
Silcrete in southwest Queensland 27

SMITH, I. E., and SIMPSON, C. J.
Late Cainozoic uplift in the Milne Bay area, eastern Papua 29

JONGSMA, D.
Marine geology of Milne Bay, eastern Papua 35

MANWARING, E. A.
Palaeomagnetism of some Recent basalts from New Guinea 55

ENGLAND, R. N.
Lamellar intergrowths of pyrophyllite and muscovite and the assemblage kyanite-pyrophyllite-quartz in quartzites from the Petermann Ranges, Northern Territory 67

DICKINS, J. M., ROBERTS, J., and VEEVERS, J. J.
Permian and Mesozoic geology of the northeastern part of the Bonaparte Gulf Basin 75

DERRICK, G. M., and GELLATLY, D. C.
New leucite lamproites from the west Kimberley, Western Australia 103

GLIKSON, A. Y.
Petrology and geochemistry of metamorphosed archaean ophiolites, Kalgoorlie-Coolgardie, Western Australia 121

GELLATLY, D. C.
Problems of provenance of the Yampi iron ores, west Kimberley region, Western Australia 191

PROTEROZOIC TILLITE AT DUCHESS, NORTHWESTERN QUEENSLAND

by

F. de Keyser

SUMMARY

A boulder clay unit in the Mount Birnie Beds near Duchess in northwestern Queensland has been recognized to be a true tillite. This unit, here named the Little Burke Tillite, is the first record of a Proterozoic tillite in northwestern Queensland, and it can be correlated with similar tillites in the Kimberleys and the Ngalia, Amadeus, and Georgina Basins.

INTRODUCTION

During field work by a combined party of the Bureau of Mineral Resources and the Geological Survey of Queensland in 1967, a boulder clay unit was found in the Mount Birnie Beds in the Duchess district, northwestern Queensland. Cautiously described as a tilloid at first (de Keyser, 1968), the unit was subsequently recognized as a true tillite during the 1968 field season. This is the first record of a Proterozoic tillite in northwestern Queensland.

GEOLOGY

The Mount Birnie Beds, named by Öpik (1960), underlie Middle Cambrian sediments in the Duchess district. A strong angular unconformity separates them from the underlying folded and metamorphosed Precambrian formation. Öpik described the Mount Birnie Beds as 'a sequence of conglomerate, sandstone, green shale, and arkose', containing fossil worm burrows; otherwise very little was known about them.

The stratigraphy of the Mount Birnie Beds was studied in some detail during the field work in 1967, when it was concluded that the sequence represents a group of formations that probably have a considerable range in age, possibly going as far back as the Proterozoic (de Keyser, 1968). The unit is exposed intermittently along the margins of the Burke River outlier, and its most complete and best developed section is located about 5 or 6 miles east-northeast of Duchess

(Fig. 1). In this section the tillite, which forms the base of the Mount Birnie Beds, reaches its maximum thickness. To the east and south it thins rapidly; the last outcrops are found about 5 miles south of the railway line, and the 'regolithic purple clay with granite fragments found southwest of Roaring Bore' (Öpik, 1961) is probably the easternmost occurrence.

The strata are preserved in a down-faulted wedge $\frac{3}{4}$ mile wide, and are surrounded by Precambrian formations except to the south, where they dip underneath Middle Cambrian cherts, siltstones, and limestones (Fig. 2). The dips and gentle fold structures in the Mount Birnie Beds are directly or indirectly a result of the faulting, and steep dips are found only along the actual fault lines. The stratigraphic section in this area is shown in Figure 3.

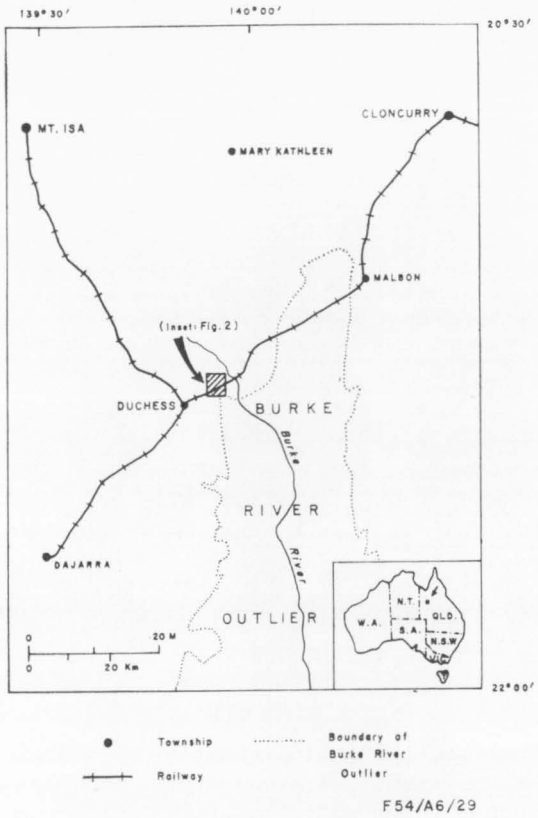
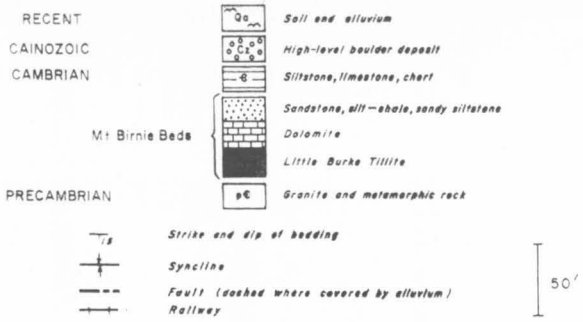


Figure 1. Locality map of the Duchess area, northwestern Queensland.

Little Burke Tillite

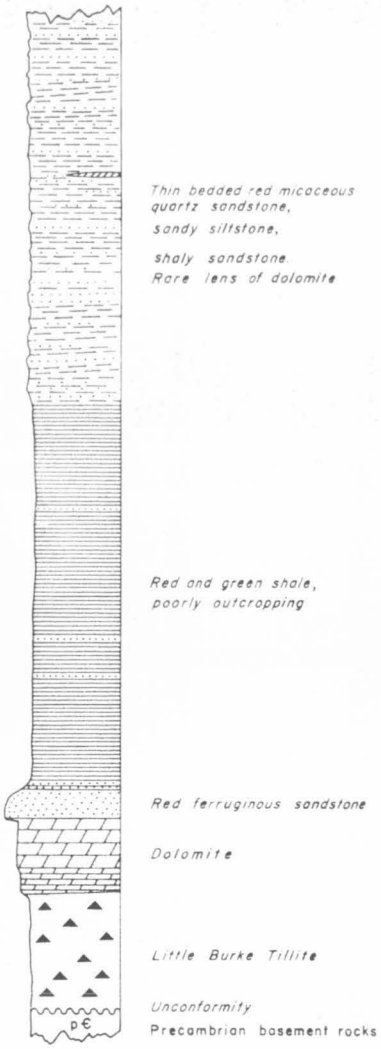
The tillite forming the base of the Mount Birnie Beds is at least 65 feet thick, and is best exposed in a section cut into the eastern bank of the Little Burke River (Fig. 2), for which reason it is here proposed to name the unit the Little Burke Tillite.





F54/A6/30

Figure 2. Geological map showing the main outcrop of the Little Burke Tillite, 6 miles northeast of Duchess.



F54/A6/31

Figure 3. Stratigraphic section of Mount Birnie Beds, measured in the Little Burke River area.

The rock is crumbly, and has the appearance of a boulder clay (Pl. 1, fig. 1), being a completely unsorted, structureless, and non-bedded deposit of a heterogeneous assortment of clasts of all sizes in a gritty, silty matrix. The clasts range in size from sand up to boulders 5 feet across. They are rounded to subrounded, commonly faceted, usually well polished with a glossy sheen, and include a very extensive range of rock types all derived from the Precambrian basement: amphibolite, calc-silicate rock, quartzite, granite, porphyry, pegmatite, conglomerate, dolomite, granulite, and a variety of schists and acid volcanics. Some boulders are very well striated (Pl. 1, fig. 2). Many, or most, of the smaller pebbles and

boulders are coated with a thin, shiny, black or rusty-brown ferruginous patina. Most of the clasts are fresh and completely unweathered, but strongly decomposed boulders are also present.

The silty matrix is deep purple or chocolate brown, and though rather crumbly in outcrop, is actually well indurated. A thin section of the matrix showed an almost complete lack of clay-sized material, the average size of the silt particles ranging from 0.02 mm upwards. The most common constituents are quartz and fine-grained dolomite rhombs, together with numerous smaller and larger rock fragments including siliceous dolomite, quartzite, rhyolite, hornblende-quartz gneiss, quartz-sericite, schist, quartz-microcline granulite, chlorite schist, quartz-biotite-feldspar gneiss, and graphitic schist. Grains of microcline, orthoclase, plagioclase, mica, biotite, apatite, zircon, tourmaline, and abundant pyrite granules or their limonite pseudomorphs are scattered throughout the groundmass. One striking feature shown in this section is the absolute freshness of all constituents, and even biotite, hornblende, and feldspars are clear and unaltered. Where chlorite does occur, it is a component of some retrograde-metamorphic rock fragments.

Glacial Origin

The evidence for a glacial origin includes the following points: presence of polished, faceted, and striated clasts, extreme diversity of rock types, complete lack of sorting, presence of very large boulders, freshness of clasts and matrix, absence of clay minerals, absence of any bedding structures. Furthermore, a comparison of the stratigraphic succession with that of the Moonlight Valley Tillite in the Kimberley region described by Dow (1965) shows a remarkable similarity between the two sections (Table 1) and, as this tillite is underlain by a glacial pavement, a glacial origin also appears to be reasonably certain for the Little Burke Tillite.

Table 1. Comparison of the Little Burke Tillite Section in Queensland with the Moonlight Valley Tillite in Western Australia

Northwest Queensland (de Keyser, 1968)		Western Australia (after Dow, 1965)	
thin-bedded quartz sandstone, sandy siltstone, siltstone	up to 250′	laminated and thin-bedded quartz sandstone and siltstone; green and red banded shale; ferruginous sandstone	Ranford Formation, 1850′
red and green fissile micaceous shale	up to 250′		
massive, red ferruginous sandstone	5′-120′	laminated pink or cream dolomite	6′-12′
thin- and medium-bedded pink or cream dolomite	5′-45′	Moonlight Valley Tillite* (underlain by glacial pavement)	0′-450′
Little Burke Tillite	0′-65′		

* Age is given as late Upper Proterozoic (Dow, 1965).

Although striated boulders have been found in mudflows and landslides, such striae are reported to be not as well developed as those associated with glacial deposits. Mudflows, moreover, are apt to be rather restricted phenomena, and do not fit the Australian picture where the distribution of the boulder rock spreads from northwest to southeast over the whole of the continent and is tied to definite stratigraphic horizons.

PLATE 1



Figure 1. Little Burke Tillite. Note glossy sheen on clasts.

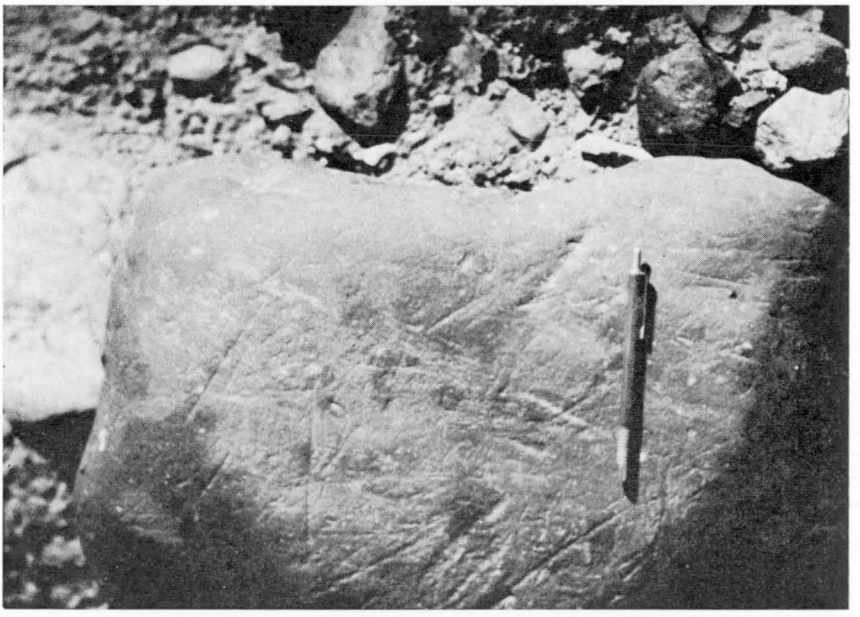


Figure 2. Striated boulder in Little Burke Tillite.

The abundance of dolomite rhombs in the matrix is common to most of the Upper Proterozoic tillites in northern Australia, and might be used by some as an argument against a glacial origin. However, consideration must be given to the probability that the Precambrian seas were considerably richer in Ca and Mg than at present, that the partial pressure of CO_2 appears to have been higher, and that the tillite contains very little clay material with which to absorb Mg. The total effect may have been that unusually large quantities of carbonates could have been dissolved in the cold glacial sea water to become trapped in the tillite, and, in the absence of clay, precipitated out as dolomite during diagenesis in a subsequent somewhat warmer climatic environment. An additional possibility is that the dolomite rhombs represent recrystallized rock flour derived from the Precambrian dolomites in the area

Age of the Tillite

The Little Burke Tillite is older than the overlying fossiliferous Middle Cambrian, and younger than the Precambrian basement. It forms the base of the Mount Birnie Beds, which have previously been described as probably Lower Cambrian in age, but which now are thought to encompass a series of deposits with a wide range of ages. The local stratigraphic succession is strikingly similar to that of the Moonlight Valley Tillite in Western Australia (Table 1), which has been demonstrated to be Upper Proterozoic. For these reasons, the age of the Little Burke Tillite is thought to be Upper Proterozoic as well, and the tillite is considered to belong to the group of Upper Proterozoic tillites known to extend in a wide belt from the Kimberley region in Western Australia through central Australia, northwestern Queensland, and South Australia to Victoria and Tasmania.

Correlations

A study of the stratigraphy and lithology of the tillites reported from the Kimberleys, the Ngalia Basin, the Amadeus Basin, and the southeastern part of the Georgina Basin (Dow, 1965; Pontifex et al., 1968; Smith, 1967; Wells, Ranford et al., 1968; Wells, Evans, & Nicholas, 1968) leads to the conclusion that the Little Burke Tillite is the equivalent of the upper one of two tillite members recognized in these areas (*see* Table 2). The lower tillite member appears to be missing from Duchess.

Table 2. Correlation of Little Burke Tillite with glacial deposits found elsewhere in Northern Australia

Western Australia/ Northern Territory (Dow, 1965; Pontifex et al., 1968)	Ngalia Basin (Wells, Evans, & Nicholas, 1968)	Amadeus Basin (Wells, Ranford, et al., 1968)	Southeast Georgina Basin (Smith, 1967, pp. 72-75)	Duchess (de Keyser, 1968)
Moonlight Valley Tillite and 'Skinner Glacials'	Unnamed glacial deposits	Olympic Member of Pertatataka Formation	Tillite in Mount Cornish Formation	Little Burke Tillite (in Mount Birnie Beds)
Fargoo Tillite	?	Glacial deposits in Areyonga Formation	Tillite in Field River Beds	—

REFERENCES

DOW, D. B., 1965—Evidence of a late Pre-Cambrian glaciation in the Kimberley region of Western Australia. *Geol. Mag.*, 102 (5), 407-14.

KEYSER, F. DE, 1968—The Cambrian of the Burke River Outlier. *Bur. Miner. Resour. Aust. Rec.* 1968/67 (Unpubl.).

ÖPIK, A. A., 1960—Cambrian and Ordovician geology, *in* THE GEOLOGY OF QUEENSLAND. *J. geol. Soc. Aust.*, 7, 89-109.

ÖPIK, A. A., 1961—The geology and palaeontology of the headwaters of the Burke River, Queensland. *Bur. Miner. Resour. Aust. Bull.* 53.

PONTIFEX, I. R., MORGAN, C. M., SWEET, I. P., and REID, A. G., 1968—Geology of the Auvergne 1:250,000 Sheet area, N.T. *Bur. Miner. Resour. Aust. Rec.* 1968/117 (Unpubl.).

SMITH, K. G., 1967—The geology of the Georgina Basin. *Bur. Miner. Resour. Aust. Rec.* 1967/61 (Unpubl.).

WELLS, A. T., RANFORD, L. C., STEWART, A. J., COOK, P. J., and SHAW, R. D., 1968—The geology of the northeastern part of the Amadeus Basin, N.T. *Bur. Miner. Resour. Aust. Rep.* 113.

WELLS, A. T., EVANS, T. G., and NICHOLAS, T., 1968—The geology of the central part of the Ngalia Basin, N.T. *Bur. Miner. Resour. Aust. Rec.* 1968/38 (Unpubl.).

CLAY MINERALOGY OF THE MIDDLE CAMBRIAN BEETLE CREEK FORMATION, GEORGINA BASIN, NORTHWEST QUEENSLAND

by

P. J. Cook and K. A. Armstrong

SUMMARY

Diffractometer analysis of several hundred samples of Middle Cambrian Beetle Creek Formation from the eastern margin of the Georgina Basin, northwest Queensland, showed that the clay fraction is composed predominantly of kaolinite; illite is common, smectite minor, and chlorite very minor. Traces of sepiolite, attapulgite, and mixed-layer clays are also present. There are no clearly defined trends in the distribution of the various clay minerals and major changes in composition commonly occur over very short distances. It is likely that this is the result of highly variable conditions of localized deposition. Phosphatic Beetle Creek Formation is richer in illite and probably formed seaward of associated non-phosphatic sediments. Similarly, pelletal phosphorites contain more illite and probably formed under more marine conditions than the muddy phosphorites ('microsphorite').

INTRODUCTION

The Georgina Basin is a Palaeozoic sedimentary basin covering an area of approximately 125,000 square miles in the Northern Territory and northwest Queensland. The present study involved an area of approximately 25,000 square miles on the eastern margin of the basin (Fig. 1), where middle Cambrian sediments are moderately well exposed.

The sedimentary succession in this area has been described by Öpik (1956; 1960), Carter & Öpik (1961a; 1961b), and Noakes et al. (1959). Smith (1970) discusses the stratigraphy of the entire Georgina Basin and also gives a comprehensive bibliography. The basement rocks are dealt with in some detail by Carter et al. (1961). Figure 2 shows diagrammatically the interrelationships of the various Middle Cambrian rock units in this area.

The discovery of major phosphate deposits in the Middle Cambrian Beetle Creek Formation by R. T. Russell in 1966 (Russell, 1967; 1968) has resulted in

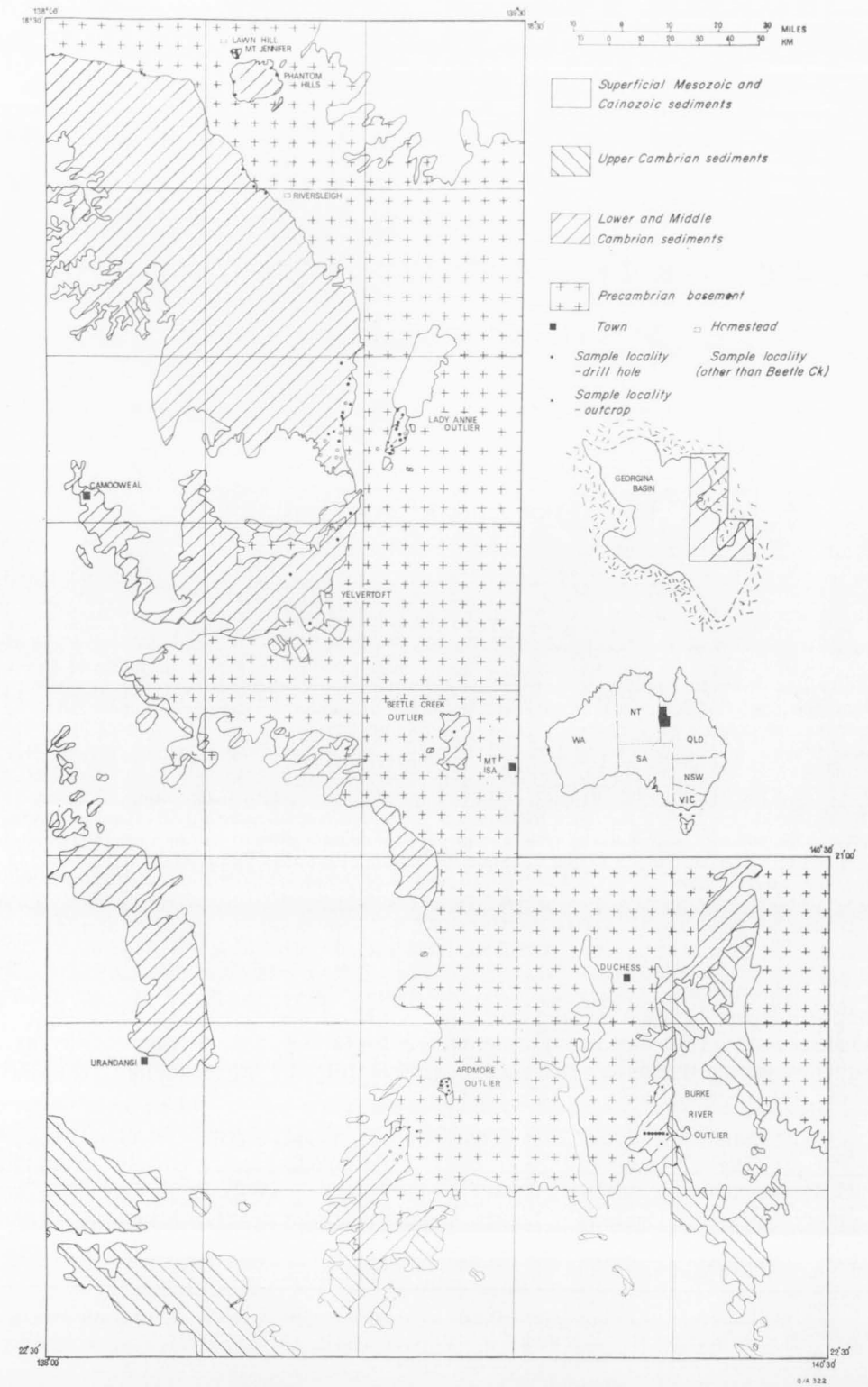
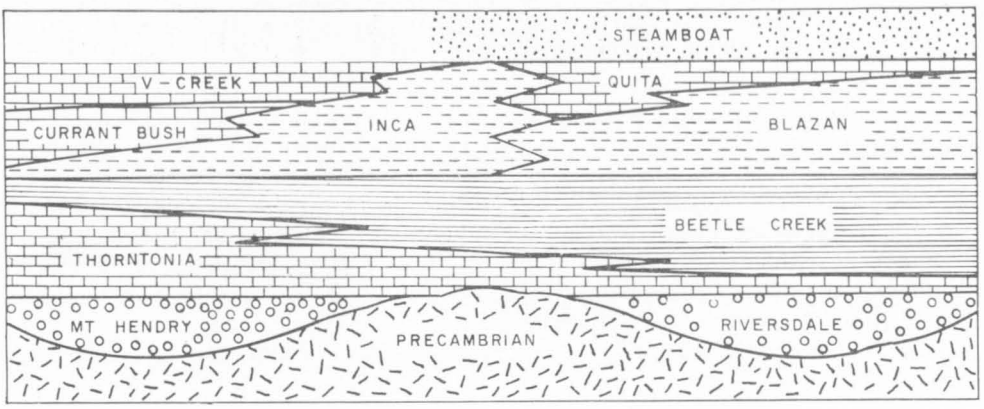


Figure 1. Map showing sample localities and the areas of Middle Cambrian sediments in the eastern part of the Georgina Basin.

a considerable amount of detailed work on the phosphorites by various mining companies and also by the Bureau of Mineral Resources (de Keyser, 1968; 1969a; 1969b). It was as an extension of this work on the Beetle Creek phosphorites that this study of the clay mineralogy was undertaken.

The Beetle Creek Formation, which is up to 300 feet thick, comprises siltstone, mudstone, chert, and phosphorite, with minor limestone and some sandstone. It overlies and interfingers with the Thorntonia Limestone and is overlain by the Inca Formation and its equivalents (Fig. 2). Fossils, particularly trilobites, are very common in places. Weathering of the unit is fairly extensive, and is thought to have removed much of the organic matter originally present in the formation; it may have also modified the mineralogy of the rocks.



Q/A / 323

Figure 2. Rock relationships of some of the Middle Cambrian units in the eastern part of the Georgina Basin.

ACKNOWLEDGEMENTS

The writers wish to express their thanks to Mr F. de Keyser of the Bureau of Mineral Resources for his advice and encouragement at all stages in this study. The assistance of the Broken Hill South Company Pty Limited and International Minerals and Chemical Development Corporation in obtaining drillhole samples and releasing unpublished information is very much appreciated. Mr D. Sadler assisted in a variety of ways.

PROCEDURE

Approximately 300 samples from 80 drillhole and outcrop localities (Fig. 1) were analysed during the course of the study. Fairly standard procedures similar to those outlined by Mueller (1967) were followed in the treatment and analysis of the samples. This involved first suspending the disaggregated sample in water, withdrawing the fraction less than 2μ in size, and from this preparing an oriented mount on a porous tile disc. The sample was then X-rayed using a Phillips PW 10 diffractometer, fitted with a spinning stage. A nickel filter and copper $K\alpha$ radiation were employed, with settings of 40 Kv and 24 MA, and a slit width of $\frac{1}{4}°$.

Each sample was subjected to three X-ray analyses: the first, following glycolation of the sample; the second, after heating the sample for two hours at 300°C;

and the third, after heating to 550°C for 30 minutes. The area under selected peaks was then measured using a planimeter, and from the relative peak areas and the peak positions, the quantitative clay mineralogy of the sample was determined.

GENERAL CLAY MINERALOGY

Using this procedure the commoner clay minerals and clay mineral groups could be identified. Generally, however, it was not possible to distinguish between various members of the groups, and throughout the following discussion the terms kaolinite, smectite, and chlorite are used for the undifferentiated groups. The association of kaolinite and chlorite presented problems in quantitative determination due to the coincidence of the (001) kaolinite peak and the (002) chlorite peak at 7°A (12.4° 2θ); in such cases it was necessary to use the method suggested by Biscaye (1964) which involves measuring the 3.5°A peaks of kaolinite and chlorite at slow scanning speeds.

The two major clay minerals present are kaolinite and illite (with kaolinite generally the more common); smectite is minor and chlorite very minor. In addition trace amounts of more poorly crystalline clay minerals are present. A consistent small peak at 12.1°A (7.2° 2θ) is thought to be sepiolite; suspected attapulgite-palygorskite (10.5°A) was also detected in a few samples. Variable (though generally trace) quantities of mixed-layer clays are present. The low amplitude of most of these peaks makes positive identification difficult, but using data given by Weaver (1956) regularly and irregularly stratified illite-montmorillonite was identified; regularly interstratified chlorite-illite may also be present.

Because the mixed-layer clays and attapulgite-palygorskite are never present in significant amounts, they will not be dealt with any further here. Similarly sepiolite is only present in trace amounts; the only possible trend discerned for sepiolite was a tendency for it to be more common in the northern part of the study area. This may be a function of more volcanic rocks (the Colless Volcanics) in the northern source area or of a more arid climate to the north in Cambrian time, as Millott (1949) has shown sepiolite to be a significant component of desert soils.

The four common clay minerals—kaolinite, illite, smectite, and chlorite—will now be discussed in some detail.

DISCUSSION

The average composition of the minus 2μ fraction of the Beetle Creek Formation is 52 percent kaolinite, 35 percent illite, 10 percent smectite, 3 percent chlorite. One of the problems in any discussion of the clay mineralogy is evaluation of the importance of post-Cambrian weathering on the assemblage. All the samples are from within the weathering zone (which in this area has a depth of 300 feet). It could therefore be argued that the clay mineralogy is more the result of Tertiary lateritic weathering than of the original assemblage, and the abundance of kaolinite would tend to support this. However, this is refuted by the fact that other Cambrian units within the weathering zone, e.g. the V-Creek limestone (*see* Table 1), contain virtually no kaolinite. Also, there is no correlation whatsoever between the percentage of kaolinite and the depth of the sample in the drillhole. It may therefore be assumed that the clay mineralogy is primarily the Cambrian assemblage, with the exception of some of the less stable clay minerals.

TABLE 1. AVERAGE CLAY MINERALOGY OF THE BEETLE CREEK FORMATION AND ASSOCIATED CAMBRIAN UNITS ARRANGED IN ORDER OF INCREASING KAOLINITE PERCENTAGE

Formation	Rock Type	No. of Samples	Major Clay Minerals			
			Kaolinite	Illite	Smectite	Chlorite
Thorntonia	dolomite	4	0	70	20	10
'Mount Hendry'*	sandstone	4	0	81	6	13
V-Creek	limestone	5	3	55	12	30
Riversdale	sandstone	6	25	73	2	0
Currant Bush	limestone	7	28	31	24	17
Beetle Creek	mudstone	120+	52	35	10	3
Steamboat	sandstone	8	53	27	20	0
Inca	mudstone	14	66	22	3	9
Blazan	mudstone	7	85	15	0	0

*Informal name used by geologists of the Broken Hill South Company.

Grim (1968) considers that marine sediments generally contain abundant illite (usually in the range 50-100 percent), whereas sediments containing predominantly kaolinite are generally only found in the fluviatile or nearshore environment. De Keyser (1969a) suggests that the Beetle Creek phosphorites formed in very shallow water in semi-enclosed basins, estuaries, lagoons, etc. The abundance of kaolinite in the Beetle Creek Formation would tend to support de Keyser's ideas on the environment.

If the mineralogy of the Beetle Creek Formation is compared with that of other Cambrian units (Table 1) the results are what would reasonably be expected, with the carbonates containing little or no kaolinite and the detrital sediments containing abundant kaolinite (up to 85 percent of the total). The exception to this is the Riversdale Formation (and its equivalent the 'Mount Hendry Formation'), which is composed of coarse detrital sediments and yet contains only minor kaolinite. However, as a general rule the clay mineralogy of the Beetle Creek Formation is intermediate between the chemical (and biochemical) marine sediments with low kaolinite and the detrital nearshore sediments with high kaolinite. If this intermediate position is extended to the environment, with the Beetle Creek Formation being deposited in areas subject to both open marine and more nearshore or fluviatile conditions, then perhaps the attendant mixing was important for the formation of phosphorites. The other Cambrian units are non-phosphatic, or only poorly phosphatic because conditions were either too marine or too nearshore or fluviatile, or because the inflow of detrital material in the nearshore environment was too great and masked any phosphate deposition.

If the clay mineralogy of the Beetle Creek Formation is examined in more detail, important variations can be seen. For instance, non-phosphatic sediments are richer in kaolinite than associated phosphatic sediments. The compositions are compared below.

Beetle Creek Formation	kaolinite (%)	illite (%)	smectite (%)	chlorite (%)
non-phosphatic	70	20	9	1
phosphatic	42	36	18	4

These differences imply that the non-phosphatic sediments were deposited under conditions which were perhaps too fluviatile or too nearshore for phosphate to form in appreciable quantities.

Differences in clay mineralogy also occur within the phosphorites. There are two main types of primary phosphorites: the pelletal phosphorite, and the so-called 'microsphorite'. (Riggs and Freas (1965) suggested the term 'microsphorite' for similar muddy phosphorites in Florida.) A third phosphorite, which is a lateritic weathering product, will be dealt with in a subsequent publication and is not discussed here.

The mineralogical differences are summarized below:

Beetle Creek Formation	kaolinite (%)	illite (%)	smectite (%)	chlorite (%)
'microsphorite'	42	36	18	4
pelletal phosphorites	38	44	18	0

These values suggest that the pelletal phosphorites, which contain a higher percentage of illite, were deposited under more marine conditions than the microsphorites, which contain a higher percentage of kaolinite and chlorite. De Keyser (1969b) came to a similar conclusion using a different line of reasoning.

Little work has been done on the clay mineralogy of other phosphorite deposits with which to compare the results obtained in this study. The only other investigation was by Cook (1970), who examined the clay mineralogy of the Phosphoria Formation. He found the average composition of the minus 2μ fraction of the Phosphoria Formation was kaolinite 20 percent, illite 70 percent, smectite 10 percent, chlorite absent. This is appreciably different from the Beetle Creek clay mineralogy. Information presently available suggests that the depositional environment for these two phosphorites was rather different and this may have influenced the clay mineral assemblage. However, numerous other factors, such as the types of rocks and the degree of weathering in the source area, may also have been of considerable importance.

One unexpected feature of the areal variation in the Beetle Creek clay mineralogy was the lack of meaningful trends. Locally, some of the trends conformed with the expected source area. In the Yelvertoft area, for instance, the percentage of kaolinite and chlorite increases eastwards towards the basement (Fig. 3). Similarly, in the Lady Annie Outlier the percentage of kaolinite increases to the west while illite increases to the east. This suggests that the provenance for the Lady Annie area was predominantly on the west side of the outlier. However, in the Riversleigh area the trends are opposite to the expected ones, with kaolinite increasing seaward and illite increasing landwards. In the Phantom Hills-Mount Jennifer area there is a similar lack of meaningful variation in the clay mineral distribution. In the Duchess area, the drillholes were insufficiently distributed within the outlier to permit contouring. However, adjacent drillholes through the Monastery Creek Phosphorite Member of the Beetle Creek Formation on the west side of the Burke River Outlier yielded very different clay mineral assemblages. The average clay mineralogy for these drillholes, arranged in their correct relative positions, is given in Table 2. Such wide compositional variations between sections only an average of 1000 feet apart suggest extremely variable conditions, with small areas of localized sedimentation.

TABLE 2. AVERAGE CLAY MINERALOGY OF DRILLHOLE SAMPLES FROM THE MONASTERY CREEK PHOSPHORITE MEMBER OF THE BEETLE CREEK FORMATION, BURKE RIVER OUTLIER

	West <—						4 miles								—> East	
Drillhole Sample	68	135	134	133	69	132	131	70	126	127	128	193	159	160	161	162
Clay Mineral (%)																
Kaolinite	58	37	36	57	42	40	41	13	35	37	38	33	0	59	5	36
Illite	32	41	55	35	49	30	38	24	41	45	41	67	100	41	20	39
Smectite	10	22	9	8	9	30	21	63	24	18	21	10	0	0	27	25

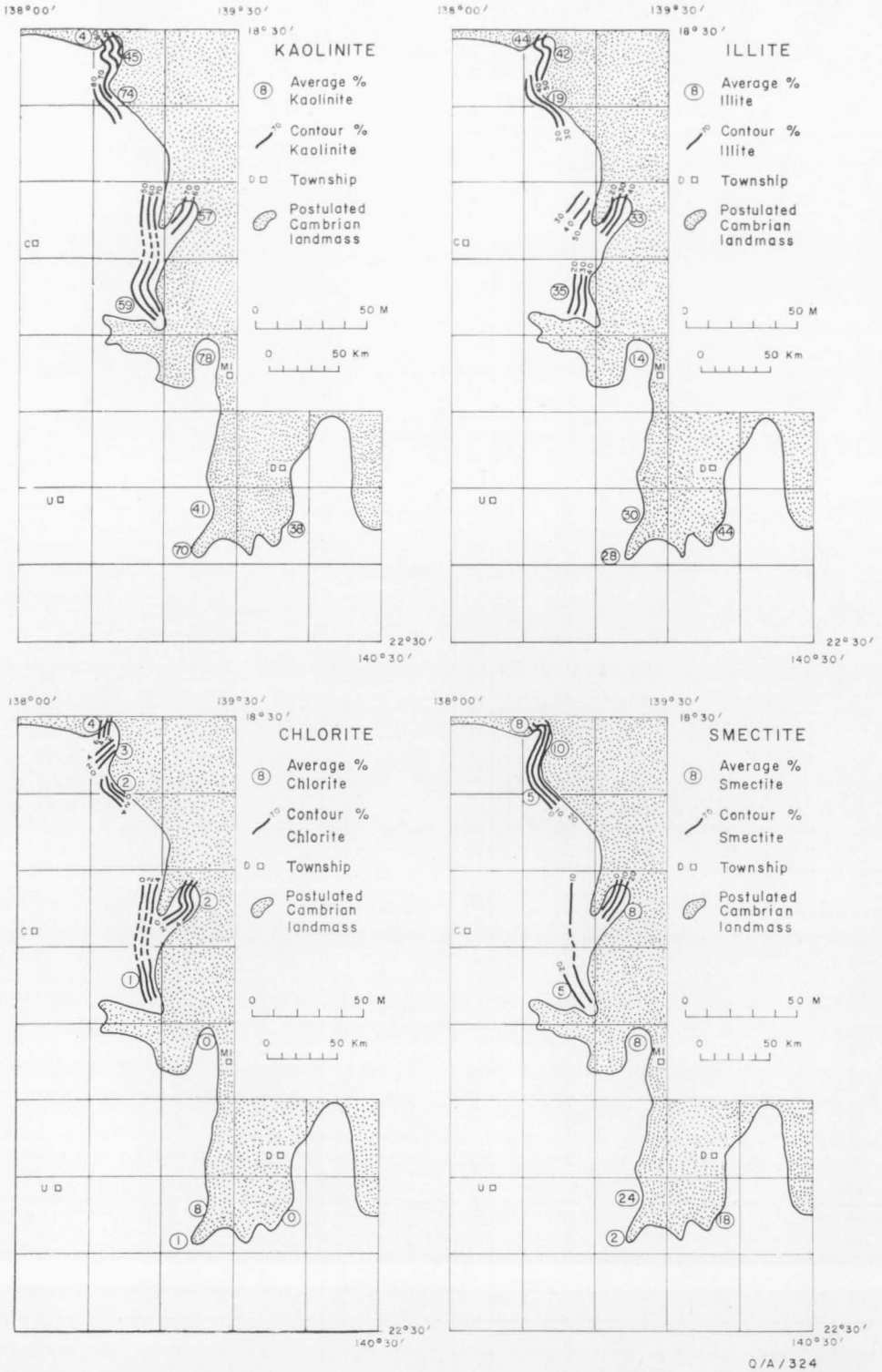


Figure 3. Variation in the clay mineralogy of the Beetle Creek Formation. The probable Cambrian palaeogeography for the east part of the Georgina Basin is also shown.

If the clay mineralogy throughout the eastern Georgina Basin is considered (Fig. 3), it is apparent that regional isopleths cannot be drawn on the percentage of particular clay minerals. This suggests that, rather than the whole of the eastern Georgina Basin being covered by a single uniform body of water, there were instead numerous fairly small discrete ephemeral areas of sedimentation which ultimately coalesced to form the body of sediment represented by the Beetle Creek Formation.

CONCLUSIONS

The minus 2μ fraction of the Beetle Creek Formation has an average clay mineralogy of 52 percent kaolinite, 35 percent illite, 10 percent smectite, and 3 percent chlorite. Traces of sepiolite, attapulgite, and mixed-layer clays are also present. Post-Cambrian weathering is not thought to have greatly modified the mineralogy.

The Beetle Creek Formation was probably deposited under shallow water, nearshore conditions. Other Middle Cambrian units, which have clay mineral compositions different from the Beetle Creek Formation, are non-phosphatic either because conditions were too marine (as in the case of the carbonates) or too fluviatile or nearshore (as in the case of the sandstones and mudstones). The lack of continuity in the pattern of variation in the clay mineralogy suggests discrete ephemeral areas of sedimentation rather than one single area of uniform sedimentation covering the entire eastern Georgina Basin.

Non-phosphatic Beetle Creek Formation contains a higher percentage of kaolinite and a lower percentage of illite and smectite than phosphatic Beetle Creek Formation. This is thought to be a reflection of the deposition of non-phosphatic sediments landward of the phosphatic sediments.

Pelletal phosphorites contain a higher percentage of illite and a lower percentage of chlorite and kaolinite than does the fine-grained phosphorite ('microsphorite'). This suggests that the pelletal phosphorites formed seaward of the 'microsphorite'.

REFERENCES

BISCAYE, P. E., 1964—Distinction between kaolinite and chlorite in Recent sediments by X-ray diffraction. *Am. Miner.*, 49, 1281-89.

CARTER, E. K., BROOKS, J. H., and WALKER, K. R., 1961—The Precambrian mineral belt of North-western Queensland. *Bur. Miner. Resour. Aust. Bull.* 51, 344 pp.

CARTER, E. K., and ÖPIK, A. A., 1961a—Explanatory Notes—Lawn Hill 4-mile Geological Series. *Bur. Miner. Resour. Aust. explan. Notes,* 21, 17 pp.

CARTER, E. K., and ÖPIK, A. A., 1961b—Explanatory Notes—Mount Isa 4-mile Geological Series. *Bur. Miner. Resour. Aust. explan. Notes,* 20, 20 pp.

COOK, P. J., 1970—The nature and origin of phosphorites in the Meade Peak Member of the Phosphoria Formation. (Manuscript.)

GRIM, R. E., 1968—CLAY MINERALOGY. 596 pp. *McGraw Hill, New York.*

KEYSER, F. DE, 1968—The Cambrian of the Burke River Outlier. *Bur. Miner. Resour. Aust. Rec.*, 1968/67, 48 pp. (Unpubl.).

KEYSER, F. DE, 1969a—On the genesis of the Georgina Basin phosphorites. *Bur. Miner. Resour. Aust. Rec.*, 1969/79, 20 pp. (Unpubl.).

KEYSER, F. DE, 1969b—The phosphate-bearing Cambrian formations in the Lawn Hill and Lady Annie Districts, northwestern Queensland. *Bur. Miner. Resour. Aust. Rec.* 1969/147, 35 pp. (Unpubl.).

MILLOT, G., 1949—Relations entre la constitution et la genèse des roches sedimentaires argileuses. *Geol. appliq. et. prosp. min,* 2.

MUELLER, G., 1967—METHODS IN SEDIMENTARY PETROLOGY. Part 1., SCHWEIZERBART. Stuttgart, 283 pp.

NOAKES, L. C., CARTER, E. K., and ÖPIK, A. A., 1959—Explanatory Notes—Urandangi 4-mile Geological Series. *Bur. Miner. Resour. Aust. explan. Notes,* 1, 16 pp.

ÖPIK, A. A., 1956—Cambrian geology of Queensland, *in* El Sistema Cambrico, su Palaeogeografia y el Problema de su Base. *Int. geol. Congr., 20th Sess., Mexico,* 1-24.

ÖPIK, A. A., 1960—Cambrian and Ordovician geology of Queensland. *J. geol. Soc. Aust.*, 7, 89-109.

RIGGS, S. R., and FREAS, D. H., 1965—Stratigraphy and sedimentation of phosphorite in the Central Florida Phosphate District. *A.I.M.E. Ann. Mtg Feb. 1965,* Preprint 65 H84, 13 pp.

RUSSELL, R. T., 1967—Discovery of major phosphate deposits in northwest Queensland. *Qld Govt Min. J.*, 68 (786), 153-57.

RUSSELL, R. T., 1968—Discovery of major phosphate deposits in northwest Queensland, Australia. *Miner. Resour. Dev. Ser. No.* 32, United Nations, New York, 241-248.

SMITH, K. G., 1970—The geology of the Georgina Basin. *Bur. Miner. Resour. Aust. Bull.* (in press).

WEAVER, C. E., 1956—The distribution and identification of mixed-layer clays in sedimentary rocks. *Am. Miner.*, 41, 202-21.

GEOLOGICAL INTERPRETATION OF A GRAVITY SURVEY OVER BASEMENT INLIERS NEAR MILLUNGERA, NORTH QUEENSLAND

by

M. D. Watts

SUMMARY

Results of a detailed gravity survey over basement inliers at Mount Fort Bowen and Mount Brown demonstate that these outcrops represent the crests of monadnocks buried by Cretaceous sediments of the Carpentaria Basin.

INTRODUCTION

At the request of BMR's Geological Branch, the Geophysical Branch made a detailed gravity survey in 1969 over two basement inliers near Millungera, north Queensland (Fig. 1). The purpose of the survey was to determine whether the outcrops are the culminations of a gentle basement swell or of more abrupt basement features.

GEOLOGY

The Millungera area lies on a complex but poorly known structure that separates the Mesozoic Carpentaria and Great Artesian Basins. Two small inliers of pre-Mesozoic basement crop out at Mount Fort Bowen and Mount Brown (Figs 2, 3) and are now considered to be on the crest of a major NW-trending basement ridge that extends to Julia Creek in the south, where the ridge is termed the St Elmo Structure. The presence of this ridge is only inferred, mainly from widely spaced water-bore data, and no detailed information is available.

Mount Fort Bowen and Mount Brown are east-tilted fault blocks of basement rock (H. F. Doutch, pers. comm.); their ages are not known. Mount Brown is composed of schist, and is possibly Precambrian; but at Mount Fort Bowen there are unmetamorphosed sandstone and conglomerate, which may be either the oldest basin sediments or infra-basin rocks.

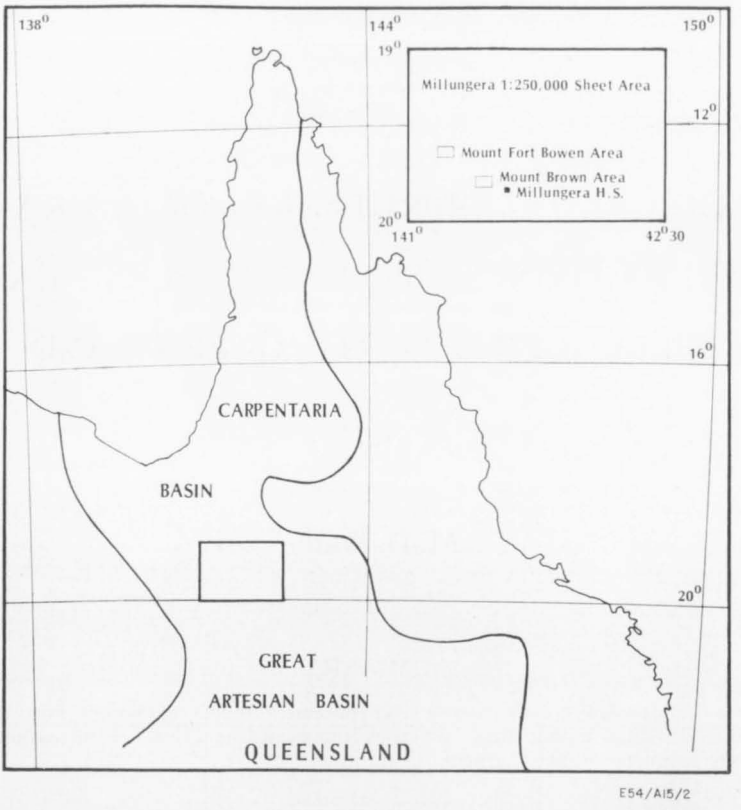


Figure 1. Location of the Millungera Sheet area, north Queensland.

INTERPRETATION OF GRAVITY DATA

Bouguer anomaly highs of 4 to 5 milligals amplitude are associated with both Mount Fort Bowen and Mount Brown. These short-wavelength features lie on the west and east flanks respectively of a major north-trending Bouguer anomaly high outlined by BMR's earlier reconnaissance gravity survey. On the basis of a comparison between regional gravity data and basement contours, the high appears to be related only to intra-basement density variations. However, the extremely close correlation between the basement outcrops and the small highs makes it clear that these Bouguer anomaly features are related at least locally to the basement topography.

Rock samples obtained from outcrops at Mount Fort Bowen have a density of 2.7 g/cm^3, while slightly weathered samples from Mount Brown suggest a density of 2.9 g/cm^3 for unweathered rock. A few measurements made on Cretaceous samples indicate a density of 2.2 g/cm^3; thus density contrasts at the two areas are 0.5 and 0.7 g/cm^3 respectively.

Quantitative analysis of the gravity data was concentrated on profiles only; adjustments to computed models were therefore necessary in order to eliminate end effects (Nettleton, 1940, p. 117). At Mount Fort Bowen the Bouguer anomaly contours are roughly circular, and so a correction factor of 1.5 was used to increase basement depths computed for a two-dimensional model. At Mount Brown, owing to the more elongate shape of the Bouguer anomaly feature, a factor of 1.1

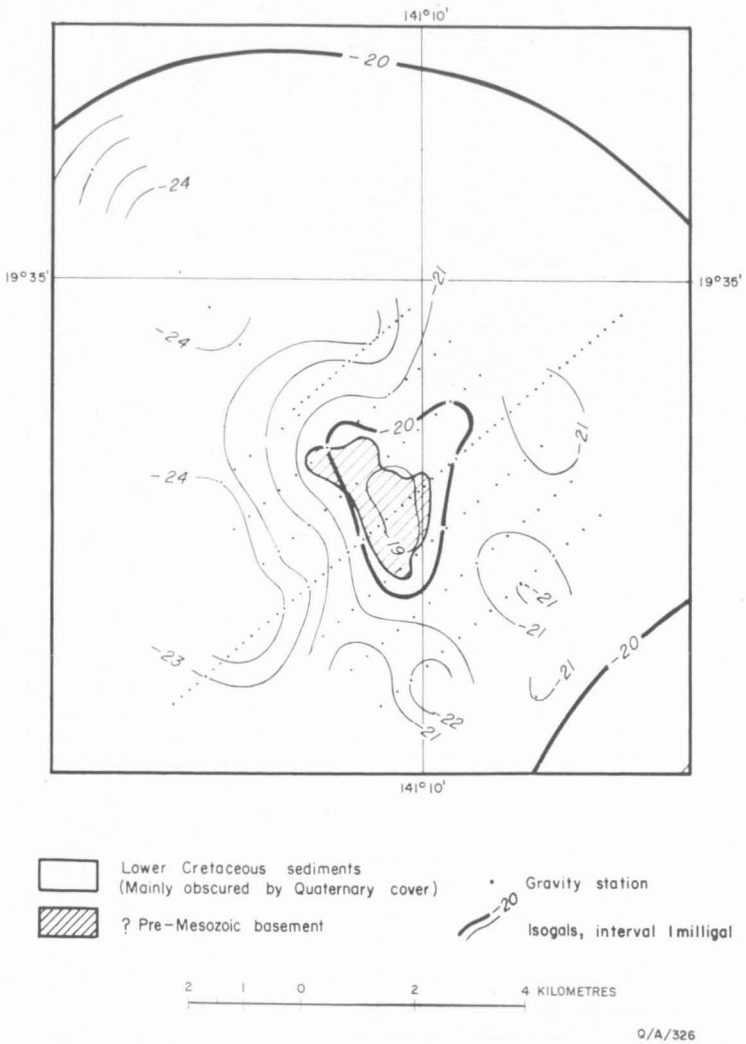


Figure 2. Surface geology and Bouguer anomaly contours of the Mount Fort Bowen area, north Queensland.

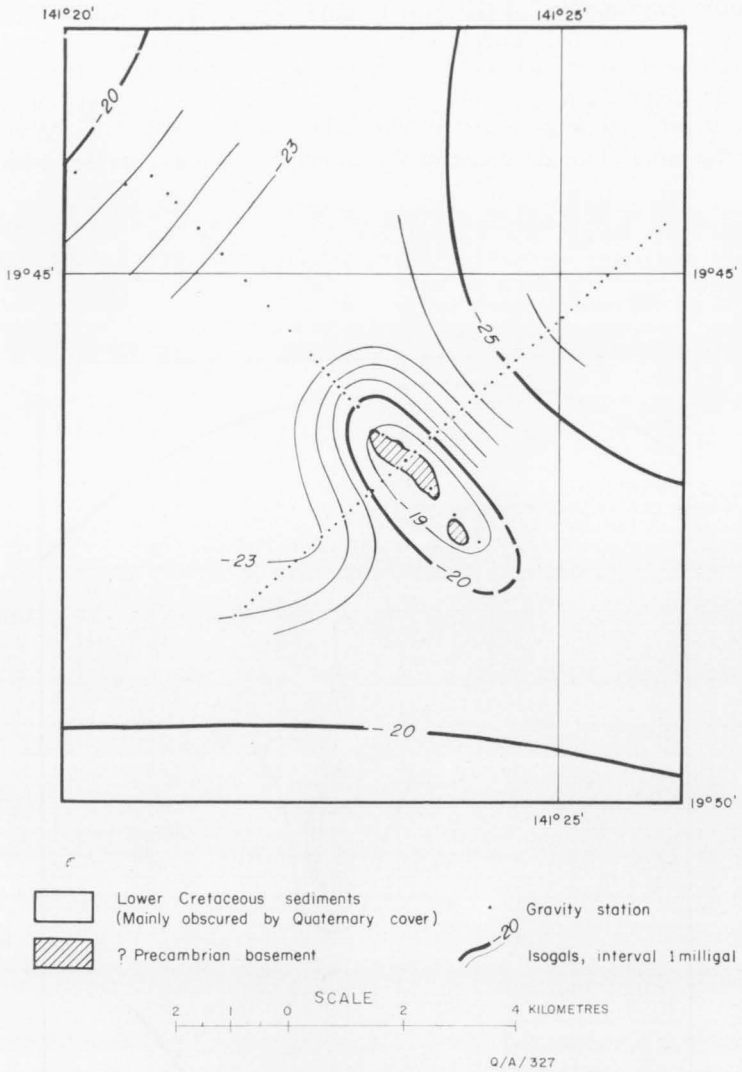


Figure 3. Surface geology and Bouguer anomaly contours of the Mount Brown area, north Queensland.

was used. Basement profiles were computed using an iterative programme (FITPLUTN) devised by R. Whitworth (in prep.). Input gravity data were corrected for the regional gradient (determined by the reconnaissance gravity survey) and reduced using a variable density to a datum plane 76 m above sea level. The final standard deviation of misfit between observed and computed profiles was 0.03 milligals for Mount Fort Bowen and 0.04 milligals for Mount Brown. The computed geological profiles are shown in Figure 4.

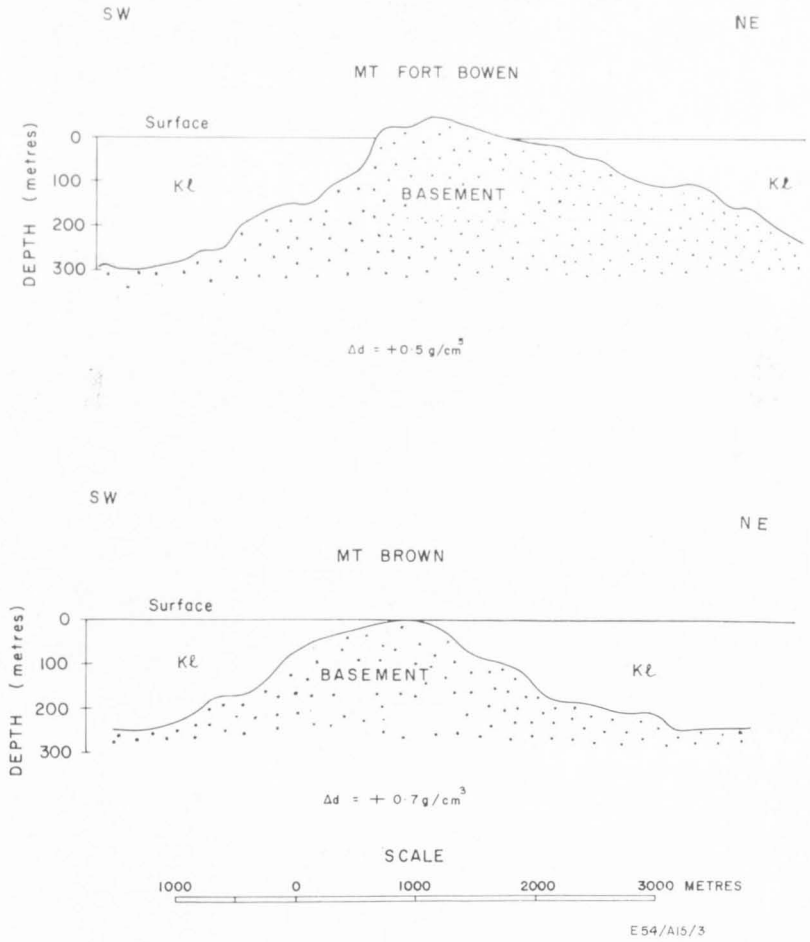


Figure 4. Basement profiles for the Mount Fort Bowen and Mount Brown areas, computed from gravity results.

CONCLUSIONS

This gravity survey has shown that rather steep basement relief is associated with the Mount Fort Bowen and Mount Brown basement outcrops. It has demonstrated that these inliers are the crests of buried hills rather than of gentle basement swells; a lack of sedimentary deformation (H. F. Doutch, pers. comm.) implies that these hills existed during the Lower Cretaceous as monadnocks rising above a general plain.

REFERENCES

NETTLETON, L. L., 1940—GEOPHYSICAL PROSPECTING FOR OIL. (New York, McGraw-Hill.)

WHITWORTH, R.—Two-dimensional interpretational programmes for gravity data. *Bur. Miner. Resour. Aust. Rec.* (in prep.).

Page 22 is blank.

SILCRETE IN SOUTHWEST QUEENSLAND

by

B. R. and Daniele A. Senior

SUMMARY

'Silcrete' is regarded as a useful lithological term for extremely siliceous sediments composed of numerous small angular to subangular quartz clasts set in an amorphous siliceous matrix. Textures and thicknesses vary, and lenticular beds of silcrete have been found. Silcrete beds are widespread in southwest Queensland, and are useful markers of general structures and folds. The silcretes are not necessarily 'duricrusts' in the sense of Woolnough's (1927) definition implying silicification of a pre-existing peneplain surface; the occurrence of multiple silcrete beds suggests that some silcretes formed by precipitation of silica in porous quartz sandstone beds below the Tertiary land surface.

INTRODUCTION

The term 'silcrete' was first coined by Lamplugh in 1902 to describe 'sporadic masses in loose material of the "greywether" type, indurated by a siliceous cement'. He later (1907) used the term silcrete for a hard sandstone or quartzite, knit together by a chalcedonic cement. Frankel & Kent (1938) referred to 'silicified rocks formerly known as "surface quartzites" but now known as silcretes in conformity with the nomenclature used by Lamplugh (1907)'.

In Australia the rock-type silcrete is described colloquially as grey billy, quartzite, siliceous duricrust, and simply as duricrust. In accordance with South African (Lamplugh, 1902; 1907; Frankel & Kent, 1938) and recent Australian usage (Williamson, 1957; Senior et al., 1968; Exon et al., 1970), silcrete is primarily a lithological term and its use should be restricted to extremely siliceous sediments.

Australian silcrete deposits are very extensive. Samples collected for analysis are from an area of approximately 70,000 square miles in western Queensland. BMR mapping shows that approximately 10 percent of this area is covered by silcrete beds averaging 6 feet, with local variations in thickness from 2 to 15 feet. The areal extent of the deposits is considerably larger if silcrete beds buried under thin aeolian sand deposits are included.

LITHOLOGY AND COMPOSITION

Silcrete is a hard grey, whitish, or buff-coloured rock composed of numerous small angular to subangular quartz clasts set in an amorphous siliceous matrix. Textures are variable owing to differences in grain size and sorting of the quartzose host sediment; they vary from fine-grained types with small scattered quartz clasts, to those with fragments of quartz up to half an inch long. In hand specimen irregular elongate cavities can be seen, and in thin section these cavities are shown to be lined with colloform structures, comprising layers of chalcedony. When hit with a hammer silcrete usually gives a marked 'ring' and breaks across quartz grains along subconchoidal fracture surfaces.

Beds of silcrete are commonly 5 to 12 feet thick, although locally they may be up to 15 feet thick. The beds may extend laterally for many miles, but lenticular beds occur. Local variations in thickness occur where former stream channels filled with quartzose sand are silicified to form silcrete (Pl. 1, fig. 1).

Vertical and subhorizontal joints in silcrete beds are common features (Pl. 1, fig. 2). Where vertical jointing is pronounced a columnar structure is characteristic; the columns terminate at the surface as a polygonal pavement, as illustrated by Wopfner (1964). Normally the silcrete bed is mantled with a veneer of several feet of silcrete cobbles and boulders. Larger joints are commonly filled with silcrete rubble forming 'pipes', and the pipe material is commonly recemented by silica and ferruginous material in the form of cement and pisolites. Breakdown of silcrete by erosion has distributed boulders and cobbles of silcrete over extensive gibber plains. The individual clasts of silcrete ('gibbers') are often iron-stained and polished with a characteristic desert varnish.

Detailed examination of the individual quartz grains shows pitting and embayments of the peripheries. In some grains transformation of quartz into chalcedony is conspicuous from the core to the edge of the grain. Frankel & Kent (1938) studied the silcrete overlying the Witteberg Series (South Africa) and found that most quartz grains were fretted and rather ragged at their edges and commonly markedly embayed. These features suggest that the siliceous matrix was enriched partly at the expense of the quartzose host sediments.

Table 1 shows results of 13 samples which were analyzed by X-ray diffraction and XRF techniques. The presence of anatase (a polymorph of rutile) is worth noting. Williamson (1957) analyzed six Australian silcretes and noted that in some samples the TiO_2/SiO_2 ratio was relatively high. Comparably high TiO_2/SiO_2 ratios characterize South African silcretes (Frankel & Kent, 1938; Frankel, 1952; Mountain, 1952). Titanium in silcrete is reported to be especially concentrated in colloform structures and syngenetic nodules (Williamson, 1957). The origin of the titanium is in doubt but it may have been concentrated and deposited from ionic or colloidal solution in a process similar to that undergone by the silica. However, the mineral anatase is present as detrital grains in most of the thin sections examined, suggesting that the titanium is derived from the sandstone host sediments.

Sample 3059 (Table 1) consists of concretionary silcrete surrounded by a softer de-silicified? zone of quartz sandstone. This sample was split into two fractions to determine the difference in composition by XRF analyses. Only very slight differences in composition occur except that loss on ignition for the hard inner zone was greater. This is interpreted as loss of water from opaline cement, with less opaline cement present in the soft outer zone.

PLATE 1

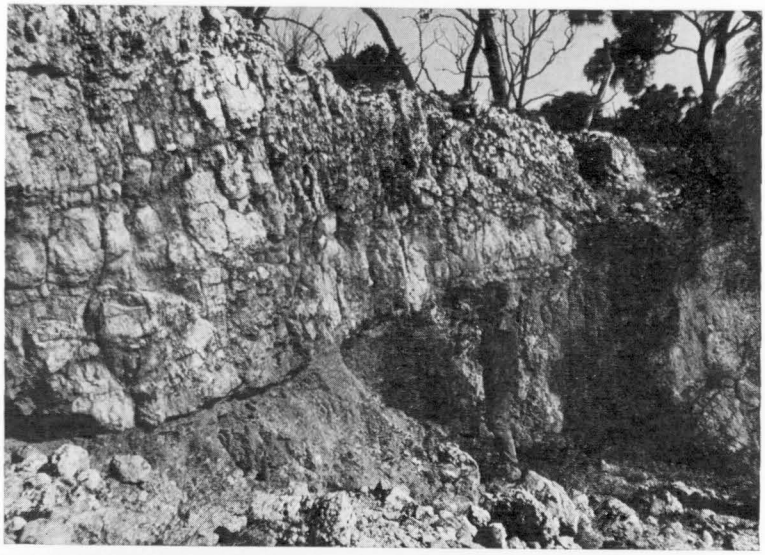


Figure 1. Channel sandstone infilling an eroded hollow at Mount Young (Toompine Sheet area Grid Ref. 315563). The sandstone is strongly silicified, forming silcrete. The head of the figure demarks the uncomformity.



Figure 2. Strong columnar and subhorizontal jointing in silcrete near Mount Koldonera (Eulo Sheet area Grid Ref. 223487).

TABLE 1. SILCRETE ANALYSES BY X-RAY METHODS OF SAMPLES FROM SOUTHWEST QUEENSLAND AND COMPARISON WITH A TYPICAL SOUTH AFRICAN SILCRETE

A. X-Ray Diffraction Analyses

Sample No.	1:250,000 Sheet Ref.	Grid Ref.	Rock Type	Mineral Identification
*1110	Barrolka SG 54-11	486669	Silcrete	Quartz, anatase (tr.)
*1027C	Cordillo SG 54-10	391736	Samples from the top, middle	Quartz, anatase (tr.)
*1027B		391736	and base of a 16-foot thick	Quartz, anatase, hematite (tr.)
*1027A		391736	silcrete bed	Quartz, anatase (tr.)
*2016	Durham Downs SG 54-15	495617	Silcrete	Quartz, anatase (tr.)
*2067		5266138	Silcrete	Quartz, anatase (tr.)
*2034		436598	Silcrete	Quartz, anatase (tr.)
*5013		495635	Silcrete	Quartz, anatase
†3059A	Connemara SG 54-3	416585	Concretionary silcrete	Quartz
*4045	Eromanga SG54-12	181657	Resilicified silcrete conglomerate	Quartz, anatase (tr.)
*4068		584692	Silcrete with opal vein	Quartz, anatase
*5035	Thargomindah SG 54-16	635641	Partly silicified quartz sandstone	Quartz, chlorite, anatase (tr.)
*6001	Bulloo SH 54-4	599517	Silcrete	Quartz, anatase

B. X-Ray Fluorescence Analyses

Sample No.	*1110	*1027A	*1027B	*1027C	*2016	*2067	*2034	*5013	†3059A (hard inner zone)	†3059B (soft outer zone)	*4045	*5035	*6001	*4068	Typical South African Silcrete‡
SiO_2	98.39	97.53	95.45	96.61	96.71	95.50	97.33	96.23	98.64	98.93	96.56	91.04	95.22	94.81	92.95
Na_2O	0.00	0.07	0.10	0.03	0.01	0.02	0.02	0.06	0.05	0.05	0.09	0.06	0.06	0.04	tr.
MgO	0.28	0.22	0.27	0.23	0.31	0.20	0.19	0.17	0.18	0.23	0.14	0.32	0.22	0.22	0.40
Al_2O_3	0.18	0.38	0.64	0.38	0.31	0.43	0.34	0.23	0.20	0.37	0.30	5.93	0.29	0.40	0.26
P_2O_5	0.05	0.03	0.11	0.11	0.03	0.03	0.06	0.02	0.02	0.13	0.06	0.03	0.03	0.05	—
K_2O	0.00	0.05	0.00	0.05	0.01	0.04	0.00	0.00	0.00	0.00	0.02	0.26	0.00	0.00	—
CaO	0.09	0.03	0.08	0.39	0.03	0.05	0.04	0.11	0.11	0.24	0.02	0.11	0.03	0.02	—
TiO_2	1.37	1.01	2.00	0.87	1.99	1.14	0.65	0.38	0.39	0.45	1.98	0.50	2.77	3.51	2.77
MnO	0.01	0.04	0.01	0.01	0.00	0.01	0.00	0.01	0.00	0.01	0.00	0.01	0.00	0.00	—
Fe_2O_3	0.02	0.05	0.05	0.13	0.08	0.03	0.05	0.03	0.03	0.12	0.03	0.44	0.02	0.04	3.60
Total	100.39	99.41	98.71	98.81	99.48	97.45	98.68	97.24	99.62	100.53	99.20	98.70	98.64	99.09	99.98
Loss on ignition	0.28	0.50	0.86	0.65	0.79	0.33	1.41	0.90	3.69	0.50	0.43	3.44	0.50	0.85	0.55

X-Ray diffraction and XRF analyses carried out in the BMR Laboratories. G. E. Berryman, analyst.

* For data retrieval at the BMR the numbers 67 (year of project) 05 (Eromanga Basin) should be used.

† For data retrieval at the BMR the numbers 66 05 should be used.

‡ Data from Frankel & Kent, 1938.

MULTIPLE SILCRETES

During a regional mapping survey by the Bureau of Mineral Resources in 1966, two silcretes were found. The Glendower Formation, which contains the silcrete beds, is a fluviatile sequence of quartzose arenaceous sediments containing minor argillaceous interbeds. Silcrete pebbles and cobbles incorporated in the sandstone beds were found along the west margin of the Thomson River (Gregory et al., 1967). Throughout this area the Glendower Formation has an obvious silcrete capping. A shallow stratigraphic hole, BMR Jundah No. 3, encountered two silcrete beds (Gregory et al., 1967); these could be interpreted as two duricrusts representing breaks in deposition.

Sprigg (1961) described more than two duricrust levels present locally in the Innamincka Dome. These silcrete beds attracted the attention of a Bureau of Mineral Resources survey in that area in 1967 (Senior et al., 1968; Senior, 1969). An exposure along the south central limb of the Innamincka Dome has three silcrete beds (Fig. 1), with each silcrete separated by several feet of friable, unsilicified quartz sandstone with minor interbeds of mudstone. These Tertiary deposits rest unconformably on the Cretaceous Winton Formation. The middle silcrete incorporates a minor depositional break and consists of 1 foot of silicified siltstone overlain by 5 feet of silicified sandstone. An important factor pertaining to the origin of silcrete is apparent here, in that the silcrete bed is formed above and below a depositional break.

The middle and basal silcrete beds are lenticular but persist for a distance of half a mile where they are eroded to form two silcrete-capped benches. The upper silcrete is largely broken-up, and downdip this fragmented silcrete merges

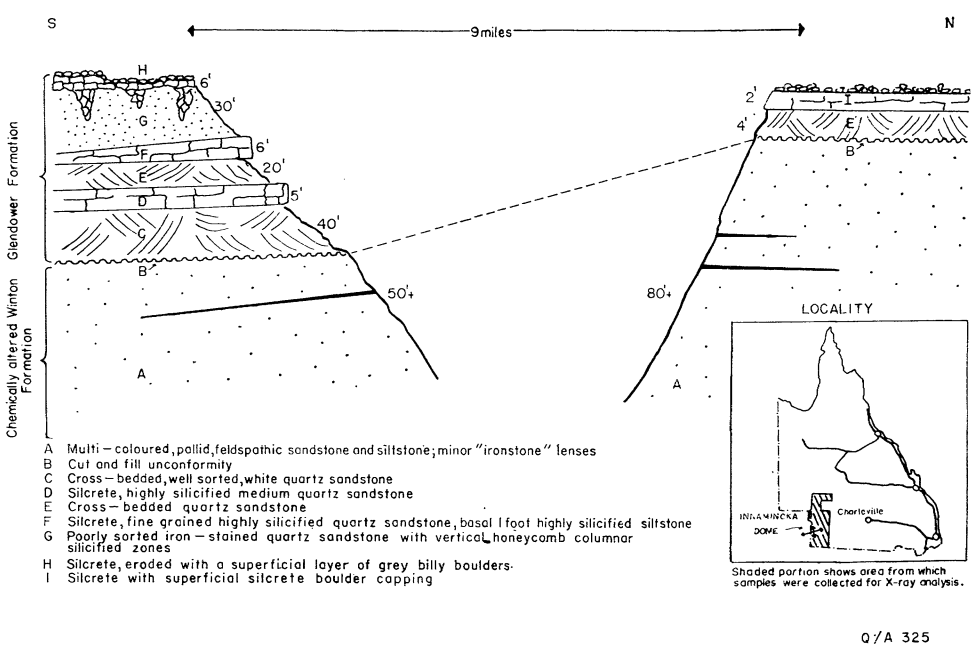


Figure 1. Diagrammatic cross section of a multiple silcrete profile from the southern limb of the Innamincka Dome and a comparison with a section from the northern limb.

with the underlying beds forming the dip slope of the southern limb of the Innamincka Dome.

Multiple silcrete beds exhibiting lenticular bedding characteristics were found at several localities in southwest Queensland, especially in the Grey Range on the Bulloo (Ingram, 1970) and Tickalara (Galloway and Senior, 1970) Sheet areas. The stratigraphic column below shows a typical example.

MULTIPLE SILCRETES IN THE GREY RANGE
(Bulloo Sheet area, Grid Ref. 599517)

47 to 52 feet	Silcrete cobbles and large boulders.
37 to 47 feet	Quartz sandstone, fine grained, friable.
7 to 32 feet	Cross-bedded quartz pebble sandy conglomerate, quartz sandstone. Abundant redeposited clasts of Winton Formation mudstone.
2 to 7 feet	Silcrete, lenticular bed.
0 to 2 feet	Quartz sandstone containing redeposited clasts of Winton Formation mudstone.
————	UNCONFORMITY. Kaolinitic sandstone and mudstone of the Winton Formation below.

Woolnough (1927) hypothesized that the hard cappings throughout Australia (including silcrete) were chemically formed rocks and equivalent to other 'case hardened' or 'armour plate' surfaces throughout Australia. He used the term 'siliceous duricrust' to describe silcrete and thought that its origin was identical to all other types of hard cappings. To describe the group collectively he coined the term 'duricrust', and maintained that the duricrust formed during an era of perfect peneplanation.

However, the lenticular characteristics of the silcrete beds imply that they are not necessarily the product of surface silicification of a peneplain and therefore are not duricrusts in the terms of Woolnough's definition.

STRUCTURAL IMPLICATIONS OF MULTIPLE SILCRETE BEDS

Numerous writers have observed that the silcrete beds have undergone tectonic disturbance. Woolnough (1927) observed monoclinal flexures in the Flinders Range, and Wopfner (1960) described tectonic features which are delineated by silcrete-capped cuestas in the Cordillo-Betoota area. Gregory et al. (1967) and Senior et al. (1968) used silcrete to delineate over forty anticlines in southwest Queensland, and successfully intersected downfolded silcrete by drilling in the Cooper Syncline.

On a regional scale silcrete beds are useful markers of general structure. Individual silcretes can be followed, particularly using airphotos, to provide structural markers for indivdual folds or parts of folds. However, the lenticular characteristics and multiplicity of beds imply that silcretes cannot be correlated over large areas. They can be used as structural markers on a regional scale because they formed as a widespread veneer of fluviatile sandstone which seldom exceeds 100 feet in thickness and the vertical distance between silcrete beds is small.

ORIGIN OF SILCRETE

We interpret that silcrete formed by movement of silica-bearing groundwater. Its movement was partially controlled by vertical differences in permeability. Argillaceous beds or lenticular sand bodies bounded by less permeable sediments

formed traps which resulted in precipitation of silica. In above average thicknesses of host sediments many traps of this kind occurred and in these favourable conditions multiple silcretes developed.

The origin of the silica in the groundwater is not known, and it was suspected that clay minerals in the Glendower Formation could have been a source. However, the fine powdery matrix in some samples subjected to X-ray analysis proved to be finely powdered quartz. Therefore, the source of the silica cement may be the quartz grains themselves, or alternatively silica originating from the unconformably underlying, deeply weathered, kaolin-rich Cretaceous sediments.

REFERENCES

EXON, N. F., LANGFORD-SMITH, T., and MCDOUGALL, I., 1970—The age and geomorphic correlations of deep-weathering profiles, silcrete, and basalt in the Roma-Amby region, Queensland. *J. Geol. Soc. Aust.*, 17, 21-30.

FRANKEL, J. J., 1952—Silcrete near Albertina, Cape Province. *Sth African J. Sci.*, 49, 173-82.

FRANKEL, J. J., and KENT, L. E., 1938—Grahamston surface quartzites (silcretes). *Geol. Soc. Sth Africa Trans.*, 40, 1-42.

GALLOWAY, M. C., and SENIOR, DANIELE, 1970—Tickalara, Qld—1:250,000 Geological Series. *Bur. Miner. Resour. Aust. explan. Notes* SH/54-3.

GREGORY, C. M., SENIOR, B. R., and GALLOWAY, M. C., 1967—The geology of the Connemara, Jundah, Canterbury, Windorah and Adavale 1:250,000 Sheet areas, Qld. *Bur. Miner. Resour. Aust. Rec.*, 1967/16 (Unpubl.).

INGRAM, J. A., 1970—Bulloo, Qld—1:250,000 Geological Series. *Bur. Miner. Resour. Aust. explan. Notes* SH/54-4.

LAMPLUGH, G. W., 1902—Correspondence. *Geol. Mag.*, 4, 575.

LAMPLUGH, G. W., 1907—The geology of the Zambesi Basin. *Quart. J. Geol. Soc. Lond.*, 53, 198-200.

MOUNTAIN, E. D., 1952—The origin of silcrete. *Sth African J. Sci.*, 48 (6).

SENIOR, DANIELE, 1969—Durham Downs, Qld—1:250,000 Geological Series. *Bur. Miner. Resour. Aust. explan. Notes* SG/54-15.

SENIOR, B. R., GALLOWAY, M. C., INGRAM, J. A., and SENIOR, DANIELE, 1968—The Geology of the Barrolka, Eromanga, Durham Downs, Thargomindah, Tickalara and Bulloo 1:250,000 Sheet area, Queensland. *Bur. Miner. Resour. Aust. Rec.* 1968/35 (Unpubl.).

SPRIGG, R. C., 1961—On the structural evolution of the Great Artesian Basin. *APEA J.*, 1961, 37-56.

WILLIAMSON, W. O., 1957—Silicified sedimentary rocks in Australia. *Am. J. Sci.*, 255, 23-42.

WOOLNOUGH, W. G., 1927—Presidential address. Part I—The chemical criteria for peneplanation (reprinted 1928 in *Econ. Geol.*, 23, 887-94). Part II—The duricrust of Australia. *J. Proc. Roy. Soc. N.S.W.*, 61, 17-53.

WOPFNER, H., 1960—On some structural development in the central part of the Great Australian Artesian Basin. *Trans. Roy. Soc. Aust.*, 83, 179-93.

WOPFNER, H., 1964—Tertiary duricrust profile on Upper Proterozoic sediments, Granite Downs area. *Geol. Surv. S. Aust. quart. geol. Notes*, 12.

LATE CAINOZOIC UPLIFT IN THE MILNE BAY AREA, EASTERN PAPUA

by

I. E. Smith and C. J. Simpson

SUMMARY

Plateaux in the Milne Bay area have been interpreted as remnants of an extensive erosion surface formed during a period of tectonic stability in Plio-Pleistocene times.

INTRODUCTION

Eastern Papua (Fig. 1) has been an area of active orogeny since the early Tertiary. Evidence presented in this paper suggests that orogenic movements may have been interrupted by a prolonged period of relative calm during Pliocene and Pleistocene times.

The geology of Eastern Papua has been outlined by Davies et al. (1968). In the Milne Bay area it is dominated by lower Miocene marine basaltic rocks with minor associated limestone, detrital sediments, and agglomerate. These are intruded by Pliocene dykes and stocks, and overlain by Pliocene volcanics in the area south of Milne Bay. The Cape Vogel Basin off the coast northwest of Milne Bay contains sediments ranging from middle Miocene to Recent. They are exposed on Cape Vogel Peninsula.

Plateaux developed on Miocene and younger rocks in the Milne Bay area were recognized by Smith during the 1968 field season (Smith et al., in prep.). Detailed air-photo examination of the plateaux east of longitude 149°54′ in the Milne Bay area suggests that they are remnants of a Plio-Pleistocene erosion surface.

THE EROSION SURFACE

Remnants of the erosion surface occur on relatively high areas in the ranges around Milne Bay. Figure 2 shows their distribution as interpreted from air photographs. Individual remnants range up to 27 sq km in area, and occur at elevations between 185 m above sea level in the southeast of the map (150°32′E, 10°26′S) and 1550 m in the northwest (150°7′E, 10°5′S). On air photographs the subhorizontal, planar surfaces are characterized by a slightly darker vegetation tone compared with the surrounding areas. Surface relief on the plateau ranges

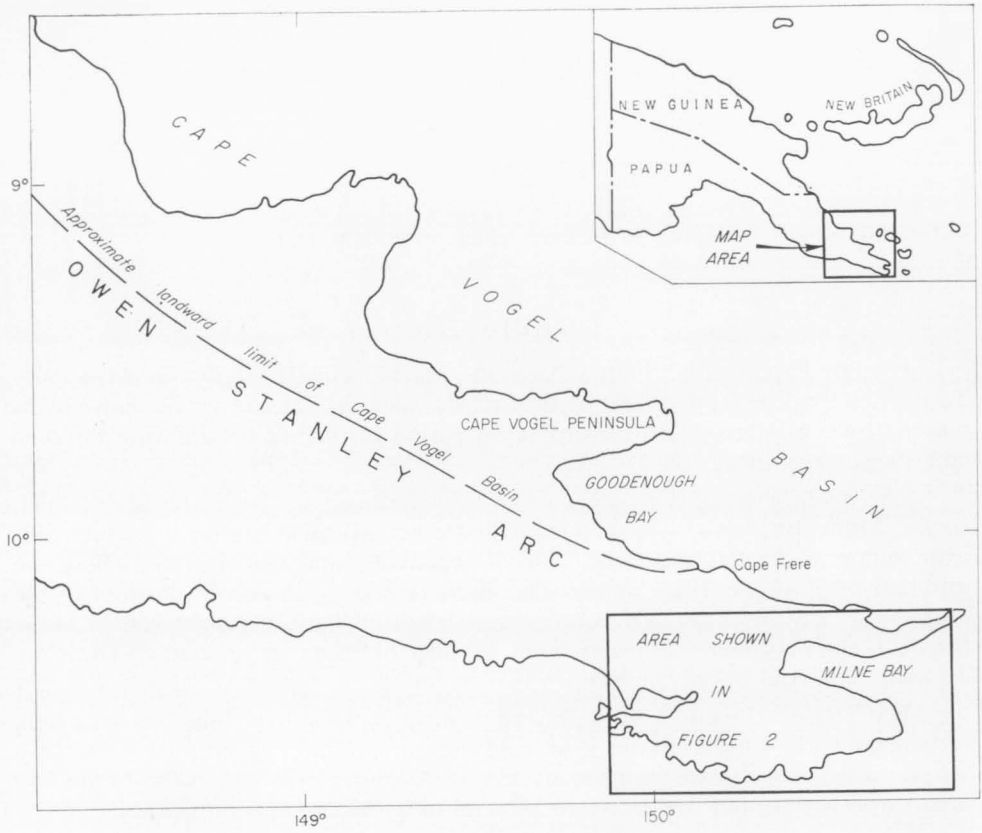


Figure 1. Locality map, Milne Bay area, Eastern Papua. The framed area around Milne Bay is shown in Figure 2.

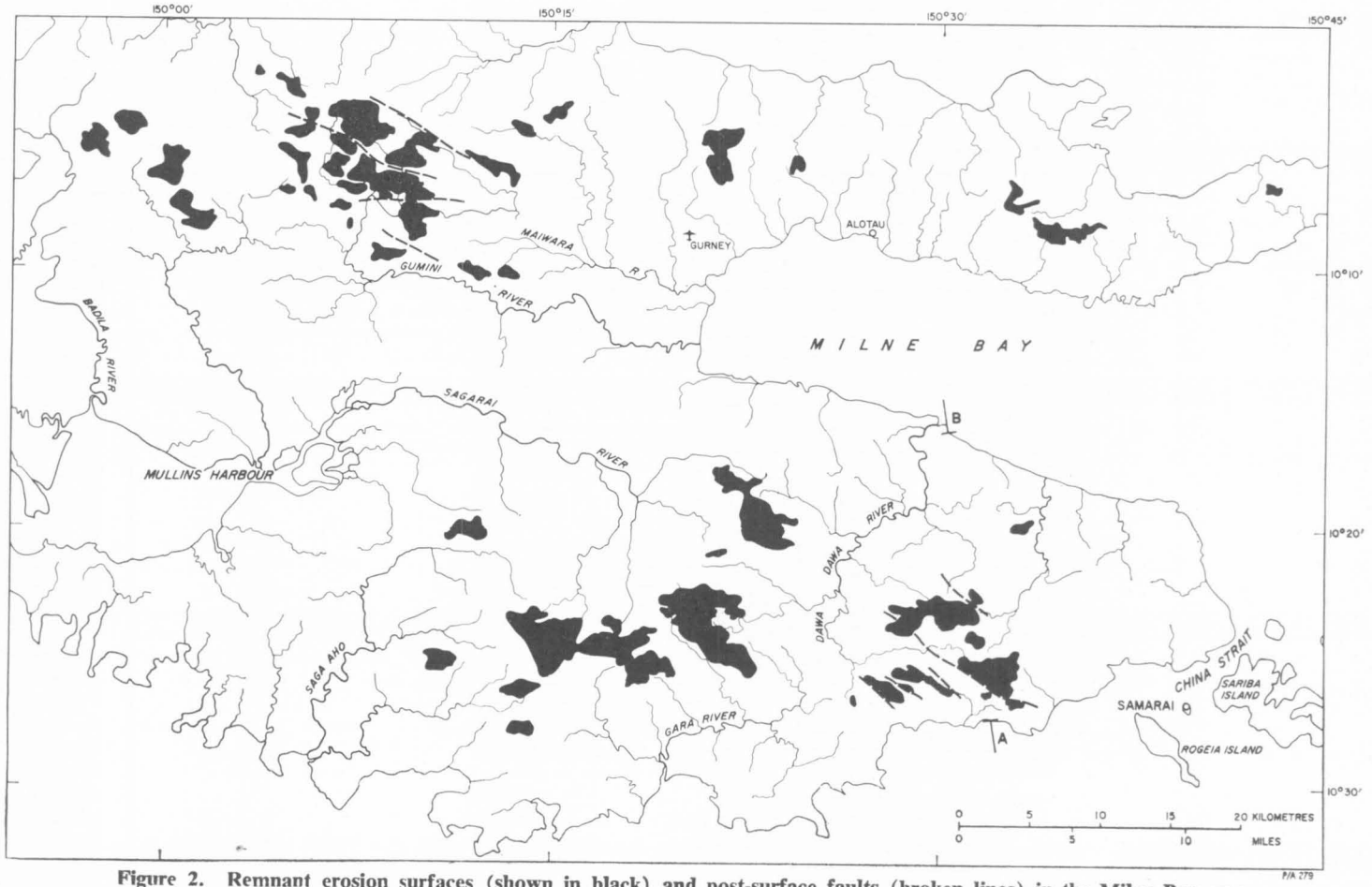


Figure 2. Remnant erosion surfaces (shown in black) and post-surface faults (broken lines) in the Milne Bay area.

up to 100 m but is normally less than 30 m. Drainage on the surface remnants is well developed but not deeply incised, except where Recent faulting has tilted them, causing localized rejuvenation and active incision. In contrast the country surrounding the surface remnants has a youthful topography with a relief of up to 900 m and deeply incised streams (Fig. 3). There is a sudden break in slope between the plateau and mountain topographies where headward erosion is actively removing the plateau remnants. Good examples of these features can be found on aerial photographs Milne Bay (CAJ 1241) 1/2091, Guaugurina Bay (CAJ 1241) 1/2068, and Sagari River (CAJ 188) 1/5154.

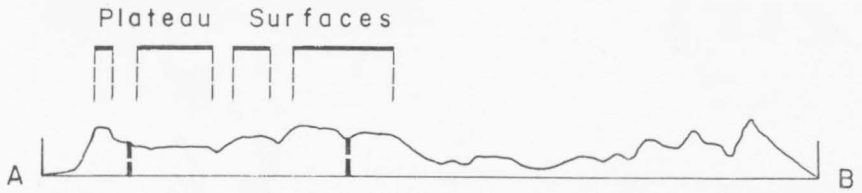


Figure 3. Profile on A-B (for location, see Fig. 2). Horizontal scale 1:200,000 $\frac{V}{H} = 4.4$.

Post-surface faulting (Fig. 2) is recognized by the presence of linear scarps separating remnants at different elevations. Block faulting predominates with vertical displacements on individual faults generally less than 100 m. Because of the faulting it has not been feasible to reconstruct the surface to obtain absolute measurements of post-surface uplift.

The age of the surface cannot be determined from existing data, but as it is developed on Miocene and (?) Pliocene rocks it is probably of late Pliocene to Pleistocene age.

DISCUSSION

The presence of this mature erosion surface is evidence of a prolonged period of tectonic standstill during the late Pliocene or early Pleistocene in the Milne Bay area. This was followed by rapid uplift as evidenced by headward erosion of rejuvenated streams.

Sedimentation in the Cape Vogel Basin suggests a similar tectonic history. The main source of sediment to the basin has been the Owen Stanley Arc forming the spine of the East Papuan peninsula. Upper Miocene to Pliocene times are represented in the basin by 4000 m of clastic sediments. These are overlain by 400 m of Pliocene claystone (Smith et al., in prep.). The presence of these fine-grained sediments indicates that by the Pliocene, uplift of the source area had ceased, allowing a more mature erosion cycle to develop.

Strong uplift along the southern margin of the basin in Recent times has raised deltaic and paralic deposits to heights of 300 m, and in the Cape Frere area coral reefs now stand at over 500 m above sea level.

NOTE ON TECTONIC HISTORY

From the foregoing discussion we postulate the following:

1. A period of orogeny during the Miocene when the Owen Stanley Arc came into existence. Uplift probably continued on a reduced scale into late Miocene times but had ceased by the early Pliocene.
2. A period of tectonic stability lasting from middle Pliocene into Pleistocene. During this time erosion in the eastern end of the Owen Stanley Arc produced an extensive area of subdued relief, and deposited fine-grained sediments in the Cape Vogel Basin.
3. Strong uplift during late Pleistocene and Recent times raised the erosion surface and produced the present rugged topography.

This study was restricted to the Milne Bay area east of longitude 149°54′. Remnants of this erosion surface could exist elsewhere in Papua.

REFERENCES

DAVIES, H. L., SMITH, I. E., CIFALI, G., and BELFORD, D. J., 1968—Eastern Papua geological reconnaissance. *Bur. Miner. Resour. Aust. Rec.* 1968/66 (Unpubl.).

SMITH, I. E., DAVIES, H. L., and BELFORD, D. J.—Geology of southeastern Papua. *Bur. Miner. Resour. Aust. Bull.* (in prep.).

Page 34 is blank.

MARINE GEOLOGY OF MILNE BAY, EASTERN PAPUA

by

D. Jongsma

SUMMARY

Bathymetry and sparker traverses have shown that Milne Bay is a graben structure which is related to the formation of the Owen Stanley fault lineament on shore and the Pocklington Shear zone which runs east to Guadalcanal. The bay floor has been sinking in Quaternary times and a thick succession of marine sediments has collected within the bay. A (?) Pleistocene unconformity observed in the sparker records indicates a rapid rate of submergence in the central southern part of the bay. A submarine trough off East Cape shows a trend similar to structural features on the D'Entrecasteaux Islands to the north.

INTRODUCTION

Milne Bay is located between latitudes 10°15′S and 10°35′S, and longitudes 150°20′ and 151°15′. The bay is bounded by two peninsulas which form the southeasternmost part of the mainland of Papua-New Guinea, and covers an area of approximately 2000 sq km (*see* Fig. 1).

During the beginning of 1968, the Marine Geology Group of the Bureau of Mineral Resources spent a total of five days in the area collecting samples and running a total of seven sparker traverses (*see* Fig. 8). The chartered survey vessel, the *Kos II,* is an ex-whale chaser, a steel ship of 125 feet overall length. It was built in 1929 and is powered by a triple expansion steam engine driving a single screw.

Milne Bay is an area of particular interest to marine geologists, sedimentologists, and geochemists. It forms part of a region which was and still is subject to much tectonic activity. As a result of this tectonic activity, the relief on the mainland of Papua-New Guinea is extremely high, while the adjacent ocean basins are deep with very steep-sided slopes. The continental shelf around Papua-New Guinea is either completely absent or in the very early stages of formation.

The purpose of this investigation is to evaluate the morphology and structural evolution of Milne Bay and its relationship within the tectonic setting of the circum-Pacific Zone of island arcs and ocean trenches by using continuous seismic profiles.

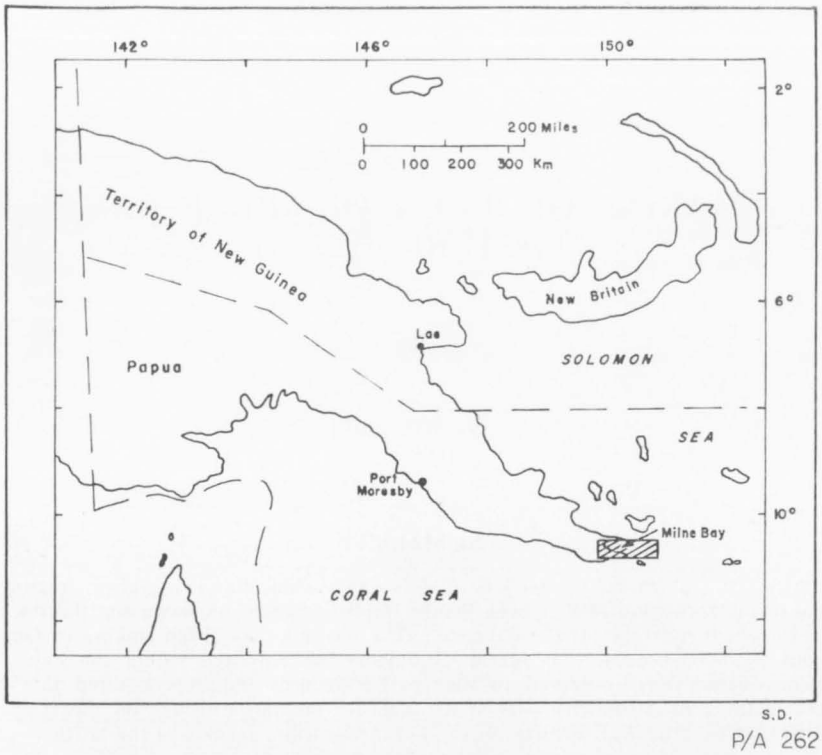


Figure 1. Locality map of the Milne Bay area, Eastern Papua.

Previous Work

Data on the marine geology of Milne Bay is scarce. The region to the south and east was the subject of reports by Krause (1965; 1967) which discussed the general tectonic framework of the northwestern Tasman Sea, the Coral Sea, and the South Solomon Sea. Previous regional geological studies on this region and gravity data collected by Milsom (in prep.) are discussed in later sections of this paper.

GEOLOGY AND PHYSICAL SETTING

Geology

Stanley (1923) gave the earliest account of the geology of the Papua area, and Thompson & Fisher (1965) discussed the geology of New Guinea with reference to the mineral deposits. Thompson (1967) has described the geological history of the region. Reconnaissance mapping by the Bureau of Mineral Resources in the last decade is the main source of information on the geology of the Milne Bay region (Davies, 1967; 1968; Davies et al., 1968). The geology of the islands off the southeastern peninsula is the subject of a further report by Smith & Pieters (1969).

Late Tertiary to Recent tectonic activity associated with the circum-Pacific zone of island arcs and ocean trenches has profoundly affected the area (Weeks, 1959; Glaessner, 1950). A number of structural provinces (Fig. 2) have been

recognized in southeastern Papua-New Guinea (Thompson & Fisher, 1965), and these provinces are retained in the following summary of the regional geology with the exception of the Ophiolite province which is divided into the Papuan Ultramafic Belt and a basalt province, as suggested by Davies (1969).

In the eastern part of the Papua-New Guinea Mainland a belt of Cretaceous and possibly older metamorphic rocks form the sialic core called the Owen Stanley Metamorphic Belt (Davies, 1968). This sialic core is separated from younger submarine basic volcanics and pelagic sediments by a discontinuous band of ultramafic rocks called the Papuan Ultramafic Belt. The Papuan Ultramafic Belt is separated from the sialic core by the Owen Stanley Fault. The Cape Vogel Basin is a structurally depressed topographically low-lying coastal zone, containing a thick succession of Miocene and Pliocene rocks (Fig. 2).

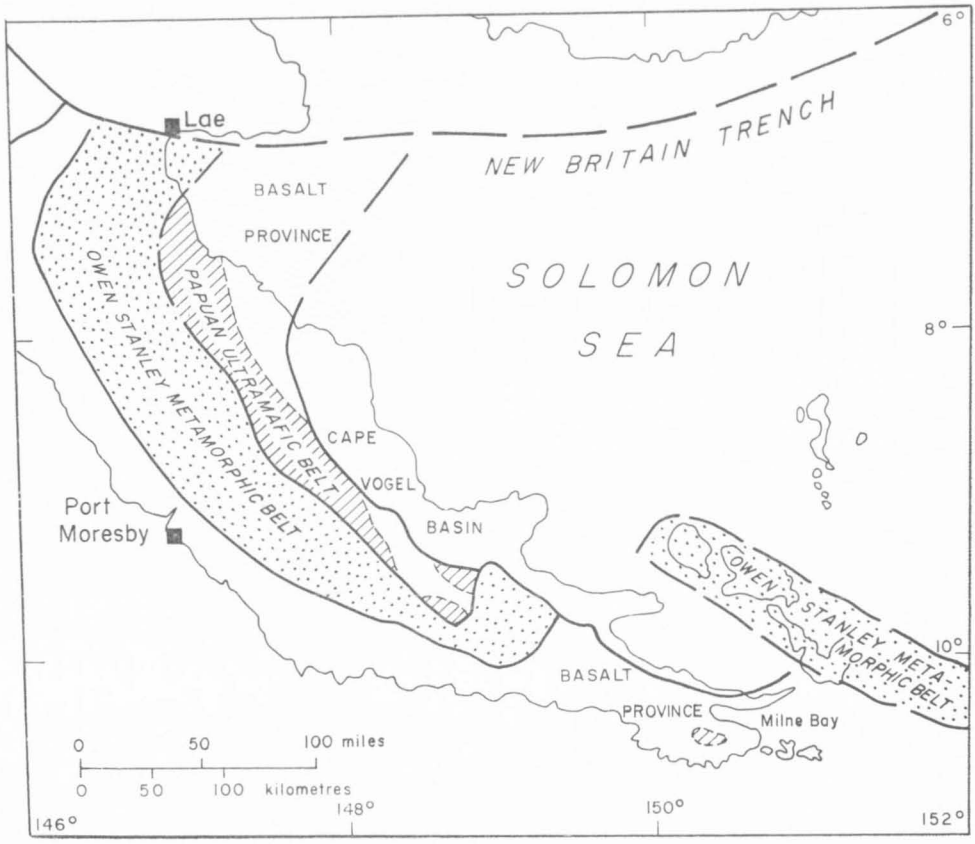


Figure 2. Principal structural units in Southeastern Papua-New Guinea. Modified after Thompson & Fisher (1965).

In the Upper Cretaceous basaltic pillow lavas were extruded, and up to 1000 m of probably deep-water limestone was deposited. Compression from the east during Eocene times caused the oceanic crust and the upper mantle to be thrust over the sialic core of Papua (Davies, 1967; *see* Fig. 3). Subsequent

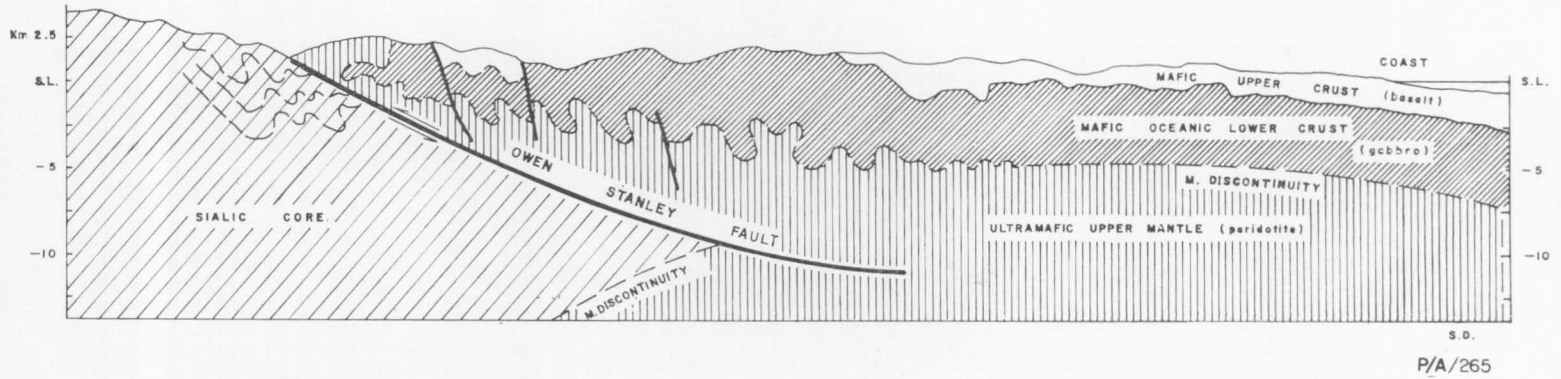


Figure 3. Collision of upper mantle with sialic core result ing in the Papuan Ultramafic Belt. After Davies (1967).

removal of this thrust sheet by erosion and gravity sliding took place, together with the development of a pile of basalt lavas and limestone on the sea floor of the Milne Bay area.

A period of quiescence ensued during Oligocene times, with little sedimentation or volcanism taking place. The upper Oligocene-lower Miocene was a period of renewed seafloor volcanic activity over a wide area. In the middle Miocene orogenic movements began which are still continuing today. Spectacular movements in a vertical sense and also strike-slip faulting in a left lateral sense occurred as a result of this orogeny. The direction of faults in the Papua-New Guinea Mainland is westerly to northwesterly. However, a markedly different trend in the structural pattern is found on the D'Entrecasteaux Islands to the north of Milne Bay—not only is the structural pattern different, but the geology of these islands also shows little similarity to the rocks around Milne Bay. Low-grade Cretaceous schists, metasediments, granite, and ultramafics are overlain by Pleistocene to Recent volcanic rocks. The rocks on these islands are believed to form part of the Owen Stanley Metamorphic Belt because of their similar lithology (Thompson & Fisher, 1965). The trend of many of the faults on the D'Entrecasteaux Islands is north-northeast. This direction is also maintained by an anticlinal fold axis on the southern part of Normanby Island (Fig. 4).

The structural geology in the region of Milne Bay is thus of interest because it is in line with the northwest-trending Owen Stanley Fault lineament. The Owen Stanley Fault may be continuous with the Pocklington Fault (Krause, 1967) which is a bathymetric feature and may be traced from the Louisiade Archipelago past Pocklington Reef to Guadalcanal. Furthermore, to the north of Milne Bay on the D'Entrecasteaux Islands faults and other structural trends are almost at right angles to the regional trend (*see* Fig. 5).

Geophysical Data

Results of a regional gravity survey of Eastern Papua by the Bureau of Mineral Resources show some features which are significant to this study (Milsom, in prep.; *see* Fig. 6). South of Milne Bay around the Ulo Ulo area a gravity high occurs, probably due to some subsurface feature such as an ultramafic body. Another gravity high occurs on the northern side of Milne Bay associated with the East Cape Gabbro. Directly eastward opposite the bay a gravity low occurs over Dawson Island. It is likely that this low extends into Milne Bay itself (Milsom, in prep.). The configuration of this gravity pattern suggests some movement of the bay relative to the land, probably a submergence of the bay floor in this region.

Topography and Coastal Geomorphology

The effective drainage area of the rivers draining into Milne Bay is part of the southern mountains and foothills of Papua. The mountains in the northwest are by far the highest, reaching elevations in excess of 1500 m, while the hills near Milne Bay are between 500 and 1000 m high. The drainage area covers about 30,000 sq. km. Three major rivers, the Maiwara, the Gumini, and the Dawa Dawa, carry most of the run-off of the area into Milne Bay. Small coastal rivers about 10 km long occur on the East Cape Peninsula and the southern margin of the bay.

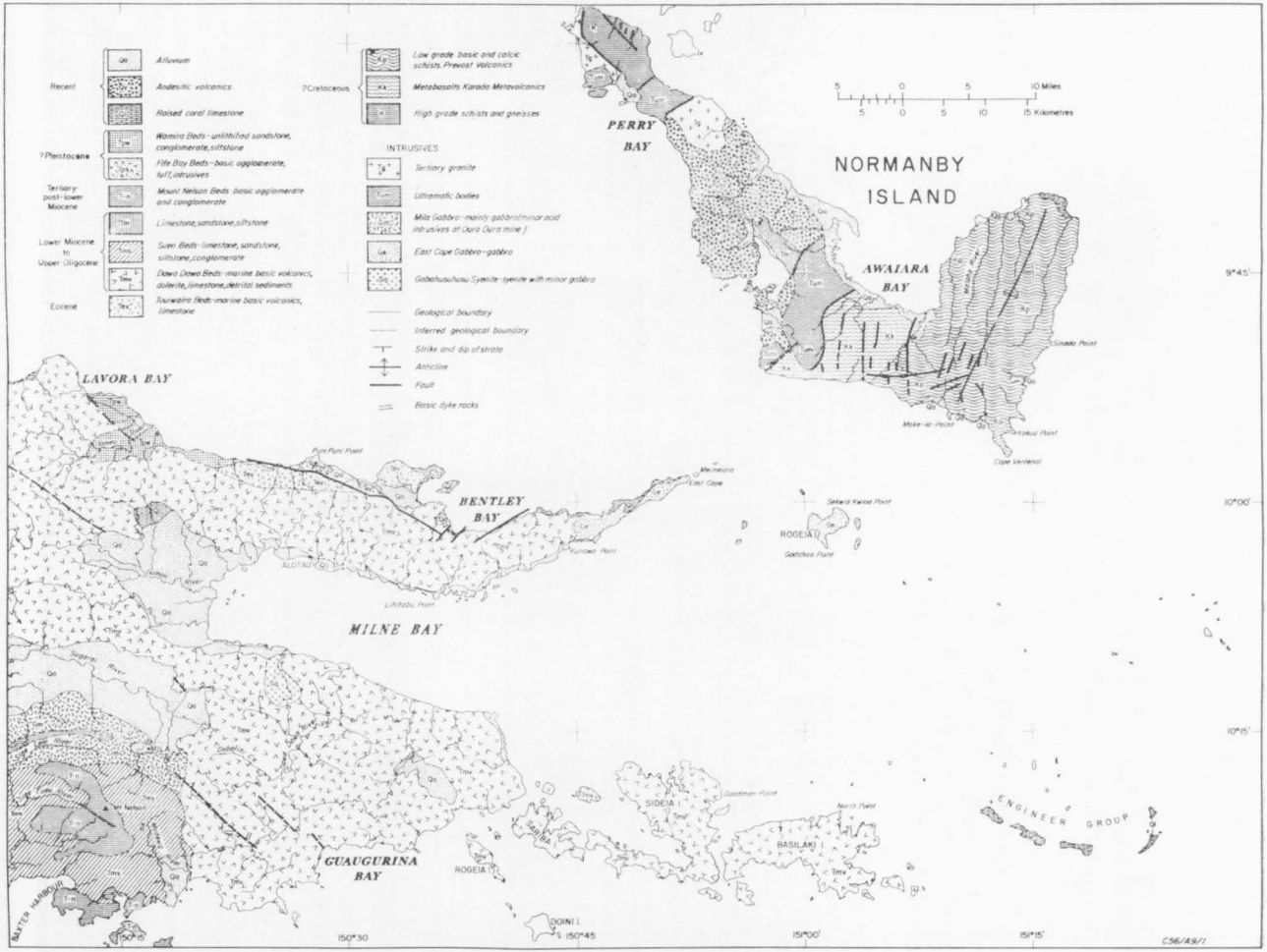


Figure 4. Geology of the Milne Bay area.

The southern coastline of Milne Bay is remarkably straight while the northern coastline is more indented. The western coastline shows convexities due to the building out of deltas at the river mouths. Swampy foreshores are found on the northwestern margin of the bay.

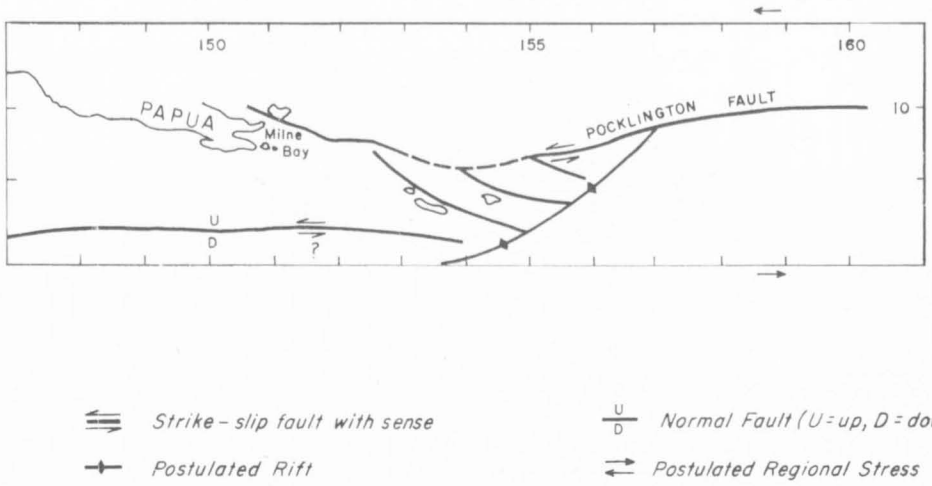


Figure 5. Position of the Pocklington Fault, as shown by Krause (1967).

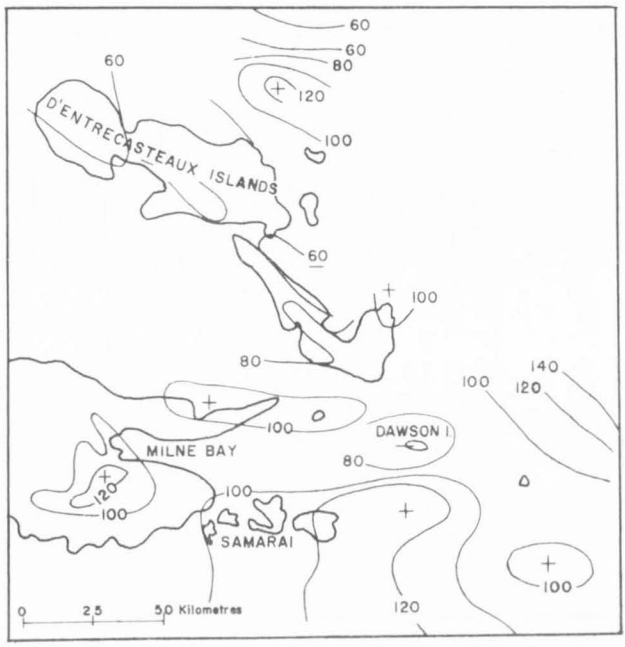


Fig. 6. Preliminary gravity map of the Milne Bay area. Data from Milsom (in prep.). Gravity highs on northern and southern margin of Milne Bay with a low near Dawson Island in line with the trend of Milne Bay.

The islands off the southern peninsula also have indented irregular margins with coral reefs surrounding most of them. These islands reach elevations of 200 to 530 m, and have swamps on their foreshores.

Some small islands with coral reefs surrounding them occur on the northeastern margin of the bay. Nuakata, the largest of these, reaches an elevation of 327 m and shows an indented margin with fringing coral reefs.

Climate

Milne Bay lies within the area affected by the southeast trade winds and the northwest monsoons. The southeast trade winds blow between May and October —they start in March when they blow intermittently, and by July and September they are steady and reach a wind force of 5 to 6 for several days. The southeast trades blow between the latitudes of 5° North and 5° South. Heavy seas in Milne Bay are very rare because most of Milne Bay is protected from the high seas by outlying islands and reefs.

From October to April the northwest monsoons often bring squalls and heavy rain in the open seas but Milne Bay is protected from the worst of these. Wind speeds in the Milne Bay area are between 3 and 4 knots for most of the year.

The climate in Papua-New Guinea is humid tropical. Temperatures for most of the year range between 65° and 95°F. Although rainfall in the Milne Bay area is less than that for most parts of Papua-New Guinea, it is very high compared with other parts of the world. The average annual rainfall is about 108 inches, as compared with up to 200 inches for some other parts of Papua-New Guinea. Because of its position, Milne Bay, which is surrounded by mountains in the northwest, receives most of its rainfall during the early part of the southeast trade winds season. The monthly rainfall at Samarai (10°37′S, 150°40′E), given in centimetres, is as follows (data from Pacific Islands Pilot, 1956):

January	17.8	July	20.6
February	19.8	August	21.8
March	25.4	September	25.6
April	24.9	October	22.0
May	30.5	November	21.3
June	28.7	December	15.5

Oceanography

There is little information available on the oceanographic conditions in Milne Bay, and most of it is in the various coast pilot volumes. The Pacific Islands Pilot (1956) discusses the currents in the narrow straits leading into the bay. China Strait in the south of Milne Bay has a current of 6 knots flowing through its narrowest part. This current diminishes to 2 or 3 knots in the wider parts of China Strait. Raven Channel, which connects Milne Bay with Goschen Strait and Goodenough Bay, has a current of about 5 knots flowing through it. A fairly weak current of about 2 knots is reported at the easternmost extremity of the bay. However, generally speaking, tidal effects are small since the difference between low and high tides in this region is only slight. The maximum difference in the height of tides is 2.7 m, while the average is 1.5 m (Admiralty Tide Tables, 1969).

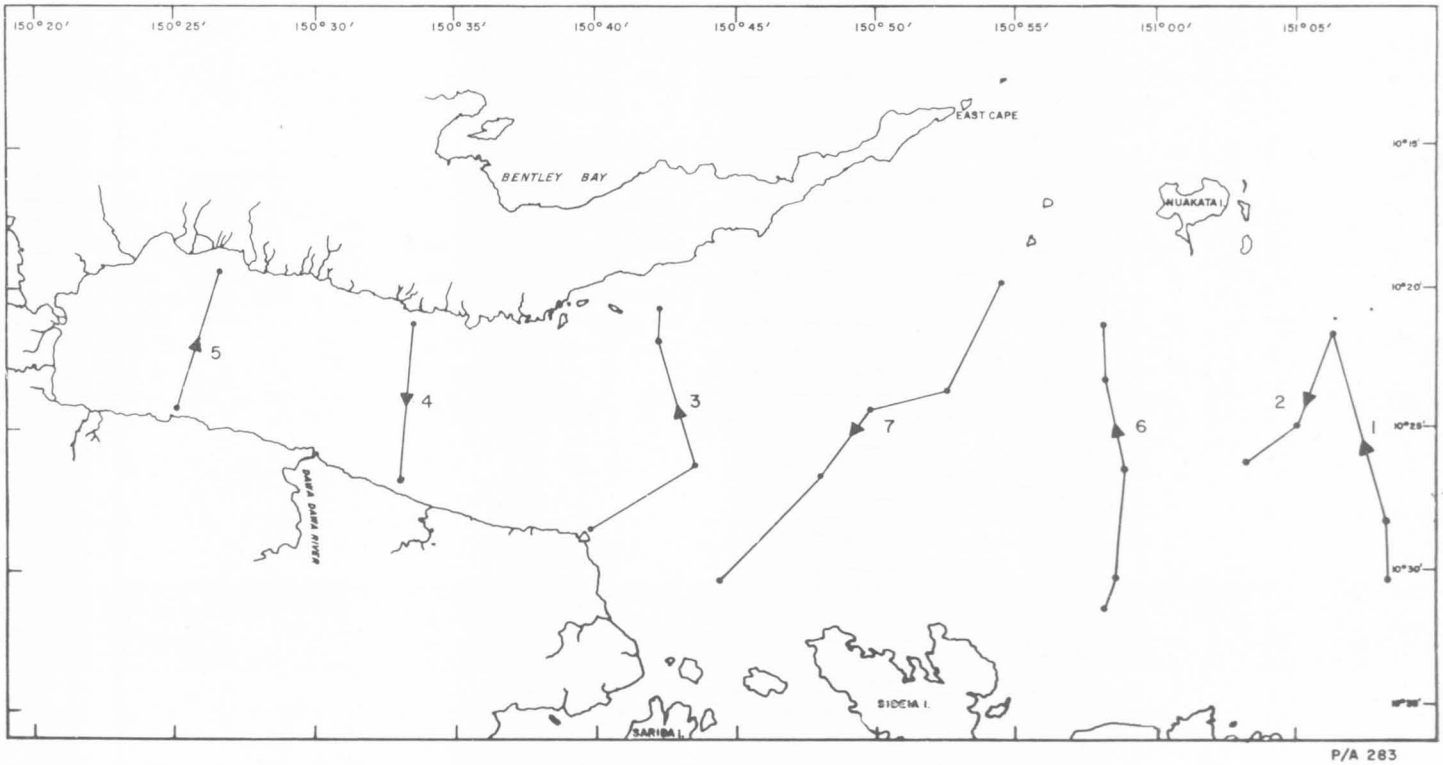


Figure 7. Sparker traverses in Milne Bay. Direction of traverse shown by arrow.

During heavy rainfalls large mountain torrents are reported to flow into the bay. The Pacific Islands Pilot (1956) mentions turbid water for a considerable distance from shore during these heavy rainfall periods. Waves in Milne Bay have small amplitude and small periods due to their small fetch, having mostly been created within the bay itself. No sufficiently large opening to the ocean is present to cause long period swells.

Bathymetry

The regional bathymetry of the South Solomon Sea is shown in Figure 7. Krause (1967) has described the bathymetry and structure of this area. Woodlark Island rests on Woodlark Ridge and to the south of it is a deep basin, the Woodlark Basin. This basin has an extremely irregular floor which is cut into a chaotic arrangement of hills, ridges, and irregular depressions about 3000 m deep. These hills have a general east-west alignment with escarpments cutting through the region in various directions.

To the south of the Woodlark Basin lies the Louisiade Archipelago which rests on the eastward extension of the Papua Peninsula. This extension of the Papuan Peninsula becomes a region of parallel structural ridges, troughs, and closed basins of which Milne Bay is one. Tagula Island, Rossel Island, and Pocklington Reef rest on a series of *en echelon* ridges (Krause, 1967).

South of the Louisiade Archipelago and the Pocklington Ridge the seafloor slopes down to the deep water of the Pocklington Trough which forms an extension of the Coral Sea Basin. The Pocklington Ridge is fault-bounded in the north and has a left lateral sense. The Pocklington Fault extends north of the Louisiade Archipelago up to the region of Milne Bay (Krause, 1967). North of Milne Bay another closed basin with a depth in excess of 1000 m occurs, bounded on the east by the D'Entrecasteaux Ridge. The D'Entrecasteaux Ridge joins in the north with the Trobriand Platform (von der Borch, 1970) and southward with the southern extension of the Papuan Peninsula. On the northern margin of Goodenough Bay, Cape Vogel is connected to the D'Entrecasteaux Ridge by a sill between Goodenough Bay and Collingwood Bay. The southern margin of this ridge slopes very steeply down to 1000 m and is probably fault-controlled. This fault may define the locus of dislocation which causes the offset of the continuation of the Owen Stanley Metamorphic Belt.

Milne Bay is a restricted basin locked in on the west by the Papuan Peninsula and on the east by coral reefs and islands. A sill at a depth of 300 m forms the connexion with the deeper ocean to the north and south (Pl. 3). Near land, on the west side, several rivers enter Milne Bay after passing through a marginal swampy delta.

On the western edge of the bay a shallow gently sloping irregular shelf occurs. The edge of this shelf occurs at about 80 m. Depth increases rapidly at the edge of this narrow shelf and at the bay margin in the north and south. Steep slopes with gradients as high as 9 in 10 occur between 80 and 250 m depth. Another break in slope occurs at about 250 m after which the gradient decreases to about 1 in 10. This slope continues down to 500 m at which point the bottom of the bay is encountered. The bottom is very flat.

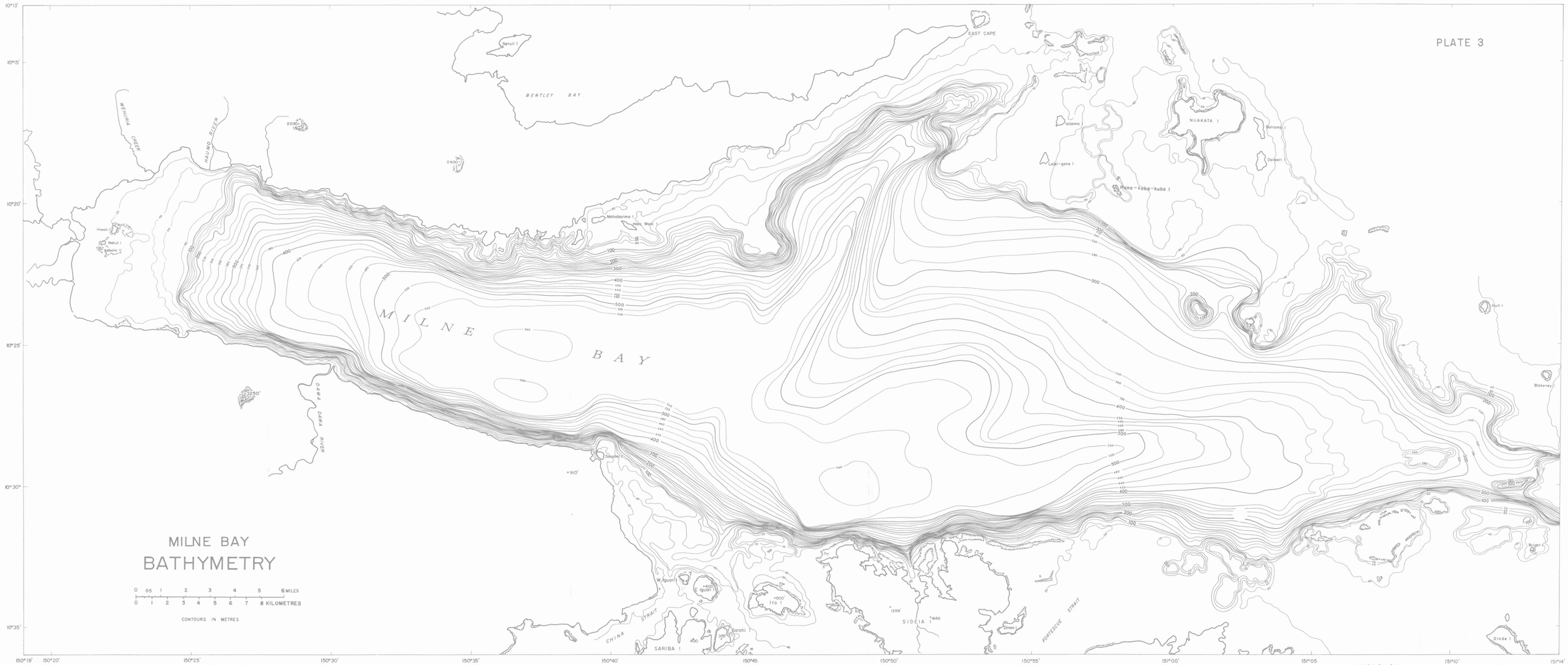


Plate 3. Bathymetry of Milne Bay, Eastern Papua.

In the northeastern part of the bay, south of Nuakata Island, the situation is slightly different. Here the initial very steep slope between 80 and 250 m is present after the edge of the rudimentary shelf is encountered. However, farther south of this steep slope a gentler increase in depth takes place. The slope in this part of the bay is about 1 in 100, and it extends for about 18 km until a channel is reached after which the depth decreases rapidly on the southern edge of the bay.

On the eastern side of Milne Bay there is a shoal which supports a few small islands. The southern end of this shoal is deeper and a channel with a maximum depth of 300 m is the connexion with other restricted basins on the submarine ridge off the Papuan Peninsula. To the south a number of shallow (20-m) channels such as China Strait and Fortescue Strait connect Milne Bay with the Coral Sea basin. Between East Cape and Nuakata Island a number of shallow connexions communicate with Goodenough Bay.

In the northern part of the bay a narrow steep-sided trough extends from the middle of the basin northeastwards parallel to East Cape peninsula. The bathymetric contours indicate a feature resembling a submarine canyon, but although no seismic data are available, it seems unlikely that this trough has been formed by erosion and a structural origin is postulated. The trough runs at right angles to other structural trends in the bay and it is probably connected with the structural features seen on Normanby Island to the north of East Cape where faults also trend northeast-southwest.

Milne Bay is the result of downfaulting of the bay floor in the form of a graben. The southern margin of the bay is obviously fault-controlled, as evidenced by the extremely steep slope. In the north a similar situation is present although the margin is slightly indented due to erosion by short rivers subsequent to faulting.

SPARKER TRAVERSES

Seven sparker traverses were run across Milne Bay (*see* Fig. 7). The sparker traverses were obtained by a continuous profiling system, comprising a 3-electrode sparkarray and a 1000 watt-second power source combined with a 7-element hydrophone and an Ocean Sonics GDR-T recorder. The recorder uses 19-inch wet paper and during these traverses was programmed at one sweep per second. This sweep speed gives a horizontal scale line interval at 36.7 m (20 fathoms) in water. Traverses were run at a speed 4.5 to 5 knots.

Plates 4-9 give photographic reproductions of the traverses, accompanied by line-drawn interpretations. The vertical scale on the line drawings are in terms of two-way travel time quoted in seconds. As a guide to depths it may be noted that the signal travels with a velocity of approximately 1.5 km/sec in water and about 1.6 km/sec in sediments. Unless otherwise stated the attitudes of reflectors mentioned refer to the apparent attitude along the line of section.

The term 'basement' is used to indicate an irregular strong reflector below which no obvious sedimentary bedding can be discerned. Note that due to bubble pulses all horizons are shown by a series of three or four lines on the original sparker records (Sargent, 1969). The sparker records are described from east to west.

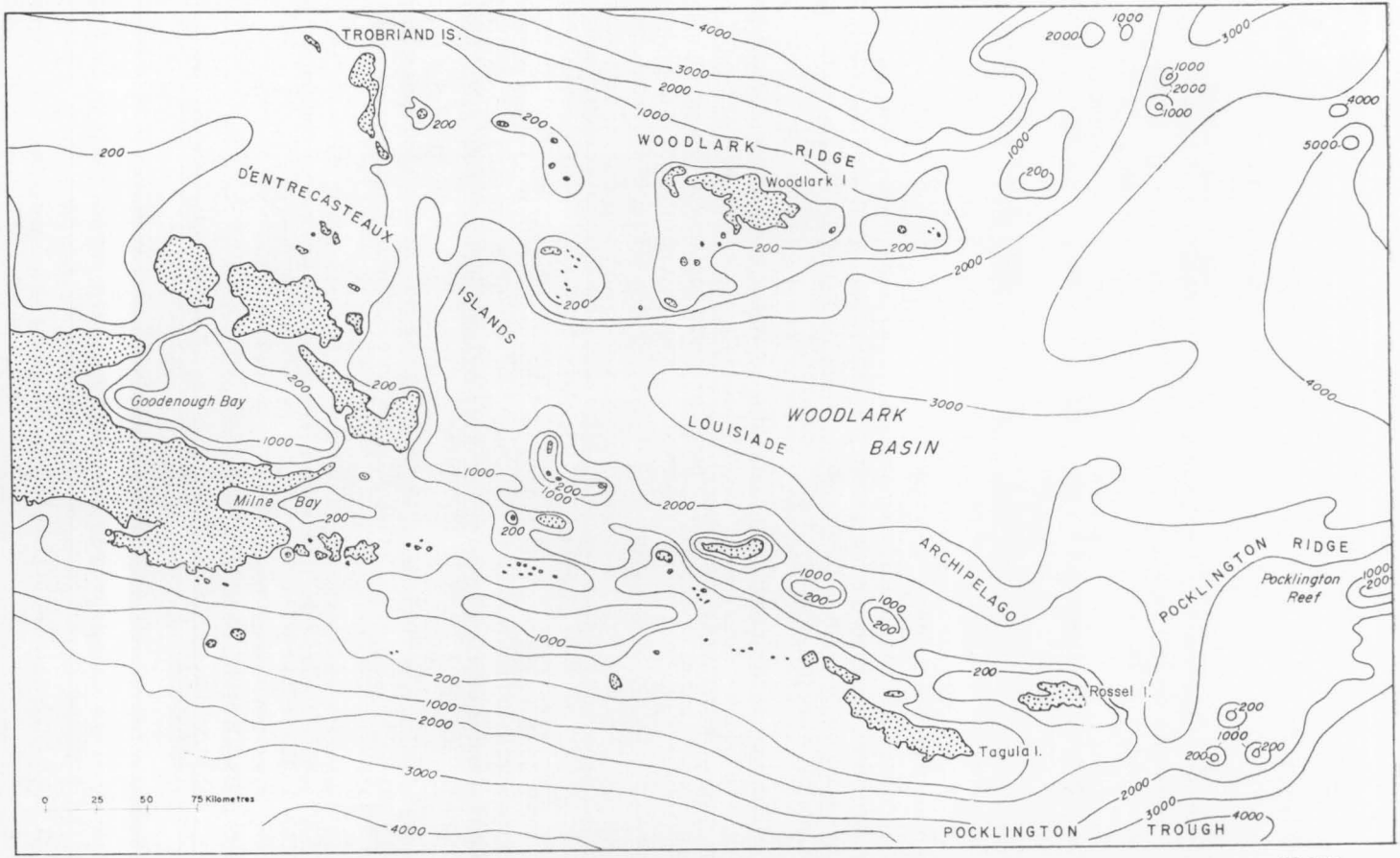


Figure 8. Regional bathymetry of the South Solomon Sea. Contours in metres.

TRAVERSE 1

The traverse runs from south to north in the easternmost part of the bay and represents an almost straight section between Shortland Reef and Cocked Hat Island. The quality of this record is excellent showing many prominent subbottom features (Pl. 4).

The floor of the bay can be seen at 1. The start of the traverse shows a shallow irregular bottom with coral reef development at 2 in a depth of 40 m. Little penetration at this point could be due either to basement rock or the presence of organic reef structures over this shallow bottom. At 3 the bottom has an almost vertical slope which becomes less steep at 150 m and gradually flattens out into a deep channel at 340 m.

At 13, two acoustically impenetrable hummocks appear which are due to basement rock forming the shoals around Nuakata Island. Another basement high crops out at 17. In between these basement highs there are subbottom strata as evidenced by reflecting horizons at 10 and 11.

A steep vertical slope at 18 marks the northern edge of the deeper basin and at 14 coral reef building can be seen on the edge of a shallow shelf which is underlain by basement rock.

A strong reflector at 6 marks an unconformity which is well displayed in this and later profiles. Onlap of the overlying sediments is evident at 12 and underlying reflectors are indicated at 7. The unconformity probably represents a low sea level stand during the Pleistocene. However, since the maximum depth of the unconformity is 425 m some submergence of the bay must have taken place to account for this depth. Maximum eustatic sealevel lowering is in the order of 120 to 125 m (Curray, 1961). The amount of subsidence in this section of the bay must thus be in the region of 300 m.

Conformity at 19 indicates the presence of a channel at the time when the unconformity originated.

A very faint unconformity below the one described occurs at 8 and since no penetration (9) can be observed below this reflecting horizon it is suggested that this is basement rock.

A water-bottom reflection occurs at 16.

TRAVERSE 2

This is a short traverse southwest. The traverse begins in shallow water, the seafloor being at 1 (Pl. 5). At the start the bottom is irregular (2) due to growth of coral reef on this shallow shelf. Little penetration below this shelf indicates that it is underlain by basement rock. The edge of the shelf is marked by a hummock (3) which is due to reef building.

Terraces occur around the indented margin of this shelf as can be seen at 4, and this feature is repeated on both sides of the submarine headland at A. Slopes at the end of this shelf are steep (5) and may be fault controlled. Sediments occupy the embayments (7) of the indented margin. Further south away from the shelf in the middle of this traverse the seafloor slopes gradually downward. Recent marine sediments occur below the seafloor at 8 and 10.

A prominent reflecting horizon at 12 has been interpreted as the continuation of the unconformity seen in Traverse 1 just to the east of this traverse. Below this unconformity further penetration shows up more sediments.

A notch in the seafloor at 11 and the bending of reflecting horizons below is due to some recent normal faulting. The possible throw of this fault is about 30 m. A water-bottom multiple reflection can be seen at 13.

Traverse 6

The traverse extends from south to north about 12 km to the west of Traverse 1. The seafloor is at 1 (Pl. 6). The start of the traverse is in shallow water with a seafloor showing irregular outlines. A coral reef on the edge of the shelf at 2, a small channel at 3, and a terrace at 4 are followed by a steady slope at 5 which is fault controlled. The slope of the floor of the bay decreases and continues to do so smoothly until a steep slope is encountered at 8 which changes to a gradual upward slope to the end of the traverse.

Conformable reflecting horizons up to a thickness of 0.2 seconds ($\pm$ 340 m) occur below the bottom at 7. These sediments border the probable basement rocks underlying the narrow shelf at the start of the traverse. At 10 below a notch (8), at the bottom of the steeply rising floor, the reflecting horizons become parabolic and are discontinuous for some distance due to a fault (9). On the other side of the fault a strong reflector at 11, 12, and 14 represents an unconformity. This unconformity may be followed for most of the traverse record, although it becomes less obvious in the latter part. However, a change in the reflecting behaviour of the horizons at 14 marks the presence of this unconformity in that part of the record.

Irregular relief at 12 indicates erosional effects during a time when this surface was subjected to subaerial erosion. This unconformity is correlated with the one visible in records of Traverses 1, 2, and 7, and indicates the indirect effects of glaciation during the late Pleistocene. Above the unconformity smooth continuous and closely spaced reflecting horizons represent the Recent sediments in this part of the bay. A water-bottom reflecting horizon is indicated at 15.

Traverse 7

Traverse 7 extends from just south of the Obstruction Islands to the southern peninsula of the mainland. Excellent penetration on this record shows very clearly the relations of the subbottom strata in the middle of Milne Bay (Pl. 7).

The bottom of the bay (1) shows a basin-shaped depression. A marked unconformity is observed at 2. This unconformity is of erosional origin and probably corresponds with the last low sealevel stand in the Pleistocene. The maximum depth of this unconformity is at 13 and is in the order of 0.6 seconds. South of 13 the record no longer contains this unconformity and it probably implies the presence of conformable beds south of 13. This maximum depth of 985 m is very much lower than the maximum low sealevel stand, which is reported to be about 125 m (Curray, 1961; 1965). Thus in this part of the bay submergence must have been in the region of 760 m. This is much more than postulated for the eastern part of Milne Bay and it is suggested that submergence here was at its

highest due to a fault connected with the formation of the trough south of the East Cape Peninsula.

Below the unconformity further penetration shows the presence of slightly distorted bedding (8) and some of these reflecting horizons are truncated near the unconformity surface (9).

Since Pleistocene times sinking accompanied by sedimentation has gone on. Continuous horizontal reflecting horizons present at (3) are Recent sediments. A thickness of 0.50 second is present in some of this section (13). Thus not only is the submergence greatest in this part of the bay, but also the locus of sedimentation is here; this thick succession of Recent deposits may represent a sediment fan at the mouth of the East Cape Canyon. Subsidence or eustatic change in sea level is also recorded in this traverse by onlapping of sediments at 6.

Small notches in the slope of the bottom (5) above these onlaps may indicate that subsidence of parts of the basin was different for different sections due to differential movement along faults. At 4 a small basin within the main basin can be discerned. Uniform closely spaced reflecting horizons indicate a well bedded sequence of sediments.

At the end of the section the bottom rises again towards China Strait. Discontinuous slightly wavy reflecting horizons occur at 10, and may indicate some slumping. Farther south at 11 well bedded sediments are encountered.

At 7 discontinuity and bending of the reflecting horizons has been interpreted as a result of faulting. The faults continue down into basement but do not extend to the top of the section, having been covered by later sedimentation.

At 12 a water-bottom multiple reflection occurs in this traverse.

Traverse 3

This traverse runs from the south, off Saraoni Island, to the north just east of the Killerton Islands. The quality of the record is poor but gross features are still discernible (Pl. 8). The bottom (1) shows undulations on a shallow narrow shelf (2, 4) probably due to presence of coral reefs. A very steep slope (3) occurs between 2 and 4. The floor of the bay at a depth of 525 m is remarkably flat, and it continues to be flat for 8 miles until the slope on the northern side of the bay is encountered.

Below the flat floor of the bay there is a succession of conformable horizontal reflecting horizons with a maximum thickness of 125 m. Basement rock occurs on the bottom of the steep slope (6), and undulating reflecting horizons occur also at the positions marked 6. These undulations are possibly due to slumping.

The upper slope at 7 is fairly uniform. Some slight penetration (9) seems to indicate some bedding below this slope. At 10 the edge of the shelf is reached again and the topography of the bottom is uneven.

A very indistinct horizon at 8 which is subparallel to the bottom slope at 7 occurs in the latter part of the record. This is possibly an unconformity related to those noted in Traverses 1, 2, 6, and 7.

TRAVERSE 4

This traverse starts in the northern part of the bay and runs south, covering the middle of the landlocked part of the bay. The bottom (1) descends steeply with irregularities until it flattens out at a depth of 480 m (Pl. 9). Irregular and wavy reflecting horizons indicate basement rock at 2. Slump structures occur at 3 and 4 on the steep slope of the bay's margin.

The central part of the traverse shows many distinct continuous and horizontal reflecting horizons underlying the flat bottom (6). Some onlapping occurs at 5 and a possible unconformity is indicated at 10. The structure at 5 may also be due to a type of deltaic prograding seen in transverse section.

At the end of the traverse near the southern margin of the bay a straight steep slope occurs which is obviously fault controlled. Some minor penetration below the bottom at 7 shows a fault.

Some irregular bedding can be seen on the upper part of this slope and under the narrow shelf (8). Water-bottom multiple reflections are observed at (9).

The maximum thickness of Recent sediments penetrated in this section is about 85 m.

TRAVERSE 5

This is the westernmost traverse in Milne Bay and covers the inner reaches in the shallow part of the bay. The traverse runs from south to north (Pl. 9).

An irregular bottom can be seen at 1 with fairly good penetration below showing very irregular reflecting horizons (3). At 2 little penetration is observed due to the presence of underlying basement rock or coral reef. Water-bottom multiple reflections are indicated by 4.

This traverse is on the edge of a prograding delta which is receiving sediments from the rivers to the west. The irregularity of the reflecting horizons is due to slumping of material down the outer slope of this delta.

CONCLUSIONS

Milne Bay is situated in a region which has been and still is tectonically very active. This bay originated as a result of faulting and is in the form of a graben. The bay itself has sunk deeper since the Pleistocene. The unconformity shown in the sparker records of Milne Bay is postulated to be of erosional origin and probably originated during the Pleistocene low sealevel stand. Curray (1961; 1965) postulates the low sealevel stand to be 18,000 years ago. Since that time the eustatic change in sea level has been a rise in the order of 125 m (Curray, 1961; 1965). From Figure 9 it may be seen that the maximum depth of the unconformity is about 900 m. Calculation of the amount of sinking since the Pleistocene results in a figure of 775 m.

Sedimentation within the bay must have been very rapid since the maximum thickness of sediment accumulated since the last low sealevel stand is about 450 m (*see* Fig. 10). This total thickness taken over a period of 18,000 years is an average of 2 cm per year. From isopachs and structure contours (Figs 9-11)

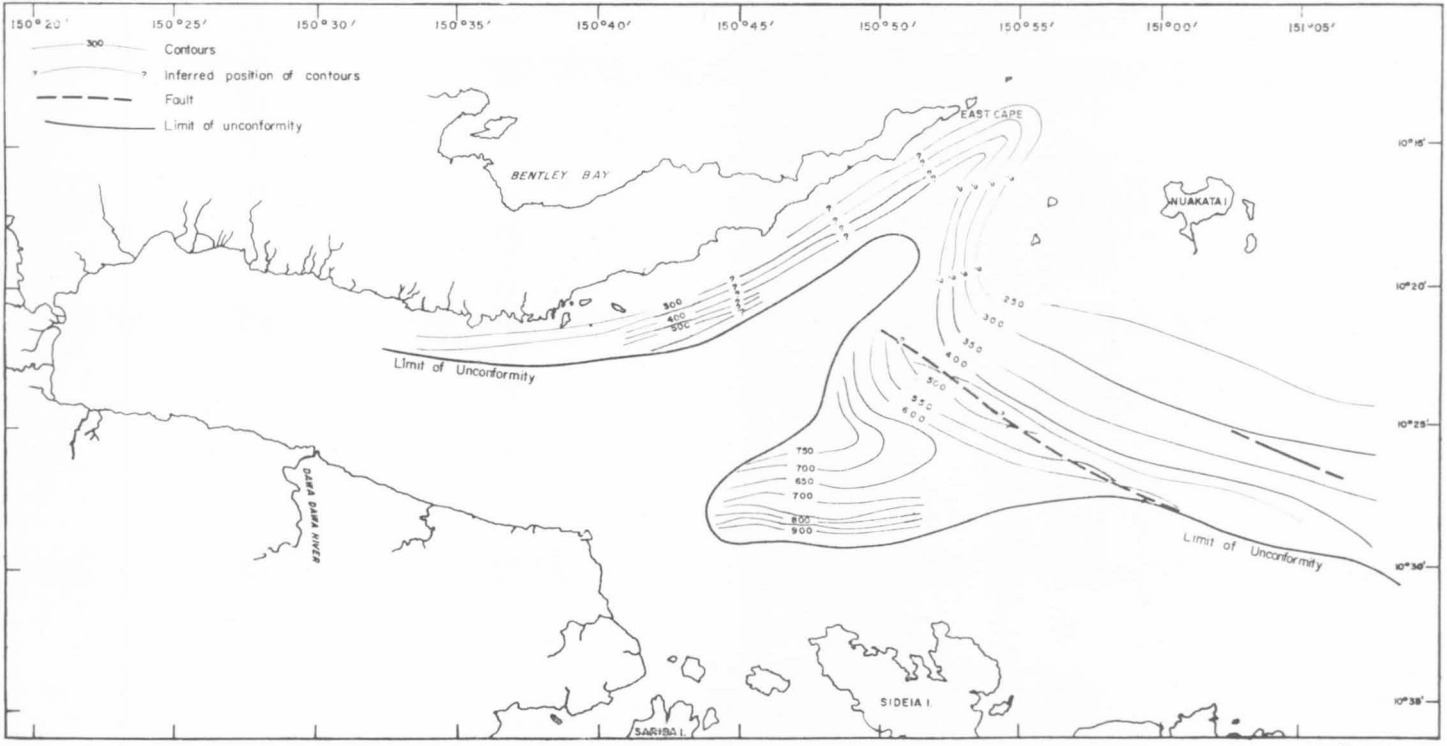


Figure 9. Structure contours on the Pleistocene? unconformity in Milne Bay. Contour interval 50 metres. Depth calculated on assumption that velocity of sound is approximately 1.5 km/sec in water and 1.7 km/sec in sediment.

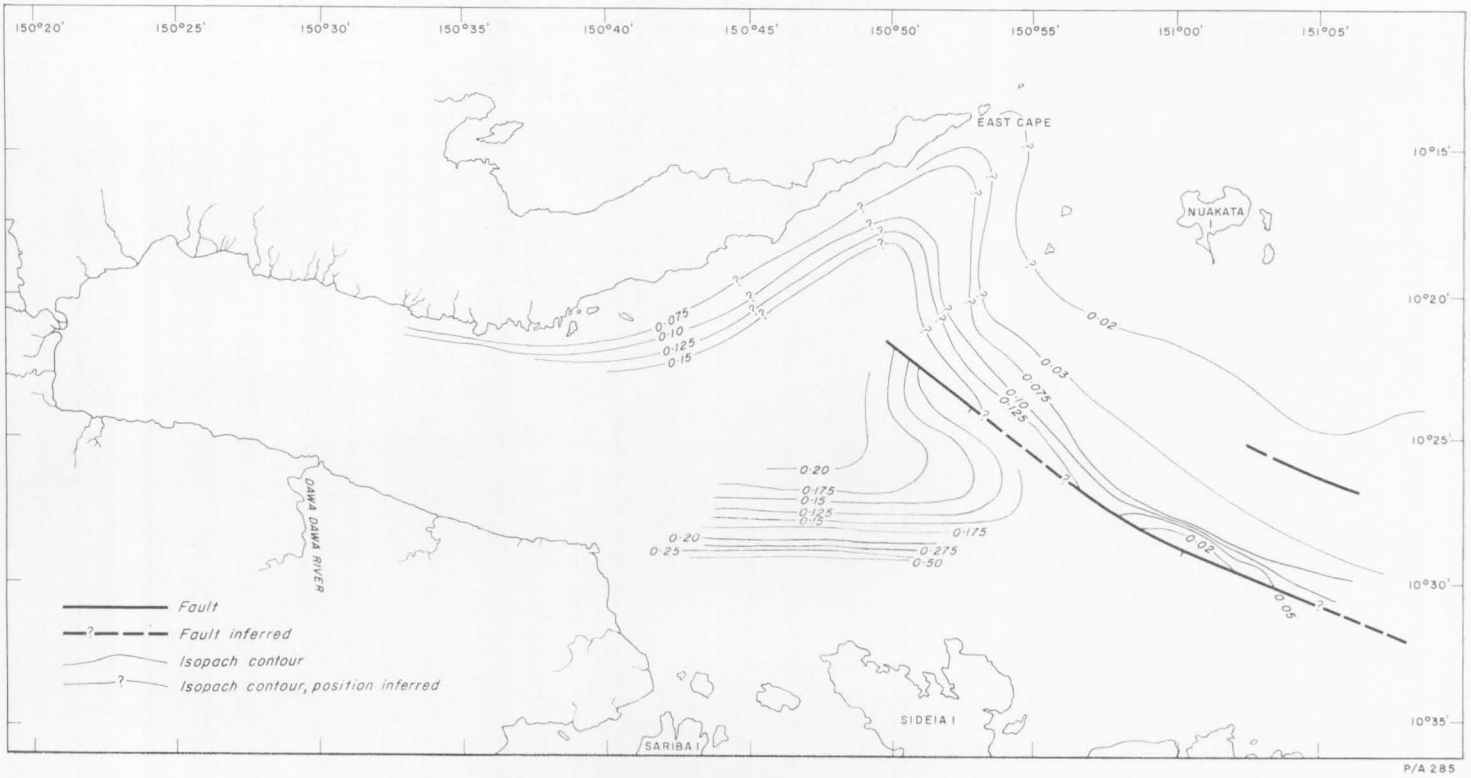


Figure 10. Isopachs of Recent sediments.

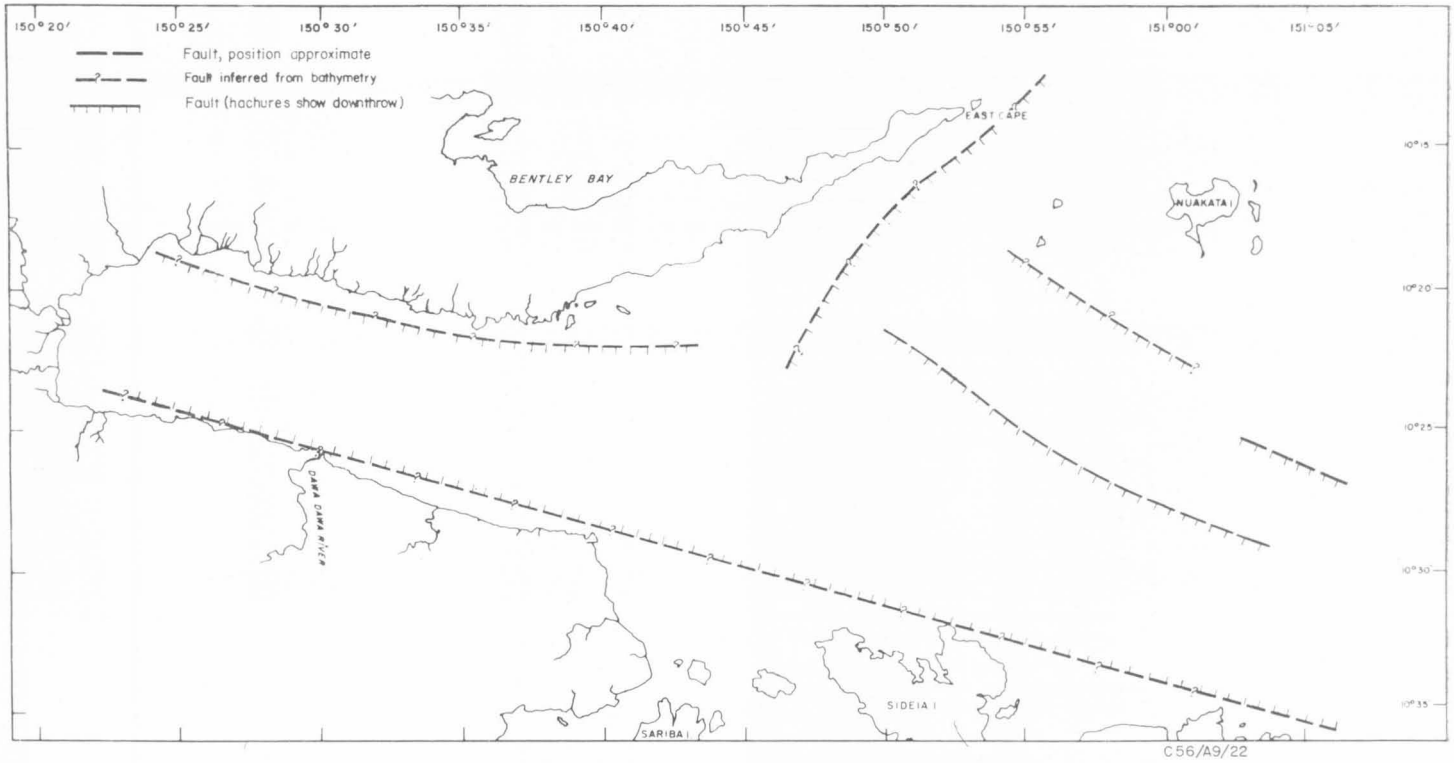


Figure 11. Structural geology of Milne Bay.

it may be seen that the locus of sedimentation is just north of the outlet of China Strait and at the mouth of the trough which runs parallel to the East Cape. This has been interpreted as a predepositional trough produced by faulting.

A structural interpretation of the bay is shown in Figure 11. Faults can be inferred from both the bathymetry and the sparker records. The west-northwest-trending faults controlling the margin of the bay are in line with the Owen Stanley fault lineament to the north. These west-northwest-trending faults are normal and movement on them has been vertical. This is similar to the post-lower Miocene movements on the Owen Stanley Fault. The northeast-trending fault-controlled trough off East Cape, on the other hand, may be genetically related to the northeast-trending structures on the D'Entrecasteaux Islands.

REFERENCES

ADMIRALTY TIDE TABLES, 1969. Vol. 3. Hydrographers of the Navy. London.

BRITISH ADMIRALTY, 1956—Pacific Islands Pilot, Vol. 1.

CURRAY, J. R., 1961—Late Quaternary sea level; a discussion. *Geol. Soc. Amer. Bull.*, 72, 1707-12.

CURRAY, J. R., 1965—Late Quaternary history, continental shelves of the United States. *in* WRIGHT JR., H. E., and FREY, D. G. (Editors), THE QUATERNARY OF THE UNITED STATES. Princeton Univ. Press, 723-35.

DAVIES, H. L., 1967—Milne Bay, Papua—geological reconnaissance. *Bur. Miner. Resour. Aust. Rec.* 1967/53 (Unpubl.).

DAVIES, H. L., 1968—The Papuan Utrabasic Belt. *Proc. 23rd Int. Geol. Congr.*, Prague.

DAVIES, H. L., 1969—Utramafics and ophiolites. *Bur. Miner. Resour. Aust. Rec.* 1969/47 (Unpubl.).

DAVIES, H. L., SMITH, I. E., CIFALI, G., and BELFORD, D. J., 1968—Eastern Papua geological reconnaissance. *Bur. Miner. Resour. Aust. Rec.* 1968/66 (Unpubl.).

GLAESSNER, M. F., 1950—Geotectonic position of New Guinea. *Amer. Assoc. Petrol. Geol. Bull.*, 34, 856-81.

KRAUSE, D. C., 1965—Submarine geology north of New Guinea. *Geol. Soc. Amer. Bull.*, 76, 27-42.

KRAUSE, D. C., 1967—Bathymetry and geologic structure of the Northwestern Tasman Sea-Coral Sea-South Solomon Sea area of the southwestern Pacific Ocean. *N.Z. Oceanog. Inst. Mem.*, 41, 46 pp.

MILSOM, J. S.—Gravity survey of Eastern Papua-N.G. *Bur. Miner. Resour. Aust. Rec.* (in prep.).

SARGENT, C. E. G., 1969—Further notes on the application of sonic techniques to submarine geological investigations, with special reference to continuous reflection seismic profiling. *9th Commonw. Min. Metall. Congr. Pap.* 28.

SMITH, I. E., and PIETERS, P. E., 1969—The geology of the Louisiade Archipelago, T.P.N.G. excluding Misima Island. *Bur. Miner. Resour. Aust. Rec.* 1969/93 (Unpubl.).

STANLEY, E. R., 1923—The geology of Papua. (*Australian Government Printer, Melbourne.*)

THOMPSON, J. E., 1967—A geological history of eastern New Guinea. *APEA J.*, 83-93.

THOMPSON, J. E., and FISHER, N. H., 1965—Mineral deposits of New Guinea and Papua, and their tectonic setting. *Proc. 8th Commonw. Min. Metall. Congr. Australia and New Zealand Pap.* 129, 115-47.

VON DER BORCH, C. C., 1970—Marine geology of the Huon Gulf Region, New Guinea. *Bur. Miner. Resour. Aust. Bull.* 127 (in press).

WEEKS, L. G., 1959—Geologic architecture of circum-Pacific. *Amer. Assoc. Petrol. Geol. Bull.* 43, 350-80.

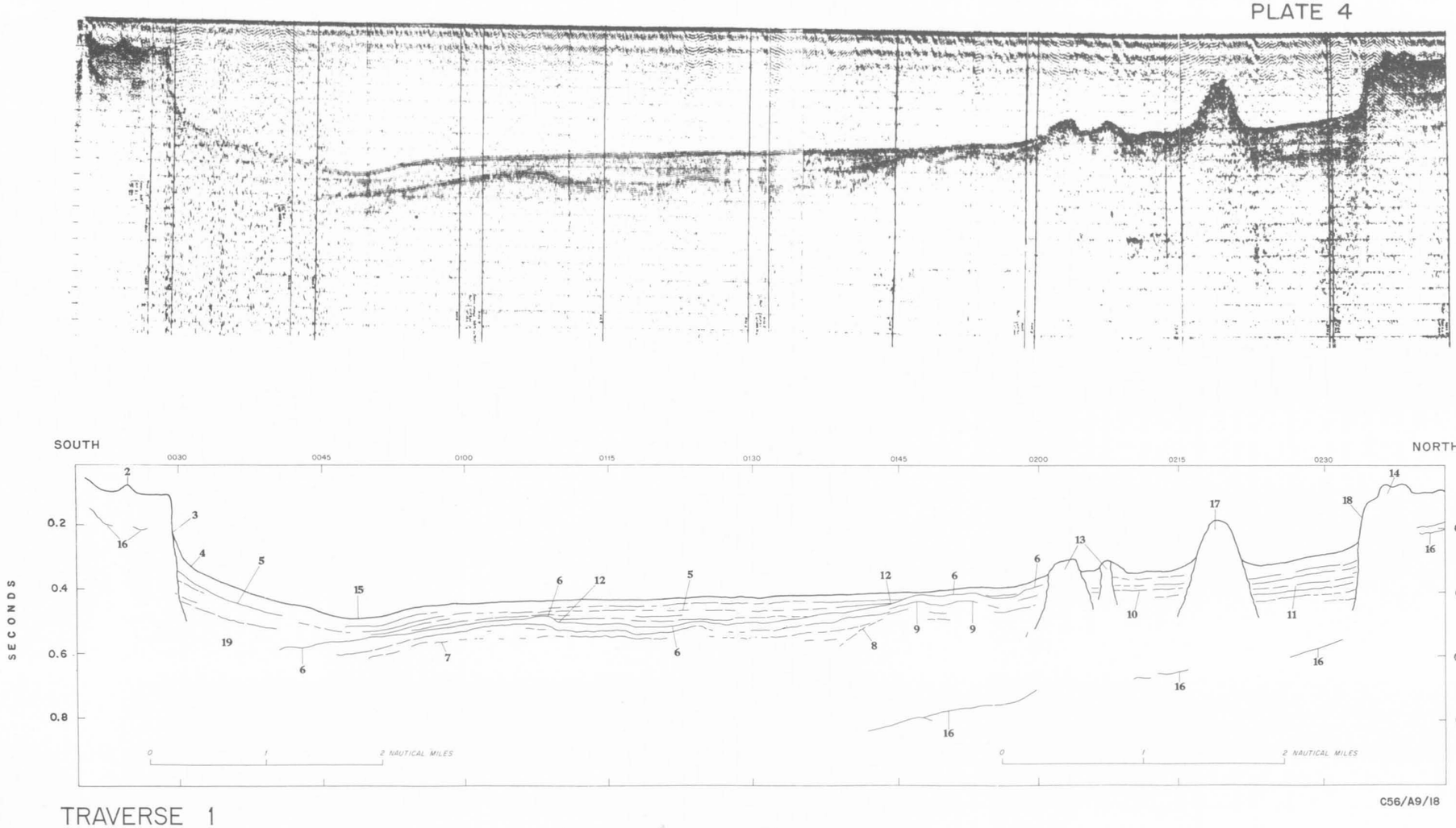
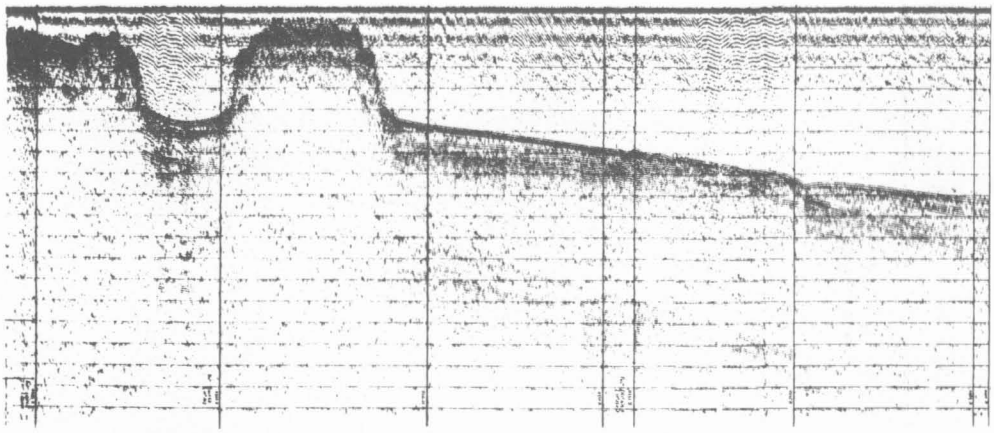
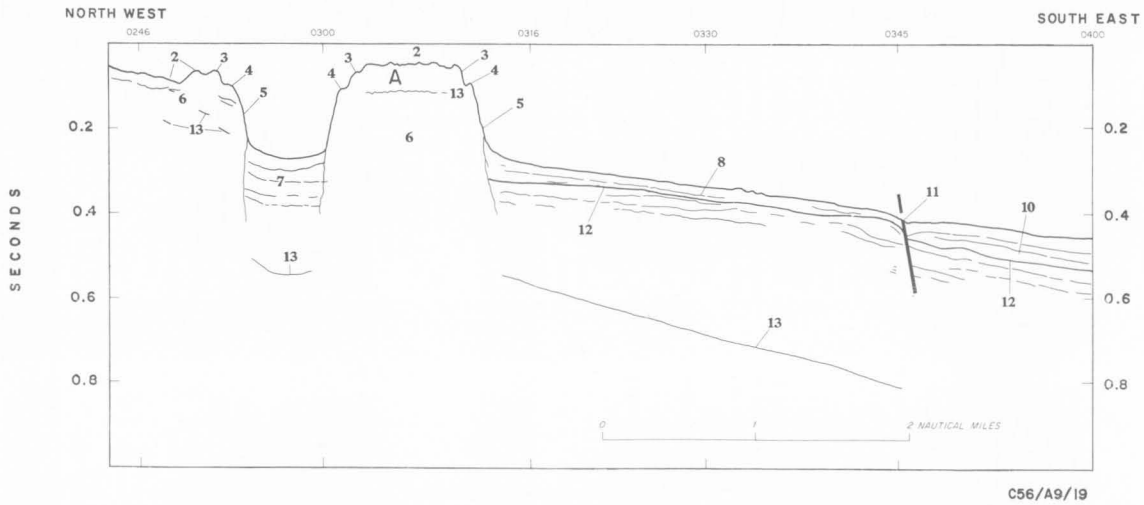


Plate 4. Sparker record and interpretation of Traverse 1.

PLATE 5

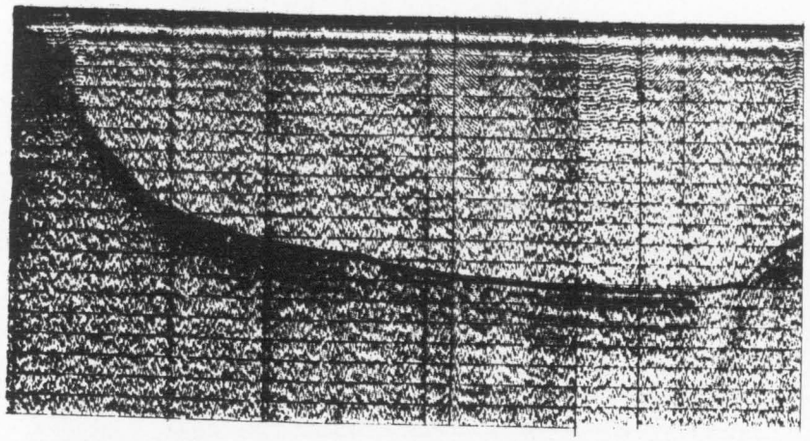


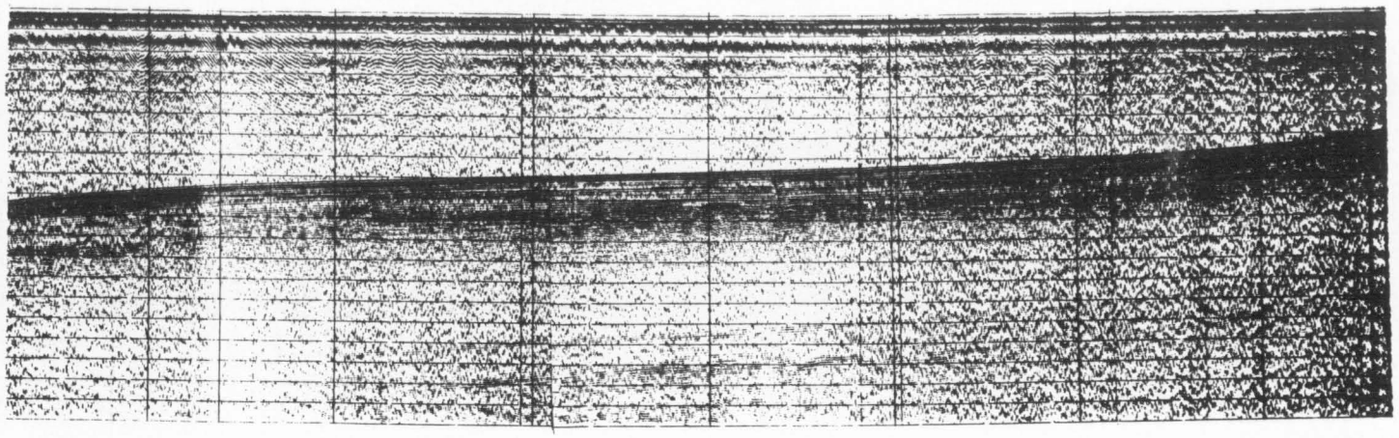


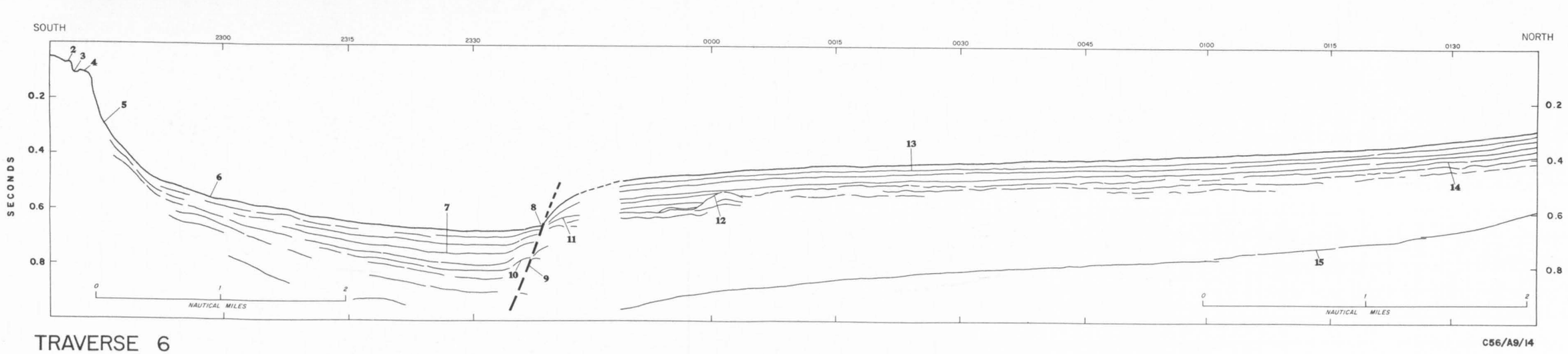
TRAVERSE 2

Plate 5. Sparker record and interpretation of Traverse 2.

PLATE 6





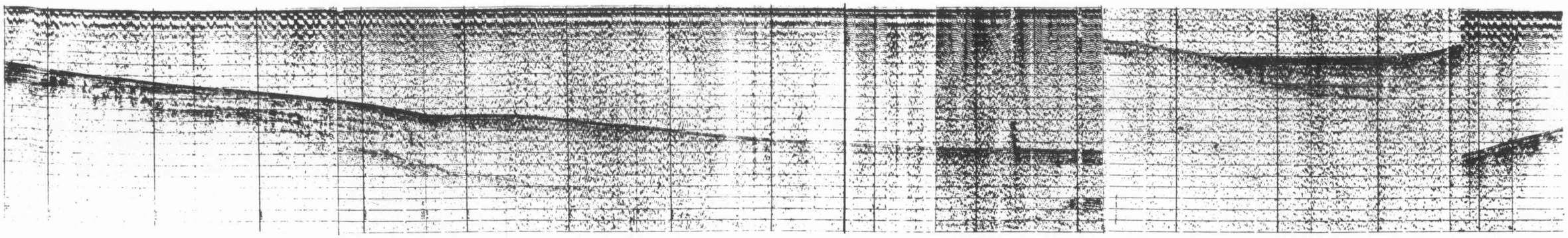


TRAVERSE 6

C56/A9/14

Plate 6. Sparker record and interpretation of Traverse 6.

PLATE 7



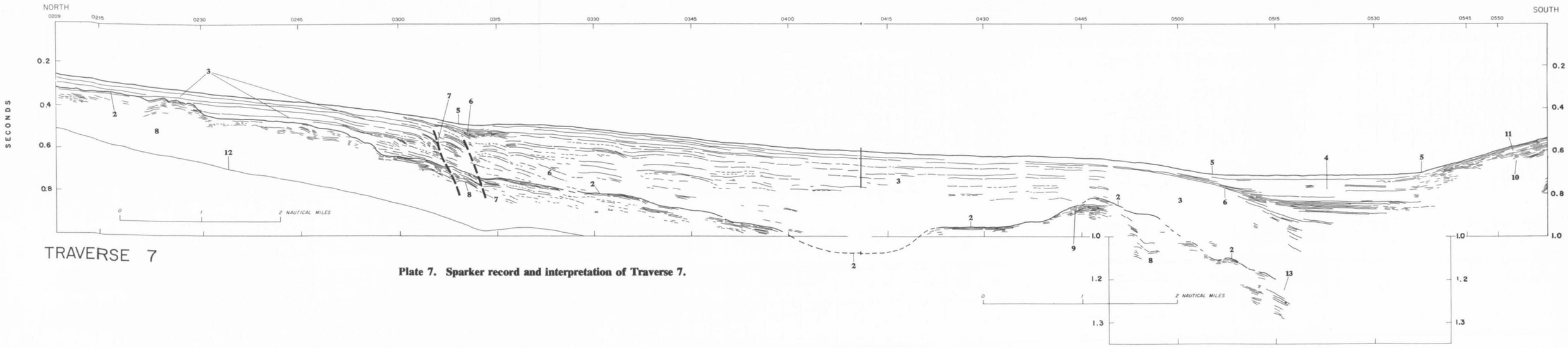
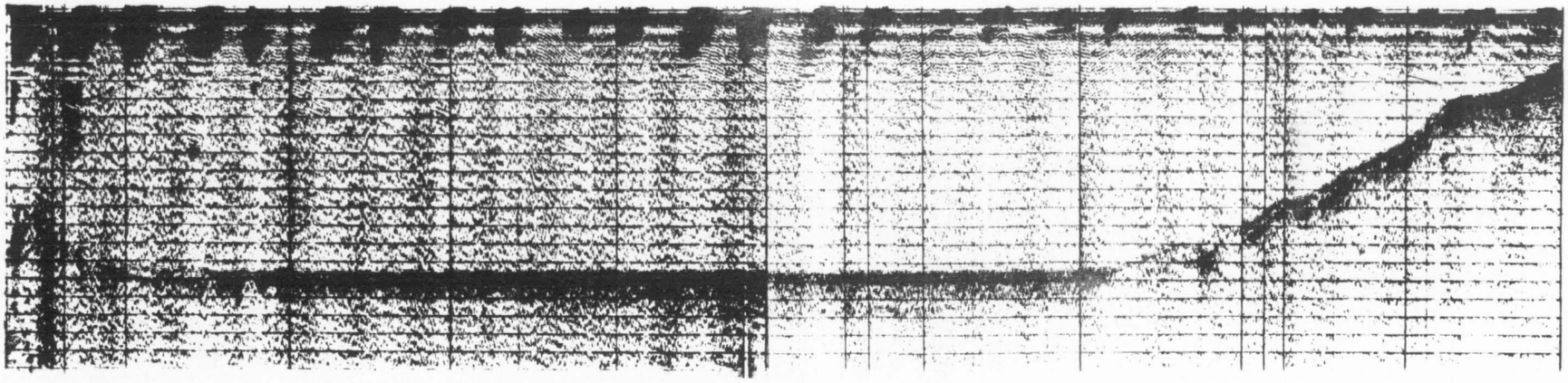
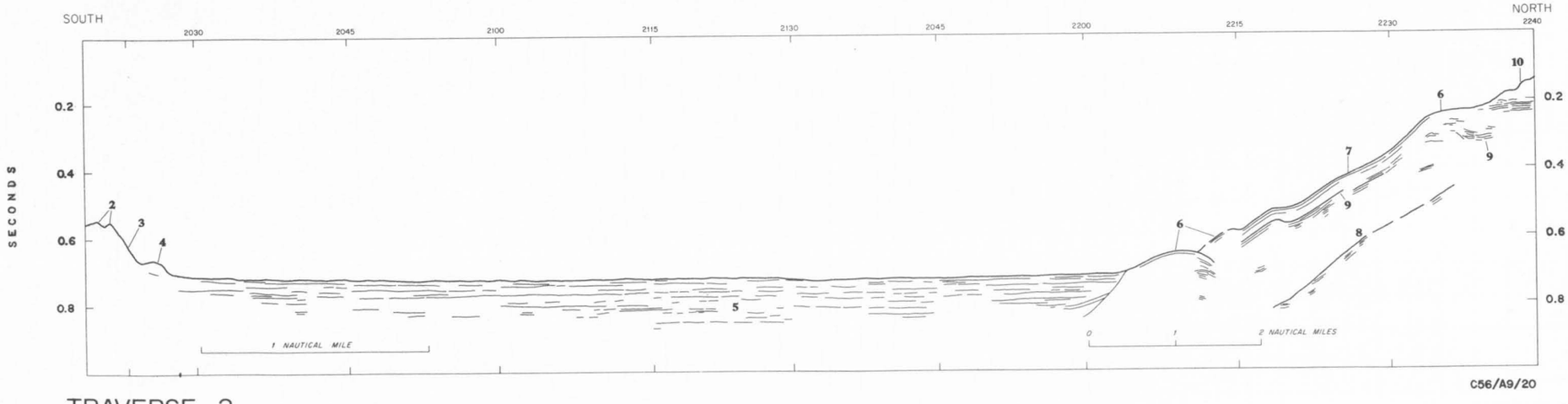


Plate 7. Sparker record and interpretation of Traverse 7.

C56/A9/15

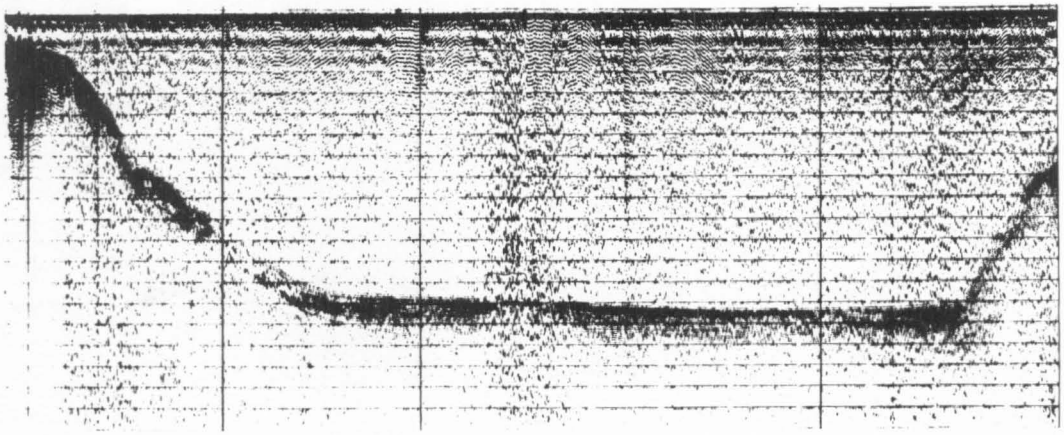
PLATE 8

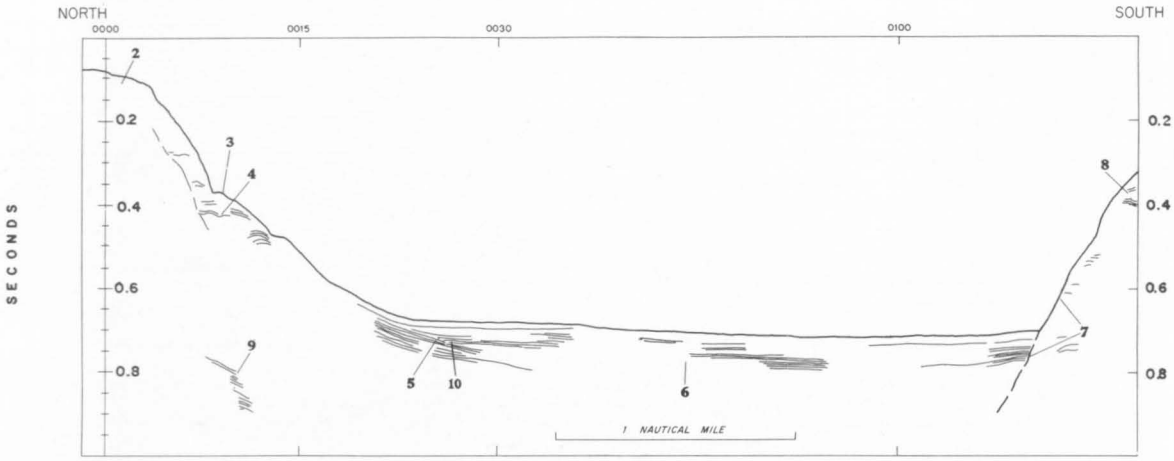




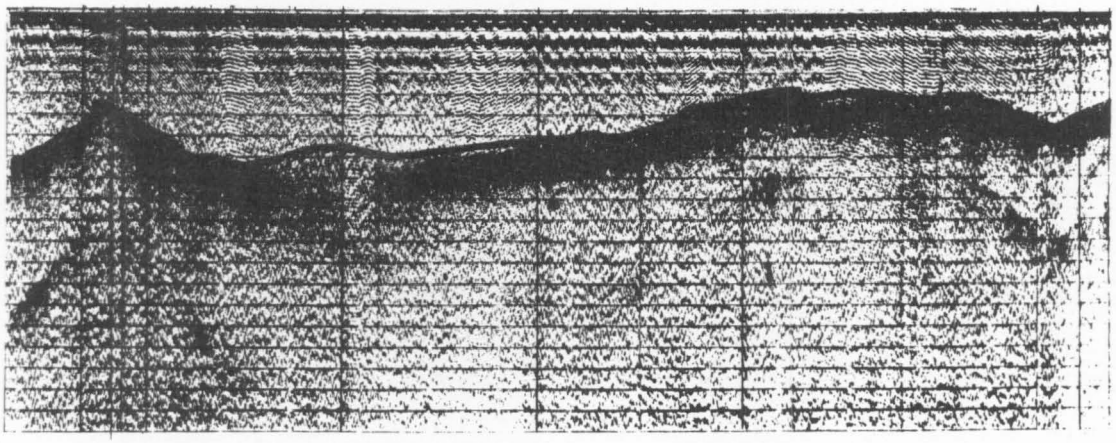
TRAVERSE 3

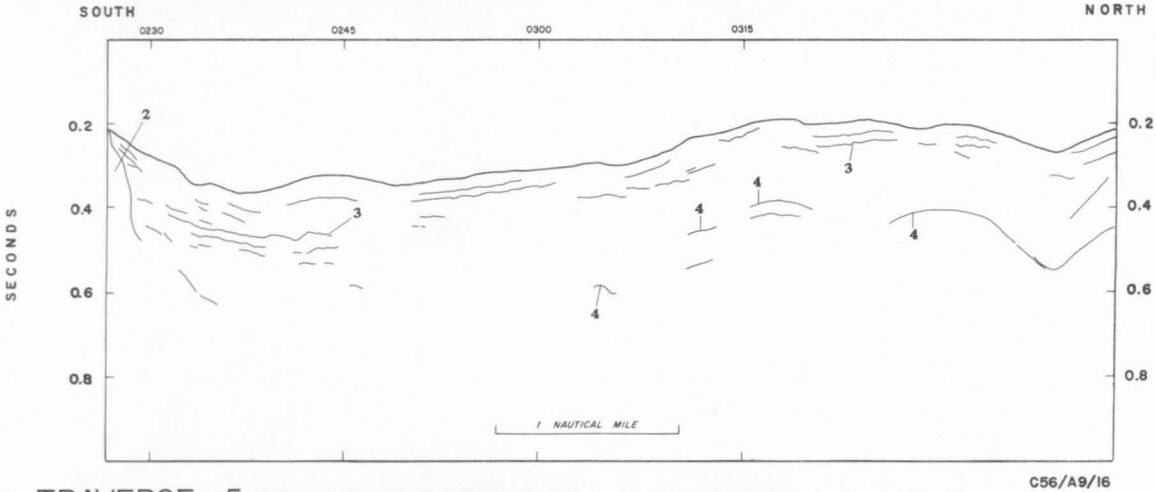
Plate 8. Sparker record and interpretation of Traverse 3.





TRAVERSE 4





C56/A9/16

TRAVERSE 5

Plate 9. Sparker record and interpretation of Traverses 4 and 5.

PALAEOMAGNETISM OF SOME RECENT BASALTS FROM NEW GUINEA

by

E. A. Manwaring

SUMMARY

The palaeomagnetic directions are given from 22 sites in the Recent basalts of New Guinea, situated within 5° of latitude of the equator. The mean direction (D = 000°, I = —16°, α_{95} = 6½°) is not significantly different from the axial dipole field direction (D = 000°, I = —8°). The data provide support for the Random Perturbation Model (Model A) of the Earth's magnetic field suggested by Irving & Ward (1964). The between-site precision (k = 21) provides an estimate of the angular dispersion θ_0 = 20° (+2°, —7°) which is related to the palaeosecular variation. This estimate is not significantly different from that estimated (Creer, 1962) by rotating the present geomagnetic field direction about the Earth's rotational axis (21°). The data suggest that the Pacific region of low non-dipole field variation (Cox, 1962) is a temporary phenomenon.

INTRODUCTION

The Territory of Papua-New Guinea and its surrounding islands lie close to the equator, and have a considerable volume of Recent volcanic material. Thus it is an important area for studies of secular variation using palaeomagnetic techniques (i.e. of palaeosecular variation), particularly from the point of view of distinguishing between the two palaeomagnetic models of the geomagnetic field—Model A of Irving & Ward (1964), and Model B of Creer, Irving, & Nairn (1959).

This area is of interest also because it lies within the Pacific region of low secular variation of the non-dipole components of the present field (Cox, 1962).

GEOLOGY AND SAMPLING

Samples of Recent volcanics were collected in 1961 from four distinct areas (*see* Fig. 1):

(a) Baluan Island. This island lies south of Manus Island, at position 147°17′E, 2°32′S. It is a volcanic island with a single peak and fringing coral reefs. It is regarded as being of Recent age because of the dissected nature of the

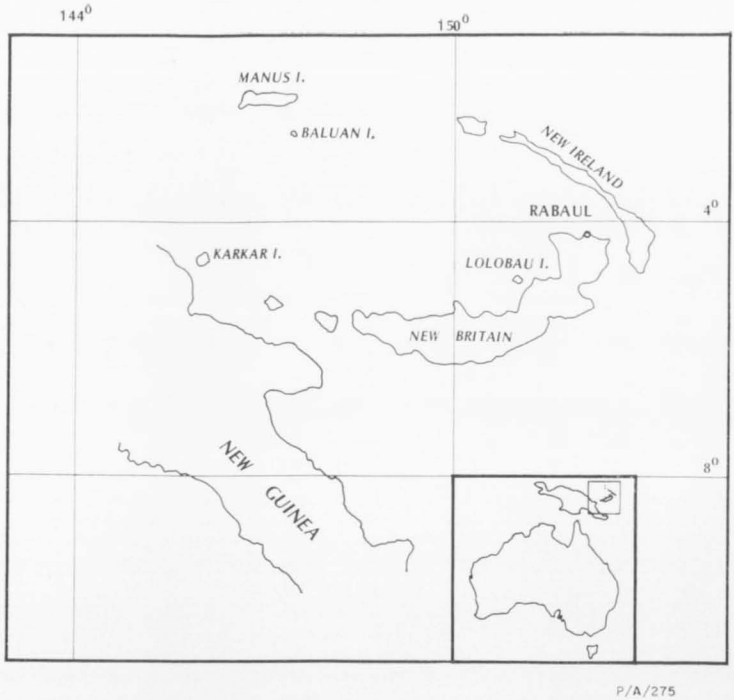


Figure 1. Locality map of the New Guinea area.

topography, the freshness of a great proportion of the volcanics, and the presence of active volcanic islands nearby.

The collection sites on this island were all near the north coast. Three rock types were collected: fine-grained vesicular basalt; vesicular basalt with scattered small feldspar phenocrysts; and vesicular basalt with a large proportion of feldspar phenocrysts up to 1 cm across. The individual flows could not be distinguished in the field because of the vegetation cover and lack of extensive outcrops, but the samples collected were all quite fresh.

(b) Karkar Island. This island consists of a single, large volcanic peak about 1800 m high, with fringing coral reefs. It lies off the north coast of New Guinea at position 145°57′E, 4°34′S, and is visible from the New Guinea coastal town of Madang. This island also is regarded as being Recent in age because of the dissected nature of the topography and the freshness of the basalts. Again, however, the individual flows cannot be distinguished because of the vegetation cover.

The collection sites were all near the northwest coast of the island. The samples collected were all vesicular basalt with feldspar phenocrysts. The proportions of both vesicles and phenocrysts varied considerably from site to site. All samples were quite fresh and unweathered.

(c) Lolobau Island. This island lies just off the north coast of New Britain, in position 151°11′E, 4°55′S. It is a volcanic caldera modified by younger cones, one of which erupted about 1905. It lies within sight of Mount Ulawun, an active volcano on the north coast of New Britain.

The samples here were collected on the south coast and in a small valley inland from this point. Two rock types were collected: a basalt with medium-sized feldspar phenocrysts and a large proportion of vesicles up to 0.5 cm across; and a basalt with extremely small feldspar phenocrysts and a few tiny vesicles. They were quite fresh.

(d) Rabaul, New Britain. The town of Rabaul lies on the northeast tip of New Britain, in position 152°12′E, 4°13′S. It is on the shores of a bay which appears to be a breached caldera flooded by the sea. The volcanics of this caldera are regarded as Recent in age since the caldera still has several small active vents. Separate flows can be distinguished in the walls of the cadera, and samples were collected from sites in different flows on the northeast and southwest sides of the bay.

The three rock types collected were vesicular basalt with feldspar phenocrysts, glassy black vesicular basalt with small feldspar phenocrysts, and glassy black basalt with small feldspar phenocrysts but consisting principally of vesicles. All samples were quite fresh. Figure 2 shows details of the sampling sites.

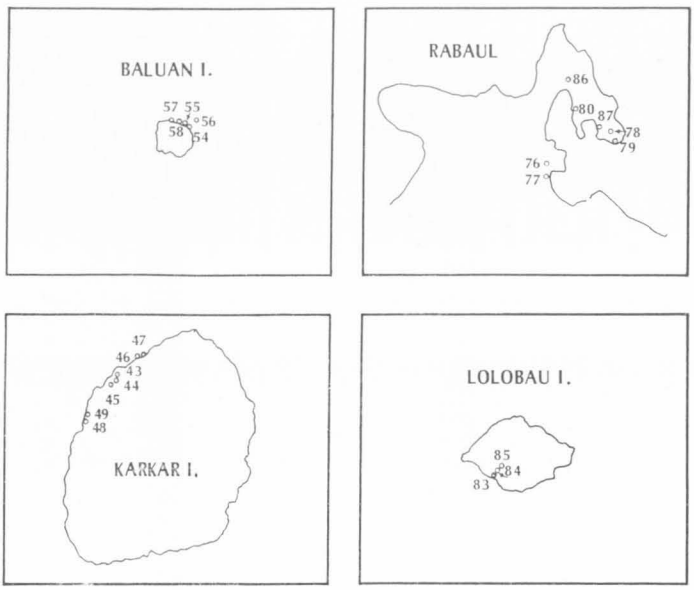


Figure 2. Details of palaeomagnetic sampling sites.

The sampling was as follows:

Area	*Number of sites*	*Number of samples*
Baluan Island	5	11
Karkar Island	7	13
Lolobau Island	3	8
Rabaul	7	12
Total	22	44

A number of specimens were cut from each sample for measurement.

Even though, in all cases except Rabaul, it was impossible to differentiate between flows in the field, it is thought that most of the sites are in different flows. The reasons for this are the differences in lithologies between most of the sites, and the distance between sites. Thus we can regard the sites as separate sampling points in time of the palaeomagnetic field.

The total time spanned by these sites is not known, but since they come from four separate areas, some still active and some not, it is thought that sufficient time is covered to give a representative coverage of the pattern of the secular variation.

PALAEOMAGNETIC RESULTS

All measurements were made on astatic magnetometers. The natural remanent magnetizations (NRMs) were measured and then, to remove any extraneous magnetic components of low coercivity, a number of specimens (pilot specimens) from each area were demagnetized in alternating magnetic fields in steps between 75 and 600 gauss (peak). The remainder of the specimens from each area were then demagnetized in that particular field which gave the closest grouping of the pilot specimen directions in each area. These demagnetized directions were then the final, cleaned directions used.

The measuring instruments and the alternating field demagnetization apparatus used were the same as, and the technique similar to, those described by Irving, Stott, & Ward (1961).

TABLE 1. MEAN PALAEOMAGNETIC DIRECTIONS OF THE NATURAL REMANENT MAGNETIZATIONS FROM EACH SITE, AND MEAN DIRECTIONS AFTER DEMAGNETIZATION

Area	*Site*	*Samples*	*NRM direction*			*Cleaned direction*			*Pole position*	
		S	D	I	R	D	I	R	°N	°E
Baluan	54	3	001	—9	2.990	003	—6	2.987	87	241
	55	2	004	—9	1.960	350	—7	1.965	88	032
	56	2	358	—19	1.990	004	—17	1.986	83	294
	57	2	355	+2	1.998	356	+4	1.989	84	102
	58	2	256	—8	1.988	310	—3	1.963	40	059
Karkar	43	1	020	—2	—	007	—14	—	83	257
	44	2	356	—11	1.980	000	—16	1.974	87	323
	45	2	357	—18	1.985	354	—26	1.996	79	357
	46	2	027	—39	1.962	023	—39	1.972	62	276
	47	2	009	—15	1.998	010	—14	1.994	79	251
	48	2	014	—25	1.951	011	—23	1.986	77	270
	49	2	356	—21	1.950	004	—17	1.975	84	293
Lolobau	83	2	359	—28	1.989	000	—24	1.981	82	332
	84	3	302	+23	1.596	335	—22	2.791	65	046
	85	3	357	—24	2.975	357	—26	2.995	81	351
Rabaul	76	1	015	—21	—	018	—19	—	72	260
	77	1	004	0	—	000	—8	—	89	152
	78	3	347	—4	2.925	350	+1	2.910	78	085
	79	1	348	—18	—	358	—17	—	85	357
	80	2	011	—25	1.975	005	—25	1.962	80	303
	86	3	007	—22	2.860	023	—19	2.985	68	256
	87	1	011	—11	—	011	—10	—	79	246

Table 1 lists the mean palaeomagnetic directions of the NRMs from each site and mean directions after demagnetization, together with the magnetic pole positions calculated from the cleaned directions. These cleaned site mean directions and pole positions are plotted in Figure 3.

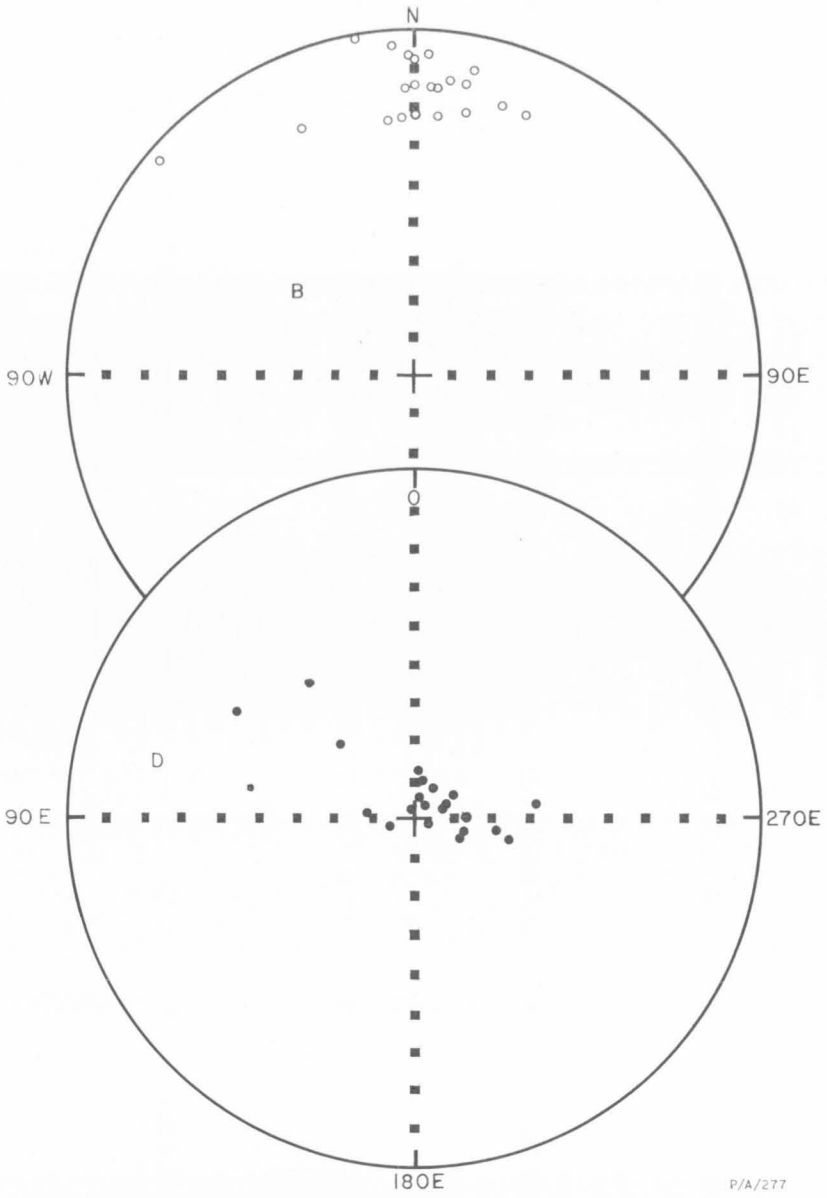


Figure 3. Equal angle stereographic plots of mean directions from all sites in the Recent basalts (B) and pole positions calculated from the site mean directions, plotted on the northern hemisphere (D).

The mean directions and poles from each area, calculated from the cleaned site mean directions, and an overall mean direction and pole, calculated from all 22 cleaned site mean directions, are listed in Table 2.

TABLE 2. MEAN DIRECTIONS AND POLES FROM EACH AREA, AND OVERALL MEAN DIRECTION AND POLE, CALCULATED FROM CLEANED SITE MEAN DIRECTIONS

Area	*Position*	*Sites*	*Samples*	*Mean direction*					*Pole position*	
		N	S	D	I	R	k	α_{95}	°N	°E
Baluan	147°17′E 2°32′S	5	11	350	—6	4.6636	12	23	80	054
Karkar	145°47′E 4°34′S	7	13	007	—21	6.8672	45	9	81	279
Lolobau	151°11′E 4°55′S	3	8	351	—24	2.9511	41	20	78	020
Rabaul	152°12′E 4°13′S	7	12	006	—14	6.8221	34	11	83	268
Overall	150°E 4°S	22	44	000	—16	20.982	21*	6½*	86	330

* From two-tier analysis.

It was thought that the geographical separation of the four collection areas might introduce an appreciable artificial scatter in the plotted directions. However, upon approximate correction for this according to the present geomagnetic field configuration, no significant difference was found. Thus the geographical scatter of the collection areas is ignored.

To test whether the distribution of the site mean directions, and of the pole positions, are in accordance with the statistics of Fisher (1953) (i.e. whether they are 'Fisherian') at the P = 0.05 level, the χ^2 test (Watson & Irving, 1957) was carried out on both distributions.

For the site mean directions,

χ^2 for D = 6.4, which is below the limit of 11.07.

χ^2 for I = 4.9, which is below the limit of 7.82.

Thus the site mean directions are a Fisherian distribution at the P = 0.05 level.

For the pole positions,

χ^2 for longitude = 16.5, which is above the limit of 11.07.

χ^2 for latitude = 11.1, which is above the limit of 7.82.

Thus the pole positions are a non-Fisherian distribution at the P = 0.05 level.

MODELS OF THE GEOMAGNETIC FIELD

When considering palaeomagnetic results, it is necessary to have some hypothetical model which expresses the average behaviour of the geomagnetic field over periods of a thousand years or more. This is because it is impossible to obtain accurate measurements of the field's configuration at a single point in time from palaeomagnetic data. Only averages taken over a period of one thousand years or more can be determined with any degree of certainty.

The simplest model is that of a geocentric axial dipole—a single dipole at the Earth's centre oriented along the axis of rotation. This model is inadequate since it does not take into account the secular variations of the geomagnetic field. Two models have been proposed:

Model A: The Random Perturbation Model was proposed by Irving & Ward (1964). This model assumes that the geomagnetic field is that of a steady geocentric axial dipole whose field is perturbed at the Earth's surface by randomly directed non-dipole fields of constant magnitude. Such a model would produce a Fisherian distribution of field directions at any one point on the Earth's surface, but the virtual pole positions calculated from these directions would form a non-

Fisherian distribution. The contrast between the Fisherian distribution of directions and the non-Fisherian distribution of pole positions would be most pronounced for directions measured at the equator.

Model B: The Whin Sill Model was proposed by Creer, Irving, & Nairn (1959). It supposes the geomagnetic field to be a geocentric dipole which undergoes random secular oscillations around the mean dipole position (the axis of rotation of the Earth). Averaged over a sufficient period of time, this model would produce a Fisherian distribution of magnetic pole positions around the mean pole position. However, the geomagnetic field directions at any point on the Earth's surface would form a non-Fisherian distribution. The contrast between the non-Fisherian distribution of directions and the Fisherian distribution of pole positions would again be most pronounced for directions measured at the equator. The distribution of directions would become nearer to Fisherian for directions measured closer to the poles.

Since the samples under consideration were collected within five degrees of latitude of the equator, the palaeomagnetic directions and poles should enable a choice to be made of the Random Perturbation or the Whin Sill model as being the more appropriate fit to these results.

As the site mean directions form a Fisherian distribution, whereas the pole positions form a non-Fisherian distribution, it is apparent that Model A (the Random Perturbation Model) is the better fit.

Fit of Data to Model A

Let $\sigma = h/H$ where H is the strength of the main dipole field, and h is the strength of the random perturbing field. Then, from Irving & Ward (1964), the circular standard deviation χ of a sample of vectors is:

$$\chi = 81/k^{\frac{1}{2}} \text{ where } k = N - 1/N - R \text{ (Fisher, 1953)}$$
$$= 46.8\ \sigma_e\ (1 + 3\sin^2 \lambda)^{\frac{1}{2}}$$

where σ_e is h/H at the equator, and λ is latitude.

For these data, $\lambda = -4°$, so that

$$81/k^{\frac{1}{2}} = 46.8\ \sigma_e \times 1.0072.$$

Therefore $\sigma_e = 0.37$ since $k = 21$.

This value of σ_e agrees closely with the estimates obtained by Irving & Ward for the present geomagnetic field, and for other palaeomagnetic data.

MAGNITUDE OF THE SECULAR VARIATION

The New Guinea Recent basalt directions can be used to estimate the dispersion of directions of the magnetic field caused by the palaeosecular variation in the New Guinea region, and this can then be compared with the estimates of Creer (1962) and Cox (1962).

Creer has calculated the angular dispersion $\theta_o = \cos^{-1}(R/N)$ of the present secular variation with respect to latitude, on the theory that the deviations from an axial dipole field around a line of latitude for a given epoch are the same as those which would occur at any point on that latitude over a long period of time. That is, the distribution of directions caused by secular variation at any point on the Earth's surface is the same as that given at that point by the rotation of the present geomagnetic field bodily about the axis rotation of the Earth. This variation includes, therefore, both the movement of the non-dipole field and the movement of the main dipole field through a circle of approximate radius $11\frac{1}{2}°$ (the angle between the rotation axis of the Earth and the present geomagnetic axis).

Cox (1962) considered separately the dispersion due to the non-dipole component of the present geomagnetic field, and the dispersion due to the superimposition of the non-dipole field on a movement of the main dipole field. For the non-dipole components only, he calculated the virtual geomagnetic poles from the non-dipole directions measured on a 10° grid covering the Earth. He found an area of low non-dipole variation in the Pacific region, and calculated the angular dispersion around lines of latitude of the virtual poles for: (a) all data; (b) data from the area of low dispersion in the Pacific region; and (c) all data except those from the Pacific region.

Analysis of Dispersion of the Recent Basalt Directions

The between-site dispersion of the palaeomagnetic directions from the Recent basalts of New Guinea is calculated as follows, after McElhinny (1967):

Source	*Degrees of freedom*	*Sum of squares*	*Mean square*	*Expectation of mean square*
Between sites	42	1.90	0.0453	$\frac{1}{2}(\frac{1}{\omega} + \frac{2}{\beta})$
Within sites	44	0.77	0.0175	$\frac{1}{2}(\frac{1}{\omega})$
Total	86	2.67		

Twenty-two sites were sampled, with between 1 and 3 samples from each site. Thus:

$$\begin{aligned} B &= 22 \\ W &= 1.90 \\ N &= 44 \\ \Sigma R_i &= 43.23 \\ R &= 41.33 \end{aligned}$$

Thus $F_{42,44} = 2.59$ which is significant.

Solving for ω and β

$$\begin{aligned} \omega &= 28.57 = 29 \\ \beta &= 34.16 = 34. \end{aligned}$$

Thus:

$$k' = \frac{1}{(\omega N)^{-1} + (\beta B)^{-1}} = 470$$

$$k = k'/B = 21.$$

The semi-angle α_{95} of the cone of 95% confidence is

$$\alpha_{95} = 6\tfrac{1}{2}^\circ$$

The angular dispersion θ_o of the directions is

$$\theta_o = \cos^{-1}(R/N) = 20^\circ$$

For B = 22, $F_{42,42} = 1.67$ at the 5% level.

Then the limits of k are:

$$k_{max} = k / 1.67 = 35$$

$$k_{min} = k / 1.67 = 13.$$

So that the limits of R are:

$$R_{max} = 21.40$$
$$R_{min} = 20.38$$

Therefore the limits of θ_o are:

$$\theta_{o\ max} = 22^\circ$$
$$\theta_{o\ min} = 13^\circ$$

Thus the true angular dispersion of the directions of magnetization of the Recent basalts lies between 13° and 22°, and the true precision k of these directions lies between 13 and 35.

TABLE 3. ANGULAR DISPERSION OF THE RECENT BASALT PALAEOMAGNETIC DIRECTIONS, OF THE TOTAL PRESENT FIELD FOR 0° LATITUDE (CREER, 1962), AND OF THE DIRECTIONS OF THE NON-DIPOLE COMPONENTS AT 0° LATITUDE (COX, 1962)

Source	*Angular dispersion θ_o of directions*
Creer (1962) at 0° latitude	21°
Cox (1962) at 0° latitude	
(a) all data	11°
(b) Pacific only	3.1°
(c) excluding Pacific	12°
New Guinea Recent Basalts	20° (max. 22°, min. 13°)

Table 3 lists the angular dispersion of the Recent basalt palaeomagnetic directions, the angular dispersion of the toal present field for 0° latitude given by Creer (1962), and the angular dispersions of the directions of the non-dipole components of 0° latitude calculated from Cox (1962). The angular dispersions of the pole positions from the non-dipole components taken from Cox are corrected to give the angular dispersions of the non-dipole field directions according to his equations:

$$d' = dC$$
$$C = \tfrac{1}{4}[1 + 3\cos^2 I + (1 + 3\cos^2 I)^{\frac{1}{2}}]$$

where d′ is the angular dispersion of the directions, d is the angular dispersion of the poles, and I is the mean field inclination (= 22°).

It can be seen from Table 3 that the dispersion of the total field from Creer (1962) lies within the limits of the results from the Recent basalts. However, the dispersion of the non-dipole components only (Cox, 1962) is too low for the dispersion of the Recent basalt directions to be attributable solely to the non-dipole components of the present geomagnetic field, especially since New Guinea lies within Cox's Pacific region of low dispersion.

Cox also considered the effect of a main dipole wobble superimposed on the non-dipole field. The precision parameter k = 21 obtained from the Recent basalts can be taken in this case to correspond to the precision of the total present non-dipole field variation superimposed on a main dipole wobble of approximately 11½°.

Let k_N = the non-dipole precision parameter for 0° latitude,

k_D = the main dipole precision parameter,

k_T = the total precision parameter.

Then $k_N = 103$ from Cox (1962, table 2),

$$k_D = (67.5°/d_m)^2$$

where d_m is the angle of wobble of the main dipole.

Then $k_D = 34.5$ for a main dipole wobble of $11\frac{1}{2}°$.

Since $1/k_T = 1/k_N + 1/k_D$, then

$k_T = 25.8$.

Correction of this precision parameter k_T, which applies to the pole positions calculated from the directions, gives the precision parameter of the field directions k_T' to be

$$k_T' = k_T/C^2 = 13.8.$$

This value of k_T' lies just within the limits of k (13 to 35) obtained from the dispersion of the Recent basalt directions.

However, if this model of Cox were true, it would mean that most of the secular variation would be due to main dipole wobble (compare $k_D = 34.5$ and $k_N = 103$). Thus the observed dispersion of pole positions must be Fisherian (i.e. must agree with model B). This is not found to be the case in the results from the Recent basalts.

It is apparent that, since these results support model A, the major part of the secular variation observed must be due to variations in the non-dipole components of the geomagnetic field (assuming that the random perturbing fields of model A are due to non-dipole components). To have produced the results obtained, these non-dipole components must have been of greater magnitude than those of the present geomagnetic field in the region.

Thus the Pacific region of low non-dipole variation (Cox, 1962) appears to be a temporary phenomenon.

CONCLUSIONS

The following deductions can be made:

(a) The mean direction (000°, —16°) is not significantly different from the geocentric axial dipole field direction (000°, —8°) at present; this supports the assumption made in palaeomagnetic work that the Earth's magnetic field, averaged over a long enough interval of time, reduces to that of a geocentric axial dipole.

(b) The dispersion of the results is in accordance with the Random Perturbation Model of Irving & Ward (1964).

(c) The rotation of the present field about the Earth's axis (Creer, 1962) can account for the magnitude of the dispersion observed.

(d) The pattern of the dispersions (directions and poles) cannot be adequately explained by a small non-dipole variation superimposed on a main dipole wobble. It seems that the dispersion is due to the secular variations of the non-dipole components, with only a small part, if any, due to variations of the main dipole field.

(e) The magnitude of the dispersion, together with point (d), suggests that the area of low secular variation of the non-dipole components in the Pacific region (Cox, 1962) is not a permanent feature of the region.

REFERENCES

COX, A., 1962—Analysis of the present geomagnetic field for comparison with palaeomagnetic results. *J. Geomagn. Geoelect.*, 13, p. 101.

CREER, K. M., 1962—An analysis of the geomagnetic field using palaeomagnetic methods. *J. Geomagn. Geoelect.*, 13, p. 113.

CREER, K. M., IRVING, E., and NAIRN, A. E. M., 1959—Palaeomagnetism of the Great Whin Sill. *Geophys. J. Roy. Astron. Soc.*, 2, p. 306.

FISHER, R., 1953—Dispersion on a sphere. *Proc. Roy. Soc.*, A, 217, p. 295.

IRVING, E., STOTT, P. M., and WARD, M. A., 1961—Demagnetization of igneous rocks by alternating magnetic fields. *Phil. Mag.*, 6, p. 225.

IRVING, E., and WARD, M. A., 1964—A statistical model of the geomagnetic field. *Pure Appl. Geophys.*, 57, p. 47.

MCELHINNY, M. W., 1967—Statistics of a spherical distribution, *in* DEVELOPMENTS IN SOLID EARTH GEOPHYSICS, 3, p. 313. (*Elsevier: Amsterdam.*)

WATSON, G. S., and IRVING, E., 1957—Statistical methods in rock magnetism. *Mon. Notes Roy. Astron. Soc.*, Geophys. Suppl., 7, p. 289.

Page 66 is blank.

LAMELLAR INTERGROWTHS OF PYROPHYLLITE AND MUSCOVITE AND THE ASSEMBLAGE KYANITE-PYROPHYLLITE-QUARTZ IN QUARTZITES FROM THE PETERMANN RANGES, NORTHERN TERRITORY

by

R. N. England

SUMMARY

Pyrophyllite-muscovite-kyanite-bearing quartzites occur in the Mannanana and Curdie Ranges, in the Petermann Ranges in the southwest of the Northern Territory. Electron probe scanning X-ray images are used to distinguish muscovite from pyrophyllite in lamellar intergrowths.

Pyrophyllite is absent in higher-grade kyanite quartzites to the east, but it occurs together with kyanite in a region at least 20 km long along strike. It is difficult to give a satisfactory explanation for the occurrence of the assemblage kyanite-pyrophyllite-quartz in terms of equilibrium, and interpretation of the muscovite-pyrophyllite intergrowth as an exsolution texture has many problems.

INTRODUCTION

The Upper Proterozoic Dean Quartzite (Forman, 1966) in which the assemblage kyanite-pyrophyllite-quartz occurs is the basal unit in the Amadeus Basin; it is the main outcropping unit in the region and overlies older granitic rocks of the Pottuyu Complex, which extends to the south towards the Mann Ranges (Fig. 1). Quite strong folding occurred during the Petermann Ranges Orogeny at the end of the Proterozoic (Forman, 1966).

Specimens were collected during a visit to the area made by D. J. Forman and the author in 1968. They were taken only from the more aluminous zones and a special effort was made to collect rocks in which kyanite was visible in hand specimen. Three separate zones occur: quartzite in this area may contain pyrophyllite at low grade, then kyanite together with pyrophyllite, and finally kyanite without pyrophyllite. Only the middle zone is characterized by lamellar intergrowths of muscovite and pyrophyllite. Quartz is of course ubiquitous and phengitic muscovite is very common.

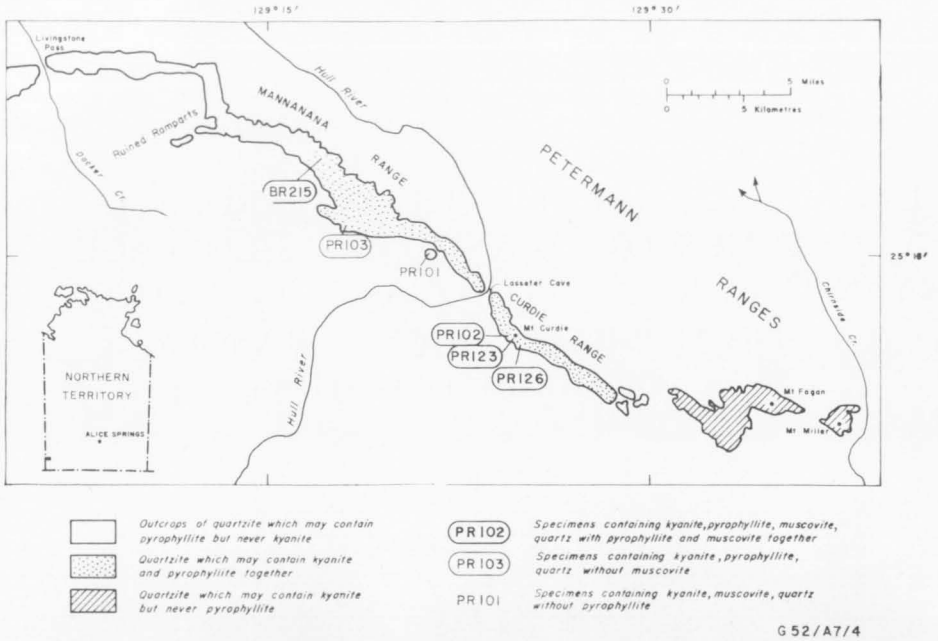


Figure 1. Sketch map of the outcrop of Dean Quartzite in the Mannanana and Curdie Ranges, showing the distribution of pyrophyllite- and kyanite-bearing rocks. Outcrop pattern from Forman (1966).

ELECTRON PROBE INVESTIGATION

X-ray scanning images were made with a Jeol J X A-3A electron probe using a specimen current of about 0.05 μ A, a beam diameter of approximately 2 μm. Electron beam scanning for sources of Al and K Kα radiation was used to distinguish pyrophyllite from muscovite (*see* Pl. 10).

PETROGRAPHY

Pyrophyllite-Quartz Zone

These quartzites are mainly medium-grained with some coarse bands and contain varying minor amounts of phengitic muscovite and/or pyrophyllite. Lamellar intergrowths of these two minerals are apparently absent. Quartz grains retain their clastic shape and show undulose extinction. Tourmaline is a common heavy accessory.

Kyanite-Pyrophyllite-Quartz Zone

Recrystallization to a medium-grained polygonal aggregate is almost complete in the first rocks to contain traces of kyanite and only a few large grains retain their clastic shape and undulose extinction. This marked textural difference between the zones with and without kyanite indicates that the latter cannot have been derived from kyanite-bearing rocks by retrograde metamorphism and therefore suggests that large-scale retrogression has not occurred.

Lamellar intergrowths of muscovite and pyrophyllite have been found only in this zone. Pyrophyllite has a roughly tabular habit; grains are generally 0.1 to 0.3 mm across and about half as thick. Continuous muscovite lamellae 5 to 50 μm thick sharing their 001 plane with pyrophyllite are almost always present in the larger pyrophyllite grains. Muscovite lamellae illustrated in Plate 10 are much more abundant than in the commoner pyrophyllite grains which contain only about two or three such lamellae. Independent plates of muscovite, similar in dimensions to the included ones, are normally quite abundant.

Muscovites are slightly stained with hydrated iron oxide (probably due to breakdown of celadonite component with later oxidation) and they can thus be distinguished with reasonable confidence from pyrophyllite. The interference colours of included muscovite are invariably lower than their host. (From almost all the optical parameters given for the two minerals it can be shown that for parallel plates of muscovite and pyrophyllite, the former will always show the lower interference colour in thin section.)

Kyanite grains in this zone are generally larger and always more abundant than pyrophyllite. They are subhedral to anhedral and most have skeletal outlines. In some specimens they are fractured and bent but never show any accompanying alteration to sheet silicates.

Kyanite-Quartz Zone

Except for the absence of pyrophyllite, these rocks are similar to those from the kyanite-pyrophyllite-quartz zone. Muscovite is still present, indicating that the grade never rose above middle amphibolite facies.

PETROGENESIS

The two main problems presented by these rocks are, firstly the origin of the interlayer texture, and secondly, the occurrence of kyanite, pyrophyllite, and quartz together over a region whose extent in one direction is at least 20 km. One would expect this assemblage to be univariant (i.e. to occur only at the isograd represented by the reaction line pyrophyllite $\rightleftharpoons$ kyanite + 3 quartz + water).

The interpretation of the lamellar intergrowths of muscovite and pyrophyllite as an exsolution texture raises a number of questions. If a small amount of muscovite component could be accommodated in the pyrophyllite lattice it would certainly exsolve as the pyrophyllite decomposed and possibly produce the texture described. The data in rows A/(B + A) and C/(A + B + C) in Table 1 show that in all specimens where the texture is well developed, about 10 to 20 times more pyrophyllite must have been present before the reaction started. It might therefore be inferred that before the reaction significant amounts (if not all) of the muscovite now present may then have been dissolved in the pyrophyllite. Unfortunately, microprobe analyses show that the mole fraction of muscovite now present in the pyrophyllite is only about 0.003 which, when compared with the calculated values in the last row of Table 1, is about a factor of 10 too small. It must be necessary, then, to postulate further exsolution, perhaps on cooling.

TABLE 1. MINERAL PROPORTIONS AND SOME CALCULATED MOLAR PROPORTIONS USING THE MOLAR VOLUME DATA OF ROBIE ET AL. (1967)

(Sufficient confidence in distinguishing pyrophyllite and muscovite has enabled the following point-counts to be made)

	PR101	PR102	PR103	PR123	PR126	BR215*
Quartz (Vol. %)	45	81	74	70	81	88
Kyanite (Vol. %)	35	15	21	26	11	0.5
Pyrophyllite (Vol. %)	0	2.2	2.5	3	4	4
Muscovite (Vol. %)	18	1.3	0	2	3	7
Others (mostly opaques) (Vol. %)	2	0.5	3	0	1	0
A. No. of moles of kyanite /100 cc	0.79	0.34	0.47	0.59	0.25	0.01
B. No. of moles of pyrophyllite /100 cc	0	0.017	0.020	0.024	0.032	0.03
C. No. of moles of muscovite /100 cc	0.13	0.009	0	0.014	0.021	0.050
A/(B + A) (A measure of the completeness of Py $\leftrightharpoons$ Ky + 3Q + W reaction)	1	0.95	0.96	0.96	0.89	0.25
C/(A + B + C) (Maximum mole fraction of muscovite which could have been accommodated in original pyrophyllite)	0.142	0.025	0	0.022	0.069	0.56

* Only one poorly developed intergrowth containing one muscovite lamella occurs in this thin section.

The very remote possibility of all the muscovite having exsolved on cooling from the present amount of pyrophyllite is only worth considering because it affords an explanation for the rather widespread occurrence of the assemblage kyanite-pyrophyllite-quartz. The addition of muscovite component to the system without it separating out as a phase raises the variance of the assemblage to 2, enabling it to be stable over a range of temperature and pressure. However, the presence of any independent grains of muscovite (which are now abundant) during pyrophyllite breakdown would cause the assemblage to again become univariant.

A more probable reason for divariance of the assemblage may be a gradual increase in the P_{H_2O} as the pyrophyllite breaks down. A similar explanation was offered by Evans & Guidotti (1966) for the co-existence over a large area of sillimanite, potash feldspar, muscovite, and quartz. Zen (1961) recorded a number of three-phase assemblages (including andalusite-pyrophyllite-quartz) in the system Al_2O_3-SiO_2-H_2O and attributed their occurrence to buffering of the H_2O activity.

However, if this assemblage is truly divariant, one would expect gradual increase in the kyanite/pyrophyllite proportion from the point of first appearance of kyanite (BR215) to the last occurrence of pyrophyllite (PR126), but Table 1 shows that in all cases except BR215 the reaction is nine-tenths or more complete. A serious explanation for this has so far eluded the author, but it may be possible that in our zeal to collect kyanite-bearing specimens we collected from areas of locally low H_2O (and/or K_2O) activity.

Retrograde metamorphism of kyanite-quartzites with a limited amount of water could produce kyanite-pyrophyllite-quartz, but there is little or no textural evidence for it. Kyanites do not appear to be altered and it is difficult to see how

the interlayer structure could have developed during retrogression. The occurrence of kyanite and pyrophyllite in the proportions observed seems to defy satisfactory explanation in terms of equilibrium and it may be possible that due to a sluggish reaction rate, a small amount of pyrophyllite has persisted beyond its normal breakdown temperature. The muscovite-pyrophyllite intergrowth may not be an exsolution texture, but could have been produced by prograde metamorphism of clays such as illite, but even this is doubtful because of the absence of clays in the rocks of lower grade than those which show intergrowths.

Temperature and Pressure Environment

The experimental data used in Figure 2 for pyrophyllite breakdown and kyanite-andalusite equilibrium are those of Kerrick (1968) and Newton (1966), respectively. Relationships for P_{H_2O} P_{load} were calculated roughly and the curve was modified to take into account the change in slope when it enters the kyanite field. The molar volume data used for the solids in the calculations were those of Robie et al. (1967) and the thermodynamic data for water were those of Burnham et al. (1969). The entropy difference between andalusite and kyanite (used to calculate the change in slope of the dehydration curve) was calculated simply from the slope of the kyanite-andalusite boundary of Newton (1966).

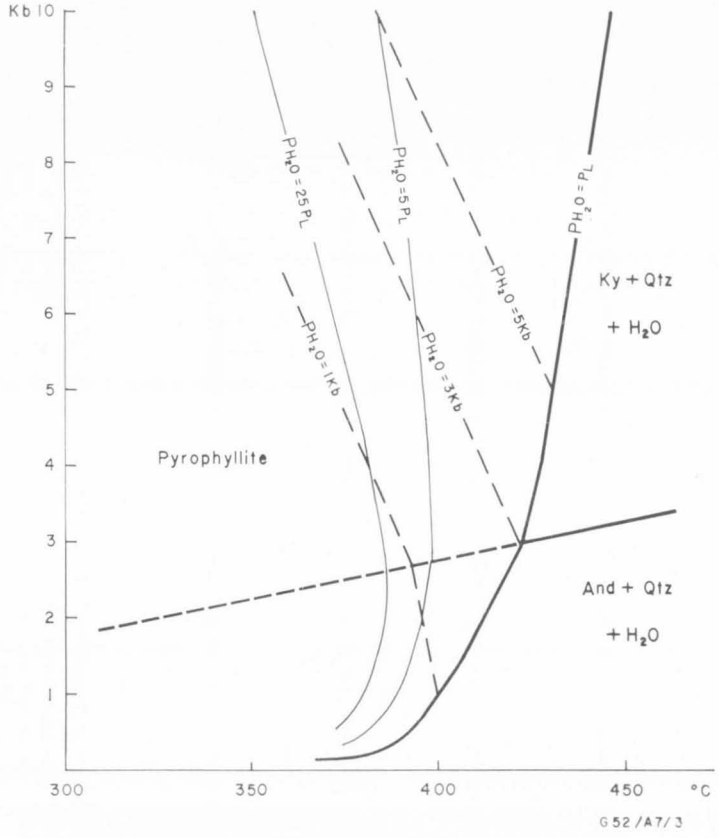


Figure 2. Pyrophyllite dehydration curve calculated from the data of Kerrick (1968) and Newton (1966).

MICROGRAPHS OF A PYROPHYLLITE-MUSCOVITE INTERGROWTH IN QUARTZITE PR126 FROM MOUNT CURDIE, NORTHERN TERRITORY.

A. Photomicrograph (plane polarized light) of a lamellar intergrowth [pyrophyllite and muscovite are almost indistinguishable here]. (x 150.)

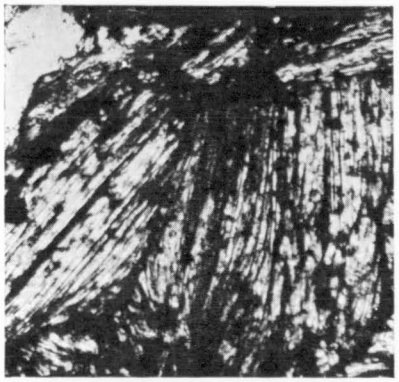
B. Scanning electron probe micrograph showing distribution of sources of Al K_α radiation from the same field of view. (x 150.)

C. Similar X-ray image of K K_α radiation showing the distribution of muscovite lamellae. (x 150.)

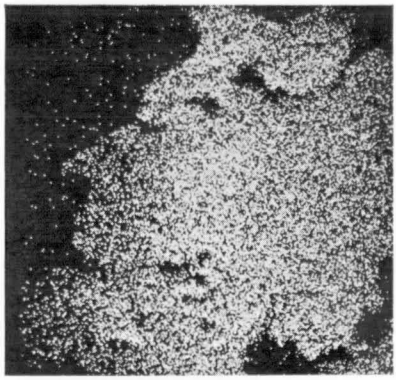
D. K radiation (heavy white dots) superimposed on Al radiation (fine grey dots). (x 150.)

E. Detail from the bottom right corner of D. (x 300.)

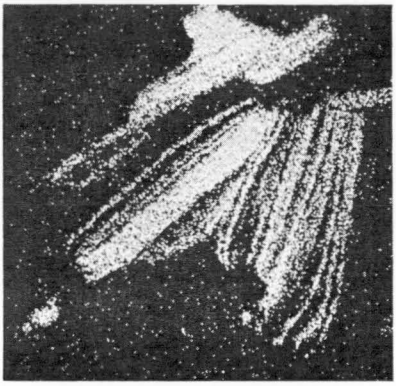
F. Distribution of Fe radiation showing the phengitic nature of the muscovite. (x 150.)
point-counts to be made)



A



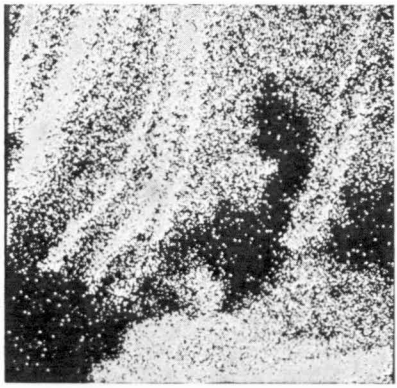
B



C



D



E



F

The kyanite-pyrophyllite-quartz rocks almost certainly formed at temperatures of 360° to 460°C and pressures greater than 3 Kb. If the water activity was buffered by the reaction at pressures lower than P_{load}, then one would expect temperatures low in this range, but if there were any significant muscovite-pyrophyllite solid solution then temperatures could be high in this range or perhaps even higher.

CONCLUSION

The interpretation of the muscovite-pyrophyllite intergrowth as an exsolution texture and kyanite-pyrophyllite-quartz as an equilibrium assemblage in these rocks has many difficulties. Even if disequilibrium is assumed it is still difficult to explain why the reaction pyrophyllite-kyanite + quartz + water is 90 percent or more complete in five out of six cases.

Acknowledgements

I am grateful to Dr D. J. Forman, who led the field party which collected the specimens, and especially to Dr E. J. Essene, Australian National University, who criticized the manuscript.

REFERENCES

Burnham, C. W., Holloway, J. R., and Davis, N. F., 1969—Thermodynamic properties of water to 1000°C and 10,000 bars. *Geol. Soc. Amer. Spec. Paper* 132.

Evans, B. W., and Guidotti, C. V., 1966—The sillimanite-potash feldspar isograd in western Maine, U.S.A. *Contr. Miner. Petrol.*, 12, 25-62.

Forman, D. J., 1966—The geology of the south-western margin of the Amadeus Basin, Central Australia. *Bur. Miner. Resour. Aust. Rep.* 87.

Kerrick, D. M., 1968—Experiments on the upper stability limit of pyrophyllite at 1.8 kilobars and 3.9 kilobars water pressure. *Amer. J. Sci.*, 266, 204-14.

Newton, R. C., 1966—Kyanite-andalusite equilibrium from 700°C to 800°C. *Science*, 153, 170-72.

Robie, R. A., Bethke, P. M., and Beardsley, K. M., 1967—Selected X-ray crystallographic data molar volumes, and densities of minerals and related substances. *U.S. geol. Surv. Bull.* 1248.

Zen, E-An, 1961—Mineralogy and petrology of the system Al_2O_3-SiO_2-H_2O in some pyrophyllite deposits of North Carolina. *Am. Miner.*, 46, 155-66.

Page 74 is blank.

PERMIAN AND MESOZOIC GEOLOGY OF THE NORTHEASTERN PART OF THE BONAPARTE GULF BASIN

by

J. M. Dickins, J. Roberts, and J. J. Veevers

SUMMARY

Most of the Permian and Mesozoic outcrops in the Bonaparte Gulf Basin are found northeast of Queens Channel. Relief and dips of the strata are low so that exposures are isolated and limited in thickness and, where fossils are absent, superpositional relationships can be difficult to establish. However, much information on the sequence has been provided by three wells drilled by Australian Aquitaine Petroleum Pty Ltd—Kulshill Nos 1 and 2 and Moyle No. 1.

North of the Moyle River probable Permian sandstone overlies the Precambrian with angular unconformity. Rocks of intermediate age are not known at the surface but Devonian and Carboniferous as well as thick Permian strata were penetrated in Kulshill No. 1 and No. 2 Wells, located south of the Moyle River. Distribution of the Palaeozoic rocks is strongly affected by a very large north-south fault running through the Kuriyippi Hills and passing north at about the mouth of the Moyle River. The fault is shown clearly by gravity and seismic work but has poor surface expression. West of the fault, Devonian, Carboniferous, and thick Permian beds are preserved, whereas to the east apparently only thin Permian unconformable on Precambrian is found.

The older Lower Permian beds, predominantly sandstones, are apparently largely non-marine with minor coal and, in places, some indication of glacial activity. The younger Lower Permian is marine with fossils of Artinskian age and is separated disconformably from overlying non-marine and marine beds. The marine beds have fossils of Upper Permian age. North of the Moyle indications of Permian fault movement are found.

The Upper Permian is overlain apparently disconformably by a formation of probable Triassic age. Cretaceous beds, with marine fossils, in places survive as remnants of a thin sheet both on the rocks of the Bonaparte Gulf Basin and on the adjoining Precambrian to the east.

INTRODUCTION

Most Permian and Mesozoic outcrops in the Bonaparte Gulf Basin are located northeast of Queens Channel in an area between the Macadam Range to the east and the Daly River to the north (Fig. 1). West of the Precambrian rocks in the Macadam Range the Permian and Mesozoic rocks crop out as low mesas, in

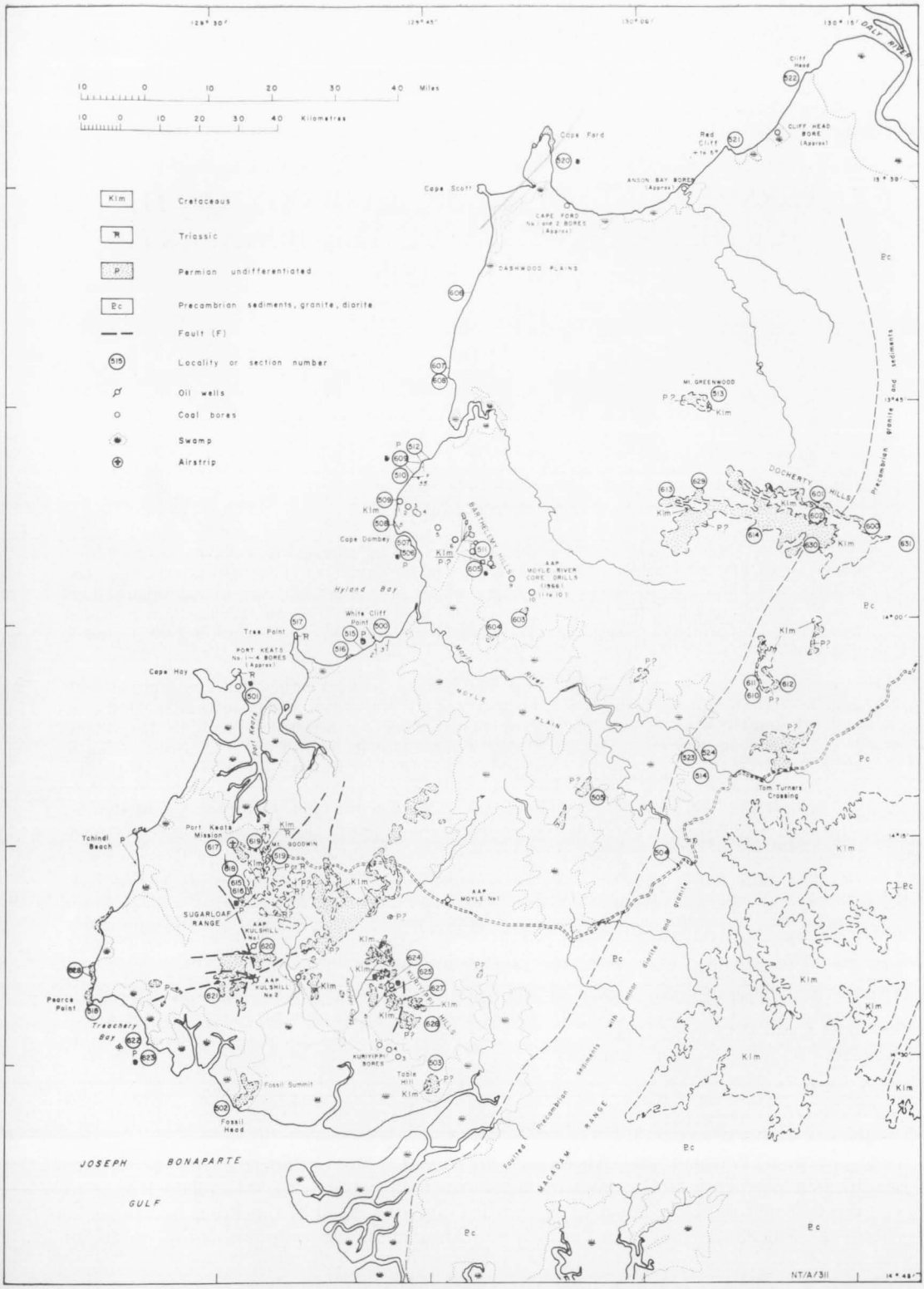


Figure 1. Geological sketch map of the northeastern part of the Bonaparte Gulf Basin, Northern Territory.

usually heavily timbered country, and as coastal outcrops. Large parts of the area are swampy, and access, apart from by helicopter, is usually difficult in normal seasons. Southeast of Queens Channel, the only known Permian outcrops are on the margins of tidal flats north of Cleanskin Bore in the Moogarooga Creek area (Veevers & Roberts, 1968).

In the subsurface, Mesozoic and Permian sediments have been penetrated by AAP Kulshill No. 1, Kulshill No. 2, and Moyle No. 1 Wells in the vicinity of Port Keats (Fig. 1), and by Arco Ltd Lacrosse No. 1 Well drilled offshore at latitude 14°17′51″, longitude 128°34′58″, 35 miles north of the coastline near Cape Domett and 53 miles west of Pearce Point. South of Queens Channel, Permian sediments have been penetrated by AAP Keep River No. 1 drilled west of Keep Inlet at latitude 15°10′05″, longitude 129°05′22″, and in AOD Bonaparte No. 1 (Veevers & Roberts, 1968).

During the period 15th to 23rd July, 1966, ten shallow holes were drilled for Australian Aquitaine Petroleum Pty Ltd north of the Moyle River, the deepest of which was 200 feet. The positions of these are shown on Figure 1, as well as the positions of five holes drilled during September-October, 1967, for Geotechnics (Aust.) Pty Ltd near the Kuriyippi Hills in search for coal. The deepest of these was 615 feet.

The work northeast of Queens Channel, which is the basis for most of this report, was carried out during September 1965 as the last part of the geological survey of the Bonaparte Gulf Basin by J. Roberts and J. J. Veevers. J. M. Dickins joined the party at this time and the survey used a helicopter from the base camp at Tom Turners Crossing. Some checking was done on the ground by Landrover. The Permian southeast of Queens Channel was examined on the ground during the earlier part of the survey.

Appendix 2 gives logs of bores put down in search of coal at Port Keats, Cape Ford, Anson Bay, and Cliff Head in the early part of the century.

We wish to thank Australian Aquitaine Petroleum Pty Ltd for their help while the field work was being undertaken and subsequently for providing information and for discussion on the geology. We would like to acknowledge co-operation with Geotechnics (Aust.) Pty Ltd, and also the air-photo interpretation work of R. Richard (BMR).

STRATIGRAPHY

Precambrian rocks crop out along the eastern margin of the basin. These have recently been described by Morgan et al. (1970). The oldest dated outcropping rocks above the Precambrian in the Port Keats area are Permian; probable Permian sandstone overlies with angular unconformity Precambrian rocks about 8 miles north of Tom Turners Crossing (locality 612) and in the Docherty Hills (locality 600). No outcropping rocks in the Cambrian to Carboniferous interval are known, but Devonian and Carboniferous sediments were penetrated beneath the Permian in AAP Kulshill No. 1 Well (Duchemin & Creevey, 1966) and Carboniferous sediments in AAP Kulshill No. 2 (Creevey, 1966). The Permian sediments are disconformably overlain by Lower Triassic and Lower Cretaceous sediments, and by superficial Cainozoic deposits.

Complete sections through the Permian, Lower Triassic, and Lower Cretaceous succession cannot be measured because of low dips and discontinuous outcrop, and fossils are essential for understanding the outcropping stratigraphical sequence; only a small part of the sequence can be established by superposition. South of the Moyle River, a varied and fairly thick sequence has thus been established; north of the Moyle River, the exposed sequence is much thinner, and probably spans a much shorter time interval. Because the information about the outcropping sequence is so incomplete, we do not propose any new formal stratigraphical names. The names Sugarloaf Formation and Kulshill Formation have been introduced informally into the literature by Guillaume (1966) and Caye (1968) for the Permian sediments penetrated by Kulshill No. 1, Kulshill No. 2, and Moyle No. 1 wells.

The following account of the stratigraphy is divided into three parts: firstly, we describe the well-dated outcrops; secondly we describe the Permian section penetrated in AAP Kulshill No. 1, Kulshill No. 2, and Moyle No. 1 wells, and compare it with the exposed sequence; and finally, we describe the remaining outcrops whose ages are known poorly, and indicate their possible relations to the established exposed sequences and to the sequence in the wells.

Well-Dated Outcrops

KURIYIPPI HILLS

The oldest dated exposed Permian sediments were found at locality 627 in the Kuriyippi Hills; here a few feet of limestone are overlain by 50 feet of thin-bedded and laminated micaceous siltstone and minor fine-grained clayey quartz sandstone with burrows. The basal limestone is a coquinite of brachiopods, pelecypods, gastropods, cephalopods, polyzoans, and foraminifers. Identifications of the brachiopods by J. M. Dickins and foraminifers by D. J. Belford (*see* Appendix 1 for details), and the polyzoans by R. K. Wass (1967) indicate correlation with the Lower Permian (Artinskian) Noonkanbah Formation of the Canning Basin (Thomas & Dickins, 1954; Thomas, 1958; Dickins, 1963). Between localities 627 and 625 the siltstone is overlain by a brown fossiliferous silty sandstone, which is correlated on the basis of fossils and lithology with the sandstone at Fossil Head. Polyzoans were obtained by Australian Aquitaine Petroleum Pty Ltd from seismic hole SP 323, at a depth of 144 feet at latitude 14°26′ and longitude 129°34′, 8 miles north-northeast of Fossil Head. Wass (1967) regards them in a general way as similar in age to the polyzoans from 627/1. The stratigraphical relationship of the seismic hole to 627/1 is not clear.

FOSSIL HEAD AND EQUIVALENT OUTCROPS

At Fossil Head (locality 502/1) there are 135 feet of brown fossiliferous silty sandstone with silt clasts and layers of siltstone and sandstone balls (Fig. 2). The basal 75 feet contains a rich marine fauna, first described by Etheridge Jr (1897; 1907), which indicates equivalence with the upper part of the Noonkanbah Formation or the lower part of the Liveringa Formation in the Canning Basin (Thomas, 1957; Dickins, 1963), which are late Artinskian or Kungurian (Lower Permian). This sandstone is also identified at localities 621 and 623, north and northwest of Fossil Head, at localities 624 and 625 in the Kuriyippi Hills, and

possibly at locality 620, a few miles southeast of Kulshill No. 1 well (Fig. 2). (Explanations for all symbols and abbreviations given in the Figures are shown in Fig. 3.)

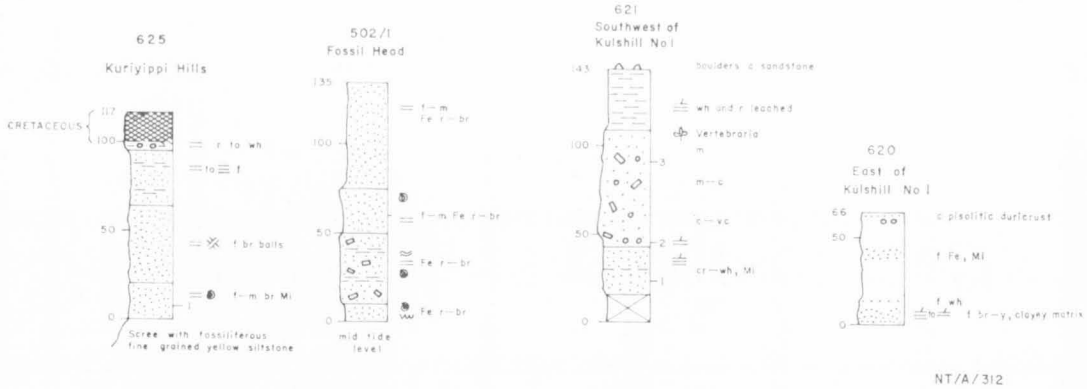


Figure 2. Lower Permian sections, Bonaparte Gulf Basin.

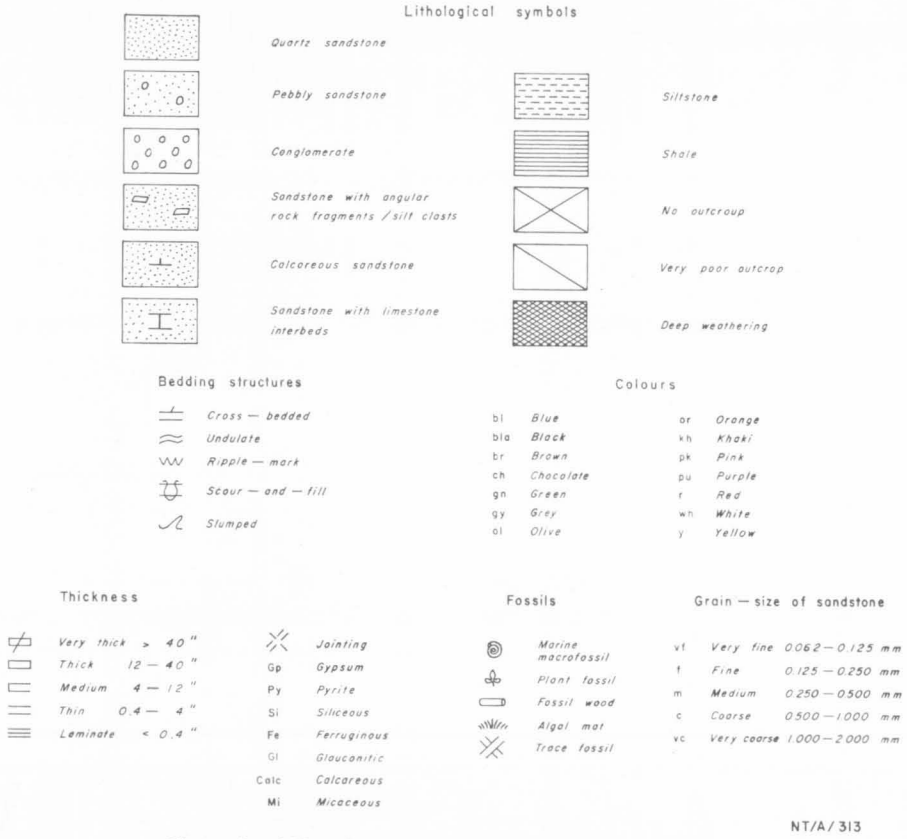


Figure 3. Abbreviations and symbols used in columnar sections.

Overlying the marine sandstone at Fossil Summit is 50 feet of cross-bedded ferruginous quartz sandstone with layers of quartzite pebbles and clay pellets. The only fossils are leaves (Thomas, 1957, p. 180) and indeterminate logs. These plant-bearing beds were seen also at Treachery Bay (locality 622) and in the hills west of Kulshill No. 2 well (locality 621).

COASTAL OUTCROPS OF UPPER PERMIAN AGE

Eight miles north along the coast from Cape Dombey (locality 512), 140 feet of fossiliferous burrowed sandstone with some interbedded claystone (Fig. 4) are exposed in low cliffs between low-tide level and a fault. Interpretation of the original lithology is hindered by deep weathering. Most of the beds are brown or yellow-brown, with an abundant matrix of clay and silt, numerous clay blebs, and lenses of coarser sandstone. Beds of fairly pure medium-grained quartz sandstone commonly grade into siltstone. Burrows, including *Rhizocorallium,* are common in the finer-grained beds. Marine shelly fossils are found mainly in the sandstone, and polyzoans in finer-grained bands. The fossils indicate correlation with the upper part (Hardman Member-Upper Permian) of the Liveringa Formation of the Canning Basin (Thomas, 1957). Thus a considerable time interval separates the marine horizon of Fossil Head from the higher marine horizon (Thomas & Dickins, 1954) and part of this interval is probably represented by breaks in the basal part of the higher horizon.

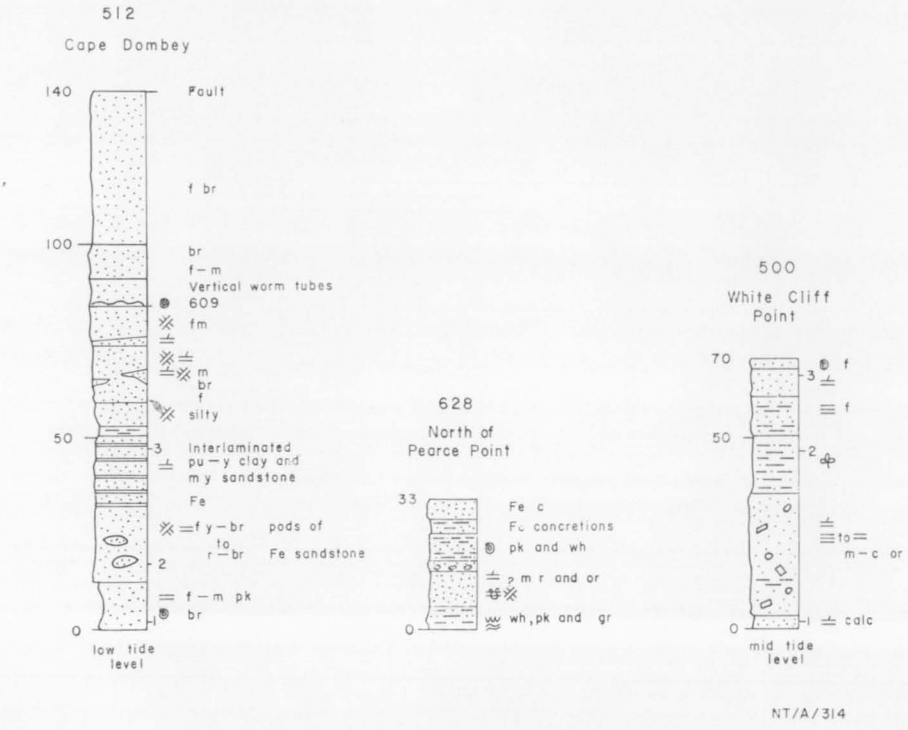


Figure 4. Upper Permian sections, Bonaparte Gulf Basin.

Other Upper Permian outcrops are found along the coast between Pearce Point (locality 628) and Tchindi Beach; at White Cliff Point (locality 500) and southwestward; south (locality 506) and north (locality 512) of Cape Dombey; and possibly at Cape Ford (locality 520). Inland, these beds underlie the Port Keats airstrip—this is a richly fossiliferous locality—and are exposed in places along the foot of the Sugarloaf Range. Erosional breaks apparently in the basal part of the Upper Permian beds were found at White Cliff Point (Fig. 4; Pl. 11, fig. 1), and north of Pearce Point (locality 628) (Fig. 4). At locality 628, the basal exposed siltstone is overlain along a deeply channelled surface by 9 feet of cross-bedded sandstone, which in turn is overlain by 2 feet of quartz pebble conglomerate containing fragments of sandstone up to 4 inches across. The conglomerate is succeeded by laminated siltstone with fenestellid polyzoans. Thomas (1957) listed a rich Upper Permian fauna consisting mainly of brachiopods, molluscs, and polyzoans from localities along the coast near Port Keats and from Port Keats airstrip and the Sugarloaf Range. He referred these to two assemblanges, C (the inland ones) and D (the coastal ones), and considered that D was possibly younger, but we consider them to be possible lateral equivalents.

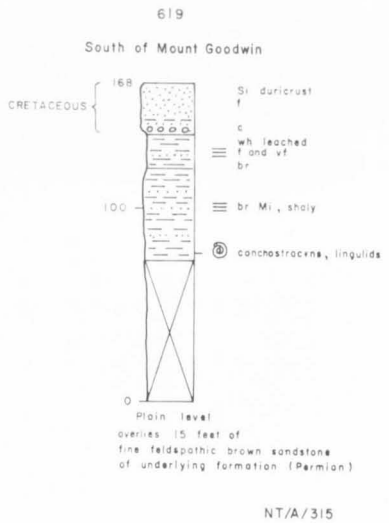


Figure 5. Triassic sequence south of Mount Goodwin.

OUTCROPS OF PROBABLE LOWER TRIASSIC AGE

Laminated micaceous sandy siltstone and shale are exposed at locality 619 (Fig. 5), south of Mount Goodwin, and near Cape Hay at the western entrance of Port Keats (locality 501). There are 12 feet of siltstone and shale with an exposed top at locality 501, and 60 feet, additionally with fine-grained sandstone, at locality 619; they overlie, above a covered interval, brown sandstone, presumably Upper Permian, and are unconformably overlain by 30 feet of duricrusted conglomeratic sandstones, presumably Cretaceous. The Triassic sediments are grey when fresh; the siltstone and shale weather buff, and the sandstone white. At Cape Hay and Tree Point, these rocks are distinctively cross-laminated. The sets are long and the dip of the cross lamination is low (Pl. 11, fig. 2). Lingulid brachiopods and vertebrate remains were collected at Cape Hay, lingulids and

estheriid conchostracens at locality 619, and lingulids, estheriids, and indeterminate plants at locality 519. The estheriid described by Etheridge Jr (1907, p. 11, pl. 8, fig. 11) apparently came from the interval 102 to 342 feet in the first three Port Keats bores near Cape Hay. Examination by J. M. Dickins suggests the estheriids comprise a single variable group, and generally resemble those from the Lower Triassic Blina Shale of the Canning Basin and also those from the Triassic outside Australia. Similar forms are known from the Permian (not, however, in the Port Keats area), but the absence of characteristic Permian conchostracans, in particular leaiids, suggests that these beds are Triassic. The specimens have been forwarded to P. Tasch, Wichita State University, Kansas, for detailed study. P. J. Jones (pers. comm.) has recorded conchostracans from Arco Petrel No. 1 at 10,512 feet (Core 8) and 10,550-10,600 feet (cuttings) which are similar to those from the Port Keats area and from the Lower Triassic Blina Shale (Canning Basin) and Kockatea Shale (Perth Basin). The lingulids do not indicate a precise age, but are valuable, with the brackish water estheriids, in indicating probable deposition in a brackish estuary or bay. Following Brunnschweiler (1954) and Thomas (1957), we correlate this sequence with the Blina Shale of the Canning Basin, whose age is now regarded as Lower Triassic (Veevers & Wells, 1961; Balme, 1963; 1969; Cosgriff, 1965).

Previously this Triassic sequence was recorded at Cape Hay, Tree Point, and in the Cape Dombey area (Thomas, 1957). In our opinion, the beds at Cape Dombey and immediately north of Cape Dombey are probably Lower Cretaceous, because, although deeply weathered, they consist of barren blocky claystone, distinct from the Triassic siltstone or shale. In addition, the dips in the Lower Cretaceous sediments of the Barthelemy Hills indicate that these rocks would probably reach sea level at Cape Dombey.

Our work shows that Lower Triassic sediments are probably widely distributed in the Sugarloaf Range. East of Mount Goodwin, at locality 519, in a gully near the track running east from Port Keats, are exposed 20 feet of yellow-brown laminated micaceous sandstone and siltstone, with lingulids and probable conchostracans and plants.

The Triassic sediments are structurally concordant with the underlying Upper Permian sequence, but this does not rule out the possibility of a hiatus and regional discordance.

OUTCROPS OF LOWER CRETACEOUS AGE

Lower Cretaceous marine fossils were found at two localities (Fig. 6). In the uppermost 12 feet of a section measured in the Barthelemy Hills (locality 605), belemnites and Radiolaria were found in a sandy micaceous shale which overlies a 6-inch pebbly sandstone; and at Mount Greenwood, belemnites were found in silty sandstone near the top of the measured section (locality 513). A. R. Lloyd has studied the shale from the Barthelemy Hills and has prepared the following: 'a sample of porcellanite (605/1) from the Barthelemy Hills, 5-6 miles east of Cape Dombey on the Cape Scott 1:250,000 Sheet area (latitude 13°56′S, longitude 129°49′E), was found to contain, in thin section, a rich radiolarian fauna. This fauna is made up of an abundance of *Arachnosphaera exilis* (Hinde, 1893) with smaller numbers of *Dictyomitra* (*Dictyomitrella*) sp. *B* and *Coscinomma* (*Cos-*

cinomma) sp. A similar fauna has been found in the Mullaman Beds around Darwin which are uppermost Albian or lowermost Cenomanian, and to the east of Newcastle Waters' (Lloyd, 1967). The Mount Greenwood belemnites were first recorded by Noakes (1949) and also mentioned by Noakes, Öpik, & Crespin (1952). The exposures at locality 513 seem to form a single unit, so that they are all regarded as Lower Cretaceous. The field relations at Mount Greenwood (which stands 245 feet above the plain) are complicated by mass movement of the claystone within the section, so that except at the top, where the strata are horizontal, the strata dip into the hillside at angles from 20° to 30°, giving the appearance of a syncline. Thus the estimated thickness of 160 feet of exposed strata is possibly excessive. At locality 605, in the Barthelemy Hills, the Lower Cretaceous section is silicified to form a duricrust, and overlies sandstone containing silt clasts which, by comparison with other rocks in the area, is regarded as Permian. The development of a siliceous duricrust is characteristic of other, barren sediments in the area regarded as Lower Cretaceous.

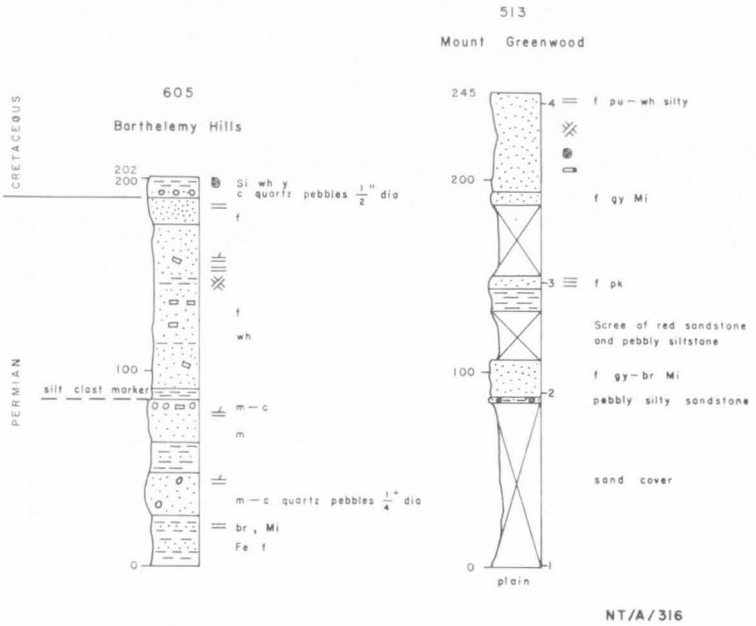


Figure 6. Sections of marine Cretaceous rocks.

Permian and Mesozoic Section in Australian Aquitaine Petroleum Wells

Kulshill No. 1 Well

According to the unpublished report of Duchemin & Creevey (1966), the AAP Kulshill No. 1 Well penetrated 180 feet of Mesozoic and 5995 feet of Lower Permian strata, underlain by Lower Carboniferous strata (Fig. 7). The Lower Permian rocks were referred to two new formations in the Port Keats Group. The lower formation, the Kulshill Formation, first used in published literature by Caye (1968), was subdivided into three parts: in ascending stratigraphical order, silicified sandstone from 5965 to 4765 feet; microconglomeratic shale from 4765

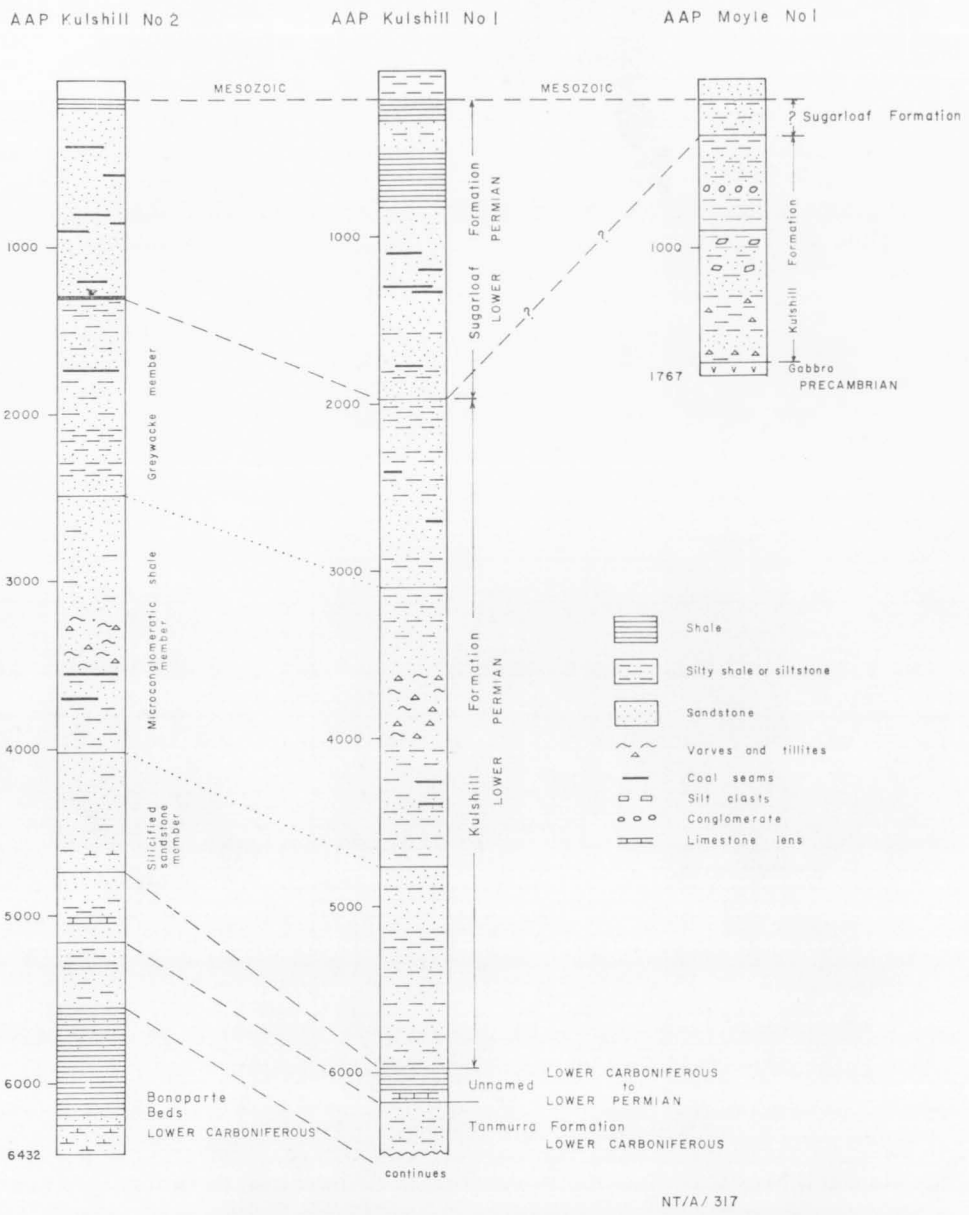


Figure 7. Generalized sequences in AAP Kulshill Nos 1 and 2, and Moyle No. 1.

to 3110 feet, subdivided into shaly sandstone (4765-4025 feet), tillite* (4025-3590 feet), and sandstone-shale (3590-3110 feet); and greywacke from 3110 to 1965 feet. The overlying Sugarloaf Formation (1965-180 feet), first used in the literature by Guillaume (1966), was subdivided into sandstone (1965-835 feet)

* The sediment described as tillite in the well reports might perhaps be rather referred to as a tillitic sediment.

and shale (835-180 feet). At the very base of the Lower Permian sequence is an unnamed unit, 210 feet thick (6175-5965 feet), of light-grey sandstone overlain by black shale with numerous thin biomicrite (limestone) beds. 'Foraminifera, ostracods, and conodonts extracted from cuttings between 6060′ and 6100′ suggest an upper Viséan to lower Namurian age for the sequence. However, spore and pollen analysis of Core 21 at the bottom of the formation shows a mixture of typical Lower Carboniferous and exclusively Permian and above, with possible Upper Carboniferous (Autunian-Stephanian) types. It is suggested that this formation may represent Lower Permian reworking of Lower Carboniferous and possibly Upper Carboniferous sediments' (Duchemin & Creevey, 1966, p. 28).

The Lower Permian sequence of this well is in part possibly glacial, as indicated by tillitic rocks (4025-3590 feet and at 5846 feet), and varves (5182 feet, and within the interval 4765-3110 feet). Coal bands occur intermittently between 4500 feet and 1000 feet, and marine fossils (polyzoans and crinoid ossicles) from near the top (400-800 feet). Virtually the entire sequence contains spores and pollen which indicate a Lower Permian age. 'The Sugarloaf is the only Permian Formation containing marine evidence. It becomes deltaic at the base' (Duchemin & Creevey, 1966, p. 1).

KULSHILL NO. 2 WELL

Kulshill No. 2 Well, drilled to a depth of 6432 feet, penetrated a Permian section similar to that in Kulshill No. 1 Well (Fig. 7). Unnamed Lower Carboniferous to Permian beds between 4745 and 5155 feet have a thickness of 410 feet compared with 210 feet in Kulshill No. 1 Well. The unnamed beds contain a mixture of Lower Carboniferous foraminifers and Permian and possibly Upper Carboniferous (?Westphalian) spores, which as in Kulshill No. 1 Well, are interpreted as a Lower Permian reworking of Lower Carboniferous and possibly Upper Carboniferous sediments (Creevey, 1966). The overlying Lower Permian Kulshill Formation between 1300 and 4745 feet is subdivided into a basal silicified sandstone member, 4020-4745 feet, a microconglomeratic shale member, 2488-4020 feet, with tillite between 3190 and 3525 feet, and a greywacke member, 1300-2488 feet. The upper part of the microconglomeratic shale member is considerably sandier than at Kulshill No. 1 Well, and is characterized by a thicker upper sandstone unit and a thinner tillitic unit. Creevey (1966) notes that the lithological distinctions between the members of the Kulshill Formation are not as clear as in Kulshill No. 1 Well, and that the lower boundary of the formation is not well defined. The Sugarloaf Formation, 104-1300 feet, which overlies the Kulshill Formation, contains a lower sandstone member, 154-1300 feet, and an upper shale member, 104-154 feet. Coal is more common in the sandstone member than in Kulshill No. 1 Well. The overlying shale member is reduced in thickness by erosion because of the higher structural position of Kulshill No. 2 compared to that of Kulshill No. 1 Well, and is overlain unconformably by Mesozoic sandstone.

MOYLE NO. 1 WELL

In Moyle No. 1 Well, sediments identified as the microconglomeratic Member of the Kulshill Formation, 900-1698 feet, overlies Precambrian gabbroic basement rock (Fig. 7). The microconglomeratic member consists of a poorly sorted tillite and shales between 1277 and 1698 feet, at the base, and an overlying micro-

conglomeratic sandstone and siltstone between 900 and 1277 feet. The micro-conglomeratic member is overlain by the greywacke member of the Kulshill Formation; the latter is penetrated between 344 and 900 feet. Overlying the Kulshill Formation, at 117 to 344 feet in the well, is a sandstone identified by Brophy (1966) as Lower Permian Sugarloaf Formation. Evidence from spores may, however, indicate a post-Permian age for the sandstone (Brophy, 1966). The uppermost beds in the well consist of Mesozoic sandstone, 60-117 feet, and soil cover, 0-60 feet.

Interpretation of the Port Keats (Cape Hay), Cape Ford, Anson Bay, and Cliff Head Bores

Original data on bores at Port Keats, Cape Ford, Anson Bay, and Cliff Head, put down in search of coal in the early part of the century, are scattered in a number of early publications. For convenience the original logs are reproduced in Appendix 2, together with a brief historical account of the bores and the references from which the information has been obtained.

The Triassic shale and sandstone and the Upper Permian marine beds are readily recognizable in the Port Keats Bores (*see also* Thomas, 1957, p. 181). In No. 1 Bore, the base of the Triassic unit can be placed at 342 feet, or slightly lower at 360 feet where the first coaly bed is reported. The boundary is placed higher than suggested by Etheridge Jr (1907, p. 12) or by Thomas (1957, p. 181) because the green fossiliferous sandstone at 469 feet corresponds to the yellow-brown fossiliferous sandstone reported from the surface outcrops. In places this sandstone could be described as green rather than yellow. In No. 2 Bore the base of the Upper Permian marine beds can be placed at 725 feet at the top of a *Glossopteris*-bearing shale band and below the brachiopod reported by Etheridge Jr (1907, p. 12) at 715 feet. No. 4 Bore, the deepest of the bores, after penetrating plant-bearing beds with coal, probably entered beds equivalent to the Fossil Head horizon and the underlying shale at about 1319 feet, being completed in a fossiliferous limestone at 1505 feet (possibly equivalent to the limestone at locality 627).

The Cape Ford No. 2 Bore may have begun in the Upper Permian marine beds, although there is no clear evidence for this, and then entered the lower sandstone unit found north of the Moyle River in which it was completed. The Anson Bay and Cliff Head Bores apparently penetrated only this lower sandstone unit, the Cliff Head Bore being completed in hard 'granite' at 728 feet.

Poorly Dated Outcrops

Keep Inlet Beds

Glover, Richardson, & McGilvray (1955) proposed the name Keep Inlet Beds for Permian tillitic sediments outcropping near tidal flats on the southern margin of Joseph Bonaparte Gulf; the name was formalized by Veevers & Roberts (1968). The beds are poorly exposed, and consist of feldspathic and lithic sandstone, locally pebbly, in situ, and a heterogeneous suite of rock fragments ranging from pebbles to boulders 3 feet across of orthoquartzite, granite, granodiorite, porphyry, schist, and subgreywacke which are thought to be glacial erratics. It is possible that these erratics have weathered from beds equivalent to the tillitic

part of the Kulshill Formation in Kulshill No. 1, Kulshill No. 2, and Moyle No. 1 Wells. Veevers & Roberts (1968) identified 578 feet of coarse-grained lithic sandstone and micaceous silty shale from the interval 60 to 638 feet in Bonaparte No. 1 Well as Keep Inlet Beds on the basis of the lithology of the sandstone and the presence of Lower Permian spores.

OUTCROPS SOUTH OF THE MOYLE RIVER

Table Hill. On the south side of Table Hill 415 feet of predominantly quartz sandstone with minor siltstone and conglomerate are exposed, capped by 25 feet of beds with a siliceous duricrust (locality 503, Fig. 8). No fossils were found. The basal 115 feet differs from the rest in containing siltstone with 'floating sand grains' (i.e. sand grains scattered through a finer matrix), and bands of scattered pebbles and cobbles in a finer-grained matrix; these may be an indication of ice activity in the area. The sediments exposed in the interval 200-415 feet are similar lithologically to those in the mesas 6 miles to the north-northwest (locality 626), described below, and the siliceous cap is probably a remnant of the widespread Lower Cretaceous. By comparison with the section in the sub-surface, this sequence is probably Permian.

Locality 626, in eastern part of Kuriyippi Hills. At locality 626, 350 feet of cross-bedded quartz sandstone with abundant feldspar and siltstone clasts, and minor siltstone are overlain by 15 feet of ferruginized claystone and sandstone. Gravity surveys (Derrington, Warren, & Burbury, 1957; Burbury, 1958; Australian Aquitaine Petroleum Pty Ltd (AAP), 1964; 1966; Langron, 1962) and seismic surveys (AAP, 1964; 1966) indicate a major fault with downthrow to the west. The fault is probably indicated in the air photographs by linear features between localities 626 and 627. The section at locality 626 therefore is probably older than that at 627; its lower limit is not known. If, as appearances indicate, it is part of the Permian sequence, it would best be placed above the possibly glacial beds of Table Hill.

Locality 505, 14 miles west of Tom Turners Crossing. At locality 505, a poorly exposed sequence of ferruginized coarse pebbly sandstone with logs is overlain by ferruginized siltstone and fine micaceous sandstone, with a few bands of fine- to medium-grained sandstone. The sequence has a low westward dip. These rocks are probably Permian but their age within this limit is unknown.

Localities 514 and 523, 6 miles west of Tom Turners Crossing. In a ridge 6 miles west of Tom Turners Crossing, pebbly feldspathic quartz sandstone and arkose unconformably overlie granite, which is exposed on the plain (locality 524). The feldspathic quartz sandstone is medium-grained, crudely laminated, purple and white, and contains pebbles of clear (granitic) quartz. In some beds the sandstone is friable, but in most it is silicified. The arkose consists of quartz and feldspar up to the size of pebbles.

The sequence of granite unconformably overlain by feldspathic quartz sandstone and arkose is essentially the same as that in the Litchfield area, 60 miles northeastward. The Litchfield arkose is Middle Cambrian (Malone, 1962; Gatehouse, 1968) so that the arkose west of Tom Turners Crossing is possibly also of Middle Cambrian age. This is no more than a speculation, and fossils should be sought in the arkose and associated sandstones at this locality.

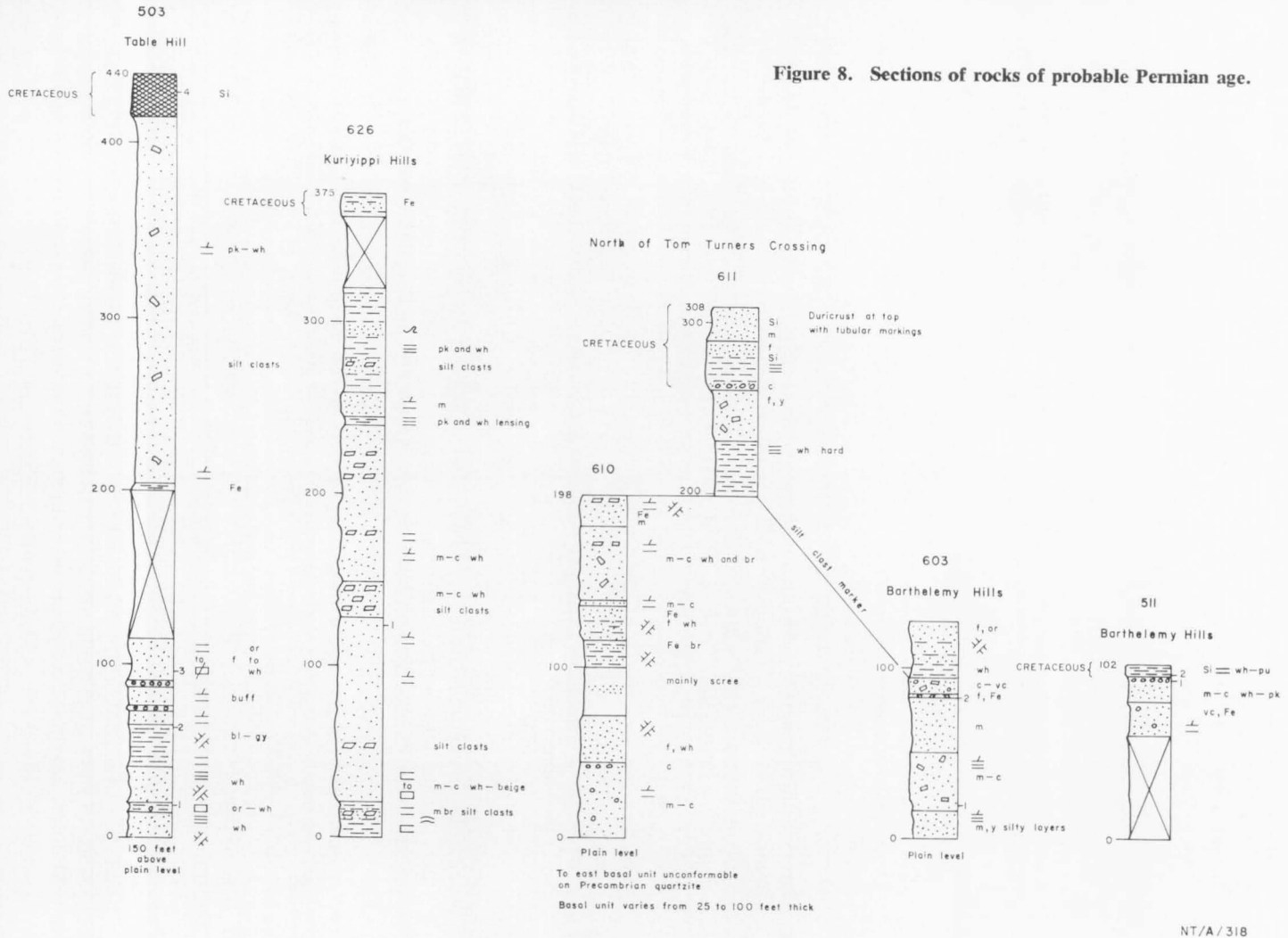


Figure 8. Sections of rocks of probable Permian age.

NT/A/318

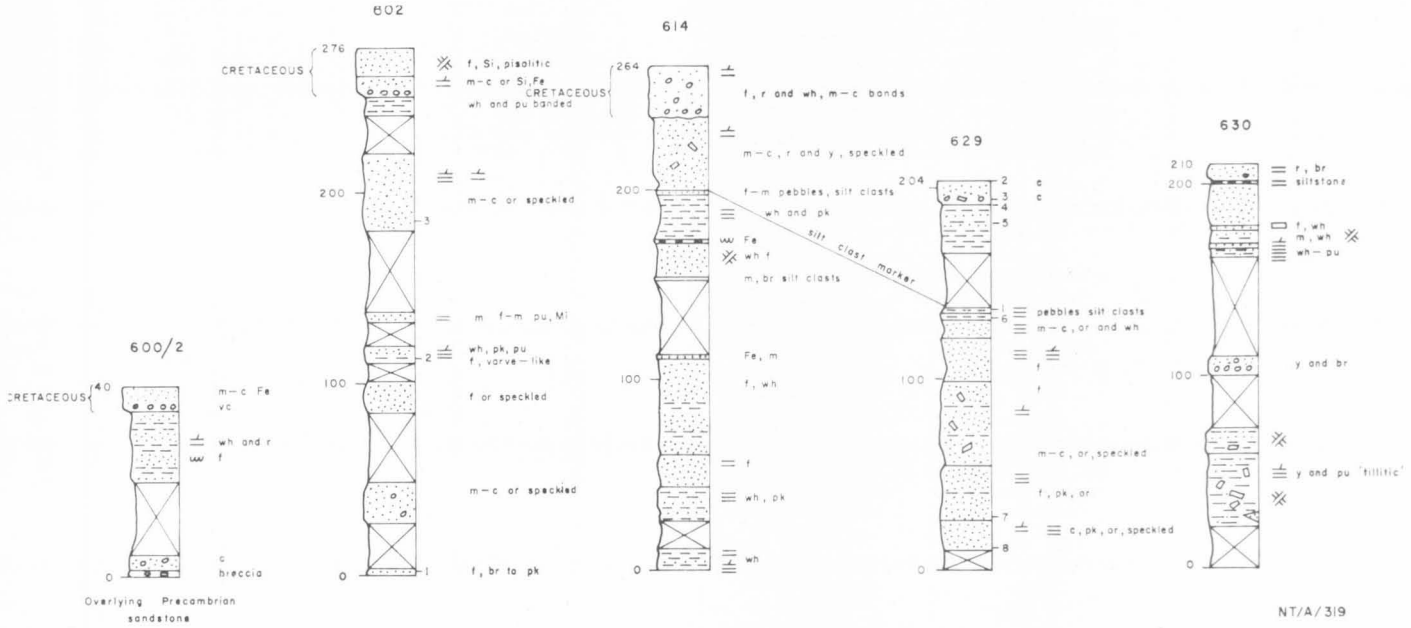


Figure 9. Sections of rocks of probable Permian age, Docherty Hills.

OUTCROPS NORTH OF THE MOYLE RIVER

Localities 600, 602, and 630. Evidence of possible glacial activity is seen at localities 600, 602, and 630 in the Docherty Hills. At locality 602, 10 feet of varve-like fine-grained sandstone and siltstone are interbedded in a sequence of sandstone and siltstone (Fig. 9). The varve-like sediments have not been recognized in either of the other localities (600 and 630) containing sediments of possible glacial origin.

In the section at locality 630 the basal beds consist of irregularly bedded 'tillitic' sediments containing pebbles and cobbles and irregular sand lenses, and are overlain by sandstone and siltstone. Both sections 602 and 630 are capped by ferruginous duricrust. Siltstone containing 'floating sand grains' occurs at locality 600.

Localities 603, 605, 611, 614, and 629. Elsewhere north of the Moyle River, the unfossiliferous sediments consist of sandstone and siltstone similar to that measured in the mesa (locality 626) 7 miles north-northwest of Table Hill. Sandstone predominates, but the proportion of siltstone and the amount of siltstone clasts varies from place to place. The sandstones are frequently cross-bedded or laminated, and some contain burrows.

In these sections a distinct silt-clast conglomerate horizon has been identified (Figs 6, 8, 9). The sequence above the silt-clast marker overlaps the fault at locality 600 in the Docherty Hills; the fault cuts the sequence below the marker bed, indicating tectonic activity during Permian time.

Lithologically the sandstone above the silt-clast marker horizon in the Barthelemy Hills (603 and 605) resembles the lowermost sandstone at White Cliff Point (locality 500), and the dip is consistent with their equivalence. The sandstone at White Cliff Point is overlain by the Upper Permian marine beds, indicating that not only is the Permian sequence north of the Moyle River thin, but the fossiliferous part of the Lower Permian sequence south of the Moyle River (including the marine beds at Fossil Head and the limestone at locality 627) has not been recognized.

Three interpretations of these data from north of the Moyle River are suggested (Fig. 10):

1. The sequence below the silt-clast marker is equivalent to the sandstone in the mesas north-northwest of Table Hill, and this is overlain with hiatus by the Upper Permian marine beds and lateral equivalents which away from the coastline lack marine fossils. Evidence supporting this interpretation comes from the sections at localities 611 and 614, where sandstone above the silt-clast horizon is greenish and has distinctive clay blebs similar to the sandstone of the Upper Permian beds. High beds also overlap the fault, suggesting that the beds below the marker horizon are of early Permian age (Fig. 10A).

2. All the strata north of the Moyle River are Upper Permian, and except near the coast are largely non-marine. The lower part of the sequence found south of the Moyle River would thus be overlapped. The 'tillitic' rocks argue against this explanation unless they are isolated remnants for which there is no evidence (Fig. 10B).

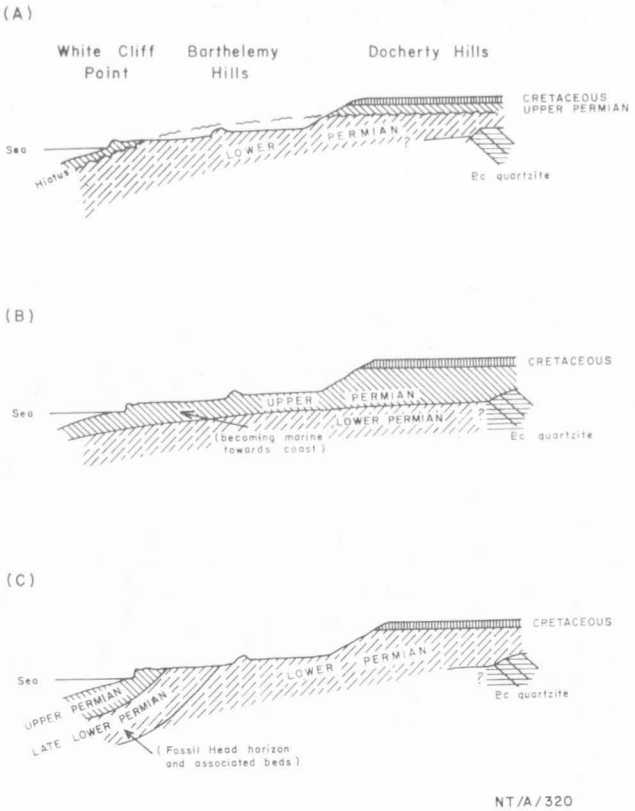


Figure 10. Interpretation of geological relationships north of the Moyle River.

3. The fossiliferous part of the Lower Permian sequence south of the Moyle is to be found between the Barthelemy Hills and White Cliff Point but is not exposed, and in this area is affected by an unidentified fault or monocline down to the west (Fig. 10C).

Red Cliff (521) and Cliff Head (522). Isolated outcrops were examined at Red Cliff and Cliff Head. At Cliff Head laminated yellow medium-grained sandstone is disconformably overlain by a breccia of sandstone fragments (Pl. 12, figs 1 and 2). No fossils were found and the age is not clear although the probable Permian north of the Moyle River appears to be represented in the sequence.

GEOLOGICAL HISTORY

Along the northeastern margin of the Bonaparte Gulf Basin probable Permian sandstone overlies Precambrian rocks with angular unconformity. No outcrops of intermediate age have so far been recognized. The geological history of the Permian and Mesozoic sequence begins with the accumulation of sandstone and siltstone in a deltaic environment in the late Palaeozoic. Drilling at Kulshill Nos

1 and 2 has shown, however, that Devonian and Carboniferous rocks occur below a thicker Permian sequence away from the margin. The Devonian and Carboniferous are controlled by an important north-south fault line (the Moyle River Fault). The early Permian sequence formed in a paralic environment—cross-bedding is very common and a few thin coal seams were developed. Possible ice activity is indicated by scattered outcrops of poorly sorted (tillitic) sediments and varve-like strata. The ice may, however, have been confined to the hinterland.

In late Lower Permian sinking led to marine transgression. Remnants of the marine sequence have been identified only west of the Moyle River Fault. In the early Upper Permian, the sea withdrew and a plant- and coal-bearing sequence was laid down. In the Upper Permian this was followed in turn by another marine transgression with local hiatus near the base. North of the Moyle River the transgression may have overlapped the Moyle River Fault. East of the fault evidence of intra-Permian faulting is shown near the eastern margin of the basin (Tom Turners Fault). The laminated siltstone and fine sandstone considered to be of Triassic age were formed in brackish estuarine or bay conditions apparently disconformably on the Permian.

The Cretaceous sequence is separated from the Triassic by a long hiatus although the dips differ little. The Cretaceous rocks are, however, much more widespread than earlier strata and this forms a basis for their separation from the Bonaparte Gulf Basin sequence. They were deposited on a very extensive surface of low relief in an environment paralic to the east and marine to the west. The sequence has thin conglomerate at the base which is overlain by fine sandstone and claystone. After the Cretaceous transgression a long period of planation and weathering ensued during which the present surface and duricrust were formed.

REFERENCES

AUSTRALIAN AQUITAINE PETROLEUM PTY LTD, 1964—Kulshill seismic and gravity Survey. Report by Compagnie Générale de Géophysique to Australian Aquitaine Petroleum Pty Ltd (Unpubl.).

AUSTRALIAN AQUITAINE PETROLEUM PTY LTD, 1966—Moyle River seismic and gravity Survey. Report by Compagnie Générale de Géophysique to Australian Aquitaine Petroleum Pty Ltd (Unpubl.).

BALME, B. E., 1963—Plant microfossils from the Lower Triassic of Western Australia. *Palaeontology*, 6, 12-40.

BALME, B. E., 1969—The Permian-Triassic boundary in Australia. *Geol. Soc. Aust. Spec. Publ.* 2, 99-112.

BROPHY, F., 1966—Well completion report, Aquitaine Moyle No. 1. Report to Australian Aquitaine Petroleum Pty Ltd (Unpubl.).

BRUNNSCHWEILER, R., 1954—Mesozoic stratigraphy and history of the Canning Desert and Fitzroy Valley, Western Australia. *J. geol. Soc. Aust.*, 1, 35-54.

BURBURY, J. E., 1958—Regional gravity survey, Bonaparte Gulf Basin, North-Western Australia. *Mines Administration Pty Ltd Rep.* N.T. 2/46 (Unpubl.).

CAYE, J. P., 1968—The Timor Sea—Sahul Shelf area. *APEA J.*, 8 (2), 35-41.

COSGRIFF, J. W., 1965—A new genus of Temnospondyli from the Triassic of Western Australia. *J. Roy. Soc. W. Aust.*, 48 (3), 65-90.

CREEVEY, K., 1966—Well completion report, Aquitaine Kulshill No. 2. Report to Australian Aquitaine Petroleum Pty Ltd (Unpubl.).

DERRINGTON, S. S., WARREN, A., and BURBURY, J. E., 1957—Preliminary geological and geophysical report, Port Keats area. Northern Territory, 1956. *Mines Administration Pty Ltd Rep.* N.T./BG/27 (Unpubl.).

DICKINS, J. M., 1963—Permian pelecypods and gastropods from Western Australia. *Bur. Miner. Resour. Aust. Bull.* 63.

DUCHEMIN, A. E., and CREEVEY, K., 1966—Well completion report, Aquitaine Kulshill No. 1. Report to Australian Aquitaine Petroleum Pty Ltd (Unpubl.).

ETHERIDGE, R., JR., 1897—The Permo-Carboniferous fossils of Treachery Bay, Victoria River, South Australia. *S. Aust. parl. Pap.*, 127 (1896), 14-16.

ETHERIDGE, R., JR, 1907—Official contributions to the palaeontology of South Australia. *S. Aust. parl. Pap.*, 55 (1906), Suppl., 1-21.

GATEHOUSE, C. G., 1968—Early Middle Cambrian trilobites of the Litchfield Area, N.T. *Bur. Miner. Resour. Aust. Bull.*, 80, 47-57.

GLOVER, J. J. E., RICHARDSON, L. A., and MCGILVRAY, E., 1955—Geological and geophysical report on the Keep River area, Bonaparte Gulf Basin. Report for Assoc. Aust. Oilfields (Unpubl.).

GUILLAUME, R. E. F., 1966—Petroleum geology in the Bonaparte Gulf Basin, N.T. *8th Commonw. Min. Metall. Congr.*, 1965, 5, 183-96.

LANGRON, W. J., 1962—Notes on a gravity survey of the Darwin-Katherine region. *In* DUNN, P. R., Alligator River—1:250,000 Geological Series. *Bur. Miner. Resour. Aust. explan. Notes* D/53-1.

LLOYD, A. R., 1967—Lower Cretaceous Radiolaria from the Northern Territory of Australia. *Bur. Miner. Resour. Aust. Bull.* 92, 115-31.

MALONE, E. J., 1962—Pine Creek 1:250,000 Geological Series. *Bur. Miner. Resour. Aus. explan. Notes* D/52-8.

MORGAN, C. M., SWEET, I. P., MENDUM, J. R., and PONTIFEX, I. R., 1970—Geology of the Precambrian and Antrim Plateau Volcanics in the Delamere, Fergusson River, Port Keats, and Cape Scott 1:250,000 Sheet areas. *Bur. Miner. Resour. Aust. Rec.* 1970/3 (Unpubl.).

NOAKES, L. C., 1949—A geological reconnaissance of the Katherine-Darwin region, Northern Territory. *Bur. Miner. Resour. Aust. Bull.* 16.

NOAKES, L. C., ÖPIK, A. A., and CRESPIN, I., 1952—Bonaparte Gulf Basin, northwestern Australia: a stratigraphical summary with special reference to the Gondwana System. *Congr. int. geol. 19 ième Sess. Alger; Symposium sur les series de Gondwana,* 91-106.

THOMAS, G. A., 1957—Oldhaminid brachiopods from the Permian of Northern Australia. *J. palaeont. Soc. India,* D. M. Wadia Jubilee Number, 2, 174-82.

THOMAS, G. A., 1958—The Permian Orthotetacea of Western Australia. *Bur. Miner. Resour. Aust. Bull.* 39.

THOMAS, G. A., and DICKINS, J. M., 1954—Correlation and age of the marine Permian formations of Western Australia. *Aust. J. Sci.*, 16 (6), 219-23.

VEEVERS, J. J., and ROBERTS, J., 1968—Upper Palaeozoic rocks, Bonaparte Gulf Basin of Northwestern Australia. *Bur. Miner. Resour. Aust. Bull.* 97.

VEEVERS, J. J., and WELLS, A. T., 1961—The geology of the Canning Basin, Western Australia. *Bur. Miner. Resour. Aust. Bull.* 60.

WASS, R. E., 1967—Permian Polyzoa from the Port Keats District, Northern Territory. *Proc. Linn. Soc. N.S.W.*, 92 (2), 162-70.

APPENDIX 1. PALAEONTOLOGICAL REPORTS

FORAMINIFERA FROM SAMPLE 627/1, BONAPARTE GULF BASIN

by D. J. Belford

This outcrop sample, collected at latitude 14°27′S, longitude 129°43′E, contains Foraminifera, Bryozoa, Algae, molluscan (pelecypod) fragments and spines. Foraminifera occurring are:

Meandrospira australae (Crespin & Belford)
Trepeilopsis australiensis Crespin
Nodosaria sp. cf. *N. tereta* Crespin
Geinitzina sp.
Calcitornella sp.
Tetrataxis ? sp.

This assemblage indicates a Permian age for the sample. *Meandrospira australae* and *Trepeilopsis australiensis* have been recorded previously only from the Callytharra Formation, or from beds stratigraphically equivalent to this formation. However, knowledge of the stratigraphical distribution of foraminifera in the Australian Permian is incomplete, and this should not be taken to indicate that the sample is to be referred to the Sakmarian stage. Foraminiferal evidence alone indicates a general Lower Permian age (Sakmarian-Artinskian stages).

MACROFOSSILS FROM SAMPLE 627/1, BONAPARTE GULF BASIN

by J. M. Dickins

Location:

Latitude 14°27′S, longitude 129°43′E, 7.2 miles north-northwest of Table Hill.

Identifications:

Pelecypods
Cyrtorostra ? sp

Brachiopods
Indet. chonetid
Strophalosia sp. (similar to species in Madeline, Coyrie and Noonkanbah Formations (KLA 76)
Large indet. orthotetid

Conclusions:

Only a few species are represented. *Strophalosia* sp. seems to indicate correlation with Madeline Formation of the Carnarvon Basin, i.e. the lower part of the Byro Group and the Noonkanbah Formation of the Canning Basin.

APPENDIX 2. PORT KEATS BORES

After the visit to the area by H. Y. L. Brown, the Government Geologist of South Australia (Brown, 1895), drilling was commenced for coal in the Port Keats area in 1905. The history of the drilling is recorded by Jensen (1913). Four bores were drilled at Port Keats and only very thin seams of bituminous coal were encountered. In April 1907, the drill was moved to Cape Ford, Anson Bay, where two bores were drilled; the first to 475 feet, and the second to 1506 feet. Artesian water was met with but no payable coal. Another bore was put down at Cliff Head and three at Anson Bay between Cliff Head and Cape Ford. No coal of interest was found. Etheridge Jr (1907) described the cores, and also described foraminifers and polyzoans from the Port Keats bores. Crockford (1943) described polyzoans.

The publications containing the drilling logs are rare and not always accessible and the logs are reproduced here for convenience. No log has been found, however, for No. 1 Bore, Cape Ford, or for a third bore reported by Jensen at Anson Bay. The logs have been reproduced as in the original, including errors.

REFERENCES

BROWN, H. Y. L., 1895—Government Geologist's Report on explorations in the Northern Territory. *South Australia parl. Pap. No.* 82, 1895.

CROCKFORD, J. M. , 1943—Bryozoa from the Port Keats Bore, Northern Territory. *Proc. Linn. Soc. N.S.W.* 14 (4), 397-418.

JENSEN, H. I., 1913—Mineral report of the Department of Mines, Northern Territory. Report of the Administration for the year 1912, 69-90.

PORT KEATS NO. 1 BORE

The total depth reached was 375 feet. The foreman's record shows—

	ft.	in.
Surface soil and rubble	4	
Yellow sandstone	10	
Sandstone	17	
Soft friable shale	52	
Blue shale	19	
Green shale, with layers of sandstone	240	
Micaceous sandstone	18	
Brown shale, with small veins of coal	1	9
Sandstone	13	
Dark shale, with coal on faces	1	
	375 ft.	9 in.

PORT KEATS NO. 2 BORE

Was put down a few feet from No. 1, and has reached a depth of 736 feet. The foreman's record shows—

	ft.	in.
The same strata were pierced as in No. 1 down to	375	
Very friable micaceous sandstone	61	11
Black graphite (proved to be carbonaceous shale)	21	

	ft.	in.
Dark shale intersected with sandstone layers	10	6
Green fossiliferous sandstone	24	6
Disturbed sandstone, with fissures and shells	36	
Black argillaceous shale	21	
Firm blue shale intersected with thin layers of sandstone	22	
Hard calcareous sandstone and limestone with shells	17	
Soft decomposed sandstone making no core	78	
Firm carboniferous sandstone	5	
Very free loose friable sandstone, making no core	53	
Black good-looking shale	5	
Friable sandstone	6	
	736 ft.	

PORT KEATS BORE NO. 3

The following is the foreman's record—

	Depth ft.	in.	ft.	in.
Surface soil and rubble	3	0	—	
White cement	6	0	—	
Yellow soft sandstone	7	0	—	
Blue shale	12	0	28	6
Firm yellow sandstone	10	0	—	
Blue friable shale	26	0	—	
Firm red clay	6	0	—	
Blue shale with fossils	269	0	338	0
Grey sandstone, portions very friable	40	0	—	
Friable micaceous sandstone	59	0	—	
Black shale	20	0	—	
Dark shale intersected with limestone layers	10	0	—	
Green fossiliferous sandstone	63	0	—	
Black argillaceous shale	25	0	—	
Green sandstone, highly fossiliferous	19	0	—	
Hard limestone, fossiliferous	12	0	—	
Coarse friable quartzitic sandstone, with water-worn pebbles	139	0	725	0
Black sandy shale	6	0	—	
Friable quartzitic sandstone	78	9	—	
Alternate sandstone and shale layers	2	0	—	
Loose quartzitic sandstone	34	0	—	
Friable carboniferous sandstone	28	0	873	0
Alternate thin layers of shale and limestone	32	0	—	
Sandstone	13	0	—	
Thin alternate layers of shale and sandstone	2	0	—	
Carboniferous sandstone	20	0	940	0
Alternate layers of sandy shale and sandstone	40	0	—	
Free friable sandstone	41	0	—	
Dark fossiliferous sandy shale having a 1/16 in. vein of coal	13	0	—	
Loose friable sandstone	20	0	1054	0
Layers of sandy shale and limestone with pyrites	13	0	—	
Loose friable sandstone	6	0	—	
Porous laminated sandstone	39	0	—	
Friable sandstone	20	0	—	
Friable laminated sandstone	10	0	1142	0

PORT KEATS NO. 4 BORE

Surface to 3 ft.	Ironstone rubble
,, 13 ft.	Sandy clay
,, 15 ft.	Soft, light coloured clay
,, 16 ft.	Red clay

Surface to 36 ft.	Dark clay
,, 56 ft.	Blue clay
,, 66 ft.	Brown clay
,, 327 ft. 6 in.	Blue clay or shale
,, 350 ft.	Sandstone
,, 352 ft.	Brown shale
,, 422 ft.	Sandstone
,, 431 ft.	Shale with sandstone layers
,, 455 ft.	Dark shale intermixed with sandstone
,, 465 ft.	Green sandstone
,, 480 ft.	Green sandstone, dark shale, and sandstone layers
,, 488 ft.	Carbonaceous sandstone, very friable
,, 514 ft.	Sandstone
,, 553 ft.	Firm dark shale
	(Definite thickness of strata not given by foreman below this depth.)
570 ft.	Layers of blue mud
589 ft.	White sandy sediment
597 ft.	Sand filled up bore 23 ft. from bottom
602 ft. 6 in.	Loose sand
616 ft.	Loose sand; washed large amount of stone and some heavy gravel from inside casing
628 ft.	Extremely soft sandy formation
648 ft.	Soft sandy formation
669 ft.	Very soft, no water returning
679 ft.	Water returning, with sediment
707 ft.	Very soft sandstone
726 ft. 6 in.	Sandstone, extremely soft
736 ft. 6 in.	Sandstone, extremely soft
752 ft. 6 in.	Sandstone
766 ft. 6 in.	Sandstone
769 ft.	Sandstone
775 ft.	Soft sandstone
796 ft.	Soft sandstone
812 ft.	Layer of shale 810 ft. to 812 ft.
820 ft.	Grey sandy shale, with soft sandstone
833 ft. 6 in.	Very soft sandstone, with thin layers of shale
846 ft.	Very soft sandstone
860 ft.	Soft sandstone
869 ft.	Firm shale
884 ft.	Firm shale, with sandstone layers
894 ft.	Sandstone, firmer at 890 ft., sandstone to 895 ft., then 1 inch shale
910 ft.	Firm carbonaceous sandstone
921 ft.	Very soft carbonaceous sandstone
931 ft.	Firm carbonaceous sandstone
942 ft.	Sandstone and shale
959 ft.	Sandstone and shale, with pyritic balls
970 ft.	Sandstone and shale, with pyritic balls
973 ft.	Very soft sandstone, with carbonaceous streaks
981 ft.	Soft carbonaceous sandstone, with a little shale
990 ft.	Loose sandstone, absorbing large quantities of water
995 ft.	Very loose sandstone
1000 ft.	Very soft carbonaceous sandstone
1007 ft.	Very soft carbonaceous sandstone
1010 ft.	Soft sandstone, losing large quantity of water
1019 ft.	Very soft sandstone
1027 ft.	Sediment troublesome
1035 ft.	Very soft sandstone
1041 ft.	Very soft sandstone
1055 ft.	Very soft sandstone, with pyrites
1068 ft.	Very soft sandstone, with little shale

1086 ft.	Soft sandstone
1100 ft.	Soft sandstone
1118 ft.	Very soft sandstone
1122 ft.	Very soft sandstone
1132 ft.	Firm sandstone, with shale layers
1143 ft.	Very soft sandstone
1146 ft.	Very soft sandstone
1149 ft.	Soft sandstone
1157 ft.	Very soft sandstone
1178 ft.	Sandstone, with small veins of coaly matter
1185 ft.	Sandstone, with large pyritic balls and veins of shale
1200 ft.	Sandstone
1205 ft.	Sandstone, with veins of coaly matter
1215 ft.	Hard and soft layers of sandstone
1229 ft.	Shale and soft sandstone
1243 ft.	Sandy shale
1253 ft.	Sandy shale
1263 ft.	Sandy shale
1273 ft.	Firm sandstone, with shale layers
1282 ft.	Sandy shale
1291 ft.	Shale and sandstone
1301 ft.	Shale and sandstone
1310 ft.	Shale and sandstone
1319 ft.	Shale and sandstone, at 1314 ft. vein of coal
1329 ft.	Shale and sandstone
1434 ft.	Sandy shale
1351 ft.	Sandstone and shale, with pyrites
1357 ft.	Sandstone
1363 ft.	Sandstone and shale
1368 ft.	Sandstone with little shale
1379 ft.	Sandstone with dark shale
1392 ft.	Shale and sandstone, with pyritic balls
1404 ft.	Dark shale and sandstone
1425 ft.	Firm dark shale
1444 ft.	Firm shale
1464 ft.	Firm shale 1457 ft. to 1458 ft.. white pipeclay running into bore
1487 ft.	Firm shale
1505 ft.	Black shale to 1499 ft., white fossilized formation to 1505 ft. (Shell limestone)

CAPE FORD NO. 2 BORE

Depth in Bore				Strata
Ft.	In.		Ft. In.	
1	0	to	140 0	Sand, very hard crust at 57 ft.
140	0	to	169 0	Very soft chalky sandstone
169	0	to	301 0	Extremely soft sandstone
301	0	to	359 0	Soft black mud
359	0	to	370 6	Blue mud of shale
370	6	to	420 0	Soft sandstone
420	0	to	444 0	Soft sandstone with gravel
444	0	to	470 0	Sandstone and gravel
470	0	to	521 0	Soft sandstone
521	0	to	537 0	Very soft sandstone
537	0	to	562 0	Firmer sandstone
562	0	to	580 0	Soft sandstone
580	0	to	588 6	Soft sandstone with ironstone bends and blue sandstone
588	6	to	593 0	Dark sandstone
593	0	to	596 0	Hard shaly sandstone with very soft layers
596	0	to	611 0	Soft sandstone with very soft muddy shale
611	0	to	631 0	Sandstone and soft shale

631	0	to	648	6	Sandstone and black shale
648	6	to	651	6	Chiefly black shale, very hard pyrites ball at 650 ft.
651	6	to	740	0	Dark shale
740	0	to	744	0	Sandstone
744	0	to	750	6	Shale
750	6	to	785	0	Black shale
785	0	to	793	0	Hard fossil sandstone
793	0	to	795	0	Hard sandstone
795	0	to	813	0	Soft green sandstone
813	0	to	816	0	Dark shale
816	0	to	822	0	Sandy shale
822	0	to	832	0	Firm sandy shale
832	0	to	845	0	Dark shale
845	0	to	852	0	Few inches of hard sandstone, then 7 ft. of shale
852	0	to	869	0	Shale with thin layers of sandstone
869	0	to	891	0	Shale
891	0	to	901	6	Shale and sandstone bars
901	6	to	911	6	Soft shale
911	6	to	925	0	Shale and fossils
925	0	to	969	6	Shale fossils 966 ft. to 969 ft.
969	6	to	976	6	Sandy shale
976	6	to	1001	8	Sandstone and shale
1001	0	to	1039	6	Shale
1039	6	to	1044	6	Soft sandstone and shale
1044	6	to	1069	0	Very soft sandstone
1069	0	to	1095	6	Soft sandstone and shale, splash of coal at 1073 ft.
1095	6	to	1103	6	Soft sandstone
1103	6	to	1116	0	Very soft sandstone
1116	0	to	1123	0	Sandstone, firmer
1123	0	to	1126	6	Soft sandstone, some of it very soft
1126	6	to	1142	0	Soft sandstone
1142	0	to	1151	0	Very soft sandstone
1151	0	to	1204	0	Soft sandstone, coal matter 1150 ft. and 1167-1168 ft.
1204	0	to	1211	0	Dark shale, vein of coal matter at 1209 ft. 6 in.
1211	0	to	1275	0	Soft sandstone, with thin layers of sandy shale
1275	0	to	1300	0	Sandstone, with small veins of sandy shale
1300	0	to	1321	0	Sandstone, with little shale—coal veins at 1317 ft.
1321	0	to	1326	0	Coarse friable sandstone
1326	0	to	1330	0	Sandstone, coal matter 1329 ft. to 1330 ft.
1330	0	to	1335	0	Sandstone, pyritic balls
1335	0	to	1346	0	Sandstone and shale
1346	0	to	1358	0	Coarse sandstone, very friable
1358	0	to	1363	0	Very soft sandstone
1363	0	to	1375	0	Coarse friable sandstone, coal matter at 1374 ft.
1375	0	to	1384	0	Soft sandstone
1384	0	to	1393	0	Very soft sandstone, shale 1393 ft.
1393	0	to	1397	0	Soft sandstone and shale
1397	0	to	1404	0	Sandstone and shale
1404	0	to	1432	0	Friable sandstone, little shale
1432	0	to	1443	0	Sandstone
1443	0	to	1459	0	Soft sandstone, shale 1445 ft. to 1454 ft.
1459	0	to	1506	0	Sandstone

CLIFF HEAD NO. 1 BORE

Depth			Strata
ft.		ft.	
1	to	15	Red sand
15	to	60	Sandy kaolin
60	to	90	Yellow sand, occasional gravel beds
90	to	100	Coarse sand and gravel

100	to	124	White sand
124	to	132	Pipeclay and thin layers of red sandstone
132	to	140	Very soft white sandstone
140	to	296	Very soft dark sandy mud, some of it of a shale nature
296	to	298	Sandstone, 2 in. bar, very hard
298	to	346	Soft dark sandstone
346	to	362	Hard gravel beds mixed with layers of soft shale
362	to	384	Gravel and sandstone
384	to	438	Gravel and large water-worn stones
438	to	455	Soft white sandstone
455	to	492	Very soft sandstone and gravel beds
492	to	500	Slightly firmer sandstone
500	to	713	Very soft sandy strata
713	to	720	Soft sandy strata, with pyritic balls
720	to	728	Hard granite

ANSON BAY NO. 1 BORE

Strata	Depth Ft.	In.
Sea sand	12	0
Blue sandy mud	3	0
Sand	30	0
Blue sandy mud and shells	4	0
Very soft sandy clay	56	0
Soft yellow sandstone	18	0
Sand and heavy waterworn boulders, quartzite	10	0
Soft yellow sandstone	134	0
Firmer yellow sandstone	8	0
Firm white sandstone	5	0
Yellow sandstone	56	0
Firm grey sandstone with small bands of shale intermixed	2	6
Highly carboniferous sandstone	1	0
Alternate thin bands of shale and sandstone	3	0
Fine grey friable sandstone	3	0
Alternate thin bands of shale and sandstone	49	0
Alternate bands of shale and sandstone	44	9
Friable grey sandstone	55	0
Dark shale, first 6 in. containing lignite	5	0
Hard grey sandstone with shale bands	1	0
Argillaceous shale	6	0
Dark ruddy shale	26	0
Hard fossilized sandstone and pyrites	2	0
Argillaceous shale	22	0
Gritty fossilized sandstone	24	0
Muddy shale, very friable	39	0
Rough sandstone with nodules of pyrites	9	0
Shale	2	0
Sandstone friable	20	0
Fossilized shale	7	0
Sandstone, friable	47	0
Alternate thin bands of shale and sandstone	20	0
Friable sandstone	15	0
Fossilized sandstone	20	0
Friable sandstone	9	0
Sandstone slightly fossilized	11	0
Friable sandstone	10	0
Fossilized sandstone	20	0
Coarse, clean sandstone, friable	30	0
Fossilized sandstone	5	0
Green agglomerate shale	4	0

Friable sandstone	22	0
Sandy shale	9	0
Sandstone slightly fossilized	18	0
Thin bands of shale and sandstone	9	0
Friable sandstone	11	0
Shale	8	9
Coal shale	3	0
Dark soft shale	7	0
Soft, slightly fossilized sandstone	4	0
Very soft sandstone	34	0
Lignite	0	3
Dark shale	0	9
Soft sandstone	6	0
Alternate layers of shale and sandstone	4	0
Sandstone slightly fossilized	15	0
Hard sandstone with pebbles imbedded	15	0
Soft sandstone	20	0
Firm sandstone with pebbles imbedded	17	0
Firm sandy shale with flint nodules	5	0
Bed of quartzite flint boulders	6	6
Hard sandstone with flint pebbles imbedded	2	6
Sandy shale	5	0
Fossilized sandstone	2	0
Firm, light sandy shale	15	6
Hard grey sandstone	5	6
Light sandy shale	6	0
Coarse friable sandstone	67	0
Flint boulders imbedded in sandstone	3	0
Soft sandstone	10	0
Firm sandy shale with pebbles imbedded	9	0
Hard gritty sandstone	4	0
Dark sandy shale	38	0
	1231	0

The bores are recorded in the following publications:

Port Keats No. 1 and No. 2 Bores—Northern Territory of South Australia. Northwestern District Reports (Geological and General) resulting from the explorations made by the Government Geologist and staff during 1905 by H. Y. L. Brown, 1906, p. 37 (Port Keats No. 1 Bore) and p. 38 (Port Keats No. 2 Bore).

Port Keats No. 3 Bore—South Australia (Northern Territory). Official contributions to the Palaeontology of South Australia by R. Etheridge Jr. and record of Northern Territory boring operations, H. Y. L. Brown, Government Geologist. Supplement to Parliamentary Papers No. 55 of 1906, 1907, p. 25.

Port Keats No. 4 Bore—Northern Territory of South Australia. Government reports on recent mineral discoveries and further record of Northern Territory boring operations by H. Y. L. Brown, Government Geologist, 1908.

Cape Ford No. 2 Bore, 0-1123 feet—Government Resident's report on the Northern Territory, 1907, by C. E. Herbert, Government Resident, ?1908, p. 8 (also contains a repetition of the log of Port Keats No. 4 Bore from 1007 feet to the bottom of the bore at 1505 feet).

Cape Ford No. 2 Bore, 1123-1506 feet, and Cliff Head No. 1 Bore—Appendix by E. C. Playford, Chief Warden for Northern Territory of South Australia in Government Resident's Report on the Northern Territory, 1908, by C. E. Herbert, Government Resident, ?1909, p. 32 (Cape Ford No. 2 Bore) and p. 38 (Cliff Head No. 1 Bore).

Anson Bay No. 1 Bore—Appendix by E. C. Playford, Chief Warden for the Northern Territory of South Australia in Resident's report on the Northern Territory, 1909, by C. E. Herbert, Government Resident, ?1910, p. 32.

Anson Bay Bore (Fig. 11)—Appendix by A. H. Cunnew in Northern Territory Report of the Acting Administrator for the year 1911, 1912, p. 52.

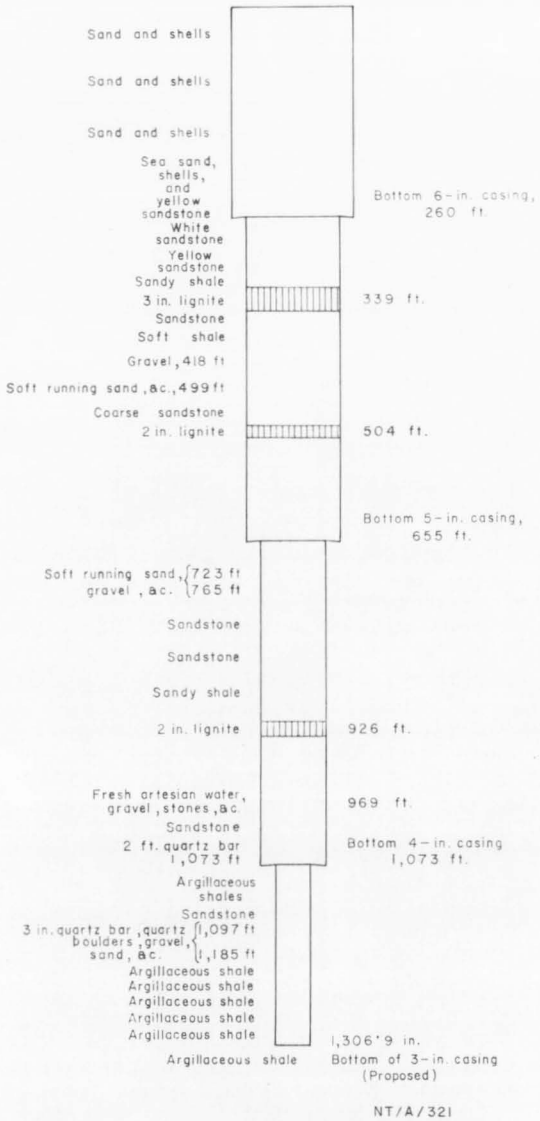


Figure 11. Rough sketch showing depths of casings, formations, artesian water supply, and seams of lignite, Coal Bore, Anson Bay, N.T., 120 miles SW of Darwin (reproduced from original).

PLATE 11

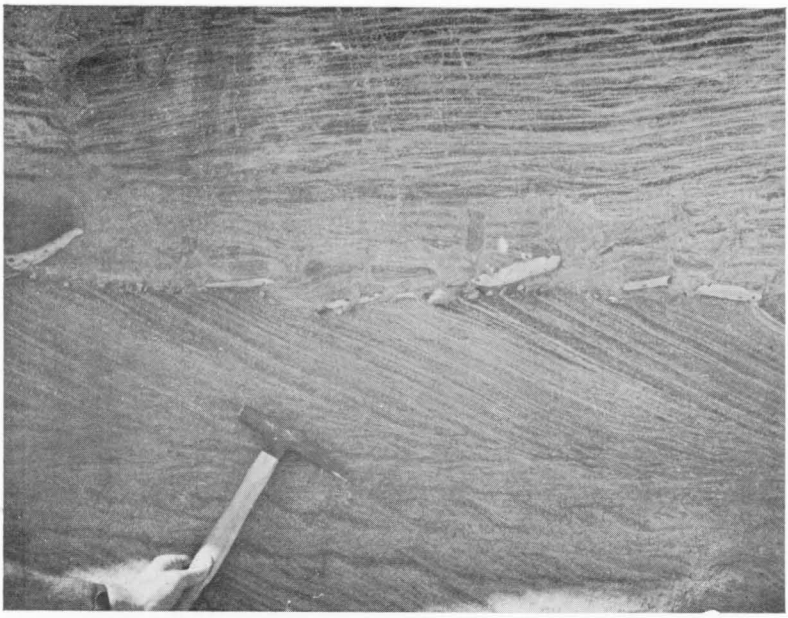


Figure 1. Disconformity on erosional break in the basal part of the Upper Permian beds at White Cliff Point.



Figure 2. Cross-bedded strata at Tree Point (locality 517) of probable Triassic age.

PLATE 12

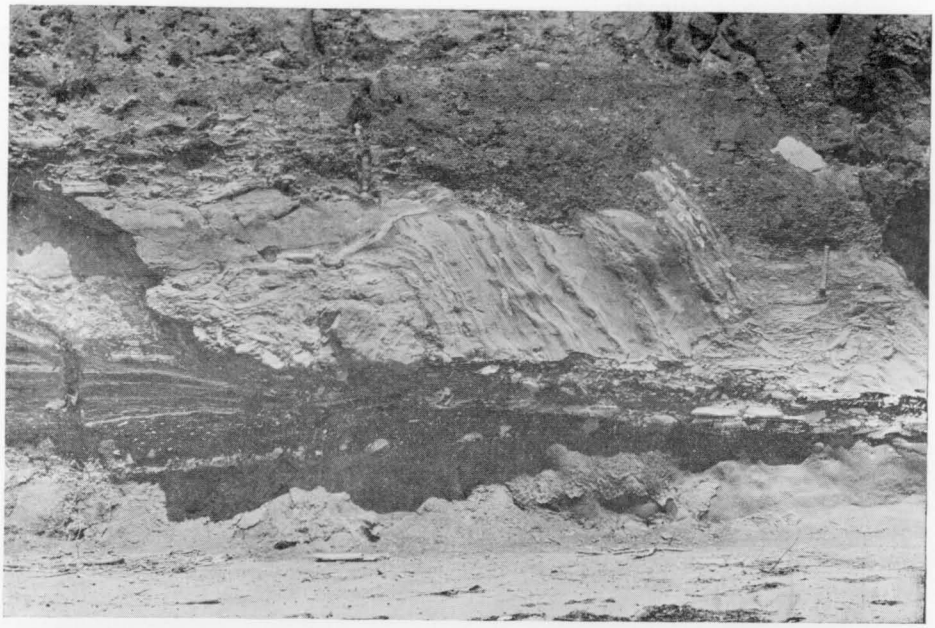


Figure 1. Cliff Head. Laminated yellow medium sandstone speckled with fragments of white siltstone disconformably overlain by a breccia of sandstone fragments, up to 6 feet across, and blue-grey quartzite in a sandstone matrix.

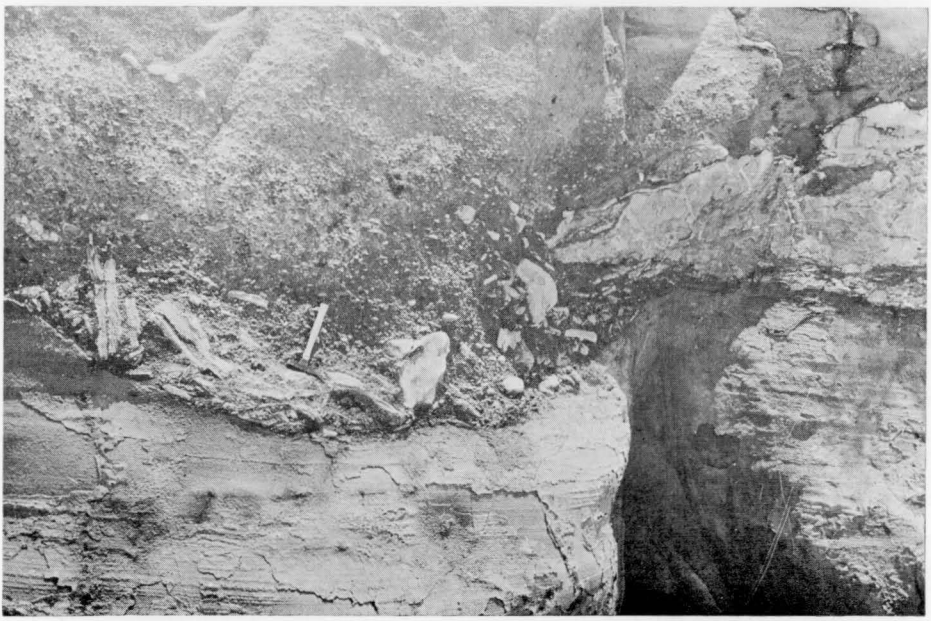


Figure 2. Detail of the disconformity at Cliff Head.

NEW LEUCITE LAMPROITES FROM THE WEST KIMBERLEY, WESTERN AUSTRALIA

by

G. M. Derrick and D. C. Gellatly

SUMMARY

Five new occurrences of Jurassic leucite lamproite have been discovered in the West Kimberley region, Western Australia. They occur as volcanic necks and vents intruding Precambrian basement rocks, Devonian limestone, and Permian sandstone, and contain lava, tuff, and agglomerate. The major rock types include various leucite lamproites, namely wolgidite, fitzroyite, mamilite, cedricite, olivine-leucite lamproite and a number of transitional rock types. Some of the plugs have a concentric structure—mamilite generally forms the outer zone and fitzroyite the inner zone.

The order of crystallization of the ferromagnesian minerals, from early to late, is olivine-phlogopite-diopside-magnophorite, but the rocks carrying these minerals as the dominant ferromagnesian phase are reversed in their order of eruption, i.e. fitzroyite (phlogopite-rich) is nearly always a late-stage phase.

INTRODUCTION

Plugs, flows, and sills of leucite lamprophyre ('lamproite') in the Kimberley region of Western Australia were first discovered by Fitzgerald (1907), and have been described in some detail by Wade & Prider (1940) and Prider (1960). Five previously unknown leucite lamproite occurrences were discovered in 1966-67, during regional mapping of the Precambrian rocks of the West Kimberley by a joint Bureau of Mineral Resources and Geological Survey of Western Australia field party. In addition one previously recorded lamproite, Old Leopold, was mapped in detail for the first time. The existence of these new lamproite occurrences has been mentioned only very briefly before (Gellatly et al., 1967; 1968). These new occurrences, which all occur in the Lennard River Sheet area, are described in this paper, and their location relative to other lamproites in the area is shown in Figure 1.

In 1967 several of the previously known occurrences were mapped and sampled in detail, and maps prepared of those where no maps previously existed. A further paper will consider the petrology and geochemistry of the new occurrences, and compare them with the previously known ones.

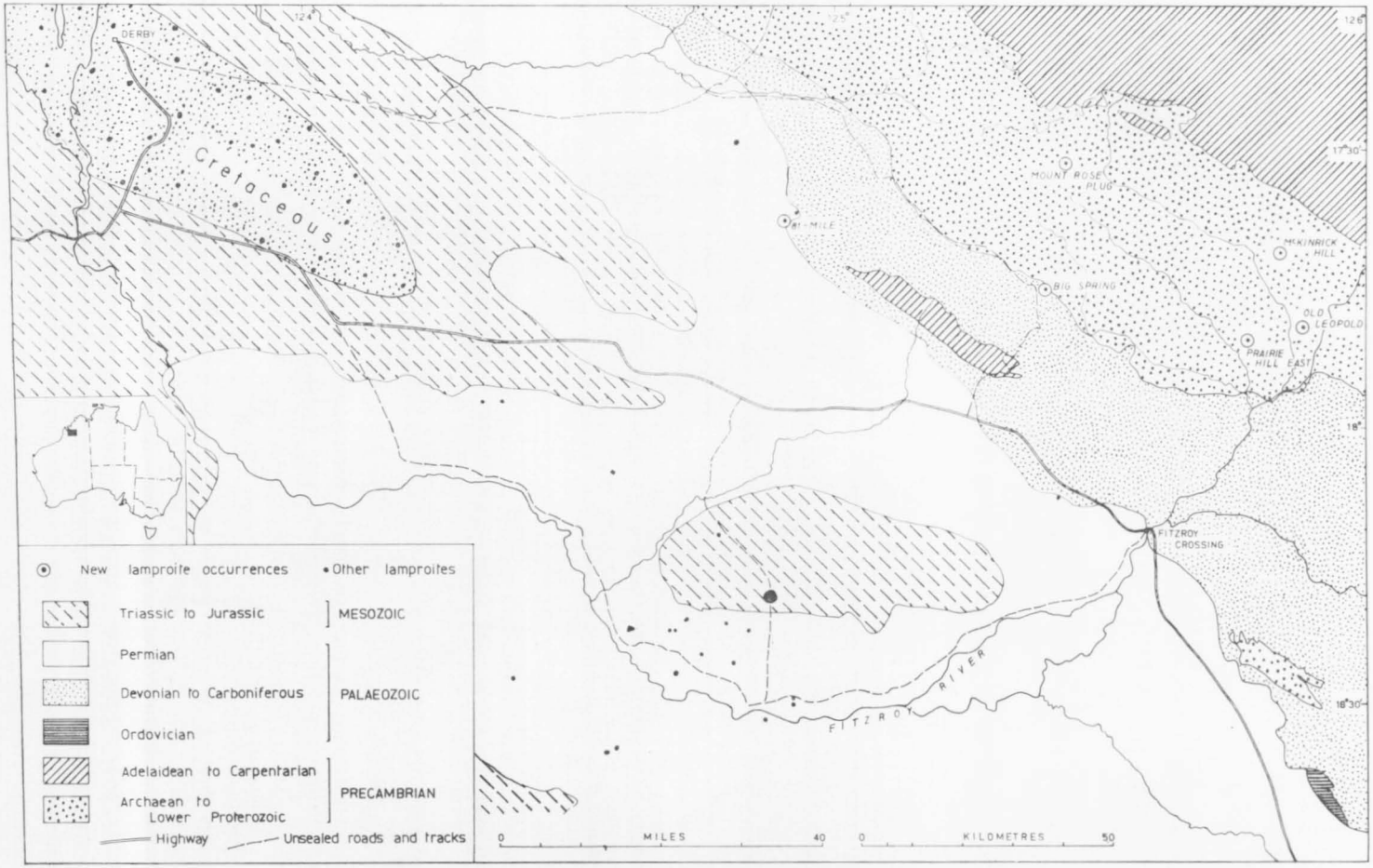


Figure 1. Distribution of leucite lamproites in the Fitzroy-Canning Basin, Western Australia.

WA/A 214

SUMMARY OF GEOLOGY

The leucite lamproites of the Kimberley region occur as volcanic plugs, vents, and flows and as intrusive sills in and adjacent to the northern part of the Fitzroy-Canning Basin. Including the new occurrences described in this paper twenty-eight are now known. They are scattered over an area of about 25,000 sq km but most are concentrated in the southwestern part of it (Fig. 1). They are mostly small circular volcanic plugs and vents ranging from a few metres across (Big Spring) up to about 3 km (Wolgidee Hills). Only one outcropping sill is known, but several thin sills have been encountered in the Associated Freney Oil N.L. Nerrima No. 1 well (Prider, 1960). Many of the volcanic centres include agglomerate, lava flows, and late-stage dykes, and generally include two or more distinct petrographic rock types. Four of the lamproites cut Precambrian rocks: all the others cut sediments ranging in age from Devonian to Triassic. No structural control is apparent in the south but most of those in the north occur close to major faults. The lamproites described here are known as Eighty-One Mile Vent, Mount Rose Plug, McKinrick Hill, Prairie Hill East, Old Leopold Hill, and Big Spring.

The age of the lamproites is considered to be Jurassic on the basis of Rb-Sr age determinations by Compston (Prider, 1960) and Kaplan et al. (1967). This is consistent with the fact that the youngest rocks cut by lamproites are Triassic. However, recent K-Ar determinations by Wellman (1971) have given early Miocene ages, from 16 to 21 m years.

NOMENCLATURE

Our nomenclature follows that of Wade & Prider (1940) and Prider (1960). The various rock types, which have been named according to the dominant ferromagnesian mineral present, are:

Fitzroyite: phlogopite-leucite lamproite
Cedricite: diopside-leucite lamproite
Wyomingite: phlogopite-diopside-leucite lamproite
Mamilite: magnophorite-leucite lamproite
Wolgidite: phlogopite-diopside-magnophorite-leucite lamproite

Each of these may carry olivine, usually altered to nontronite, or to ? hydrotalcite (Prider & Cole, 1942). Priderite is a constant accessory.

A number of transitional types occur, and these have been designated by compound names (e.g. cedricite-mamilite).

The unusual minerals from the lamproites include:

(a) *Magnophorite*: an amphibole allied to kataphorite (Prider, 1939), with magnesia dominant over iron, and potash greatly dominant over soda. It shows unusual pleochroism: X = colourless to pale yellow, Y = reddish pink, like X in hypersthene, and Z = pale to lemon yellow.

(b) *Wadeite*: a potassium zirconium silicate (Prider, 1939; Henshaw, 1955) similar in many respects to zircon, but flattened in the 'C' direction.

(c) *Priderite*: a rutile-like mineral exhibiting a peculiar lamellation parallel to the 'base' of the prisms. Its formula is $(K, Ba)_{1.3}$ $(Ti, Fe)_8O_{16}$ (Norrish, 1951).

EIGHTY-ONE MILE VENT

Outcrops of leucite lamproite about 4 km west-southwest of Mount Percy have been named the Eighty-One Mile Vent from the nearby 81-mile post in the Derby-Halls Creek telegraph line. This vent is roughly circular and about 300 m in diameter. It is surrounded by sand plains overlying sandstone of the Permian Grant Formation. The lamproite forms a prominent topographic horseshoe structure and is conspicuous on air photographs. The vent was first noted in 1967 by the writers during regional mapping of the nearby Precambrian, but specimens examined by Prider (1960, p. 72) and labelled 'from N5, WSW of Mount Percy', could also be from this vent.

Field Occurrence

The outcrop consists mainly of a prominent ring of massive scarp-forming lamproite dipping inwards towards a small soil-covered basin (Pl. 13, fig. 1). This massive fine-grained lamproite is underlain by tuff and agglomerate with thin intercalated lamproite flows, and is overlain by moderately coarse-grained phlogopite-rich lamproite (Fig. 2). A measured section across the western rim is given in Figure 3.

Tuffaceous sandstone, lapilli tuff, and agglomerate make up 24 m of the exposed thickness of volcanic material and probably persists in depth. The agglomerate and tuff are commonly vesicular and contain abundant subrounded to angular lapilli and blocks of quartz sandstone up to 20 cm. The matrix of the tuff is predominantly of sand grains cemented by opaque brown altered lamproitic material. Lamproite fragments are rare in the lowermost exposed beds but increase in abundance upwards in the sequence. The topmost tuff grades upwards into lamproite lava through a progressive increase in lamproite fragments and lamproite matrix and a corresponding decrease in sandstone fragments.

The thin lava flows intercalated with the tuff and agglomerate are similar to the flow of massive lava which forms the principal outcrop. They are fine-grained, grey to grey-green in hand specimen, and contain sparse small (1 mm) phenocrysts of phlogopite. They are mostly non-amygdaloidal, but one specimen contains 1- to 2-mm elongate amygdales. Subrounded fragments of altered sediment are present locally, especially near the base of the main flow. Columnar structure is present locally.

The topmost flow is characterized by abundant 3-mm phlogopite phenocrysts and is non-amygdaloidal. The upper part of this flow is obscured by soil cover in the centre of the vent. No contact with the underlying fine-grained flow has been observed but it is assumed from petrographic differences that the two flows are distinct.

Petrography

The rocks range in composition from mamilite-fitzroyite, through fitzroyite-mamilite to fitzroyite. Modal analyses are given in Table 1 and are plotted on Figure 8.

The fitzroyite is coarsely porphyritic with phlogopite occurring as phenocrysts up to 3 mm showing narrow dark borders, and as microphenocrysts in a brown chloritic groundmass. Other microphenocrysts include leucite, diopside, priderite, acicular apatite, and rare serpentinized olivine.

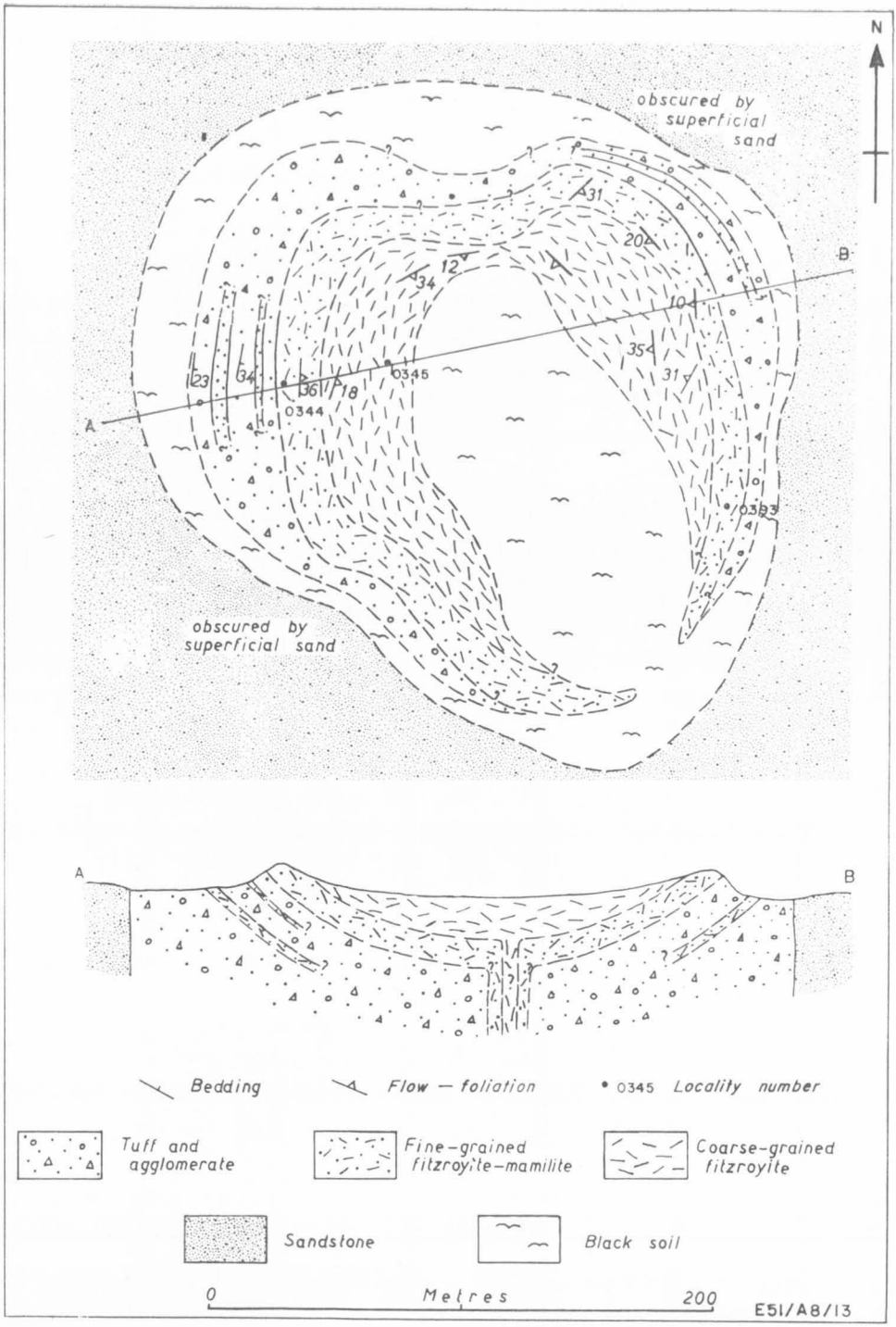


Figure 2. Plan and cross section of Eighty-One Mile Vent.

TABLE 1. MODAL ANALYSES OF LAMPROITES FROM THE WEST KIMBERLEY, WESTERN AUSTRALIA

	Mount Rose Plug					Eighty-One Mile			Prairie Hill East				Old Leopold Hill			McKinrick Hill
	0343	0335	0336	0337	0338	0344	0345	0393	0011	0012	0013	0397[7]	0003	0001	0001 vein	0016
Leucite (phenos)	16.3	20.6	23.4	8.0	27.3	—	—	—	30.8	28.7	46.2	55	33.0	34	—	—
(matrix)	—	45.0	—	50.4	—	57.3	1.8	20.1	—	—	—	—	—	—	—	—
Phlogopite	17.4	4.6	15.0	0.4	13.4	6.0	20.0	5.1	5.9	—	tr	—	5	3.6	—	0.4
Diopside	6.0	1.7	8.0	0.5	7.5	0.4	1.0	—	4.6	4	4.6	12	7	5.2	—	—
Olivine pseudomorphs	2.6	3.1	1.1	8.7	3.1	0.3	—	—	7.5	9.1[4]	11.5	6	0.4	tr	—	11.5
Magnophorite	18.9	20.0	0.4	23.7	0.3	20.4	—	0.2	7.5	9.6	6.7	5	14	12.2	—	—
Priderite	0.8	3.0	5.9	2.6	4.4	6.0	1.2	—	8	8.3	4.4	2	9.3	12.4	62.4	—
Groundmass	38.0	0.5	46.2	0.9	44.0	9.6	75.7	57.6	34.6	39.2	26.5	20	30[1]	28.0	—	67.3[5]
Amygdales and/or vesicles	—	—	—	4.8	—	—	—	{ 6.3[6] 9.8[8]	—	—	—	—	—	—	—	—
Apatite	—	tr	—	—	—	—	0.3		1.1	1.1	0.1	—	tr	2.3	—	—
Others	—	—	—	—	—	—	—	0.9[5]	—	—	—	—	1.3[2]	2.3[2]	37.6[3]	—
Rock fragments	—	1.5	—	—	—	—	—	—	—	—	—	—	—	—	—	20.8
Total	100.0	100.0	100.0	100.0	100.0	100.0	100.0	100.0	100.0	100.0	100.0	100	100.0	100.0	100.0	100.0

1. Includes ?sanidine.
2. Aegirine and trace wadeite.
3. Quartz and opal 24.6; aegirine 13.
4. Pseudomorphs possibly after diopside as well as olivine.
5. Includes some vein material (3.2%) and fine-grained leucite.
6. Quartz: some or all may be recrystallized xenocrysts.
7. Ring dyke; estimated mode only; abundant fresh leucite and some fresh olivine.
8. Zeolite.

Rocks intermediate between fitzroyite and mamilite are all fine-grained, with phenocrysts of phlogopite up to 1.5 mm prominent; and microphenocrysts of leucite (showing internal cruciform structure), phlogopite, and magnophorite. Small needles of priderite are generally conspicuous. An amygdaloidal lava (0392*) contains amygdales of silica, zeolite, and opaque isotropic material; those filled with silica show an outer rim of fibrous silica surrounding a core of a single quartz grain, which suggests they are probably quartz xenocrysts which have undergone partial or complete melting.

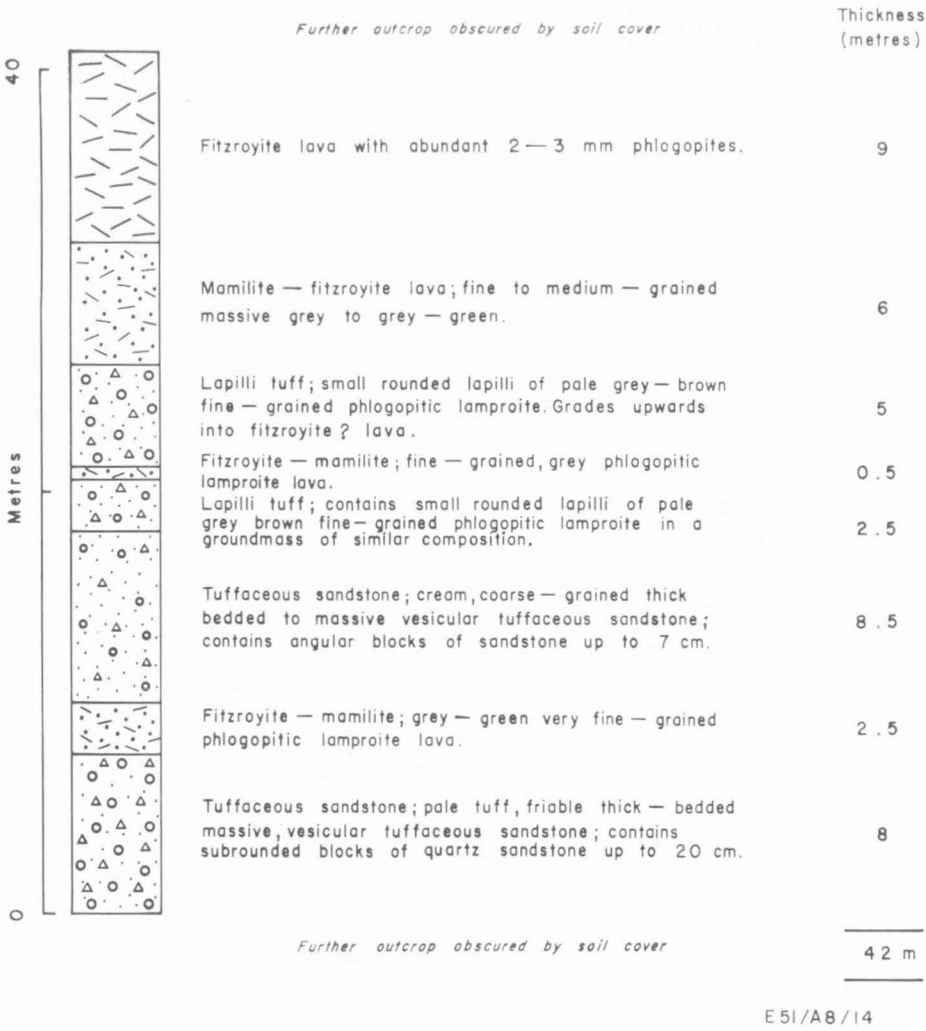


Figure 3. Measured section, western rim, of Eighty-One Mile Vent.

* BMR registered numbers. All numbers below 0334 have the prefix 66.16; those above have prefix 67.16.

A lamproite lapilli tuff (0393) contains lapilli of fine-grained porphyritic phlogopite lamproite, some of which is highly amygdaloidal; most amygdales contain an outer border of quartz surrounding a core of zeolite. Interstitial material is mainly recrystallized quartz grain aggregates and fragments of opaque material bordered by green chlorite (? nontronite).

MOUNT ROSE PLUG

Field Occurrence

This lamproite body is an intrusive plug, cutting probably Archaean metasediment of the Halls Creek Group about 3.2 km southwest of Mount Rose. It occurs within 1.6 km of a prominent zone of transcurrent faulting. The plug is roughly circular in outcrop plan and about 80 m in diameter (Fig. 4; Pl. 13, fig. 2). It is well exposed near the margins, but the central part is obscured by phlogopite-bearing black soil and detritus from the lamproite. The lamproite carries vegetation distinct from the surrounding spinifex cover of the Halls Creek Group.

Flow foliation near the margins of the plug mostly dips inwards at 50° to 65°. A contact with phyllite of the Halls Creek Group on the eastern margin is vertical. The surrounding phyllite is only slightly metamorphosed and shows no deformation even close to the lamproite contact.

The plug consists of an outer zone of friable weathered grey-green, phlogopite-poor mamilite and an eccentric inner zone of phlogopite-rich fitzroyite-wyomingite containing conspicuous phenocrysts of phlogopite and diopside up to 3 mm long.

Petrography

Five specimens have been examined. Modal analyses of these are given in Table 1. The dominant rock types are mamilite and wyomingite with one intermediate type close to wolgidite in composition.

Specimens from the outer zone (0335, 0337) are of mamilite. They are almost entirely crystalline and contain phenocrysts of leucite and very rare phlogopite, diopside, and olivine pseudomorphs in a groundmass of small (0.05 mm) leucites, rare prismatic crystals of priderite, and abundant poikilitic magnophorite crystals studded with small leucite inclusions. Olivine occurs as elongate euhedral crystals pseudomorphed by a micaceous mineral (? hydrotalcite). One specimen is vesicular.

Specimens from the inner zone (0336, 0338) contain abundant phenocrysts of phlogopite up to 3 mm long and less abundant elongate diopside phenocrysts, and rare olivine pseudomorphs in a cryptocrystalline chloritic groundmass containing microphenocrysts of leucite, phlogopite, priderite, and diopside. In 0338 one olivine pseudomorph contains small granules of green spinel. An intermediate type (0343) resembles these, but in addition contains abundant poikilitic crystals of magnophorite, less groundmass, and also has partially resorbed phlogopite phenocrysts.

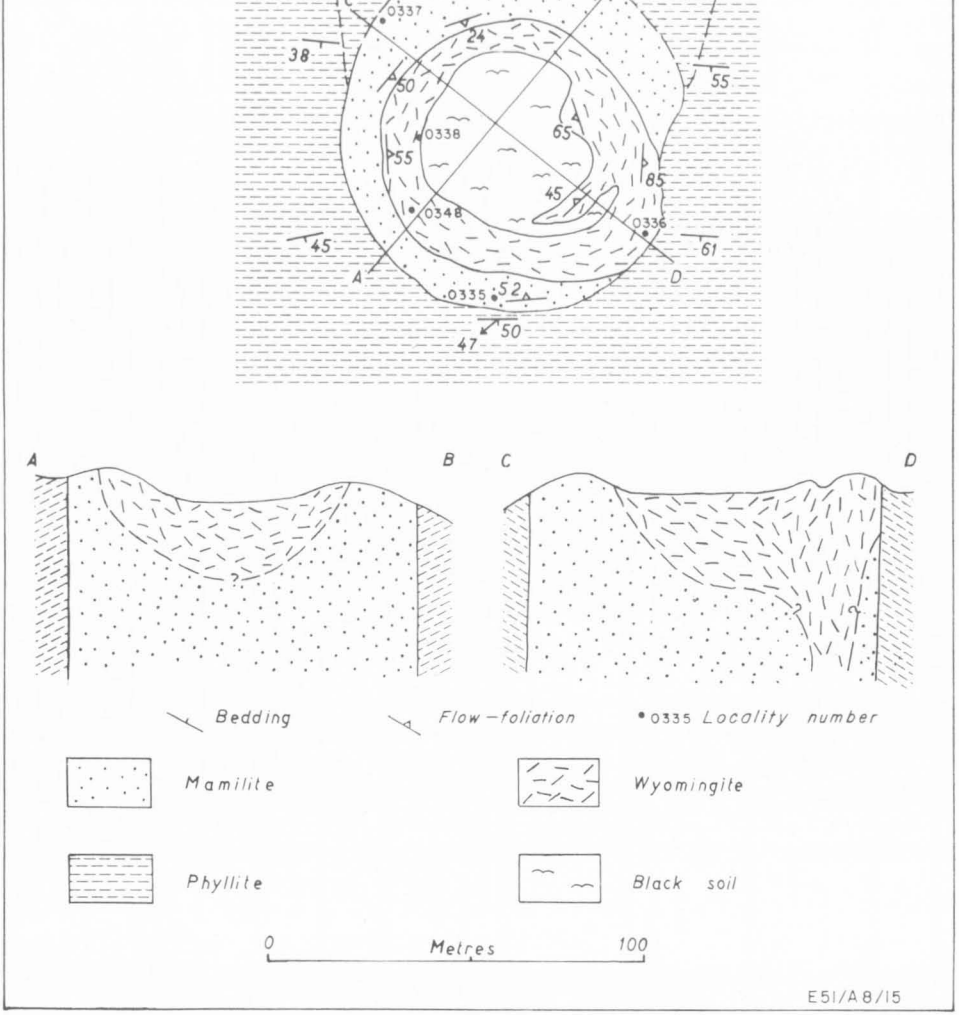


Figure 4. Plan and cross section of Mount Rose Plug.

McKINRICK HILL

McKinrick Hill is an olivine-leucite lamproite situated 19 km north-northwest of Old Leopold Downs, in a broad east-southeast-trending belt of sheared Precambrian volcanics and granite.

Field Occurrence

The lamproite forms a low rise about 20 m high, elongated in a southwest-northeast direction and plunging gently to the southwest (Pl. 14, fig. 1). It is

earthy brown and massive, with scattered xenoliths of metamorphosed acid volcanics, green and red jasper, and xenocrysts of quartz and feldspar. Jointing and outcrop shape suggest the lamproite fills a pipe which plunges steeply to the southwest. Joint planes from 10 cm to 1 m apart form elongate saucer-shaped structures with dips ranging from 80° at the pipe margins to 2° at the pipe centre (Fig. 5). Discontinuous streaks of siliceous or zeolitic material coat most of the joint planes. Strike of the joint planes parallels the contact with the country rock, which shows some brecciation and metamorphism.

A small pod of dull green earthy phlogopite lamproite occurs a few metres east of the main hill, and is xenolith-free.

Petrography

There appears to be no major variation in rock type within the main body of lamproite. A typical specimen (0016) is a cedricite: it contains microphenocrysts and rock and mineral fragments set in a fine-grained matrix. Euhedral phenocrysts pseudomorphous after ?olivine are common, and are 0.2-0.3 mm long. They are altered to a colourless to pale green micaceous mineral (? hydrotalcite) with some cryptocrystalline silica, and are strongly aligned. Microphenocrysts of leucite, average diameter 0.04 mm, are also present. They show abundant oriented inclusions, and skeletal cruciform growth structures.

The groundmass is pale green and very fine grained, with aggregates of priderite common. Xenolithic fragments include feldspar grains and rock fragments up to 0.8 cm, derived from the Whitewater Volcanics. Lamproitic fragments contain shattered crystals of phlogopite with resorbed margins, and fine-grained green material with abundant fine-grained laths of magnophorite. Most fragments are rimmed by fine-grained glassy limonitic material. ?Barite is scattered through the rock, which resembles the lower flow at Mount North (Prider, 1960, p. 76).

OLD LEOPOLD HILL

This plug was first recorded by Harms (1959) but was not mapped in detail until the BMR survey in 1966. The name was first used by Prider (1960), and is derived from the abandoned Old Leopold Downs homestead 3.2 km to the south, near the Fitzroy River.

Field Occurrence

The plug forms a prominent dark conical hill rising 45 m above sandy plains and bouldery outcrop of Lennard Granite (Pl. 14, fig. 2). Harms (1959) considered the rock to be a dyke, but steeply inclined flow foliation and the semicircular outline of the western contact with granite indicate that it is an inclined plug, plunging steeply to the southeast (Fig. 6). The northern and southern contacts with granite and aplite are sharp, but soil and talus obscures the eastern part of the plug. Small cliffs are present near the top of the hill; at their base some subhorizontal columnar jointing occurs.

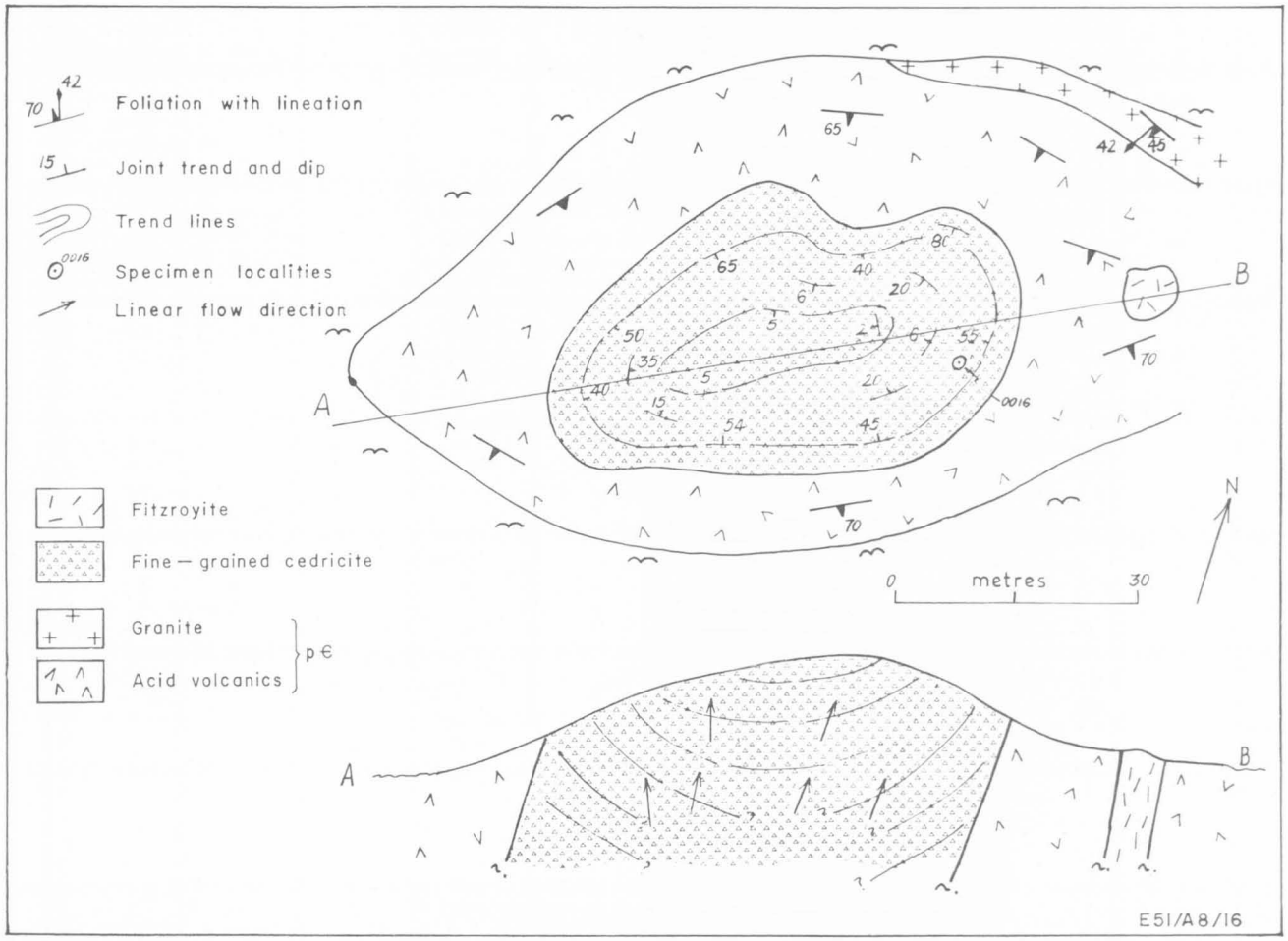


Figure 5. Plan and cross section of McKinrick Hill.

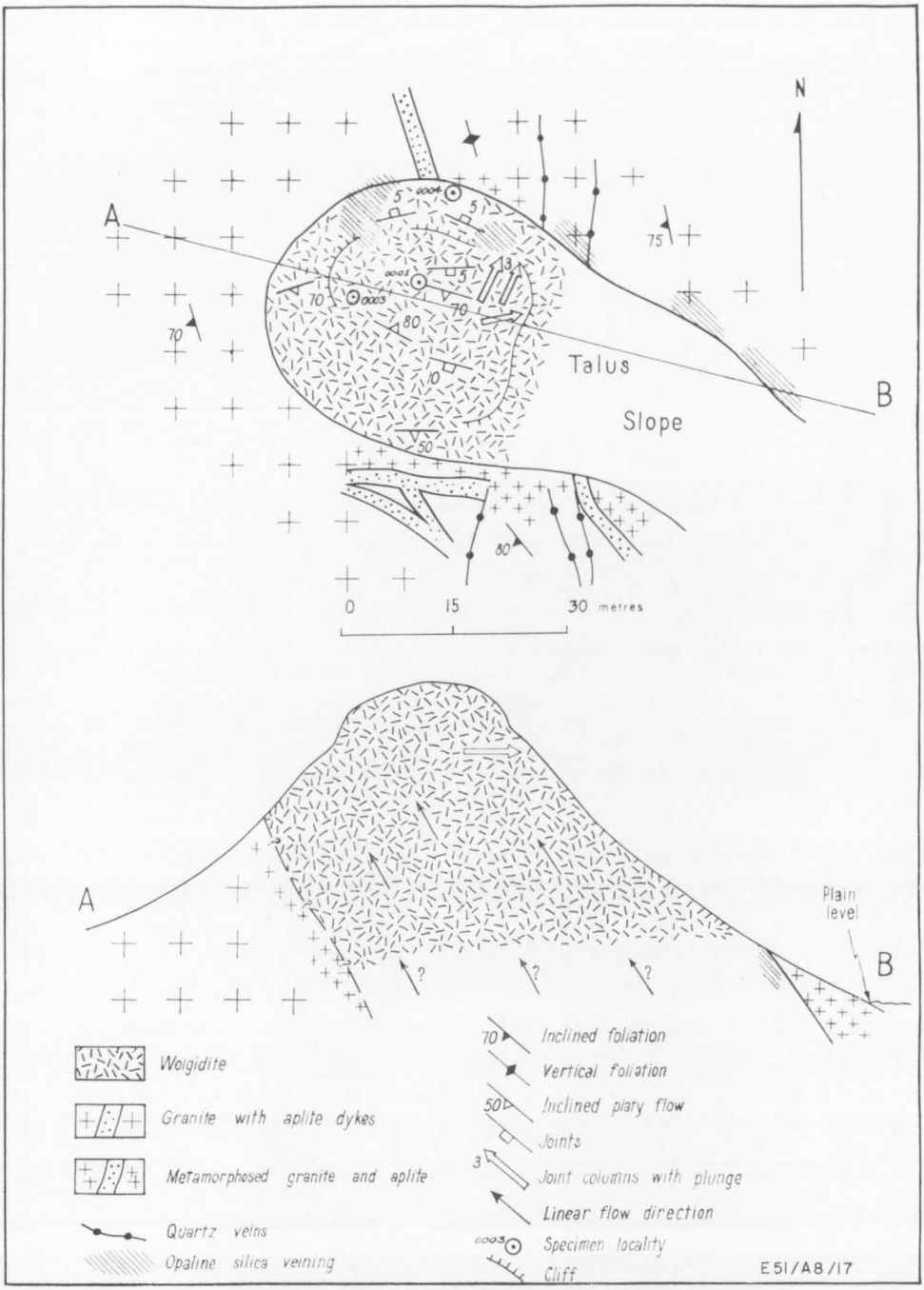


Figure 6. Plan and cross section of Old Leopold Hill.

The lamproite is grey-brown, and is uniform throughout; prominent phlogopite, diopside crystals up to 3 mm long, and leucite are abundant. Pale green to cream opaline silica masses occur on the northern and northeastern slopes of the plug; the granite and aplite in this area are brecciated and silicified, and veined by masses of dark grey-brown chalcedonic silica.

Petrography

All three specimens examined show similar textures and mineral assemblages. They are medium- to coarse-grained wolgidite. Modal analyses of two of them are listed in Table 1.

Leucite forms phenocrysts from 1.3 to 0.04 mm diameter, and most crystals are totally altered to aggregates of quartz, chalcedony, ?zeolite, turbid grey orthoclase, and some carbonate. ?Sanidine laths and pale green amphibole occur in altered leucite in 0003. Diopside phenocrysts from 3 mm to 0.4 mm long form stout, fresh, flow-oriented euhedra with poorly developed (010) prism faces. Magnophorite appears to have preferentially crystallized along diopside prism faces, and poikilitically encloses small leucite euhedra. Phlogopite occurs as corroded phenocrysts 2 to 3 mm in diameter and smaller unaltered grains in the groundmass. The margins of some grains contain priderite and a grey turbid alteration product, possibly ?leucoxene. Aegirine-augite and rare wadeite occur scattered throughout most samples.

A narrow veinlet of quartz, chalcedony, priderite, and aegirine-augite cuts 0001. Magnophorite in the rock is more intensely pleochroic adjacent to the vein. Estimates of birefringence and extinction angle of aegirine-augite indicate a Fe^{3+} ion content of between 0.45 and 0.50 (Deer et al., 1966).

PRAIRIE HILL EAST

Prairie Hill East is a lamproite plug 2.4 km east of Prairie Hill and 9.6 km west of Old Leopold Yard, in the Lennard River Sheet area. It was found during regional mapping in 1966.

Field Occurrence

The lamproite (in association with Precambrian granite and Devonian sandstone) forms a hill elongated in a northeasterly direction and surrounded by soil plains. The lamproite itself occupies a slight depression in the central part of the hill (Fig. 7). Immediately to the northeast of the main hill are slight rises of granite and sediment, enclosing poorly exposed lamproite, probably forming a ring dyke (Fig. 7; Pl. 15, fig. 1). A discontinuous sill of vesicular lamproite up to 20 cm thick intrudes the Devonian sediments on the southeast flank of the hill.

In the main plug platy and linear flow indicates a steep plunge to the southwest. Platy flow at the lamproite margins parallels the contact with the older rocks. Locally the shallow-dipping sandstones have been upturned by intrusion of the lamproite and have outward dips of up to 70°. Both the granite and Devonian rocks are metamorphosed; the latter, mainly coarse-grained sandstone and conglomerate, have a characteristic apple-green colouration, and are extensively veined by white chalcedony and opaline material.

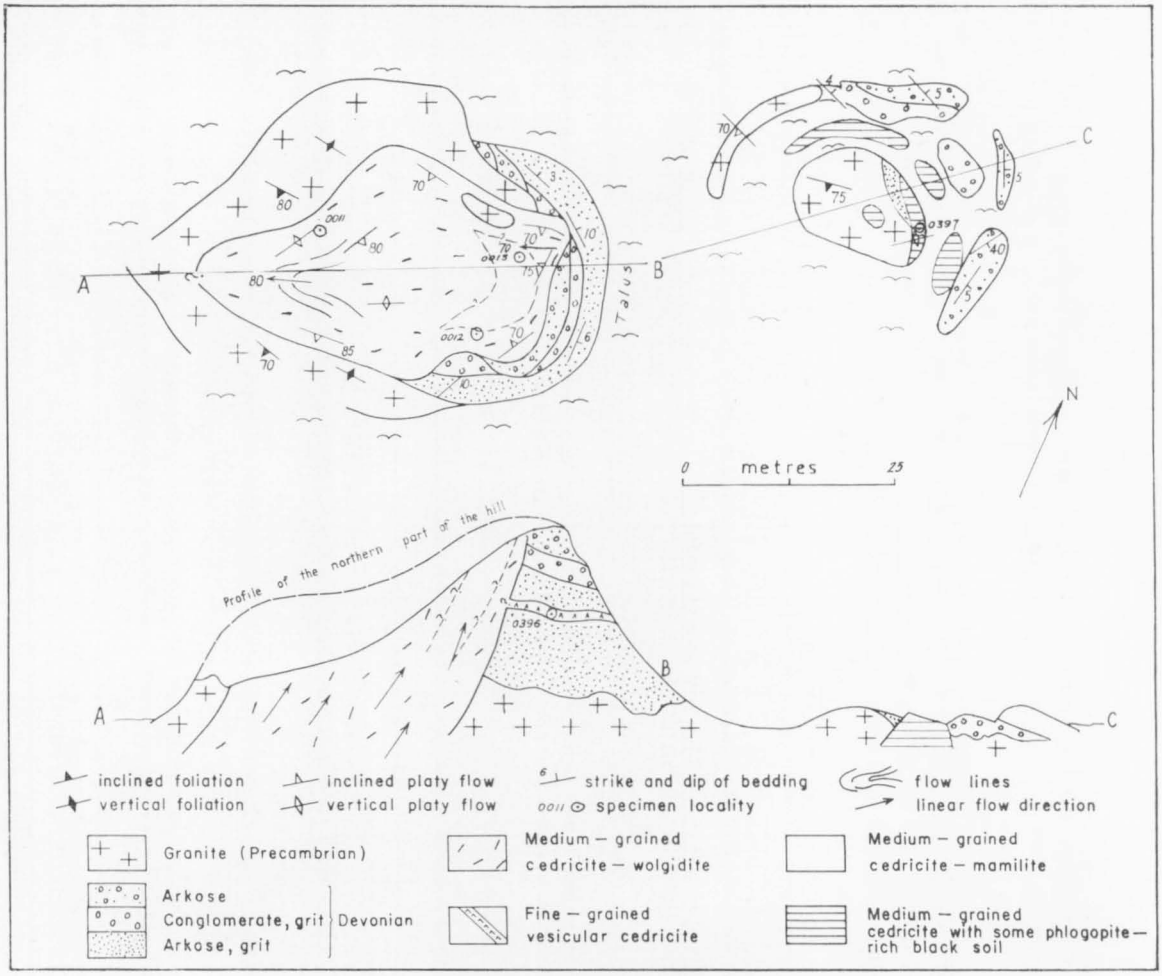


Figure 7. Plan and cross section of Prairie Hill East.

E51/A8/18

The main lamproite is moderately homogeneous and resembles the Old Leopold plug, but is fine-grained and contains fewer phenocrysts of phlogopite. A crescentic zone at the northeast end of the plug contains no phlogopite phenocrysts.

Petrography

Most specimens from the main plug are transitional between cedricite and mamilite, and cedricite and wolgidite. The outer zone (0011) is a fine- to medium-grained wolgidite characterized by rare phlogopite phenocrysts, abundant altered leucite, diopside, magnophorite, and priderite. Green ?nontronite after olivine is common; opaline material and chalcedony corrodes phlogopite and diopside. The latter poikilitically encloses leucite, stubby apatite, and slivers of magnophorite. The orange-brown serpentiferous groundmass contains very fine-grained leucite, apatite, priderite, phlogopite, calcite, and magnophorite with some chlorite and a fibrous zeolite.

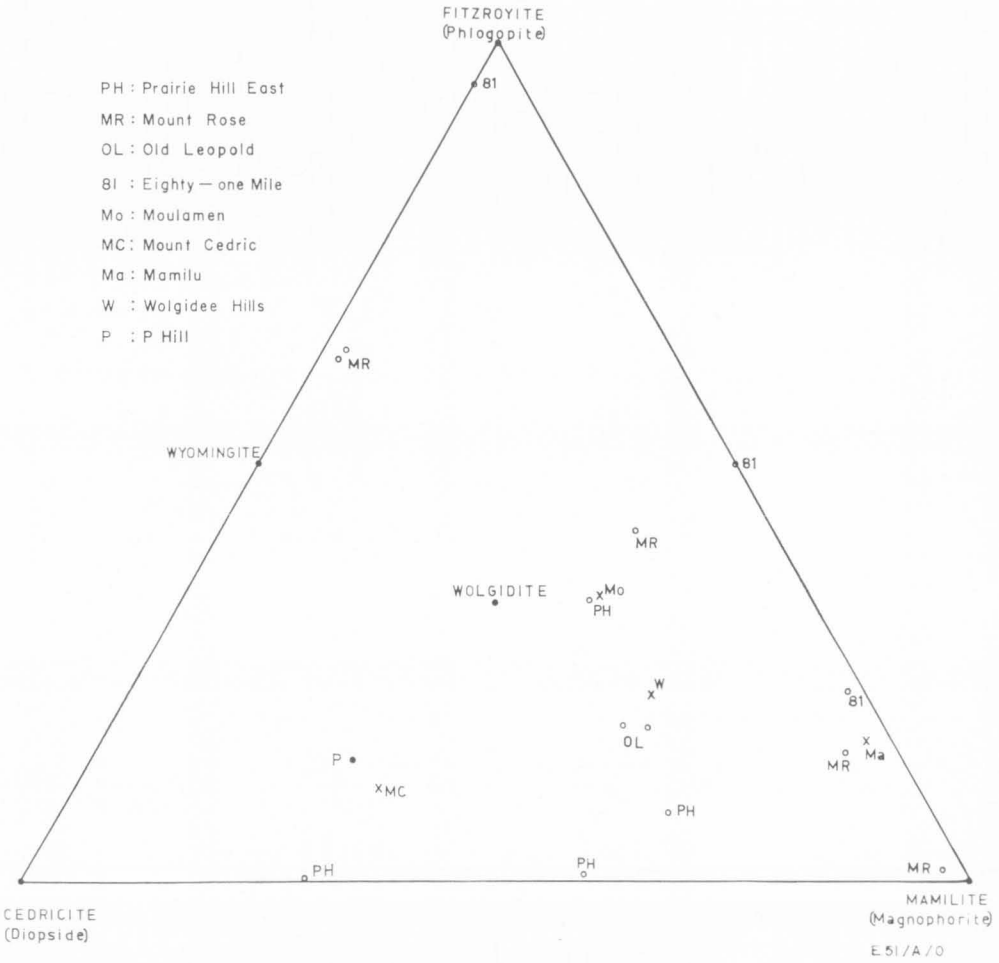


Figure 8. Plot of lamproite modal analyses.

The inner zone deficient in phlogopite contains cedricite-mamilite (0012, 0013). These rocks are similar to 0011 but contain only trace amounts of phlogopite and are more extensively carbonated. Specimen 0013 contains more abundant leucite, and relatively coarse-grained prisms of priderite up to 0.8 mm long.

The ring dyke to the northeast of the main plug is cedricite (Table 1). Fresh, coarse-grained euhedra of leucite and an almost complete absence of phlogopite are characteristic of this rock. It is unique in that some fresh olivine is still present in highly altered pseudomorphs now composed mainly of ?hydrotalcite and chlorite. Diopside, magnophorite, and priderite are also present, in an apple-green chloritic matrix. This specimen comes from the inner zones of the ring dykes. The outer zone is covered by phlogopite-rich black soil, probably overlying a zone of fitzroyite.

The vesicular sill (0396) is a very fine-grained fitzroyite, with average grain size 0.01 to 0.02 mm. Phlogopite, ?leucite, priderite, and pseudomorphs after ?olivine are present, together with coarse xenocrysts of microcline derived from either the granite basement or Devonian sandstones.

BIG SPRING LAMPROITE

This occurrence is located in a soil plain about 1.6 km east of Big Spring Bore; the only outcrop is a low mound of loose bouldery breccia about 8 m by 5 m (Pl. 15, fig. 2). It occurs close to the contact between Precambrian Whitewater Volcanics and Devonian Pillara Limestone, and contains fragments of both these units. The fragments are generally pale green and are similar to metamorphosed sediments at Prairie Hill East. Thin section examination has failed to reveal any lamproite material and the characteristic colour is the only suggestion of lamproite activity. The matrix of the breccia is a metamorphosed arkose or acid volcanic.

The occurrence is probably of cryptovolcanic origin, similar to Mount Abbott (Prider, 1960).

DISCUSSION

In most of the new occurrences the order of crystallization of the minerals is similar to that noted by Prider, with olivine first and magnophorite the last mineral to crystallize. An exception is a medium-grained wolgidite from Old Leopold, where some diopside was subpoikilitically enclosed by phlogopite phenocrysts, suggesting that diopside crystallized before phlogopite. Diopside is rimmed by magnophorite, but only the latter encloses small leucite crystals; this suggests a period of fine-grained leucite crystallization after crystallization of diopside. Priderite, some diopside, and rare wadeite are also enclosed by magnophorite.

A general order of crystallization is as follows, from early to late: olivine-phlogopite-$\left\{\begin{matrix}\text{large leucite} \\ \text{diopside}\end{matrix}\right\}$-small leucite-priderite-magnophorite.

Aegirine-augite at Old Leopold is widely scattered through the rock and in late-stage veinlets, and is probably contemporaneous with magnophorite.

It is interesting to note that although phlogopite is early in the crystallization sequence and magnophorite late, the rocks carrying these minerals as the dominant ferromagnesian phase are reversed in their order of eruption, i.e. the mamilites (magnophorite-rich) are early and the fitzroyites (phogopite-rich) are late. The presence of a late fitzroyite phase, either as flows or dykes, is a feature common to many of the lamproite vents and is presumably a fundamental feature of the crystallization and differentiation processes of the lamproite magma.

This sequence of eruption noted above, and the structure of many of the vents and plugs (especially Eighty-One Mile and Mount Rose) differ from that inferred by Prider (1960, fig. 12). We hope to discuss these features more fully in a future paper which will compare the chemistry and petrology of these new occurrences with the other lamproites in the region.

REFERENCES

DEER, W. A., HOWIE, R. A., and ZUSSMAN, J., 1966—AN INTRODUCTION TO THE ROCK-FORMING MINERALS. (Longmans, London.)

FITZGERALD, W. V., 1907—Reports on portions of the Kimberleys (1905-6). *W. Aust. parl. pap.* No. 6.

GELLATLY, D. C., SOFOULIS, J., DERRICK, G. M., and MORGAN, C. M., 1967—West Kimberley Mapping Project. *Bur. Miner. Resour. Aust. geol. Brch,* Ann. Summ. of Activities, 46-8.

GELLATLY, D. C., SOFOULIS, J., DERRICK, G. M., and MORGAN, C. M., 1968—The older Precambrian geology of the Lennard River 1:250,000 Sheet area SE. 51-8, Western Australia. *Bur. Miner. Resour. Aust. Rec.* 1968/126.

HARMS, J. E., 1959—The geology of the Kimberley Division, Western Australia, and of an adjacent area of the Northern Territory. *M.Sc. Thesis, Adelaide Univ.* (Unpubl.).

HENSHAW, D. E., 1955—The structure of wadeite. *Miner. Mag.,* 30.

KAPLAN, G., FAURE, D., ELLOY, R., and HEILAMMER, R., 1967—Contribution à l 'étude de l'origine des lamproites. *Bull. Centre Rech. PAU-SNPA,* 1 (1), 153-59.

NORRISH, K., 1951—Priderite, a new mineral from the leucite lamproites of the West Kimberley area, Western Australia. *Miner. Mag.,* 29.

PRIDER, R. T., 1939—Some minerals from the leucite-rich rocks of the West Kimberley area, Western Australia. *Miner. Mag.,* 30.

PRIDER, R. T., 1960—The leucite lamproites of the Fitzroy Basin, Western Australia. *J. Geol. Soc. Aust.,* 6 (2), 71-118.

PRIDER, R. T., and COLE, W. F., 1942—Alteration product of olivine and leucite lamproites from the West Kimberley area, Western Australia. *Am. Miner.,* 27.

WADE, A., and PRIDER, R. T., 1940—Leucite-bearing rocks of the West Kimberley. *Quart. J. geol. Soc. London,* 96, 39-98.

WELLMAN, P., 1971—The age and palaeomagnetism of the Australian Cenozoic volcanic rocks. *Ph.D. Thesis, Aust. Nat. Univ.* (Unpubl.).

Page 120 is blank.

PLATE 13

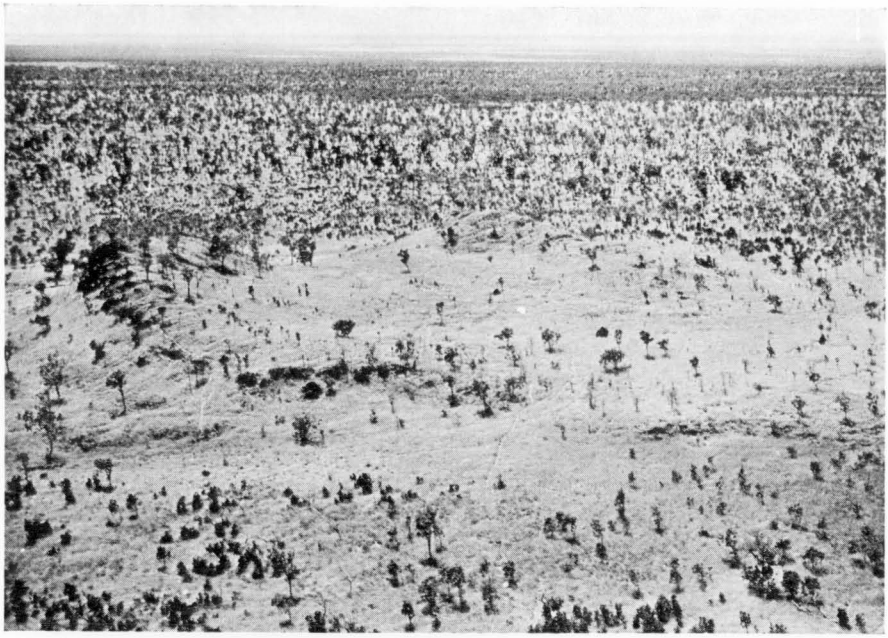


Figure 1. Eighty-One Mile Vent, looking northeast.

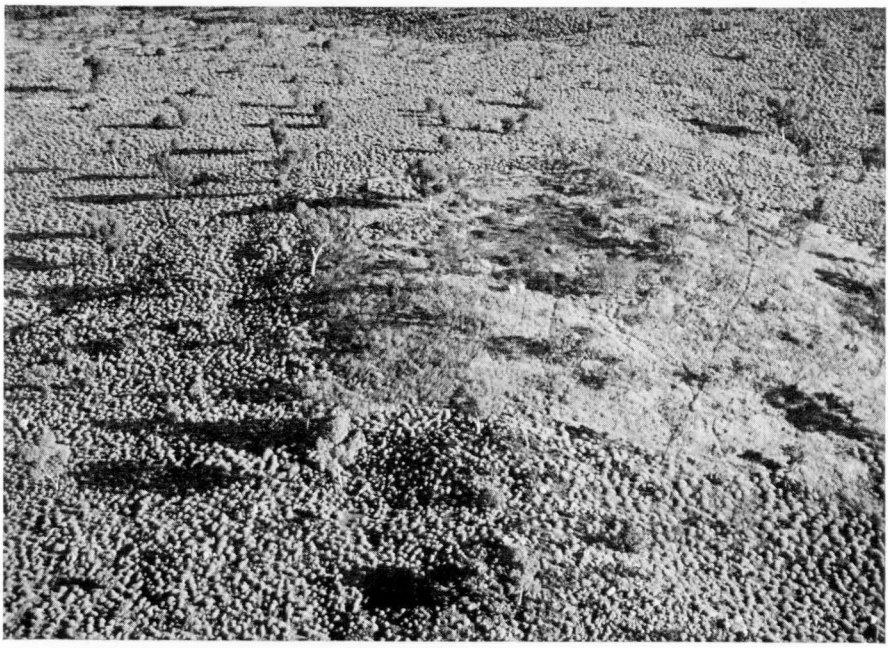


Figure 2. Aerial view of Mount Rose Plug.

PLATE 14

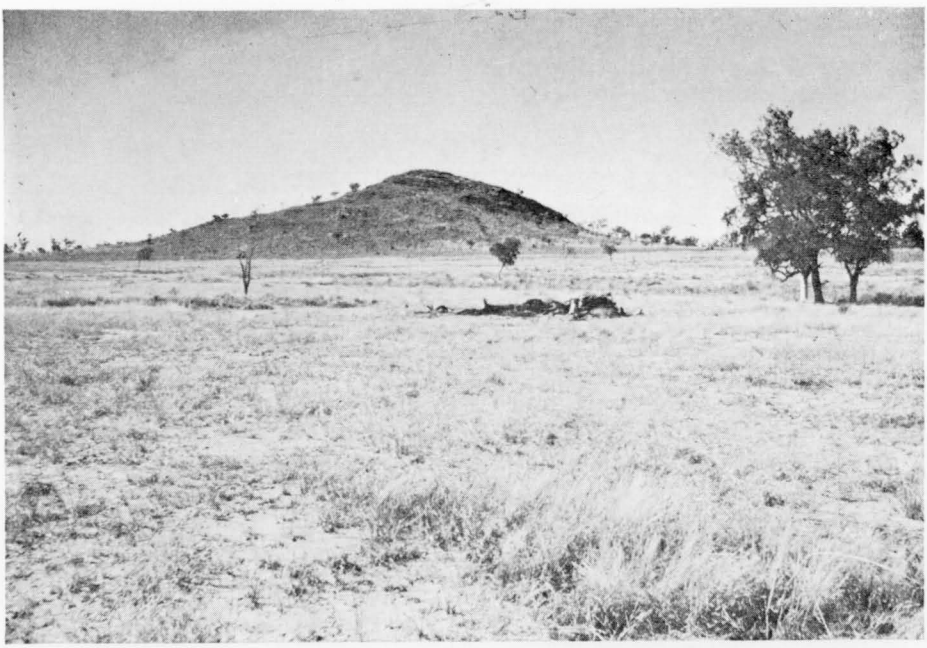


Figure 1. McKinrick Hill, viewed from the northwest.



Figure 2. Old Leopold Plug, looking west.

PLATE 15

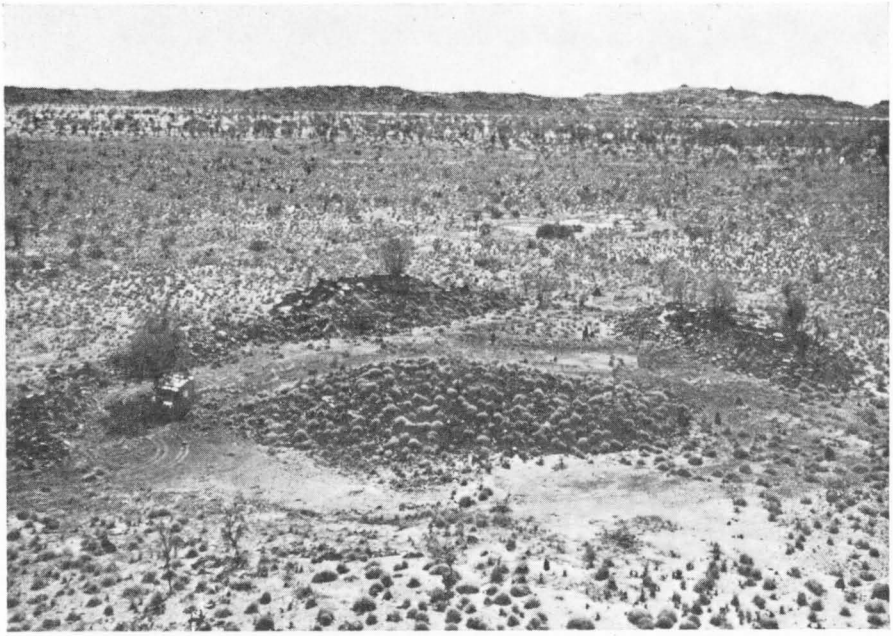


Figure 1. Ring dyke structure, Prairie Hill East.

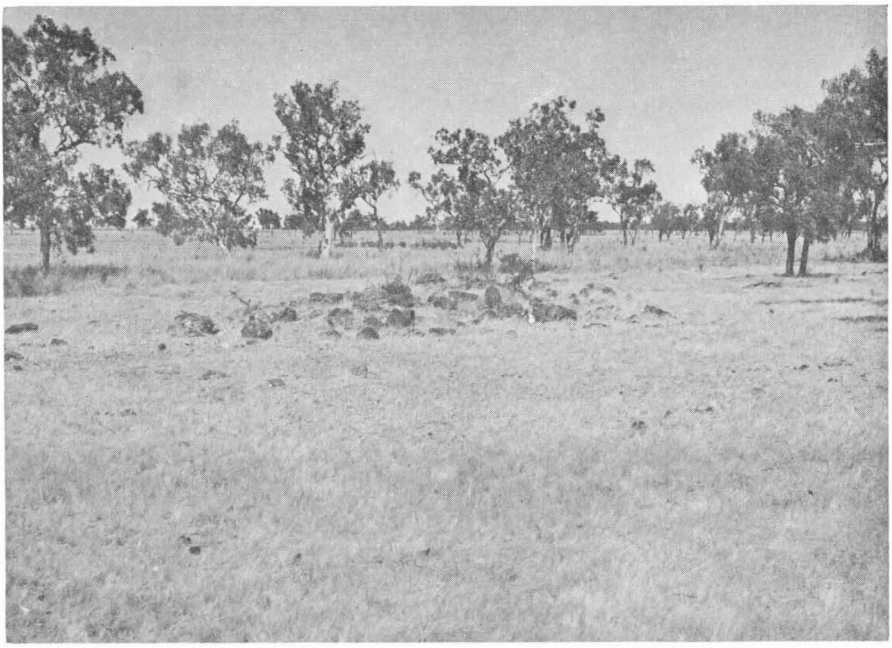


Figure 2. Big Spring, a cryptovolcanic structure.

PETROLOGY AND GEOCHEMISTRY OF METAMORPHOSED ARCHAEAN OPHIOLITES, KALGOORLIE-COLGARDIE, WESTERN AUSTRALIA

by

A. Y. Glikson

SUMMARY

The field relationships, petrology, and geochemistry of pillowed metabasalts, metadolerites, metapyroxenites, serpentinites, and sodic metaporphyries incorporated in a 20,000-metre-thick geosynclinal succession between Coolgardie and Kalgoorlie, Western Australia, are considered. These ophiolites—or greenstones, as they are commonly termed—occur as stratiform complexes spatially distinct from sedimentary zones. A cyclic weakening of igneous activity was associated with a transition from ultrabasic and basic rocks to intermediate and acid sodic rocks. The ultrabasic components occur preferentially at low stratigraphic levels of ophiolite complexes, the emplacement of which is interpreted in terms of multiple extrusion and intrusion of the products of partial melting of the mantle. The meta-igneous suite is calc-alkaline, and is characterized by a low potash content. The metabasalts are consistent with oceanic tholeiites. Genetic relationships between the basic members of the ophiolite suite and sodic porphyries are suggested by field relationships and geochemical affinities. Metamorphism of the ophiolites reached the upper greenschist facies, as indicated by a transition from the actinolite-calcic plagioclase assemblage to the hornblende-intermediate plagioclase assemblage. Plagioclases with a wide range of composition, actinolites, and hornblendes co-exist in the same assemblages. Compositional relationships between plagioclase, amphibole, chlorite, and host rock are considered. The metamorphism has probably been of the low-pressure type, and was characterized by low water and carbon dioxide pressures.

The occurrence of ultrabasic to basic and acid igneous cycles, the thickness of the volcanic sequences, the abundance of serpentinites and pillow lavas, and the nature of the associated metasediments suggest a correlation between the Archaean greenstones and typical Alpine ophiolites. The ultrabasic-basic assemblages are akin to a correlation supported by the chemistry of the metabasalts. Basal ophiolite belts may well be representative of a primordial Achaean oceanic crust.

Submitted: November, 1969.

CONTENTS

	Page
Introduction	123
Stratigraphy	123
Correlation of Ophiolite Belts	126
Petrography	128
Mineralogy	140
Geochemistry	150
Metamorphism of the Ophiolites	167
Origin of the Ophiolites	172
Conclusions	184
References	186

INTRODUCTION

The greenstones of southwestern Western Australia have been a subject of great interest ever since gold was discovered in Coolgardie by Paddy Hannan in 1895. In spite of numerous observations carried out since the turn of the century, the association of gold and of recently discovered nickel deposits with the greenstones is not fully understood. Early workers regarded the greenstones as diorites. The origin of these rocks from low-grade metamorphism of basic igneous rocks, however, was subsequently recognized from abundant relict pillow structures, varioles, and amygdales, and the remnant ophitic, porphyritic, and trachytic textures. Most workers classified the greenstones in terms of a two-fold division, 'Older Greenstones' and 'Younger Greenstones', representing the extrusive phases and intrusive phases, respectively (Simpson & Gibson, 1912). Prider (1961) reviewed the terminology and problems associated with the greenstones, and pointed out the confusion which existed with respect to the origin and metamorphism of these rocks. Since then, petrological and geochemical studies of the greenstones in the Kalgoorlie-Norseman area contributed considerably to the understanding of these rocks. The more detailed studies were carried out by students of the University of Western Australia (e.g. Blockley, 1956; Mazzuchelli, 1962; Burt, 1962; Bekker, 1963; Doepel, 1965; Hudson, 1966; Williams, 1967). Bekker (1963), on the basis of work in the Norseman mines, gave one of the most comprehensive petrographic accounts ever written on greenstones. The porphyries of the Eastern Goldfields of Western Australia, which are consistently associated with the greenstones, have been the subject of an extensive geochemical study by O'Beirne (1968).

The present paper is based on part of a Ph.D. study of a type section of the Kalgoorlie System (Glikson, 1968). Because of the typical Alpine geosynclinal characteristics of the sequence, in the sense of Glaessner & Teichert (1947), Kay (1951), and Aubouin (1965), the greenstones are referred to as ophiolites. The petrographic, mineralogical, and geochemical features of the rocks are described, and conclusions with respect to their original characteristics and metamorphism are considered.

ACKNOWLEDGEMENTS

This paper is based on a part of a Ph.D. thesis submitted to the University of Western Australia. Supervision of the thesis work by Dr G. J. H. McCall and Dr K. J. Mills is gratefully acknowledged. I would like to thank Dr P. J. Cook and Mr K. Townley for their suggestion to publish this paper as a Bureau of Mineral Resources publication, and Mrs J. Owen for editing the manuscript.

STRATIGRAPHY

The Yilgarn Block and the Pilbara Block are the oldest parts of the Australian Precambrian Shield (Wilson et al., 1960). The Yilgarn Block, covering about 480,000 sq km in the southwestern part of Western Australia, is made up essentially of granitic gneisses and granites enclosing isolated metamorphic belts elongated in a north-northwest direction (Fig. 1). These belts consist of greenstones and metasediments and represent the remnants of an Archaean system defined by Prider (1965) as the Kalgoorlie-Yilgarn Succession and referred to by

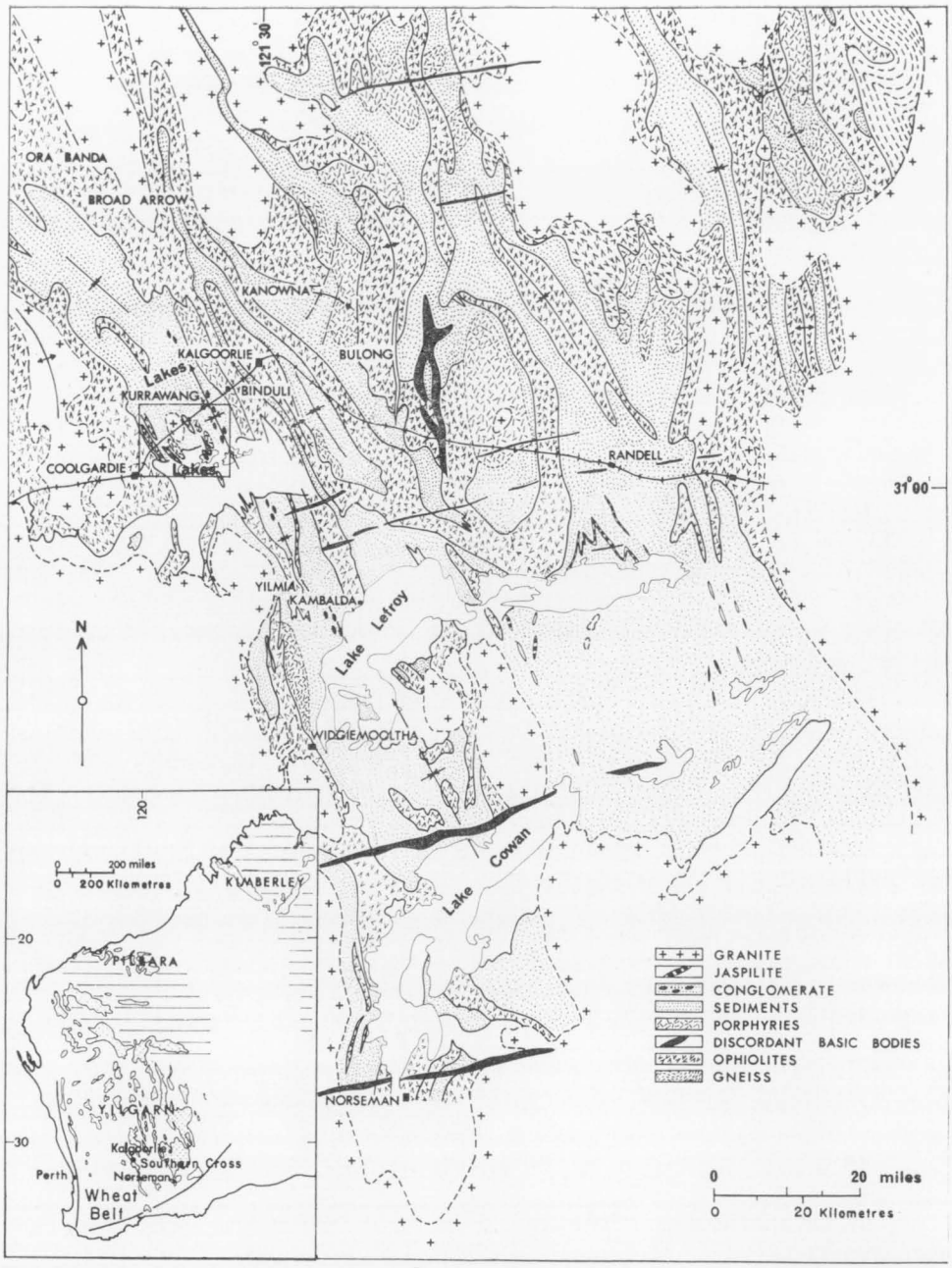


Figure 1. Geological map of the Kalgoorlie-Norseman area, compiled from sketch maps of the Geological Survey of Western Australia. The framed area represents the Coolgardie-Kurrawang sequence.

McCall et al. (1967) as the Kalgoorlie System. The metamorphic grade recognized in these belts shows a progressive increase from east to west, with the greenschist facies, the amphibolite facies, and the amphibolite and granulite facies prevailing in the Kalgoorlie-Norseman area, the Southern Cross area, and the Wheat Belt respectively (Fig. 1).

The greenstones and metasediments which crop out within the broadly defined area between Norseman, Ora Banda, and Randell constitute one of the most extensive relics of the Kalgoorlie System. Because of the rich gold and nickel ores discovered in the area, the Kalgoorlie-Norseman rocks have been investigated more thoroughly than other Archaean belts of the Eastern Goldfields of Western Australia. The western zone of the Kalgoorlie-Norseman area includes abundant ophiolites and acid metaporphyries associated with thick sedimentary sections. The rocks are steeply folded on north-northwest-trending axes, and mildly cross-folded on east-west-trending axes. The sequence underwent low-grade regional metamorphism, dated as 2665 $\pm$ 25 m.y. (Turek, 1966).

One of the major structures in the Kalgoorlie-Norseman area is the Kurrawang Syncline, the axis of which can be traced for nearly 160 km (Sofoulis, 1966). Outcrops associated with the lake country of the Coolgardie-Kurrawang area afford the study of a relatively well exposed section across the western flank of the Kurrawang Syncline. The base of the Coolgardie-Kurrawang sequence consists of thick stratiform ophiolites intruded by granite, whereas the top is defined by the Kurrawang Beds, exposed in juxtaposition with the axial zone of the Kurrawang Syncline (Fig. 2). Metamorphosed ophiolites and sodic metaporphyries constitute about 50 percent of the Coolgardie-Kurrawang sequence. Stratiform ophiolites predominate at low stratigraphic levels, and are extensively interspersed with metasediments at intermediate stratigraphic levels, where they are commonly accompanied by sodic metaporphyries. Individual igneous bodies range in thickness from a few inches to several thousand feet. The meta-igneous rocks associated with the Coolgardie-Kurrawang sequence are divided into three units on the basis of their stratigraphic position (Fig. 2). These units are given informal stratigraphic names, and are as follows (from base to top):

Coolgardie ophiolites: 6600 m (minimum thickness). A sequence consisting of pillowed and massive metabasalts, stratiform metadolerite, metapyroxenite, serpentinite, and small bodies of sodic metaporphyries, with common pelitic intercalations. The base is intruded by granites, whereas the top grades into the Gunga meta-argillites and the Mount Robinson ophiolites.

Mount Robinson ophiolites: 3300 m (approximately). This unit consists of pillowed metabasalts intruded by metadolerites and metapyroxenites and abundantly accompanied by sodic metaporphyries. These rocks are intermittently intercalated with the meta-argillites which prevail at lower levels of the Mungari beds.

Red Lake ophiolites: 6600 m (approximately). This unit consists of pillowed and massive metabasalts, metadolerites, and metapyroxenites, abundantly accompanied by sodic metaporphyries. The igneous units are associated with and occur mainly at lower sections of the Black Flag metasediments (Fig. 2).

Meta-igneous rocks decrease gradually toward the top of the Black Flag unit, and have not been found within the Kurrawang beds.

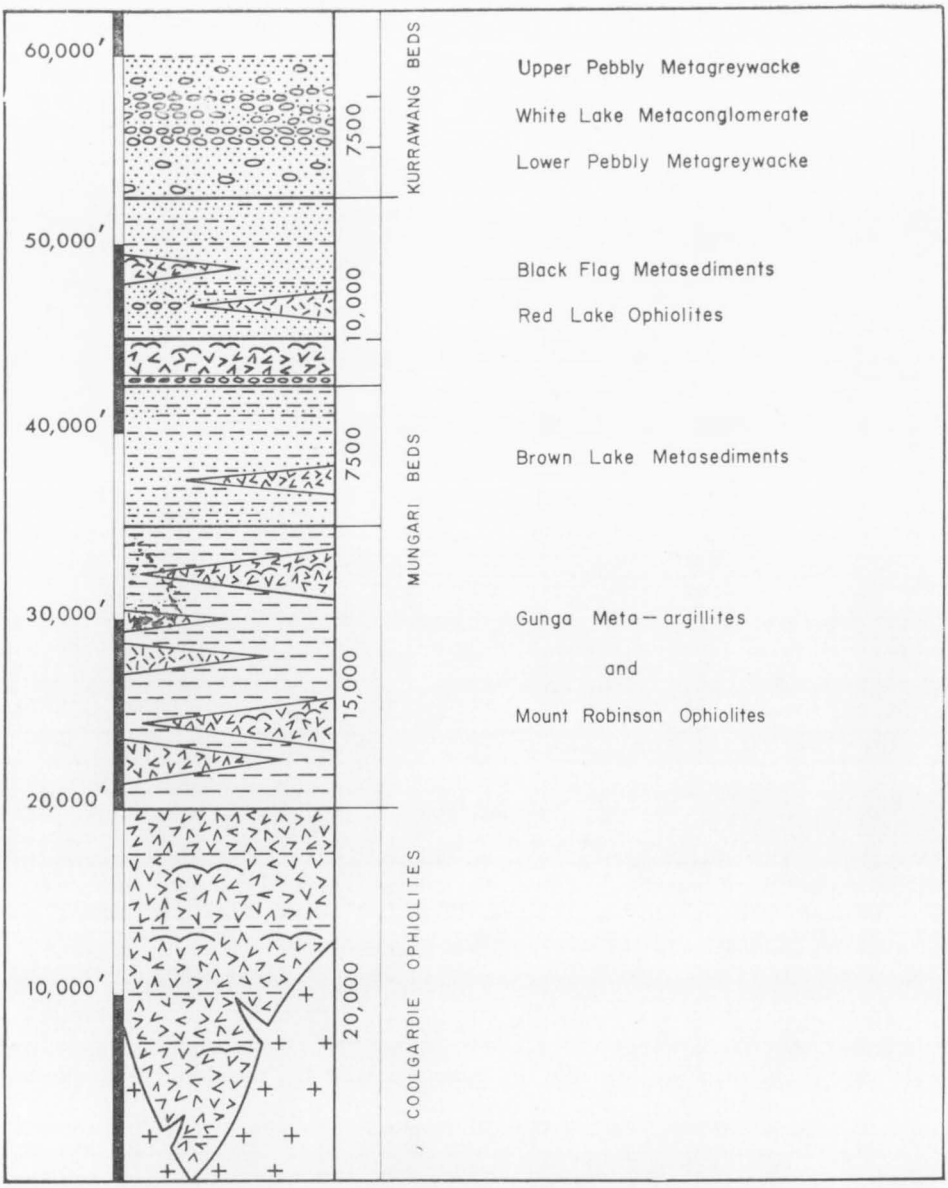


Figure 2. Composite columnar section of the Coolgardie-Kurrawang sequence. Thickness figures are approximate.

CORRELATION OF OPHIOLITE BELTS

The basic and ultrabasic meta-igneous formations tend to form conformable belts distict from zones of a predominantly sedimentary nature. These belts are clearly shown on airborne magnetic maps (Fig. 3). Studies of the ophiolite belts indicate their complexity in both composition and field relationships (Blockley, 1956; Mazzuchelli, 1962; Bekker, 1963; Doepel, 1965; Hudson, 1966; Williams, 1967). Figure 4 shows the general stratigraphy of ophiolite sequences in several parts of the Kalgoorlie-Norseman area.

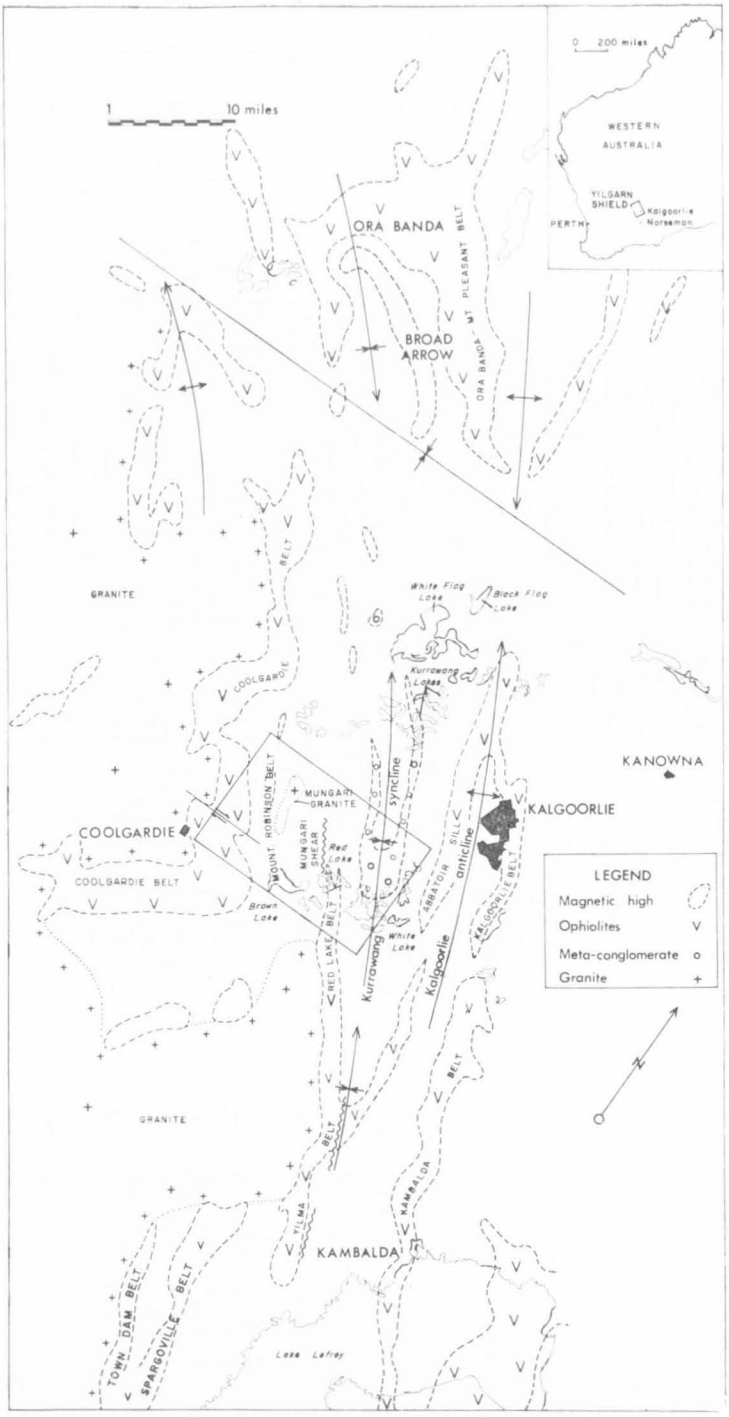


Figure 3. Structural sketch map of the Kalgoorlie region, showing the distribution of high-magnetic belts. The map is based on air-borne magnetic maps prepared by the Bureau of Mineral Resources. The framed area is mapped on the scale of 2 inches to the mile (Glikson, 1968).

A similar pattern of distribution of ophiolite belts has been described by McCall et al. (1967) from the western part of the Lake Lefroy area, about 80 km south-southwest of Kurrawang (Fig. 1). Three major ophiolite belts have been distinguished in this area (from top to base): the Yilmia belt (divided into a main eastern belt, and a minor western belt), the Spargoville belt, and the Town Dam belt. The Yilmia belt can be stratigraphically correlated with the Red Lake ophiolites with a high degree of certainty. Such a correlation had been suggested by Honman (1914). Both belts are continuous along strike and display a similar range of rock types, including pillowed metabasalts, metadolerites, and chlorite-tremolite metapyroxenites. The relationships between the Spargoville and the Town Dam belts, and the Mount Robinson ophiolites and the Coolgardie ophiolites, are more difficult to assess. While no continuous tracing along the strike of the basal ophiolites of the Lake Lefroy-Kalgoorlie area is possible because of intervening granite (Fig. 3), it is apparent from the general structural outline that these belts occupy similar stratigraphic positions with respect to the axis of the regional Kurrawang-Lake Lefroy syncline. One difficulty involved in this correlation, however, is the difference in facies of the metasediments associated with the Spargoville and Town Dam belts, and those associated with the Coolgardie and Mount Robinson ophiolites. The stratigraphically low ophiolites of the Lake Lefroy area are associated with metapelites, metasandstones, and metaconglomerates (McCall et al., 1967), whereas the Coolgardie and Mount Robinson belts are associated with mainly pelitic metasediments.

A possible stratigraphic equivalence of the Red Lake ophiolites to the Kalgoorlie greenstone belt is indicated in Figure 3. A probable correlation of the Yilmia belt with the Kambalda belt, which constitutes the southern continuation of the Kalgoorlie greenstone belt, was suggested by McCall et al. (1967). Assuming that these correlations are correct, it follows that the Red Lake-Yilmia belt and the Kalgoorlie-Kambalda belt represent one and the same phase of basic igneous activity. In as much as the Coolgardie ophiolites, the Town Dam belt, and the Norseman greenstones are stratigraphically consistent, they represent together the earliest major phase of basic igneous activity recorded in the Eastern Goldfields of Western Australia.

PETROGRAPHY

Pillowed Metabasalt

Pillowed metabasalts are well exposed about 2.5 km south-southeast of Coolgardie (Pl. 16). Lenticular, planoconvex, and concavoconvex pillow shapes are common. The effects of tectonic deformation on pillow shapes is small to moderately strong. The pillows fit tightly into each other, leaving little interstitial leucocratic mesostasis between them. In outcrop the pillows are well defined from each other due to their dark-green quenched shells (Pl. 16, fig. 1), which are contrasted with their light green cores spotted by lenticular patches up to 3 mm long. Microscopically, the pillow interiors consist of a sheared aggregate of microcrystalline acicular amphibole and xenoblastic untwinned plagioclase in approximately equal amounts. The plagioclase (oligoclase) mosaics delineate vague microlitic outlines, usually aligned parallel to the axes of columnar amphibole aggregates. Quartz is a common minor constituent of the groundmass. Opaques and leucoxene are common accessories. The megascopic spotting of the pillow

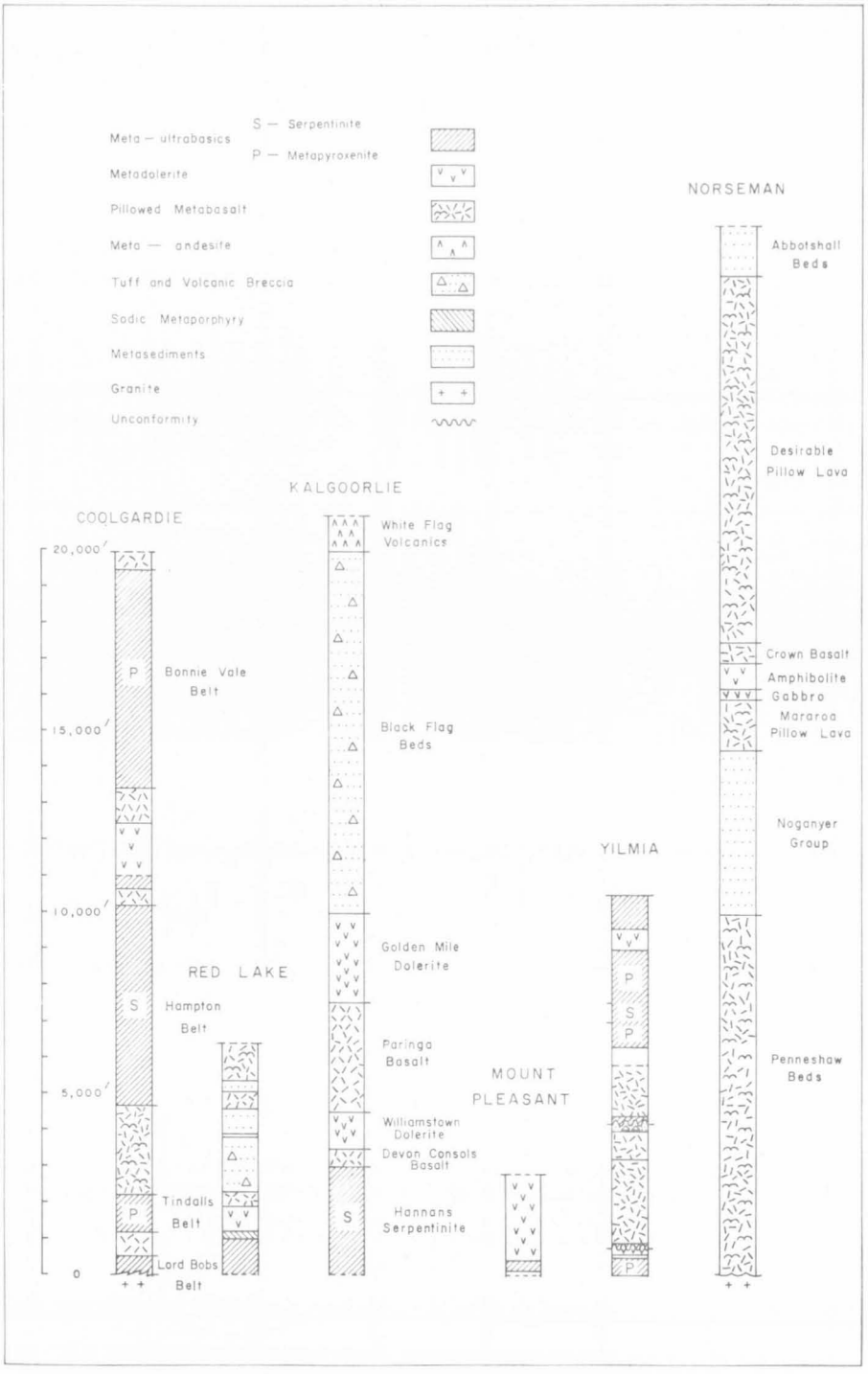


Figure 4. Stratigraphy of the ophiolite sequences of Coolgardie, Red Lake, Kalgoorlie (Woodall, 1965), Mount Pleasant (Mazzuchelli, 1962), Yilmia (Doepel, 1965), and Norseman (Bekker, 1963).

cores is caused by variations in the ratio of amphibole to plagioclase, the leucocratic lenses being considerably higher in feldspar. No relict igneous textures are associated with these lenses. The transition from pillow core to shell involves the gradual increase in the abundance of amphibole. Subhedral to euhedral microphenocrysts of andesine and subhedral to euhedral pseudomorphs of recrystallized plagioclase accompanied by quartz are sparsely distributed in the transition zone (Pl. 16, fig. 2). The quenched pillow shells are about 10 mm thick, and consist of a dense, matted, moderately sheared aggregate of fibrous microcrystalline amphibole associated with accessory plagioclase, quartz, and opaques. The shells may include subhedral pseudomorphs of plagioclase consisting of granoblastic sodic plagioclase and quartz, and of acicular amphibole (Pl. 16, fig. 2).

Individual pillows are frequently separated by thin veneers of leucocratic aphanitic mesostasis. In thin section this material is composed of microcrystalline to very fine-grained aggregates of granoblastic albite and quartz, intergrown with very fine-grained prisms of amphibole, and accompanied by minor chlorite, clinozoisite, epidote, sphene, and opaques.

Pillowed Variolitic Meta-andesites

Pillowed meta-andesites with variolitic and porphyritic margins are included in the Mount Robinson and Red Lake ophiolites (Pl. 17). The pillows fit well into each other, leaving little room for interstitial matrix. Locally, convex pillow tops are deflected downwards due to projections from overlying pillows. Pillow cores are usually light green to green, and are characterized by a delicate dark green spotting caused by cumuloblastic aggregates of amphibole. The pillow margins, up to 10 mm thick, are riddled with lenticular varioles and fine-grained phenocrysts of plagioclase (Pl. 17, fig. 1). The varioles may be up to 10 mm across. The transition from the pillow interior into the variolitic-porphyritic margin is accomplished by the development of vaguely defined bulbous leucocratic masses evolving into individual spheroids which gradually diminish in size and concentration toward the pillow rim. This pattern is interpreted in terms of the development of varioles through the emanation of late-magmatic liquids from the pillow interior into the still-plastic shells. The actual rims of the pillows are devoid of varioles, and may be heavily spotted by phenocrysts of plagioclase. Neither varioles nor phenocrysts are present in the cores.

In thin section, the cores are resolved as uneven-grained assemblages comprising cumuloblasts of fine-grained acicular to prismatic amphibole set in turbid matrices of microcrystalline sodic plagioclase, quartz, accessory opaques, and apatite. The plagioclase may display weakly defined outlines of microlites arranged in fan-shaped aggregates, indicative of relict variolitic texture. Veinlets of prehnite associated with clouding of the plagioclase may be present. The prehnite may also occur as microporphyroblasts set in matrices of quartz and amphibole, with chlorite and opaques as minor components. The recrystallized varioles consist of granoblastic aggregates of microcrystalline sodic plagioclase, bladed crystals of amphibole, accessory quartz, and opaques. Also present in the pillow shells are subhedral to euhedral phenocrysts of calcic plagioclase, which are usually partly recrystallized and heavily clouded by saussurite, amphibole, epidote, calcite, and quartz. The recrystallized plagioclase ranges from albite to labradorite. Both the varioles and the phenocrysts are embedded in a very fine-grained base composed

of prismatic and bladed amphibole accompanied by minor plagioclase, opaques, apatite, chlorite, and sphene. This aggregate is probably the metamorphosed equivalent of the chilled glassy margins of the pillow.

Pillowed Porphyroblastic Meta-andesites

Pillowed meta-andesites displaying the development of porphyroblastic textures are common in the Red Lake ophiolites (Pl. 18). The pillows are circular in plan, and ellipsoidal to concavoconvex in cross section. Base diameters range up to 1.5 m, and thicknesses up to 70 cm. The pillows fit tightly into each other, and are well defined by interpillow ultramafic mesostases (Pl. 18). Segregations and veins of carbonate are widespread, and commonly transgress interpillow boundaries. Narrow shear zones consisting of alternating bands of meta-andesite and ultramafic chlorite-amphibole rocks are present. The emplacement of the ultramafic bands along these shears indicates a syntectonic to post-tectonic origin of the ultrabasic material. In thin section no relict igneous texture is retained. The cores display well developed porphyroblastic and cumuloblastic textures, with very fine-grained to fine-grained crystals and clusters of amphibole (hornblende) set in microcrystalline matrices of plagioclase, amphibole, and carbonate. Porphyroblasts are coarser-grained and more abundant in pillow interiors than in the margins, which are bounded abruptly by a chlorite-amphibole mesostasis.

Unlike the cores, the pillow shells are aphanitic and light grey. In thin section the mineralogy and texture of the shells differ from those of the cores as follows:

(1) The amphibole-plagioclase ratio in the margins is lower than in the cores.

(2) The amphibole porphyroblasts in the margins are finer-grained and less well defined than in the cores.

(3) There is little or no carbonate in the margins.

The boundary between the pillow margin and the interpillow mesostasis is abrupt. In thin section, the ultramafic rock is resolved as an aggregate of fine- to medium-grained euhedral amphibole (hornblende) crystals developed at the expense of microcrystalline to very fine-grained chlorite. The amphibole may be pocked by inclusions of microcrystalline albite, and may be bodily deformed into S-shapes. Accessory minerals are epidote, biotite, apatite, tourmaline, and rod-like opaques.

Garnet-rich brecciated pillowed meta-andesites crop out within the Red Lake ophiolites, and form an irregular mass surrounded by non-brecciated garnet-free pillowed meta-andesites. The breccia fragments are set in an ultramafic matrix, not unlike the interpillow mesostasis described above. Both the fragments and the ultramafic matrix are heavily charged with porphyroblasts of garnet. Except for the occurrence of garnet porphyroblasts, the breccia fragments are texturally and compositionally similar to the cores of pillowed porphyroblastic meta-andesites.

Pillowed Metavolcanics from Lake Lefroy and Norseman

Well preserved microlites of calcic plagioclase (oligoclase to labradorite) are displayed by pillow interiors in Norseman (Bekker, 1963). The microlites are often arranged in pilotaxitic textures. Typical of the Norseman metabasalts is the high degree to which the primary plagioclase has been preserved in spite of the greenschist facies metamorphism.

Fine- to medium-grained lath-like plagioclase crystals are developed in cores of pillows described by Muhling (1965) from the Lake Lefroy area. This occurrence may be similar to that of pillowed spilites displaying transitions from variolitic margins to ophitically textured cores, described by Reed from New Zealand (1957). Pillowed dolerites have also been described by Yagi (1960) from Japan.

Leucocratic patches and lenses characterized by feldspar-amphibole ratios higher than those of the surrounding matrix were described from metabasalt pillow cores in Norseman (Bekker, 1963). No relict igneous textures are displayed by the leucocratic aggregates. It is likely that these textures represent recrystallized varioles.

Nonporpyhritic pillow shells composed of uniform aggregates of fibrous submicrocrystalline amphibole were described from Norseman (Bekker, 1963), Lake Lefroy (Muhling, 1965), and Lake Cowan (Hudson, 1966). Porphyritic pillow shells riddled with recrystallized phenocrysts of plagioclase also occur in the shells of pillowed metabasalts at Yilmia (Doepel, 1965). Bekker (1963) pointed out that lath-like crystals of calcic plagioclase may be common at metabasalt pillow margins at Norseman, whereas only microlitic plagioclase is present in the cores.

Porphyritic Meta-andesites

Massive outcrops of greenish grey meta-andesites and tourmalinized meta-andesites occur in the Red Lake area. In thin section the meta-andesites consist of microphenocrysts of plagioclase and amphibole set in microcrystalline matrices of plagioclase, amphibole, and biotite. Biotite-rich and tourmaline-rich meta-andesites are common, and are regarded as the altered equivalents of the relatively fresh meta-andesites. In thin section the altered meta-andesites consist of very fine-grained to fine-grained subhedral and anhedral equant crystals of intermediate to sodic plagioclase and of equant microphenocrysts of amphibole (actinolite), set in turbid microcrystalline aggregates of plagioclase and amphibole, with biotite, quartz, tourmaline, sphene, and opaques forming accessory constituents. The plagioclase phenocrysts are slightly recrystallized, considerably corroded at their margins, and may be clouded at their centres.

Basic Flow-Breccia

A horizon approximately 7 m thick of polymictic basic flow-breccia is well exposed at the promontory of the Red Lake peninsula (Pl. 19, fig. 1). Stratigraphically, this horizon overlies a thin slate intercalation, which in turn overlies pillowed variolitic-porphyritic meta-andesites, associated with bands of meta-dolerite and metapyroxenite. The stratigraphic top of the flow-breccia is eroded. The lateral extension of the flow-breccia is about 200 yards. In places, the flow-breccia directly overlies strongly brecciated pillowed meta-andesites. The rocks are composed of subangular to lenticular pebble-sized fragments of microlitic meta-basalt, porphyritic metabasalt, meta-andesite, acid volcanics, and metapyroclastic rocks. No variolitic fragments similar to the underlying variolitic-porphyritic pillowed meta-andesites were encountered in the flow-breccias. Sedimentary fragments are absent. The igneous fragments are embedded in a finely comminuted pyroclastic matrix associated with eutaxitic flows and fragments of metamorphosed volcanic glass, referred to in the following as 'metatachylyte'.

Chilled fragments of metabasalt displaying metatachylytic margins are common. The flow-breccia is moderately sheared, with the fragments lying with their longest axes parallel to each other, and oriented at vertical to subvertical attitudes. The megascopic structures and textures of the breccia are beautifully pronounced on varnished surfaces (Pl. 19, fig. 2; Pl. 20, fig. 1).

Study of the flow-breccia in thin section is complicated by extensive metamorphic reconstitution. Nevertheless, the retention of recrystallized microphenocrysts, lath-like crystals, microlites, and longulites of plagioclase, as well as the preservation of original fragmental boundaries, facilitates the recognition of the main primary elements of the flow-breccia. The petrographic designation of the fine-grained metavolcanic fragments as metabasalt, meta-andesite, and acid volcanic rocks, is tentatively based on the amphibole-plagioclase ratio of these rocks. In the following, the various fragment types will be individually described.

Metabasalt and meta-andesite fragments. In hand specimen these fragments are dark green to light green, and slightly mottled in appearance. Microscopically, they consist of recrystallized microlites and equant phenocrysts of plagioclase set in matrices of amphibole and plagioclase, with accessory sphene, opaques, and clinozoisite (Pl. 20, fig. 2). Microlitic plagioclase is characteristic of the metabasaltic fragments. The meta-andesite fragments include both microlitic and microporphyritic plagioclase.

Acid volcanic fragments. Although quantitatively minor, the acid fragments stand out in outcrop because of their leucocratic aspect. Microscopically, they consist of microcrystalline aggregates of granoblastic plagioclase, quartz, and sheaf-like amphibole. Some of these fragments include microlitic plagioclase, arranged in parallel or slightly diverging groups, which may be associated with slender feather-like aggregates of amphibole. The sodic composition of the plagioclase and the low amphibole-plagioclase ratio suggest the acid igneous parenthood of the fragments. No phenocrysts have been found, which distinguishes these fragments from sodic metaporphyries.

Metadolerite fragments. Although quantitatively minor, metadolerite fragments stand out in outcrop due to their megascopic subophitic texture (Pl. 19, fig. 2). In thin section, the metadolerites display lath-like prisms of labradorite twinned according to the Carlsbad law, and to a lesser extent according to the albite law. The plagioclase is patchily clouded by saussurite, and is riddled with submicrocrystalline needles of amphibole, often oriented with their *c*-axes parallel to cleavage directions in the host feldspar. Amphibole also occurs as fibrous aggregates located at interstitial positions, and may protrude into the feldspar. Both the plagioclase and the amphibole are partly replaced by granular calcite. Recrystallized plagioclase accompanied by quartz occurs as granoblastic intergranular aggregates. The opaques are preferentially associated with the amphiboles. Some metadolerites show a progressive obliteration of primary igneous textures, recrystallization and saussuritization of the plagioclase and by redistribution of the amphibole. Amphibole may occur as fibrous bundles aligned in crude nematoblastic textures.

Chilled metabasalt fragments. Thin selvedges of microcrystalline amphibole which are considered metatachylyte coatings are often associated with metabasalt, meta-andesite, acid metavolcanics, and metadolerite fragments (Pl. 20). In some cases these selvedges are particularly well developed, and may occupy more than half the diameter of the fragment. Wherever the selvedge is thickly developed, the

transition from the metatachylyte into the fragment core is gradual, as contrasted with the usually sharp boundaries between these selvedges and the interfragmental matrix of the flow-breccia. As a rule, the smaller the diameter of the fragment, the better developed is the metatachylyte selvedge. These relationships can be understood in as much as the coated fragments represent chilled basalt fragments, that is, basaltic fragments which have been marginally fused during their transportation in the magma. If this is correct, the relatively thicker development of metatachylyte selvedges in smaller fragments can be interpreted, for smaller fragments could be expected to melt more quickly than larger ones.

Alternatively, the coated fragments can be considered as chilled micropillows in which the cores have crystallized due to a slower rate of cooling. Microscopically, the crystallized cores of the chilled metabasalt fragments display an irregularly textured assemblage of plagioclase, saussurite, amphibole, and clinozoisite, with epidote, quartz, and opaques as minor constituents. Vaguely outlined microphenocrysts of recrystallized plagioclase are sparsely distributed throughout the rock. Some lenticular leucocratic aggregates may be associated with 'flow-tails', consisting of bunches of plagioclase microlites located in continuation with the lenses.

Fragmental matrix and eutaxitic flows. The interfragmental matrix of the flow-breccia displays finely microbrecciated textures, which are usually well pronounced due to differences in composition between the microfragments and the interstitial groundmass. The microfragments are composed of a felted aggregate of acicular submicrocrystalline amphibole and of granoblastic plagioclase accompanied by minor sphene and opaques. The interstitial matrix consists of granoblastic plagioclase and a subordinate amount of acicular amphibole. Some fragments are characterized by the comb-like texture of their amphibole aggregates.

The metatachylyte consists of dense assemblages of fibrous submicrocrystalline amphibole, often abundantly accompanied by chlorite and minor opaques. These aggregates assume three modes of occurrence, as follows:

(1) As selvedges and chilled margins of meta-andesite, metabasalt, and meta-dolerite fragments.

(2) As streamlined tongues, eutaxitic flames, and streaks associated with the finely comminuted interfragmental groundmass.

(3) As smaller angular fragments embedded in the interfragmental groundmass.

Metatachylytic tongues may project into microfragmental matrix. These amphibolitic flames usually grade into small fragments of metabasalt, or may enclose small fragments.

Recrystallized phenocrysts of plagioclase may be engulfed by the metatachylyte flows. As a rule, boundaries of the metatachylyte flames and tongues with the fragmental matrix are well defined. Boundaries with the larger fragments, on the other hand, are either sharp or gradual. The significance of the metatachylyte elements with respect to the origin of the flow-breccia is considered in the following section.

Origin of the amphibolitic flames. In considering the nature of the flames, tongues and selvedges of amphibole, and of the chlorite-amphibole assemblages described above, two alternative interpretations are possible:

(1) The amphibole and chlorite-amphibole aggregates have originated by means of metamorphic segregation.

(2) The amphibole and chlorite-amphibole aggregates represent metamorphosed basic volcanic glass, or metatachylyte.

The first interpretation seems compatible with the frequent association of the aggregates in question with fragment-matrix boundaries, as well as with concordant microjoints in the rock. The bulk of the evidence, however, seems to favour the second interpretation.

Assuming an igneous origin for the amphibole and chlorite-amphibole aggregates, the flow-like elements, the fragment coatings, and the fragmental elements can be interpreted as eutaxitic flows, chilled margins, and glassy fragments, respectively. The occurrence of angular fragments would be difficult to explain in terms of metamorphic segregation. Furthermore, amphibolitic aggregates have not been found within the igneous fragments. This feature, while understandable in terms of an igneous origin, can be hardly explained in terms of metamorphic segregation. The composition and the texture of the amphibolitic aggregates are similar to those of pillow margins. Since the latter can be safely regarded as the metamorphosed equivalents of volcanic glass, a similar origin is implied for the amphibolitic aggregates of the flow-breccia.

METADOLERITES

Metadolerites are widespread throughout the Coolgardie-Kurrawang sequence, and occur within stratiform ophiolite belts, or as independent sills intruded into metasediments. Some metadolerite bodies are coarser grained in their centres than in their margins. No contact-metamorphic effects have been discerned in the sedimentary wall rocks. On the other hand, sodic metaporphyries in contact with metadolerites may contain abundant amphibole. Due to their relatively coarse grain-size when compared with metabasalts and meta-andesites, the metadolerites have retained certain primary mineralogical and textural features to a relatively high degree. Metadolerites from several localities display well preserved subophitic textures (Pl. 21, fig. 1), and often include little-recrystallized primary calcic plagioclase. However, no pyroxene has been retained by the metadolerites An entire transition from subophitic metadolerites to completely reconstituted amphibolites retaining no relict igneous textures can be demonstrated. In thin section, subophitic texture may be well preserved. Partly recrystallized fine- to medium-grained lath-like crystals of plagioclase are partly or completely enwrapped by fine- to medium-grained amphibole. The plagioclase may be normally zoned, and in some cases reversely zoned. It may be twinned on the Carlsbad and albite laws. Clouding by microcrystalline amphibole and cryptocrystalline saussurite is widespread. Biotite, quartz, clinozoisite, and apatite may also be included in the feldspar. Partial recrystallization of the plagioclase into granoblastic aggregates ranging from albite to labradorite in composition is present. The actinolite commonly occurs as short prismatic subhedral crystals which appear to occupy original pyroxene positions, and enclose the feldspar ophitically or subophitically.

The actinolite is commonly rimmed by acicular hornblende, which also forms aggregates independent of the actinolite. Biotite is a common minor constituent

usually developed at the expense of amphibole. Other accessories are quartz, subhedral and granular sphene, and leucoxene, which often substitutes for or encloses armoured relics of skeletal ilmenite (Pl. 21, fig. 2).

A progressive obliteration of the original igneous texture is achieved through redistribution of the amphibole. The effect of propylitization on the metadolerites is represented by fan-shaped aggregates of chlorite and granular calcite which may be developed at the expense of both plagioclase and amphibole. Replacement of amphibole is particularly well pronounced along cleavage planes. The end product of the complete propylitization of metadolerites is represented by rocks displaying ghost doleritic texture in hand specimen. Microscopic examination of these rocks shows that they consist of calcite, sericite, chlorite, and quartz. Calcite is mainly concentrated within the outlines of pre-existing lath-like crystals of plagioclase, which accounts for the megascopically discernible doleritic texture of the rocks.

Amphibolites

Amphibole-plagioclase assemblages showing no relict igneous textures are most widespread in the Coolgardie-Kurrawang area. These rocks are commonly associated with basic meta-igneous rocks, the origin of which is shown by relict igneous textures and structures. Amphibolites also occur as individual bodies, not necessarily associated with rocks of proved igneous parenthood. Wherever amphibolites are associated with igneous elements, such as pillows, varioles, amygdales, or flow-textures, they evidently represent the reconstituted derivatives of basic igneous rocks. In interpreting the origin of amphibolites with no relict igneous elements, the following considerations are pertinent:

(1) The amphibolites may form discrete stratiform bodies, displaying sharp contacts with their wall rocks. This mode of occurrence is consistent with that of meta-igneous sills or flows which retained their igneous textures.

(2) A continuous textural transition from little recrystallized metadolerites and metabasalts into amphibolites can be demonstrated.

(3) No relict sedimentary structures or textures are displayed by the amphibolites.

(4) The mineralogy of the amphibolites is similar to that of the basic meta-igneous rocks.

(5) The chemical composition of the amphibolites is consistent with that of the metabasalts and metadolerites in the area.

(6) The high iron and magnesia contents of the amphibolites are not compatible with the compositions of normal sedimentary rocks.

(7) The amphibolites do not have enough lime to be considered derivatives of impure dolomites.

It is accordingly concluded that the amphibolites represent the recrystallized equivalents of the basic meta-igneous rocks.

Meta-ultrabasic Rocks

Meta-ultrabasic rocks are common throughout the igneous sequence of the Coolgardie-Kurrawang area. Serpentinites are found only in the Coolgardie ophiolites, and are not described in this section. The Mount Robinson and Red Lake ophiolites comprise numerous chlorite-tremolite rocks, occasionally displaying relict cumulate textures. The chemical composition of these rocks indicate that they have been derived from pyroxenites. In the Mount Robinson and Red Lake belts, the meta-ultrabasics are preferentially located at low stratigraphic levels of the igneous sequences. The chlorite-tremolite assemblages are deep green in hand specimen, and are particularly susceptible to shearing, which accounts for the usually poor preservation of primary igneous textures in these rocks. In thin section the weakly sheared metapyroxenites contain densely packed pseudomorphs of tremolite after pyroxene. The former presence of pyroxene is suggested by the short prismatic form of the pseudomorphs, which may be up to 1 mm long. The pseudomorphic tremolite aggregates are irregularly transected by fine microfractures composed of submicrocrystalline chlorite, possibly representing the fracture pattern within the original pyroxene. The pseudomorphs are set in a microcrystalline aggregate of chlorite and tremolite, accompanied by accessory feldspar, quartz, and opaques.

Shearing of the metapyroxenites results in the progressive elimination of the pseudomorphs. An advanced stage of obliteration of the blastocumulate texture is represented by sheared aggregates of microcrystalline tremolite separated by tremolite-chlorite aggregates. This textural pattern is represented in hand specimen by the alteration of dark green patches (the tremolite aggregates) and light green matrix (the tremolite-chlorite aggregates). With extreme shearing, the chlorite-tremolite metapyroxenites develop a conspicuous schistosity. Microscopically, these rocks consist of ropy aggregates of fibrous tremolite and submicrocrystalline chlorite accompanied by opaques. Some chlorite-tremolite rocks display a porphyroblastic development of the tremolite, which occurs as fine- to medium-grained columnar crystals embedded in a microcrystalline base of chlorite.

Talc-tremolite meta-ultrabasics are similar in hand specimen to chlorite tremolite assemblages. In thin section these rocks consist of radiating aggregates of tremolite, and of talc aggregates. The talc occurs as cryptocrystalline to microcrystalline scales, mostly occupying interstitial positions with relation to the radiating tremolite tuffs, and is accompanied by saussurite and by accessory albite.

Sodic Metaporphyries

Sodic metaporphyries occur as stratiform to lenticular bodies up to 1000 m thick. The extensive pre-existence of sodic porphyries contemporaneous with the deposition of the Mungari Beds and the Kurrawang Beds is shown by the abundant pebbles of sodic porphyry, as well as by the sodic composition of the tuffaceous metagreywackes. In outcrop, the metaporphyries appear as massive, folded (Pl. 22, fig. 1), or strongly sheared, light-coloured, grey, and black rocks. The strongly sheared and dark-coloured varieties are characterized by abundant sericite and biotite, respectively. The phenocrysts are usually megascopically discernible, and may be up to 10 mm across. In thin section (Pl. 22, fig. 2), the sodic metaporphyries consist of phenocrysts of albite and/or oligoclase, which may be accom-

panied by phenocrysts of quartz. No potash feldspar has been encountered. The phenocrysts are set in matrices of sodic plagioclase and quartz, which may be accompanied by chlorite, biotite, sericite, amphibole, and opaques, and less commonly by sphene and epidote. Apatite is usually present. Calcite may assume quantitative importance in many metaporphyries.

The metaporphyries of the Eastern Goldfield of Western Australia have been referred to by various workers as dacite porphyries (Blockley, 1956), rhyodacite porphyries (Mazzuchelli, 1962), rhyolites (Horwitz & Sofoulis, 1965), and porphyroids (Bekker, 1963). Differences in the nomenclature of the porphyries reflect the confusion which exists with respect to the magmatic versus metasomatic, and intrusive versus extrusive origin of these rocks. A comprehensive study of the porphyries of the Kalgoorlie region carried out by O'Beirne (1968) indicates that the bulk of these rocks are of magmatic origin, and that both intrusive and extrusive phases are present. In most cases, however, little structural or textural evidence affording the discrimination of intrusive from extrusive porphyries is present.

Because the porphyries are considered to have undergone regional metamorphism, they are referred to as sodic metaporphyries. These rocks are consistent with keratophyres, as defined by Howell (1960).

The thickest bodies of sodic metaporphyries in the Coolgardie-Kurrawang area are associated with the Mount Robinson and Red Lake ophiolites. Hosts of small bodies of sodic metaporphyries are associated with ophiolites and to a lesser extent with metasediments throughout the Coolgardie-Kurrawang sequence. Stratiform bodies of sodic metaporphyry are commonly located along boundaries of ophiolites and metasediments. No discordant relationships between the metaporphyries and metasediments have been observed. Owing to poor exposure, however, the precise nature of the contacts could not be assessed. Sodic metaporphyries adjacent to ophiolites are often characterized by the occurrence of amphibole as a minor or major constituent. It is reasonable to ascribe this feature to magmatic contamination upon the emplacement of the porphyritic magma. The possibility of an origin of the amphiboles due to metamorphic diffusion of iron, magnesia, and lime into the sodic porphyries, however, cannot be excluded. Altered metabasalts adjacent to sodic metaporphyry bodies at the Surprise Gold Mine (southeast of Coolgardie) display the following zonation pattern:

(1) The actual contact with the porphyry is rimmed by amphibole, which is developed at the expense of biotite and chlorite. Amphibole may also occur away from the contact.

(2) The amphibolitic zone is bounded by a usually thick zone consisting mainly of biotite, accompanied by minor chlorite.

(3) The internal zone consists of chlorite. Chlorite and biotite may replace each other, but biotite is mostly younger.

The sequence of crystallization, with chlorite, biotite, and amphibole being younger than each other in this order, indicates the influx of potash and lime in the vicinity of the sodic metaporphyry.

According to O'Beirne (1968), porphyries of the Kalgoorlie region occur in a variety of forms: as flows, sills, dykes, ring necks, and plugs. The sodic metaporphyries of the Coolgardie-Kurrawang sequence display two principal modes of occurrence, as follows:

(1) Stratiform to lenticular, usually thick bodies of metaporphyry, commonly associated with oligomictic porphyry breccias and porphyry conglomerates. On the basis of considerations made later in this paper, these bodies are regarded as volcanic flows.

(2) Thin stratiform and lenticular bodies of porphyry, regarded as sills.

Some metaporphyry bodies display slight shearing effects, whereas in others shearing is well pronounced, and is often associated with a high degree of sericitization of the feldspar. These factors indicate that the porphyries have been emplaced before the onset of metamorphism. The pre-folding age of at least some metaporphyries is indicated by the isoclinal folding of sills of sodic metaporphyry. That the emplacement of the porphyries preceded folding is also indirectly indicated by the association of these rocks with derivative porphyry conglomerates and tuffaceous greywackes. It is reasonable to assume that most of the sodic metaporphyries represent the acid phase of the geosynclinal igneous suite.

Subdivision of the sodic metaporphyries is facilitated by the type of phenocrysts present, as follows:

(1) Sodic quartz metaporphyries—phenocrysts of quartz are present along with phenocrysts of albite and/or oligoclase.

(2) Sodic metaporphyries—phenocrysts of albite and/or oligoclase are present, and are accompanied by few or no phenocrysts of quartz.

(3) Sodic amphibole metaporphyries—phenocrysts of albite and/or oligoclase are set in matrices rich in amphibole; no phenocrysts of quartz have been observed in these rocks.

In thin section the sodic metaporphyries consist of short prismatic to equant phenocrysts of sodic plagioclase. Complex twinning according to the Carlsbad, albite, and pericline laws is common. Tabular crystals tend to display discontinuous checker-board twinning patterns on their (100) faces, whereas prismatic crystals are more often twinned according to the Carlsbad law alone. Optical discontinuities within the feldspar are common. Sericitization of the plagioclase is ubiquitous, and is developed to varying degrees. The microcrystalline scales of sericite are generally aligned along the cleavage planes of the host crystal. Variations in the density of distribution of the sericite within plagioclase phenocrysts may define concentric zones, indicative of pre-existing zonation patterns of the feldspar. The degree of sericitization usually decreases from the core of the phenocrysts outwards. The quartz phenocrysts are usually rounded or deeply corroded and embayed. Undulatory extinction is common. The groundmass adjacent to the boundaries of quartz phenocrysts is relatively rich in sericite, reflecting the abundance of feldspar in the immediate vicinity of the phenocryst. The groundmass itself consists of turbid aggregates of microcrystalline albite, quartz, and sericite, accompanied by clots of biotite and by finely disseminated opaques. Some metaporphyries carry accessory epidote. In some specimens, the groundmass consists of short microlites of feldspar.

The mineralogy of amphibole-bearing sodic metaporphyries differs from that of sodic quartz metaporphyries by virtue of the abundant amphibole in the groundmass and the absence of quartz phenocrysts. These rocks are either associated with boundaries of sodic metaporphyries and ophiolites, or constitute independent bodies. In hand specimen the rocks differ little from amphibole-free metaporphy-

ries. In thin section, they consist of lath-like to equant microphenocrysts of sodic plagioclase unevenly scattered in a matrix composed of microcrystalline granoblastic albite and quartz, fibrous bundles of micro-crystalline amphibole, biotite, and accessory opaques.

The biotite is developed at the expense of the amphibole. The latter constituent is almost invariably confined to the groundmass. The phenocrysts are clouded by submicroscopic inclusions, decreasing in concentration toward the margins. Inclusion-free zones also coincide with cleavage planes. Continuous to discontinuous twinning according to the albite, pericline, and Carlsbad laws may be present.

MINERALOGY

PLAGIOCLASE

Relict Igneous and Recrystallized Plagioclase

Plagioclase is the predominant leucocratic component and the sole feldspar of the basic meta-igneous rocks and the sodic metaporphyries. On the basis of differences in the textural mode of occurrence and the composition of the feldspar, a two-fold classification into relict igneous (primary) plagioclase and recrystallized plagioclase is possible. While most basic meta-igneous rocks in the Coolgardie-Kurrawang sequence contain only recrystallized plagioclase, some metabasites and most acid metaporphyries have partly retained their igneous feldspars. The main characteristics of the feldspar classes, and the reasoning underlying their separation from each other, are given below.

Igneous plagioclase. Subhedral to euhedral microphenocrysts and lath-like crystals of plagioclase are common in metavolcanic rocks and in metadolerites, respectively (Pl. 21, fig. 1; Pl. 23, fig. 2). In the basic meta-igneous rocks these feldspars commonly range in composition between andesine and labradorite, and less frequently correspond to oligoclase and bytownite. The calcic and intermediate plagioclase feldspars are usually clouded to varying degrees by saussurite, clinozoisite, sericite, sphene, calcite, amphibole, and chlorite. The plagioclase feldspars of sodic metaporphyries range from albite to sodic oligoclase in composition (Pl. 21, fig. 1; Pl. 23, fig. 2). In the basic meta-igneous rocks these feldspars patterns of which often represent a pre-existing normal zonation of the plagioclase.

The basis for considering the above-described class of plagioclase feldspars as igneous is as follows:

(1) The rocks of the Coolgardie-Kurrawang sequence are metamorphosed according to the greenschist facies (Glikson, 1968). According to most workers, no metamorphic crystallization of calcic plagioclase is possible within this range of metamorphic conditions (e.g. Turner & Verhoogen, 1960; Brown, 1962; Deer et al., 1963). The occurrence of andesine, labradorite, and bytownite in the ophiolites, therefore, is better interpreted in terms of a retardation of metamorphic reactions.

(2) The common occurrence of well-preserved crystal outlines of the plagioclase feldspars of both the basic and the acid meta-igneous rocks favours an igneous rather than metamorphic origin.

It appears likely that the compositions of the primary plagioclases have in most cases been modified to varying degrees through the development of clouding products and by incipient recrystallization. Thus, the growth of amphiboles at the expense of plagioclase has been associated with a partial depletion of the feldspar in lime and alumina.

Recrystallized plagioclase. The igneous plagioclase crystals may be recrystallized to varying degrees into microcrystalline aggregates of granoblastic plagioclase ranging in composition from albite to labradorite. Individual grains of plagioclase may be discretely rounded or display sutured outlines, they may display undulating extinction, or merge imperceptibly into each other. Recrystallized grains are relatively free of inclusions, and are rarely twinned. Recrystallized plagioclase feldspars are usually more sodic than co-existing relict igneous plagioclase feldspars. A two-fold classification of the metamorphic plagioclase in terms of recrystallized plagioclase confined to original plagioclase positions, and of redistributed plagioclase, can be made on a textural basis. Upon complete redistribution of the plagioclase, the primary textural identity of the meta-igneous rocks is lost, and the rocks are classified as amphibolites.

Most metadolerites contain both igneous and recrystallized plagioclase. Fine-grained metavolcanic rocks commonly display a thorough recrystallization of the feldspar, accompanied by little redistribution of the recrystallized products. The groundmass plagioclase of the sodic metaporphyries probably underwent metamorphic crystallization. The absence of flow textures in these aggregates could partly result from metamorphic reconstitution. The clear rims of sodic plagioclase typical of many phenocrysts may represent either metamorphic growth or recrystallization. Late-magmatic growth is an alternative explanation for this feature. It appears that the higher the lime content of the plagioclase, the more it is prone to clouding and recrystallization. This appears to explain the fact that the sodic metaporphyries, and to a lesser extent the meta-andesites, have retained their original igneous textures to considerably higher degrees than the basic meta-igneous rocks.

Compositional relationships. Figure 5 shows the relationships between the compositions of igneous plagioclase feldspars and their recrystallized equivalents in basic meta-igneous assemblages. In all the specimens with co-existing plagioclases, the metamorphic plagioclase is higher in the albite molecule than the igneous plagioclase. These relationships indicate that recrystallization of the latter is associated with a loss of lime and alumina, which have conceivably been incorporated in the formation of amphibole. Figure 5 also suggests sympathetic relationships between the composition of metamorphic plagioclases and co-existing igneous plagioclases.

The plagioclase compositions have been determined by optical methods, with igneous plagioclase compositions based on measurements of twinning, and the metamorphic and recrystallized plagioclase compositions based on measurements of the refractive indices. Both the igneous and recrystallized feldspars display a range of composition in each rock. The compositional data presented in this paper apply to the most calcic plagioclase encountered in each group. Thus, for example, the recorded existence of granoblastic andesine in any particular assemblage does not necessarily imply the absence of oligoclase or albite.

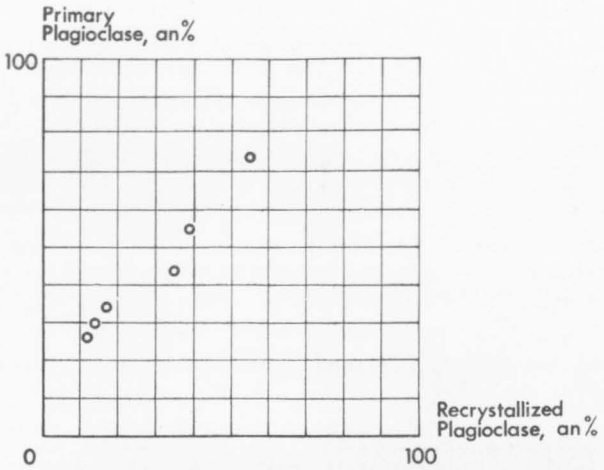


Figure 5. Co-existing 'primary' (relict igneous) plagioclase feldspars and metamorphic (recrystallized) plagioclase feldspars in basic meta-igneous rocks of Coolgardie-Kurrawang. Each point represents the composition of the most calcic metamorphic plagioclase present in the rock.

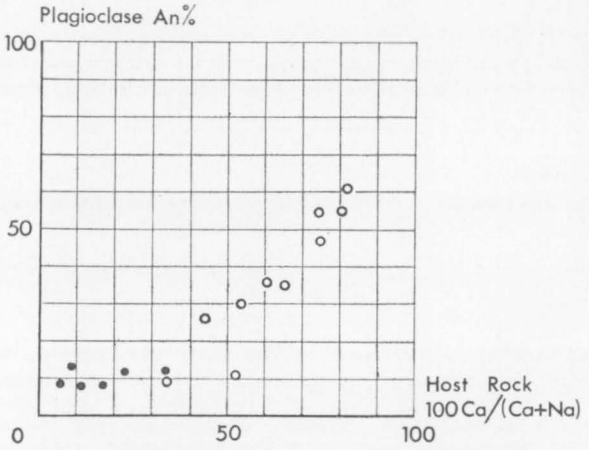


Figure 6. Relationships between modal plagioclase compositions and the 100Ca/Ca+Na values of the host rocks in basic meta-igneous rocks and sodic metaporphyries. The 100Ca/Ca+Na values are calculated from the equivalent cation percentages. Open circles—plagioclases of basic meta-igneous rocks; solid circles—plagioclases of sodic metaporphyries.

Zonation of plagioclase. Weak normal compositional zonation is commonly displayed by both igneous and recrystallized plagioclase feldspars of the basic meta-igneous rocks. The igneous plagioclase crystals of some metadolerites consist of cores of calcic plagioclase which grade outward into margins of sodic plagioclase. The zonation pattern within plagioclase grains appears to be controlled by their boundaries with adjacent amphiboles. These relationships may also be present where the amphibole projects into the plagioclase. Because the amphibole is clearly a metamorphic rather than a relict igneous constituent, it follows that the zonation of the plagioclase is at least partly metamorphic in origin.

It is likely that the release of lime and alumina represented by the normal zonation was associated with the formation of the amphibole and with the replacement of actinolite by hornblende.

Plagioclase-host rock relationships. Relationships between the distribution of lime and soda in plagioclase feldspars and in the corresponding host rocks are explored by comparison of the respective 100Ca/Ca+Na values (Fig. 6). For each rock, the composition of the most calcic plagioclase present is considered. The positive trend displayed in Figure 6 indicates that the abundance of the anorthite molecule in the plagioclase feldspars is sympathetically related to the lime-soda ratio of the host rocks. The 100Ca/Ca+Na value of each analyzed host rock is higher than the optically derived 100Ca/Ca+Na value of the incorporated plagioclase. These relationships suggest that the co-existing amphiboles have a higher lime-soda ratio than the corresponding host rock, thus compensating the relatively low lime-soda ratio of the plagioclase.

Amphibole

Amphiboles constitute a major and commonly the sole ferromagnesian phase present in the intermediate, basic, and ultrabasic meta-igneous rocks of the Kalgoorlie region. Some sodic metaporphyries are rich in amphibole as well. In classifying the amphiboles of the basic and intermediate meta-igneous rocks, the following considerations are pertinent:

(1) The amphiboles do not exhibit the deep colours and pleochroic schemes characteristic of alkali amphiboles.

(2) The amphiboles do not display the multiple twinning characteristic of cummingtonites and grunerites.

(3) The amphiboles do not display the positive optic sign and the low optic angle characteristic of paragasite and ferrohastingsite, respectively.

The range of the optical properties of the amphibole (refractive indices, optic angles, and extinction angles) is consistent with that of the tremolite-ferroactinolite series, of common hornblende, and of the edenite and tschermakite series. While common hornblende cannot be distinguished from the two latter series by optical means, the distinction of actinolites from hornblendes is facilitated by measurements of the refractive indices. Distinguishing the iron-rich members of the tremolite-ferroactinolite series from hornblendes, however, is not straightforward. In Figure 7 the optical data of amphiboles cited from Shido and Miyashiro (1959) and from Deer et al. (1963, vol. 2, tables 38, 40) are plotted on the $2V_x/N_z$ diagram, along with the optical data for amphiboles from the Coolgardie-Kurrawang sequence. The discontinuous curves are those given by Shido & Miyashiro

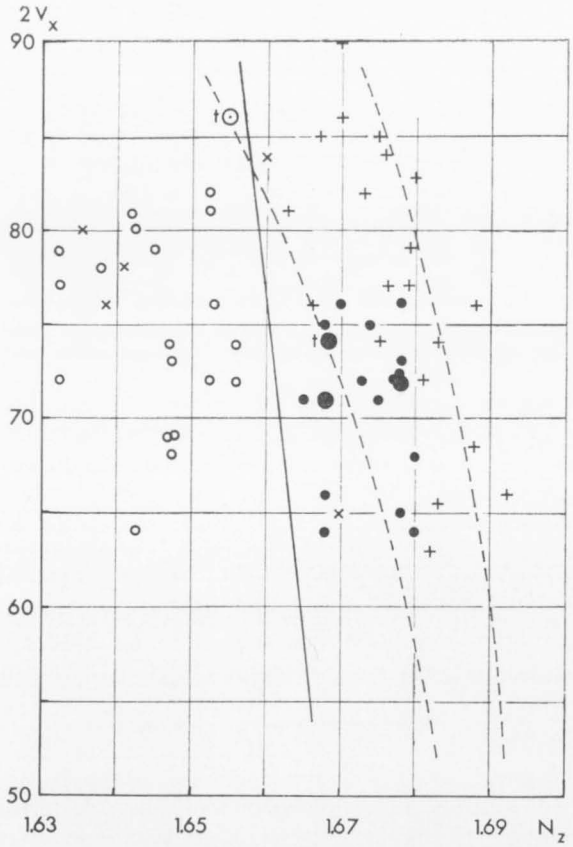


Figure 7. Relationships between the optic angle ($2V_x$) and the refractive index (N_z) of amphiboles. The discontinuous curves (Shido & Miyashiro, 1959) define the fields of amphiboles collected from three metamorphic zones in the Abukuma Plateau, Japan. The continuous line is located at the gap between the field of hornblendes and the field of tremolites-actinolites from Coolgardie-Kurrawang. Crosses—hornblendes (data cited from Deer et al., 1963, vol. 2, table 40; Shido & Miyashiro, 1959); oblique crosses—actinolites (data cited from Deer et al., 1963, vol. 2, table 38); solid circles—hornblendes from the Coolgardie-Kurrawang area; large solid circles—analyzed Coolgardie-Kurrawang hornblendes (Table 1); open circles—actinolites and tremolites from the Coolgardie-Kurrawang area; large open circle and large solid circle marked with (t)—analyzed co-existing actinolite and hornblende.

(1959) for the distinction of amphiboles collected from each of three metamorphic zones defined in the Abukuma Plateau, Japan. The amphiboles of the Coolgardie-Kurrawang area plot on two fields separated from each other by a well-defined gap, which is represented by a straight line.

Following Shido & Miyashiro (1959), the amphiboles which lie to the right of this line are hornblendes, whereas the amphiboles which plot to the left of this

line are actinolites and tremolites. Shido & Miyashiro (1959) interpreted the separation of the field of actinolites from that of hornblendes as representative of a compositional immiscibility gap between these amphiboles under the metamorphic conditions in which they crystallized, which was confirmed by their study of the chemical properties of the amphiboles. That the gap between the field of the hornblendes and the actinolites of the Coolgardie-Kurrawang metabasites is located slightly to the left of the curve for the Abukuma Plateau is not necessarily surprising, for Shido and Miyashiro allowed for shifts in the position of their curve for various metamorphic terrains. Zoned amphiboles with cores of actinolite and rims of hornblende are common in the metadolerites (Pl. 23, fig. 2). The sharp boundary between the rims and the cores supports the possibility of an immiscibility gap between the amphiboles.

While the amphiboles which plot on the low-N_z field are clearly tremolites and actinolites, distinguishable from each other by their refractive indices, the amphiboles which plot on the high-N_z field could be either hornblendes or ferroactinolites. Since these minerals cannot be discriminated from each other on the basis of their optical properties (Deer et al., 1963), three of the amphiboles which fall into the high-N_z field were separated by electromagnetic and gravitative methods from their host rocks, and were analysed for silica and alumina (Table 1). The high alumina content of the analyzed amphiboles indicates they are hornblendes rather than ferroactinolites. As ferroactinolite is characteristic of iron-rich rocks the occurrence of this mineral in the Coolgardie-Kurrawang ophiolites is also unlikely because of their normal iron contents (Tables 4, 6).

TABLE 1. SILICA AND ALUMINA CONTENTS OF AMPHIBOLES IN METADOLERITES FROM THE COOLGARDIE-KURRAWANG SEQUENCE

Description	*Classification**	*SiO_2 wt.%*	*Al_2O_3 wt.%*
Fibrous Z—blue-green	Hornblende	49.00	15.70
Cores of light green amphibole rimmed by blue-green amphibole	Actinolite rimmed by hornblende	53.00	8.75
Columnar to acicular Z—blue-green	Hornblende	49.20	11.50

* Based on the $2V_x/N_z$ diagram (Fig. 7).

The significance of the absorption colours of amphiboles with relation to their composition is not clear. In considering this problem it appears that, although most hornblendes (as determined according to the $2V_x/N_z$ diagram) display blue-green colours, blue-green actinolites and light green hornblendes are by no means uncommon. It must consequently be concluded that the absorption colours of the amphiboles cannot provide a reliable guide to their composition.

Composition of the amphiboles. In using the $2V_x/N_z$ diagram (Fig. 7) as a basis for classification of the amphiboles, it is apparent from the plot distribution that both actinolites and hornblendes are present in the Coolgardie-Kurrawang ophiolites. These amphiboles predominate in both the basic and intermediate meta-igneous rocks, and may often co-exist in the same assemblages, with the hornblende forming rims around the actinolite. Tremolites are the characteristic but not the exclusive amphiboles of the meta-ultrabasic rocks.

Using correlation charts from Deer et al. (1963), the refractive indices of the actinolites and the hornblendes can be correlated with their 100Mg/Mg+tot.Fe+Mn values. The ranges of optic values and compositions for each of the amphibole types are as follows:

	N_z	$2V_x$	$Z \wedge c$	$\frac{100Mg}{Mg+tot.Fe+Mn}$
Tremolites	1.6325-1.655	64°-82°	18°-31°	81-93
Actinolites	1.647 -1.660	69°-86°	18°-28°	57-76
Hornblendes	1.665 -1.680	64°-76°	17°-29°	57-69

According to Miyashiro (1957), the refractive indices of co-existing amphiboles and chlorites are positively related to the ratio of ferrous iron to magnesia of the host rocks. Leake (1965) suggested that the composition of hornblendes in metamorphic rocks is mainly controlled by host rock composition. In order to investigate the relationships between composition of the amphiboles of the Coolgardie-Kurrawang ophiolites and the composition of the corresponding host rocks, the respective 100Mg/Mg+tot.Fe+Mn values are compared (Fig. 8).

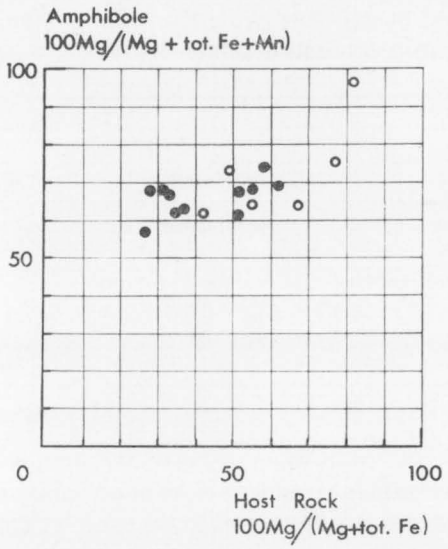


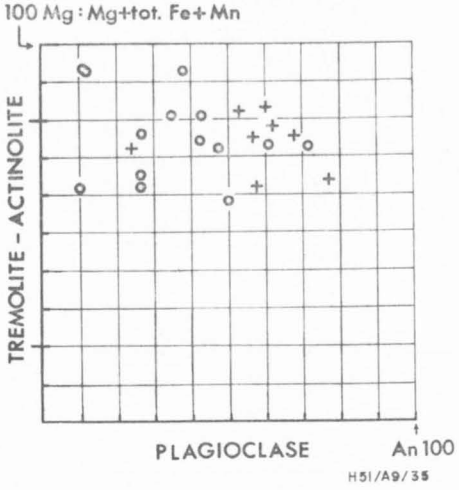
Figure 8. Relationships between the 100Mg/(Mg+tot. Fe+Mn) ratios of amphiboles (optically deduced) and the 100Mg/(Mg+tot. Fe) of host rocks. Open circles —actinolites, solid circles—hornblendes.

Chemical values of the host rocks are calculated on the basis of their chemical analyses using the equivalent cation percentages, whereas chemical values of the amphiboles are optically deduced. The following observations are pertinent:

(1) The amphiboles and the host rocks are roughly sympathetically related with respect to the 100Mg/Mg+tot.Fe+Mn ratios.

(2) The actinolites tend to fall in the field corresponding to high 100Mg/Mg+tot.Fe values of the host rocks. It follows that rocks of magnesian composition are more likely to include actinolite than hornblende.

Amphibole-plagioclase relationships. Investigations of the relationships between co-existing amphiboles and plagioclase feldspars in metamorphic assemblages by Leake (1965) showed that both constituents display a progressive decrease in their Na/Na+Ca ratios with rising metamorphic grade. The relationships between



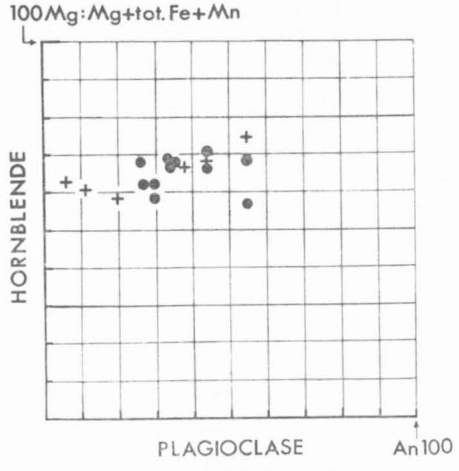


Figure 9. Compositional relationships between co-existing amphiboles and plagioclase feldspars of basic meta-igneous rocks of the Kalgoorlie area. Open circles—actinolites from the Coolgardie-Kurrawang area; crosses—amphiboles of rocks from various parts of the Kalgoorlie region (data cited from Mazzuchelli, 1962; Doepel, 1965; Hudson, 1966).

these minerals with respect to their alumina-silica ratios are affected by the role of host rock composition and of pressure. Figure 9 shows the compositional relationships between amphiboles and plagioclase feldspars of the Coolgardie-Kurrawang ophiolites and ophiolites from other parts of the Kalgoorlie-Norseman area. In plotting the anorthite content of plagioclases against the 100Mg/Mg+tot.Fe+Mn values of co-existing actinolites and co-existing hornblendes, the following relationships are apparent:

(1) No systematic trends of variation are displayed by the actinolite-plagioclase and hornblende-plagioclase diagrams.

(2) The range of composition of plagioclase feldspars co-existing with actinolites is wider than for those co-existing with hornblendes. Labradorites are commonly associated with actinolites, but are rarely associated with hornblendes, which usually co-exist with andesines and oligoclases.

The preferential association of hornblendes with plagioclase feldspars less calcic than labradorite can be understood in terms of the distribution of alumina in the basic meta-igneous assemblages. Assuming isochemical metamorphism, the alumina necessary for the development of hornblende from pyroxene and from actinolite was probably derived from the anorthite molecule of the plagioclase feldspar. An association of hornblendes with plagioclase feldspars depleted in the anorthite component can thus be expected. This is not necessarily the case with plagioclase feldspars associated with actinolites, partly because of the low alumina content of the latter as compared with hornblendes. The implications of these relationships with respect to the metamorphic grade are discussed later.

Chlorite

Chlorite is an important component of the meta-ultrabasic assemblages, of propylitized basic meta-igneous rocks, and of metamorphosed volcanic glass. This mineral is also a common although minor accessory of the metabasalts, the meta-andesites, and the metadolerites. On the whole, the abundance of chlorite in basic meta-igneous rocks is surprisingly low when compared with low-grade metamorphic rocks elsewhere. The composition of the chlorites has been deduced from their refractive indices, birefringence values, and optic signs, using correlation charts by Hey (1954). The optical data and the compositions of chlorites of the Coolgardie-Kurrawang ophiolites, in part determined by the author and in part cited from Blockley (1956), display the following features:

(1) Meta-ultrabasic rocks are characterized by aluminous chlorites, notably pycnochlorite.

(2) The chlorites of basic and intermediate meta-igneous rocks are mostly of aluminous composition.

(3) Chlorites of metamorphosed volcanic glass and of interpillow mesostases are typically ferroan in composition.

The composition of the chlorites is probably largely affected by host rock compositions (Miyashiro, 1957). In Figure 10 the tot.Fe/tot.Fe+Mg values of the chlorites are compared with corresponding values of the host rocks (calculated from the equivalent cation percentages). The positive trend indicates a high sensitivity of chlorite composition in relation to changes in host rock composition. The preferential occurrences of ferroan chlorites in metamorphosed volcanic glass reflects the high ratio of total iron to magnesia characteristic of pillow selvedges. The same relationships apply to interpillow mesostases. The high magnesia contents of the meta-ultrabasic rocks control the composition of the incorporated chlorites, which are invariably of magnesian-aluminous compositions. In plotting the 100Mg/Mg+tot.Fe+Mn values of the amphiboles against the tot.Fe/

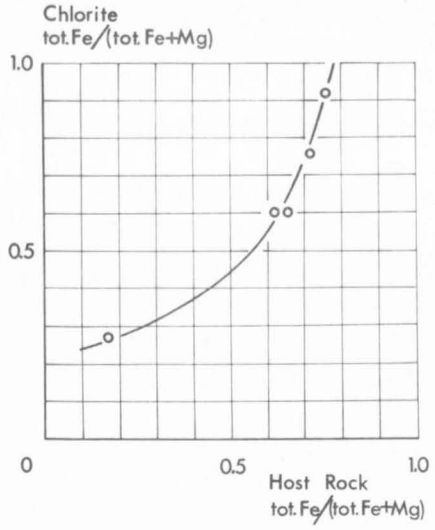


Figure 10. Comparison of tot. Fe/(tot. Fe+Mg) ratios of chlorites (optically deduced) and of the corresponding host rocks.

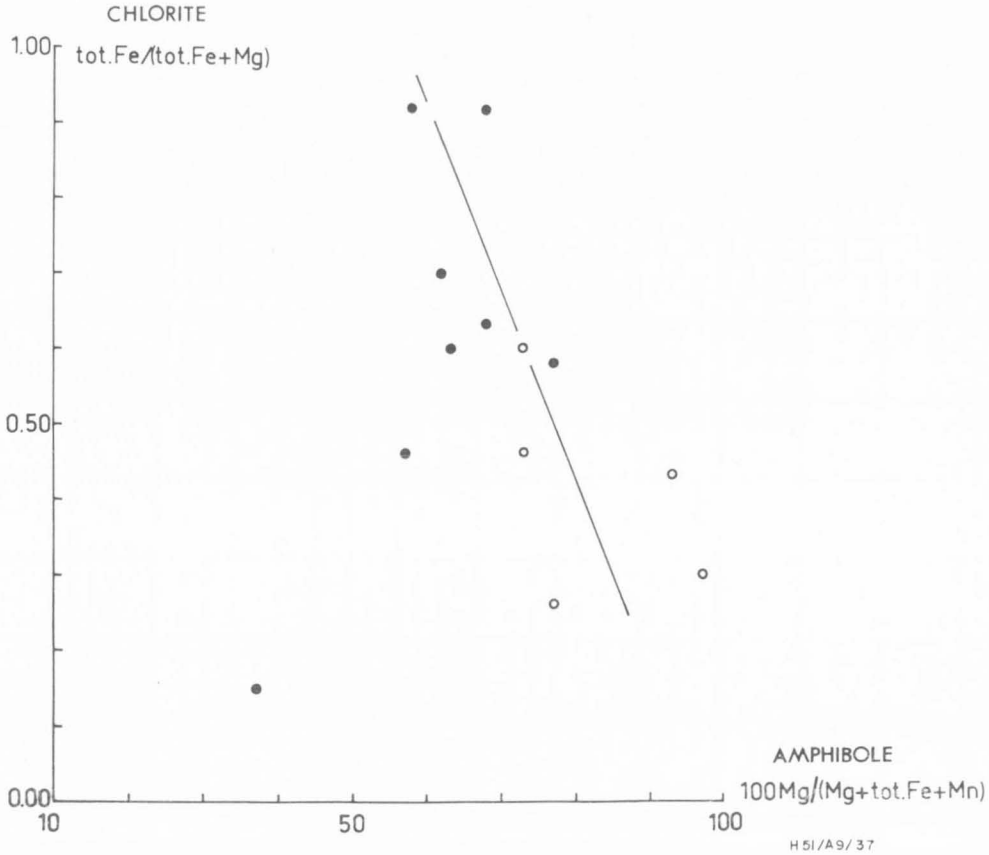


Figure 11. Comparison of the tot. Fe/(tot. Fe+Mg) values of chlorites, and the 100 Mg/(Mg + tot. Fe+Mn) values of co-existing amphiboles. Open circles—actinolites and tremolites, solid circles—hornblendes.

tot.Fe+Mg values of the co-existing chlorites (Fig. 11), it appears that actinolite-tremolite and hornblende are preferentially associated with magnesian and ferroan chlorite, respectively. There is therefore an indication of sympathetic relationships between the magnesia-iron ratios of co-existing amphiboles and chlorites.

GEOCHEMISTRY

The chemical data on which this chapter is based includes twenty-one analyses by the author, thirteen analyses cited from Joplin (1963), and four analyses by O'Beirne (1968). The degree to which the chemical composition of the meta-igneous rocks is representative of their original composition depends on the importance of subsequent diagenetic and metasomatic processes. The review of possible modifications of primary compositions, therefore, must precede any considerations on chemical characteristics of the original rocks.

Carbonated, saussuritized, propylitized, and silicified basic meta-igneous rocks are common in the general Kalgoorlie-Coolgardie area, and are particularly abundant along sheared zones associated with the rich auriferous ores of the Golden Mile of Kalgoorlie. The chemical variability of altered basic meta-igneous rocks of the Golden Mile is represented by four analyses cited from Joplin (1963) and given in Table 2.

TABLE 2. ALTERED BASIC META-IGNEOUS ROCKS FROM THE GOLDEN MILE OF KALGOORLIE, COMPARED WITH OCEANIC THOLEIITE
(Data from Joplin, 1963)

	(1)		(2)		(3)		(4)	(5)
Oxide, wt.%								
SiO_2	53.97		48.08		42.38		35.04	49.4
TiO_2	1.55		0.84		0.66		2.57	2.4
Al_2O_3	14.80		14.13		9.77		9.67	14.4
Fe_2O_3	0.48		1.64		0.92		18.68	3.3
FeO	0.10		4.53		10.76		—	8.2
MnO	0.05		0.13		0.26		tr.	0.17
MgO	1.96		4.94		11.25		4.97	7.8
CaO	3.57		8.20		9.38		4.77	10.5
Na_2O	7.30		1.68		0.18		2.93	2.2
K_2O	0.88		2.76		0.05		2.25	0.45
H_2O+	0.37		1.76		5.98		—	0.82
H_2O-	0.05		0.18		0.17		—	—
CO_2	4.86		11.33		8.95		8.38	—
P_2O_5	0.21		0.33		0.12		—	—
Other constituents								
FeS_2	9.04	FeS_2	0.07	FeS_2	tr.	S	5.49	
Cr_2O_3	0.04	V_2O_3	0.10	Cr_2O_3	0.12	Fe	4.80	
V_2O_3	0.40	B_2O_3	0.02	V_2O_3	0.04	Cu	0.14	
Total	99.63		100.72		100.69		99.99	99.64

(1) Carbonated quartz dolerite; Boulder, Kalgoorlie. Analyst, J. N. A. Grace.
(2) Carbonated dolerite; Boulder, Kalgoorlie. Analyst, D. G. Murray.
(3) Propylite; Kalgoorlie. Analyst, E. S. Simpson.
(4) Chlorite schist; Boulder, Kalgoorlie. Analyst, Helms.
(5) Average of 282 oceanic tholeiites (Manson, 1967).

These analyses are compared with oceanic tholeiitic basalt (Manson, 1967). The most obvious feature displayed by these rocks is enrichment in carbon dioxide. Loss of lime, soda, ferrous iron, ferric iron, and magnesia are common, although not consistent features. It appears that alteration took place according to more than one scheme, and was at times of a highly complex nature. Similar observations were made by Bekker (1963) in the gold mines of Norseman. A detailed study of mineralization and of associated wall-rock alteration has been carried out by G. Bartram (pers. comm.).

As contrasted with the metasomatized ophiolites, most basic meta-igneous assemblages observed in the Coolgardie-Kurrawang area show little evidence of chemical reconstitution. The least altered metabasites are characterized by the following properties:

(1) Only minor amounts of typical alteration products like calcite, sericite, chlorite, epidote, and prehnite are present in these rocks.

(2) Primary calcic plagioclase may be retained.

(3) The amphibole may occupy original pyroxene positions.

(4) Igneous textures may be well preserved.

As will be shown later in this paper, the chemical compositions of the little-altered meta-igneous rocks fall into the range of the various average igneous rocks. It is reasonable to assume therefore that rocks showing the above features behaved as approximately chemically closed systems during metamorphism. In selecting specimens for chemical analysis, the least altered rocks were chosen. Likewise, the chemical analyses cited from Joplin (1963) do not include carbonate-rich rocks and rocks which were classified by Joplin as metasomatically altered. Nothwithstanding the above considerations, the possibility of deviations from isochemical metamorphism should be constantly borne in mind, and is particularly relevant in conjunction with the pillowed metavolcanics.

META-ULTRABASICS

Analyses of two chlorite-tremolite rocks and three serpentinites are given in Table 3. Petrochemical classifications of the meta-ultrabasic rocks indicate that the chlorite-tremolite rocks and the serpentinites can be considered metamorphosed pyroxenites and peridotites, respectively. That the chlorite-tremolite assemblages represent metapyroxenites was suggested earlier on the basis of the retention of blastocumulate textures in some of these rocks. Likewise, serpentinites in the Coolgardie ophiolites display pseudomorphs and armoured relics of olivine (Blockley, 1956).

According to the equivalent norm, the original pyroxenites consisted of about 50 percent magnesian hypersthene, about 25 percent magnesian pyroxene, 10 to 25 percent calcic plagioclase, and accessory olivine. The chemical analyses of the chlorite-tremolite rocks are comparable with the average pyroxenite calculated by Nockolds (1954). According to Rittman's (1952) classification of volcanic rocks, the analyses of the chlorite-tremolite rocks correspond to pigeonite basalt and to mafic olivine basalt. A classification according to Niggli's magma-type clasification (Burri, 1964) defines the rocks as strongly femic, alkali-poor, and lime-normal.

TABLE 3. CHEMICAL ANALYSES OF SERPENTINITES AND METAPYROXENITES FROM THE KALGOORLIE-COOLGARDIE AREA, COMPARED WITH THE AVERAGE PERIDOTITE AND PYROXENITE OF NOCKOLDS (1954)

	(1)	(2)	(3)	(4)	(5)	(6)	(7)
Oxide, wt. %							
SiO_2	44.97	39.35	39.06	43.54	49.80	49.20	50.50
TiO_2	0.16	0.60	0.51	0.81	0.42	0.06	0.53
Al_2O_3	4.66	6.15	3.36	3.99	8.24	3.65	4.10
Fe_2O_3	2.92	4.75	2.77	2.51	3.58	4.11	2.44
FeO	5.24	5.17	5.93	9.84	8.09	8.72	7.37
MnO	0.03	1.21	0.77	0.21	n.d.	n.d.	0.13
MgO	30.61	28.51	32.94	34.02	18.68	20.92	21.71
CaO	0.18	3.10	2.43	3.46	9.47	9.00	12.00
Na_2O	abs.	0.73	0.12	0.56	0.61	0.21	0.45
K_2O	abs.	0.15	0.08	0.25	0.06	0.03	0.21
H_2O+	9.78	9.05	8.38	0.76	2.14	2.91	
H_2O-	0.92	0.14	0.54	0.05			
CO_2—	0.06	abs.	2.88	—	—	—	—
Cr_2O_3	0.26	0.40	0.24	—	—	—	—
Other constituents							
FeS_2	0.09	V_2O_3 tr.	V_2O_3 0.01				
		NiO 0.36	SO_3 0.37				
		FeS_2 abs.	BaO abs.				
Total	99.95	99.68	100.65	100.00	101.09	98.81	99.91

TABLE 3.—*continued*

Equivalent molecular norms								
Or		—	0.5	0.25	—	0.5	0.5	1.0
Ab		—	5.0	0.50	—	5.5	1.5	4.0
An		0.5	14.7	9.12	—	19.0	9.0	8.5
C		5.1	—	—	—	—	—	—
Di	Wo	—	0.6	1.36	—	11.0	14.8	20.0
	En	—	0.5	1.27	—	9.3	12.6	17.4
	Fs	—	0.1	0.09	—	1.7	2.2	2.6
Hy	En	74.6	29.7	29.33	—	37.9	45.0	26.2
	Fs	5.2	1.3	2.09	—	7.1	7.6	4.2
Ol	Fo	10.5	39.6	48.75	—	3.3	1.5	11.4
	Fa	0.6	1.5	3.39	—	0.3	0.6	1.5
Il		0.4	1.4	1.00	—	0.6	0.2	0.8
Mt		3.1	5.1	2.85	—	3.8	4.5	2.4
Hm		—	—	—	—	—	—	—
Q		—	—	—	—	—	—	—

(1) Serpentinite; 356 M.P. on railway line, Coolgardie. Analyst, W. Inglis.

(2) Serpentinite; Hannans Lake, Kalgoorlie. Analyst, C. C. Williams.

(3) Serpentinite; Mt Hunt, Kalgoorlie. Analyst, H. Bowley.

(4) Average peridotite (Nockolds, 1954).

(5) Sheared chlorite-tremolite metapyroxenite; Coolgardie-Kurrawang. Analyst, A. Y. Glikson.

(6) Chlorite-tremolite metapyroxenite; Coolgardie-Kurrawang. Analyst, A. Y. Glikson.

(7) Average pyroxenite (Nockolds, 1954).

TABLE 4. CHEMICAL ANALYSES OF METABASALTS AND PILLOWED METABASALT OF THE COOLGARDIE OPHIOLITES, AND METATACHYLYTE FROM THE RED LAKE FLOW-BRECCIA

	(1)	(2)	(3)	(4)	(5)	(6)	(7)	(8)	(9)	(10)
Oxide, wt. %										
SiO_2	50.00	51.71	50.41	50.37	50.27	49.56	56.95	49.00	56.15	54.10
TiO_2	1.77	0.56	0.35	0.90	1.29	0.57	1.14	1.40	1.17	0.52
Al_2O_3	13.75	15.17	17.23	9.02	13.61	14.97	12.18	14.69	10.69	10.08
Fe_2O_3	3.32	0.86	0.21	0.84	10.36	0.98	3.66	6.54	3.95	4.60
FeO	11.68	8.17	9.68	9.15	9.87	9.20	6.78	10.31	7.21	11.92
MnO	0.18	0.16	0.07	0.14	0.15	0.21	n.d.	n.d.	n.d.	n.d.
MgO	5.97	9.60	13.45	6.77	6.16	8.54	4.85	8.12	5.18	8.45
CaO	8.41	11.90	6.51	12.02	9.10	14.68	10.00	9.50	9.95	8.75
Na_2O	2.67	1.99	1.60	1.65	1.71	0.84	1.58	1.79	1.60	1.17
K_2O	0.57	0.14	0.04	0.03	0.05	0.12	0.10	0.16	0.11	0.02
H_2O+	1.63	2.03	1.35	1.18	1.48	1.49	1.73	1.21	1.68	1.21
H_2O-	0.09	0.22	0.11	0.14	0.01	0.13				
CO_2	abs.	0.19	abs.	0.04	0.01	0.05				
P_2O_5	0.13	0.06	0.63	0.13	0.27	0.20				
Cr_2O_3	0.02	0.16	0.06	—	—	—				
FeS_2	—	0.09	tr.							
Total	99.95	100.59	99.64	100.58	99.75	100.18	100.85	100.21	101.69	109.82

TABLE 4.—*continued*

Equivalent molecular norm										
Or	3.5	0.5	0.5	0.2	0.3	0.5	0.5	1.0	0.5	0.1
Ab	19.0	14.0	11.0	11.5	12.5	6.0	14.5	16.6	15.0	11.5
An	27.2	28.5	32.5	42.2	19.8	35.0	34.8	25.7	33.5	24.2
C	—	—	—	—	—	—	—	—	—	—
Wo	6.6	12.8	—	7.3	11.5	16.0	6.7	9.0	6.8	9.2
En	17.2	27.2	37.4	19.0	18.2	24.2	13.8	23.4	14.6	14.4
Fs	12.4	11.0	14.2	11.8	5.6	12.8	6.8	9.6	7.0	12.6
Il	4.2	1.2	0.6	2.0	3.2	1.2	1.4	2.0	1.6	2.0
Mt	3.4	0.8	0.2	0.8	11.5	0.9	3.9	7.1	4.2	5.2
Hm	—	—	—	—	—	—	—	—	—	—
Q	6.5	4.0	1.6	5.2	17.4	3.4	17.6	5.6	16.8	20.8

Analyses 1-6 are cited from Joplin (1963). Analyses 7-10 by A. Y. Glikson.

(1) 'Basic lava', Burbanks; Collgardie; analyst, W. Inglis.
(2) 'Amygdaloidal basalt', Coolgardie; analyst, W. Inglis.
(3) 'Basalt', Lord Bobs; Coolgardie; analyst, B. W. Stenhouse.
(4) 'Basalt', Coolgardie; analyst, B. W. Stenhouse.
(5) 'Porphyritic basalt', Bellbird; Coolgardie; analyst, B. W. Stenhouse.
(6) 'Ultrabasic lava', Coolgardie; analyst, B. W. Stenhouse.
(7) Quartz-amphibole-plagioclase metabasalt pillow core; Coolgardie ophiolites.
(8) Plagioclase-amphibole metabasalt pillow shell; Coolgardie ophiolites.
(9) Average of metabasalt pillow (analyses 7 and 8).
(10) Metatachylyte from basic flow-breccia.

The normative assemblages of the serpentinites consist of up to one-half magnesian olivine, between one-third and three-quarters magnesian hypersthene, and minor diopside. A comparison of the chemical analyses of the serpentinites with Nockolds' (1954) average igneous rocks indicates a similarity to average peridotite. According to Rittman's classification, the serpentinites correspond in composition to picritic basalts. On the basis of Niggli's magma-type classification, the serpentinites are very strongly femic, alkali-poor, and lime-poor rocks.

The most obvious difference between the chlorite-tremolite rocks and the average pyroxenite, and between the serpentinites and the average peridotite, is the considerably higher water content of the metamorphic rocks. Except for this feature, the deviations of the meta-ultrabasic rocks from the corresponding average igneous rocks are relatively minor, and lie within the normal range of compositional variability of igneous rocks.

METABASALTS

Chemical analyses of six metabasalts of the Coolgardie ophiolites, a pillowed metabasalt of the Coolgardie Ophiolites, and metatachylyte from the Red Lake flow-breccia, are presented in Table 4. The normative assemblages calculated from the chemical analyses of the metabasalts consist of calcic plagioclase, pyroxene, and accessory ilmenite and magnetite. Normative quartz is invariably present, and may occasionally be of quantitative importance. The minor normative orthoclase molecule is probably incorporated in the plagioclase feldspars in the actual assemblages, for no orthoclase and little or no biotite are incorporated in the rocks. The composition of the normative plagioclase feldspars ranges between An 59 and An 82. Using the classification of Poldervaart & Hess (1951), the compositions of the normative pyroxenes can be correlated with augites, subcalcic augites, and less often with subcalcic ferroaugite and hypersthene. According to Rittman's (1952) classification scheme, the rocks can be defined as basalts, quartz basalts, olivine-andesine basalts, and pigeonite basalts. The Coolgardie metabasalts are notably low in soda and potash when compared with Nockolds' (1954) central basalt and tholeiitic basalt. The lime contents of most metabasalts, on the other hand, are similar to those of central basalt and tholeiitic basalt. These relationships are reflected by the high lime-soda indices, and by the high anorthite contents of the normative plagioclases of the metabasalts (Table 4). The alkali-poor and lime-normal to lime-rich nature of the metabasalts is also indicated by Niggli's magma-type classification.

As is evident from the chemical characteristics of the metabasalts, no correlation with spilitic basalts is possible. Another difference between the average Coolgardie metabasalt and the average spilite is the high titania content of the spilite (Table 5). Because of their low to intermediate alumina contents, no correlation can be made between the metabasalts and high-alumina basalts. The metabasalts are characterized by the presence of normative quartz and by low alkali contents, and are therefore consistent with tholeiitic basalts. According to Engel et al. (1965), tholeiitic basalts can be divided into two major groups displaying different chemical properties, and characteristic of different geotectonic settings, as follows:

TABLE 5. COMPOSITION OF THE AVERAGE COOLGARDIE METABASALT COMPARED WITH THE AVERAGE KEEWATIN METABASALT AND VARIOUS AVERAGE BASALTS

	(1)	(2)	(3)	(4)	(5)	(6)
Oxide, wt. %						
SiO_2	51.21	49.83	51.33	50.83	49.4	49.65
TiO_2	0.94	0.94	1.10	2.03	2.4	1.57
Al_2O_3	13.71	14.64	18.04	14.07	14.4	16.00
Fe_2O_3	2.93	30.03	3.40	2.88	3.3	3.85
FeO	9.28	8.77	5.70	9.06	8.2	6.08
MnO	0.15	0.21	0.16	0.18	0.17	0.15
MgO	7.95	7.36	6.01	6.34	7.8	5.10
CaO	10.36	10.46	10.07	10.42	10.5	6.62
Na_2O	1.72	2.02	2.76	2.23	2.2	4.29
K_2O	0.15	0.23	0.82	0.82	0.45	1.28
CO_2	0.04	0.33	—	—	—	1.63
P_2O_5	0.23	0.19	0.16	0.23	—	0.26
Total	98.67	98.01	99.55	99.09	98.82	96.48
Na/K	11.5	8.8	3.4	2.7	4.9	3.3
Fe^{+3}/Fe^{+2}	0.31	0.34	0.59	0.31	0.40	0.63

(1) Average of seven Coolgardie metabasalts.
(2) Average of 53 Keewatin metabasalts (Wilson et al., 1965).
(3) 'Central basalt' (high-alumina basalt), average of 56 analyses (Nockolds, 1954).
(4) Normal tholeiitic basalt and dolerite, average of 137 analyses (Nockolds, 1954).
(5) Average of 282 oceanic tholeiitic basalts (Manson, 1967).
(6) Average spilite, based on 92 analyses (Vallance, 1960).

Oceanic tholeiitic basalts. Most of these rocks have been dredged from the Mid-Atlantic Ridge and the East Pacific Rise. This group is characterized by high Na/K ratios (above 10), low Fe_2O_3/FeO ratios (below 0.2), and extremely low K, Ba, P, Pb, Sr, Th, U, and Zr contents.

Continental tholeiitic basalts. These rocks occur as flood eruptions over the continents. Most continental tholeiites have higher Si, K, Ba, Cs, Pb, Rb, Sr, Th, U, and Zr contents than oceanic tholeiites.

In comparing the metabasalts of the Coolgardie ophiolites with the above types (Table 5), the following points are pertinent:

(1) The metabasalts are characterized by extremely low potash percentages; the average of seven Coolgardie metabasalts is 0.15 percent K_2O.

(2) The Coolgardie metabasalts have high to very high Na/K ratios, with an average ratio of 11.5.

(3) Most metabasalts have low to very low Fe_2O_3/FeO ratios; the average ratio is 0.31.

It appears from the foregoing comparison that the Coolgardie metabasalts compare favourably with oceanic tholeiites. This conclusion is supported by the low alumina percentages of the metabasalts, as Hamilton (1965) considered oceanic tholeiites to be characteristically low in alumina when compared with the circum-Pacific basalt-andesite-rhyolite association. This author also noted the compositional uniformity of tholeiitic basalts of oceanic domains, as contrasted with the heterogeneity of the circum-Pacific association.

METADOLERITES

Unlike the metabasalts, the metadolerites associated with the Mungari Beds are similar in composition to the average tholeiitic andesite of Nockolds (1954). Chemical analyses of five metadolerites, and the corresponding norms, are presented in Table 6, along with the average tholeiitic andesite. Four analyses are comparable to average tholeiitic andesite, and one to normal tholeiitic basalt. While two analyzed metadolerites of the Red Lake ophiolites have andesine and labradorite as normative constituents, analyzed metadolerites of the Mount Robinson Ophiolites are characterized by normative oligoclase and andesine, reflecting their higher soda contents. The normative pyroxenes can be correlated with augites. Normative quartz is invariably present.

In classifying the analyzed metadolerites according to Rittmann's (1952) classification system, the compositions of these rocks correspond to those of andesine basalt, olivine-andesine basalt, and pigeonite basalt. The differences between the

TABLE 6. CHEMICAL ANALYSES OF METADOLERITES OF THE RED LAKE AND MOUNT ROBINSON OPHIOLITES, COMPARED WITH THE AVERAGE THOLEIITIC ANDESITE OF NOCKOLDS (1954)

	(1)	(2)	(3)	(4)	(5)	(6)
Oxide, wt. %						
SiO_2	54.72	51.94	53.94	52.61	56.40	51.43
TiO_2	1.31	0.38	1.60	2.12	1.06	2.60
Al_2O_3	11.01	15.45	12.82	11.07	12.60	13.05
Fe_2O_3	3.81	3.25	0.10	5.91	3.89	3.36
FeO	7.37	7.70	14.86	11.42	8.60	9.74
MgO	5.78	7.19	4.38	4.34	4.81	5.28
CaO	11.50	8.90	8.20	6.65	5.35	8.78
Na_2O	1.45	3.22	4.02	4.75	4.95	3.18
K_2O	0.46	0.22	0.24	0.32	0.20	1.04
H_2O+ / H_2O-	2.37	0.58	0.61	1.09	1.02	—
Total	99.78	98.83	100.77	100.28	98.88	99.33
Equivalent molecular norm						
Or	3.0	1.0	1.0	1.5	1.0	6.5
Ab	13.5	29.5	37.0	43.5	46.0	30.0
An	23.5	27.5	16.3	8.8	12.0	18.5
Wo	14.8	7.0	10.0	10.0	6.0	10.6
En	17.0	20.4	21.2	12.4	13.8	15.0
Fs	7.4	9.0	12.4	11.0	9.2	9.4
Il	1.8	0.6	2.2	3.0	1.6	3.8
Mt	4.2	3.5	0.1	6.3	4.1	3.6
Q	14.8	1.5	—0.2	3.5	6.3	2.6

Analyses 1-5 by A. Y. Glikson.

(1) Quartz-plagioclase-actinolite metadolerite fragment in flow-breccia, Red Lake ophiolites.
(2) Hornblende-actinolite-plagioclase metadolerite, Red Lake ophiolites.
(3) Ilmenite-rich hornblende-actinolite-sodic plagioclase metadolerite, Mount Robinson ophiolites.
(4) Hornblende-actinolite-sodic plagioclase metadolerite, Mount Robinson ophiolites.
(5) Fine-grained quartz-amphibole-sodic plagioclase amphibolite. Collected from the margin of a stratiform metadolerite, Mount Robinson ophiolites.
(6) Average tholeiitic andesite (Nockolds, 1954).

Red Lake metadolerites and the Mount Robinson metadolerites are well expressed by their classification according to Niggli's magma-type scheme. The Red Lake metadolerites are defined as femic, alkali-poor, and lime-normal, whereas the Mount Robinson metadolerites are defined as femic, alkali-intermediate, and lime-normal. In conformity with the metabasalts of the Coolgardie ophiolites, the metadolerites have extremely low potash values, and very high soda-potash ratios. The average metadolerite is high in silica, total iron, and soda, and low in alumina, magnesia, and lime, as compared with the average metabasalt. When compared with the average meta-andesite of the Red Lake ophiolites, the metadolerites tend to be lower in silica and higher in total iron, magnesia, and lime.

META-ANDESITES

Chemical analyses and norms of two pillowed meta-andesites, a brecciated pillowed meta-andesite, a porphyritic meta-andesite, and an altered porphyritic meta-andesite are given in Tables 7 and 8. In calculating the bulk compositions of the pillowed meta-andesites, the volumetric relationships between the cores and the shells were taken into consideration. The classification of the average composition of a porphyritic variolitic pillowed meta-andesite of the Red Cross ophiolites according to Rittmann's (1952) scheme defines the rock as labradorite dacite. However, in comparing the average pillow composition with Nockolds' (1954) average dacite and average tholeiitic andesite, it appears that a better match is achieved with the latter average with respect to the alumina, total iron, magnesia,

TABLE 7. CHEMICAL COMPOSITION OF META-ANDESITES AND ALTERED META-ANDESITES OF THE RED LAKE OPHIOLITES, COMPARED WITH THE AVERAGE THOLEIITIC ANDESITE AND DACITE

	(1)	(2)	(3)	(4)	(5)	(6)	(7)
Oxide, wt. %							
SiO_2	61.15	52.53	61.22	60.20	61.50	51.43	63.58
TiO_2	0.84	2.24	2.23	0.60	0.69	2.60	0.64
Al_2O_3	13.07	14.19	15.70	15.37	15.54	13.05	16.67
Fe_2O_3	2.14	4.34	2.10	2.69	4.89	3.36	2.24
FeO	6.60	10.37	7.00	2.80	1.72	9.74	3.00
MnO	—	—	0.17	—	—	0.19	0.11
MgO	4.33	3.35	1.47	6.04	3.49	5.28	2.12
CaO	8.87	7.77	6.00	7.80	4.20	8.78	5.53
Na_2O	1.68	3.58	1.75	3.92	4.85	3.18	3.98
K_2O	0.06	0.14	0.36	0.18	2.00	1.04	1.40
H_2O+ } H_2O-	0.94	1.40	1.51	1.33	1.42	0.87	0.56
Total	99.68	99.91	99.51	100.93	100.30	99.52	99.83

Analyses 1-5 by A. Y. Glikson.

(1) Average composition of porphyritic amygdaloidal meta-andesite pillow, Red Lake ophiolites.
(2) Average composition of porphyroblastic meta-andesite pillow, Red Lake ophiolites.
(3) Composite sample of brecciated garnetiferous pillows, Red Lake ophiolites.
(4) Porphyritic actinolite-oligoclase meta-andesite, Red Lake ophiolites.
(5) Porphyritic biotite-amphibole-plagioclase meta-andesite, Red Lake ophiolites.
(6) Average tholeiitic andesite (Nockolds, 1954).
(7) Average dacite and dacite obsidian (Nockolds, 1954).

and lime contents. Thus, classification of these rocks as metadacites according to Rittmann's scheme is based on their high silica contents, and is not consistent with the other chemical properties of the rocks. It is possible that the pillow cores underwent either late-magmatic or diagenetic silicification processes. In this case, the anomalous silica content of the average pillow composition can be neglected, and a reasonably good match with the average tholeiitic andesite is obtained.

The classification of pillowed porphyroblastic meta-andesites of the Red Lake ophiolites according to Rittmann's scheme defined the average composition of the pillow as pigeonite andesite. The average pillow composition (Table 7) compares well with Nockold's average tholeiitic andesite. Normatively, the rock consists of about 50 percent andesine (An 40), and is saturated in silica. In classifying the pillowed meta-andesites according to Niggli's magma-type classification, both the porphyritic-variolitic pillows and the porphyroblastic pillows are defined as femic,

TABLE 8. COMPOSITIONAL VARIATIONS WITHIN META-ANDESITE PILLOWS, RED LAKE OPHIOLITES

	Porphyritic-variolitic meta-andesite pillow				Porphyroblastic meta-andesite pillow		
	(1)	(2)	(3)	(4)	(1)	(2)	(3)
Oxide, wt. %							
SiO_2	61.94	62.60	67.90	54.00	52.54	63.94	41.00
TiO_2	0.86	0.80	0.69	0.69	2.34	2.05	1.68
Al_2O_3	12.86	15.12	9.25	14.95	14.48	14.26	11.76
Fe_2O_3	2.16	0.01	0.91	1.96	4.36	1.36	7.21
FeO	6.38	3.85	1.93	8.59	9.94	6.38	17.81
MnO	n.d.	n.d.	n.d.	n.d.	0.12	n.d.	n.d.
MgO	4.13	3.34	1.26	6.18	2.94	1.90	8.09
CaO	8.80	7.50	12.85	9.55	8.00	4.50	8.25
Na_2O	1.68	3.13	0.10	1.68	3.84	4.10	1.00
K_2O	0.06	0.16	0.03	0.07	0.13	0.13	0.22
H_2O (total)	0.87	2.36	2.59	1.55	1.32	0.59	2.83
Total	99.74	98.87	99.01	99.22	99.89	99.21	100.85
Equivalent molecular norm							
Or	0.5	1.0	0.5	0.5	0.5	0.5	1.0
Ab	17.5	29.5	1.0	17.5	36.0	38.0	9.5
An	27.3	27.5	26.8	33.0	23.0	21.0	29.3
Wo	7.0	4.4	17.4	6.4	7.4	0.8	7.8
En	11.8	9.6	3.8	17.8	8.4	5.4	24.0
Fs	7.4	4.9	1.6	11.2	9.4	6.4	21.6
Il	1.2	1.2	1.0	1.0	3.4	2.8	2.4
Mt	2.4	0.1	1.6	2.3	4.8	1.5	8.1
Q	24.9	21.8	46.8	10.3	7.1	23.6	—3.7

All analyses by A. Y. Glikson.

(1) Quartz-amphibole-plagioclase meta-andesite pillow core.

(2) Amphibole-quartz-plagioclase meta-andesite pillow core.

(3) Prehnite-quartz segregation in pillow core.

(4) Porphyritic-variolitic quartz-plagioclase-hornblende meta-andesite pillow shell.

(1) Porphyroblastic carbonated amphibole-plagioclase meta-andesite pillow core.

(2) Amphibole-quartz-plagioclase meta-andesite pillow shell.

(3) Chlorite-hornblende inter-pillow mesostasis.

alkali-poor, and lime-normal. Another feature common to both the porphyritic-variolitic meta-andesites and the porphyroblastic meta-andesites is a very low potash content, as compared with the average tholeiitic andesite.

Porphyritic massive meta-andesites occurring in the Red Lake ophiolites are classified according to Rittmann's method as dacites. However, as indicated by the high total iron, magnesia, and lime contents of these rocks (Table 7), and on the basis of the same considerations as those made above in connexion with the porphyritic variolitic pillowed meta-andesites, the rocks are better defined as meta-andesites. A classification according to Niggli's magma-type system indicates a semi-femic, alkali-poor, and lime-normal composition for the fresh rock. The second analyzed rock (Table 7) is considered an altered equivalent of the massive meta-andesite, and is depleted in lime and magnesia, and enriched in potash (incorporated in biotite).

Zonation of Volcanic Pillows

Variations in the abundance of chemical components within pillows were recorded by Vuagnat (1949), and were studied by Vallance (1960; 1965). Vuagnat observed relatively high concentrations of silica and soda in pillow cores, and relatively high concentrations of ferrous iron, ferric iron, and magnesia in pillow shells. The distribution pattern of lime has been found to be generally variable. In variolitic pillows, however, the lime content is relatively high in the cores (Vuagnat, 1949). Vallance (1965) confirmed the tendency of soda and silica to be concentrated in pillow cores, and related the sympathetic relationships between these constituents to their fixation in feldspar. Potash and titania are frequently higher in pillow selvedges than in the cores.

Figure 12 shows the chemical zonation patterns within pillowed metabasalts and meta-andesites from the Kalgoorlie-Norseman area. In three pillows silica is higher in the cores, and ferric iron, ferrous iron, and magnesia are higher in the shells. The acid shell developed in the Red Lake porphyroblastic pillowed meta-andesite constitutes an exception, which can be explained in terms of a loss of iron and magnesia to the ultramafic interpillow mesostasis. With the exception of the porphyritic-variolitic meta-andesite pillow, the alumina content of the pillows is higher in the cores than in the shells. This feature is understood in terms of the higher feldspar content of the pillow interiors.

No consistent trends of variation with respect to lime and alkalies are displayed by the pillows. In two cases, however, the percentage of soda is higher in the cores than in the shells.

Chemical variations within the pillows are reflected by changes in mineralogy and texture through the pillows. While pillow interiors are usually uniform in composition, pillow peripheries commonly display a well-developed concentric zonation. These variations are usually consistent. With a single exception, the ratios of ferromagnesian minerals (mainly amphibole) to leucocratic minerals (feldspar and quartz) in the pillow shells are higher than in the corresponding pillow cores. The increase in the abundance of amphibole upon transition into the shell is usually associated with a decrease in grain size. Some pillow selvedges include phenocrysts of calcic plagioclase and/or their recrystallized equivalents. Except for the pillowed metabasalts described by Doepel (1965) from Yilmia, Lake Lefroy, neither phenocrysts of plagioclase nor their recrystallized equivalents have been observed in pillow interiors.

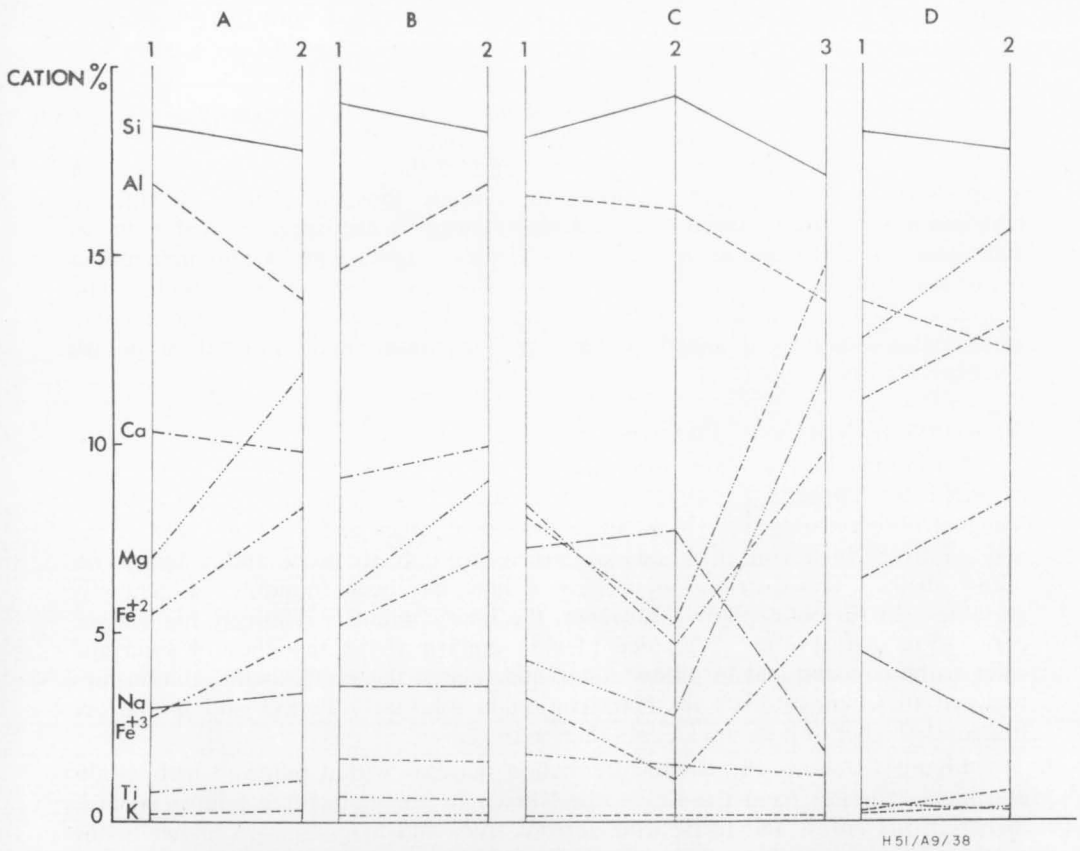


Figure 12. Chemical variations within metabasite pillows.

A. Pillowed metabasalt; Coolgardie ophiolites (Table 4). (1) pillow core, (2) pillow shell.

B. Pillowed porphyritic-variolitic meta-andesite (Table 8). (1) pillow core, (2) porphyritic-variolitic pillow shell.

C. Pillowed porphyroblastic meta-andesite (Table 8). (1) porphyroblastic pillow core, (2) pillow shell, (3) chlorite-hornblende interpillow mesostasis.

D. Pillowed metabasalt (Yilmia; Doepel, 1965). (1) saussurite-amphibole pillow core, (2) pyroxene-saussurite-amphibole pillow core.

Sodic Metaporphyries

A comprehensive geochemical study of the metaporphyries has been carried out by O'Beirne (1968). In Table 9 the analyses of five sodic metaporphyries collected from stratiform and lenticular bodies located in the Mungari Beds are presented. The metaporphyries are characteristically high in silica and soda, and low in potash. Potash-rich metaporphyries reported by O'Beirne (1968) from other areas within the Kalgoorlie region have not been found in the Coolgardie-Kurrawang sequence.

The average metaporphyry calculated on the basis of the seven analyses consists of approximately 70 percent silica, 15 percent alumina, nearly 5 percent total iron and magnesia, about 3 percent lime, more than 5 percent soda,

TABLE 9. CHEMICAL ANALYSES OF SODIC METAPORPHYRIES ASSOCIATED WITH THE MUNGARI BEDS

	(1)	(2)	(3)	(4)	(5)	(6)
Oxide, wt. %						
SiO_2	73.24	73.20	66.60	72.69	66.77	73.66
TiO_2	0.45	0.34	0.52	0.31	0.37	0.22
Al_2O_3	14.73	14.68	16.23	15.42	15.48	13.45
Fe_2O_3	0.19	0.01	1.69	0.76	2.15	1.25
FeO	0.32	0.85	2.21	1.37	0.32	0.75
MnO	0.02	—	—	0.02	0.07	0.03
MgO	1.01	0.43	1.40	2.40	4.76	0.32
CaO	1.16	1.20	4.10	0.71	3.39	1.13
Na_2O	5.62	6.18	4.76	6.61	6.44	2.99
K_2O	0.88	1.23	0.57	0.05	0.10	5.35
H_2O+	0.55	0.63	0.41	0.11	0.09	0.78
H_2O-	0.23			0.09	0.17	—
Total	98.40	98.75	98.49	100.54	100.11	99.93
Equivalent molecular norm						
Or	5.5	7.0	3.5	0.5	0.5	31.7
Ab	51.0	56.0	43.5	58.0	56.5	25.1
An	6.0	6.0	20.5	3.5	12.8	5.0
C	2.6	1.1	0.5	3.4	—	0.9
Wo	—	—	—	—	1.4	—
En	2.8	1.2	4.0	6.6	12.8	0.8
Fs	—	1.0	1.8	1.0	—	—
Il	0.4	0.4	0.6	0.4	0.4	0.5
Mt	—	0.1	1.8	0.8	—	1.9
Hm	0.1	—	—	—	1.5	—
Ru	0.1	—	—	—	0.1	0.2
Q	31.5	27.2	23.8	25.8	14.0	33.2

(1) Quartz-albite metaporphyry; Red Lake ophiolites. Analyst, W. R. O'Beirne.

(2) Biotite-quartz-oligoclase metaporphyry; Mount Robinson ophiolites. Analyst, A. Y. Glikson.

(3) Amphibole-quartz-albite metaporphyry; Mount Robinson ophiolites. Analyst, A. Y. Glikson.

(4) Biotite-quartz-albite metaporphyry; Red Lake ophiolites. Analyst, W. R. O'Beirne.

(5) Tremolite-quartz-albite metaporphyry; Red Lake ophiolites. Analyst, W. R. O'Beirne.

(6) Average calc-alkali rhyolite + rhyolite obsidian. Average of 22 analyses (Nockolds, 1954).

and under 1 percent potash. The average normative assemblages consist of about two-thirds sodic plagioclase, and about one-quarter quartz. Biotite-rich varieties and amphibole-rich varieties are relatively high in potash and lime, respectively, and are relatively high in total iron and magnesia. In comparing the average sodic metaporphyry with Nockolds' (1954) average calc-alkali rhyolite (Table 9), the porphyries appear relatively high in silica, lime, and soda, and relatively low in alumina, magnesia, and potash. Classification of the sodic metaporphyries according to Rittmann's (1952) system defines these rocks as rhyolites. Similar rocks have been referred to as sodic rhyolites by workers on the Archaean of the Canadian Shield (e.g., Wilson et al., 1965).

Geochemical Affinities

Variation diagrams for the meta-igneous rocks show a consistent increase in silica and alkali contents by the serpentinites, metapyroxenites, metabasalts, metadolerites, meta-andesites, and sodic metaporphyries, in this order. This trend is associated with a general increase in alumina. The increase in these oxides is associated with a concomitant decrease in magnesia. Total iron and lime are high in the metapyroxenites, metabasalts, and metadolerites, and are relatively low in the serpentinites, meta-andesites, and sodic metaporphyries.

In plotting the normative An+C:Ab:Or ratios (Fig. 13), the following features are apparent:

(1) The meta-igneous rocks are very low in normative orthoclase in comparison to average basalts, andesites, and dacite (Nockolds, 1954).

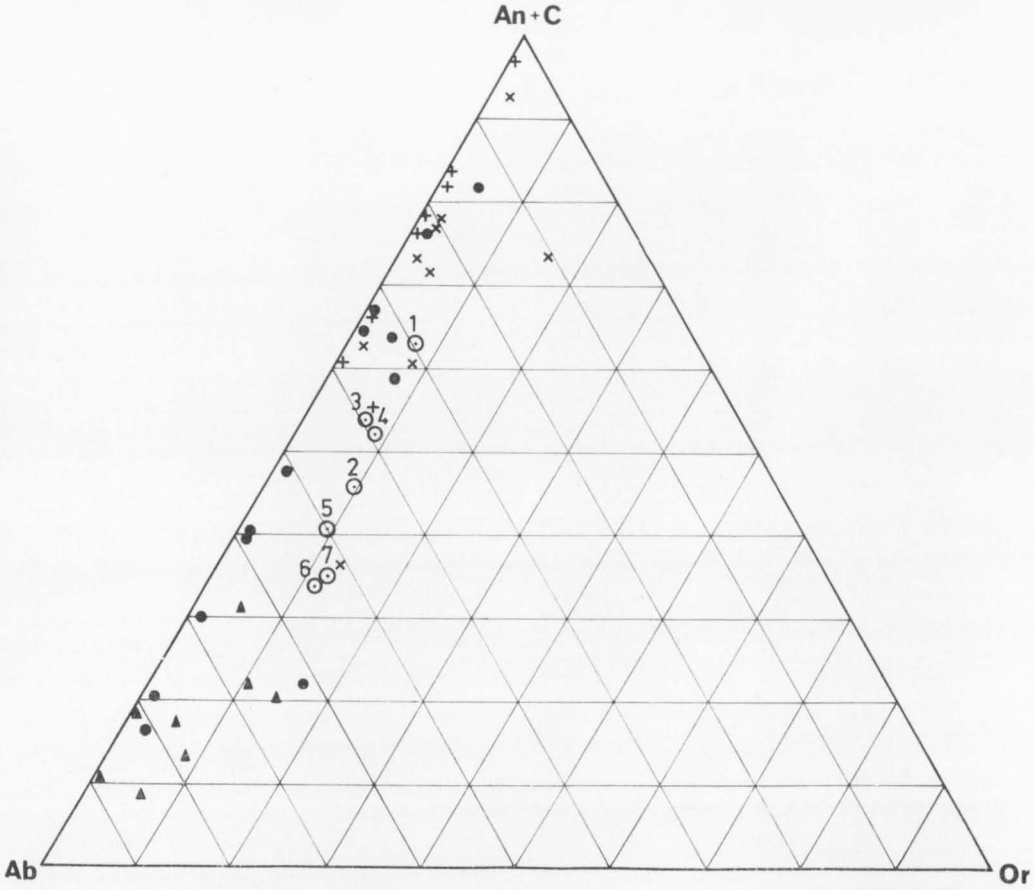


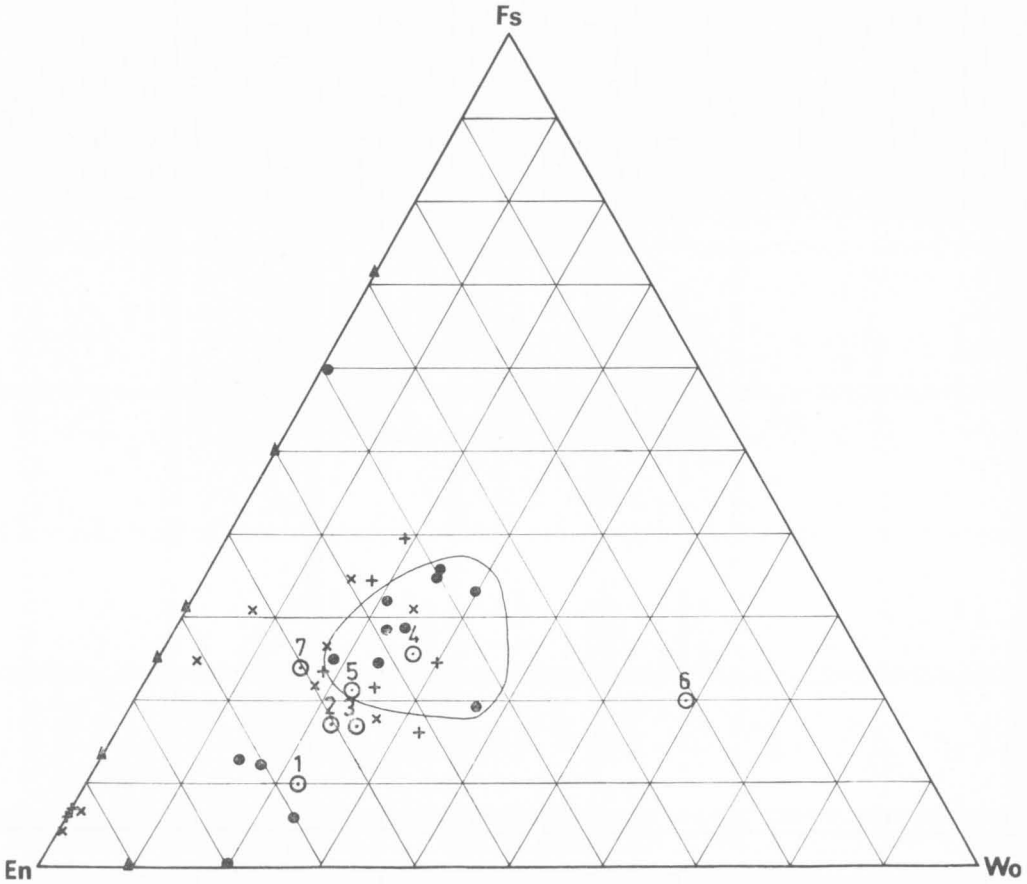
Figure 13. An+C:Ab:Or diagram for meta-igneous rocks of the Kalgoorlie-Coolgardie area. Solid circles—ophiolites associated with the Mungari Beds; crosses—Coolgardie metabasalts; oblique crosses—Kalgoorlie metabasites; triangles—sodic metaporphyries; numbered open circles—average igneous rocks (Nockolds, 1954). (1) Average pyroxenite, (2) central (high-alumina) basalt, (3) normal alkali basalt, (4) normal tholeiitic basalt, (5) average andesite, (6) average tholeiitic andesite, (7) average dacite.

(2) The Coolgardie metabasalts are relatively high in the anorthite molecule.

(3) The sodic metaporphyries are high in the albite molecule.

The Fs:En:Wo diagram (Fig. 14) reflects the similarity of the normative pyroxenes of the metabasalts to the normative pyroxene of normal tholeiitic basalt. The general chemical affinities of the ophiolites and of the sodic metaporphyries are represented by plots on Figures 15 and 16. The two diagrams indicate the calc-alkaline to calcic affinities of the igneous suite.

Although the plots of the ophiolites and sodic metaporphyries on Figure 15 scatter rather widely, it is possible to delineate alkali-silica and lime-silica curves representing the average variation trends. The intersection of these curves falls within the calcic range (above 60 percent silica). The chemical affinities of individual analyses can be assessed by means of the calculation of Rittmann's sigma index: $\sigma = (Na_2O+K_2O)^2/SiO_2 - 43$, which constitutes the basis for a chemical classification of igneous rocks into a 'Pacific' suite (calc-alkaline), 'Atlantic' suite (sodic), and a 'Mediterranean' suite (potassic). These suites are further divided



Firgue 14. Fs:En:Wo diagram for meta-igneous rocks of the Kalgoorlie-Coolgardie area. (Symbols as for Fig. 13.) Circle defines the field of the tholeiitic metabasalts.

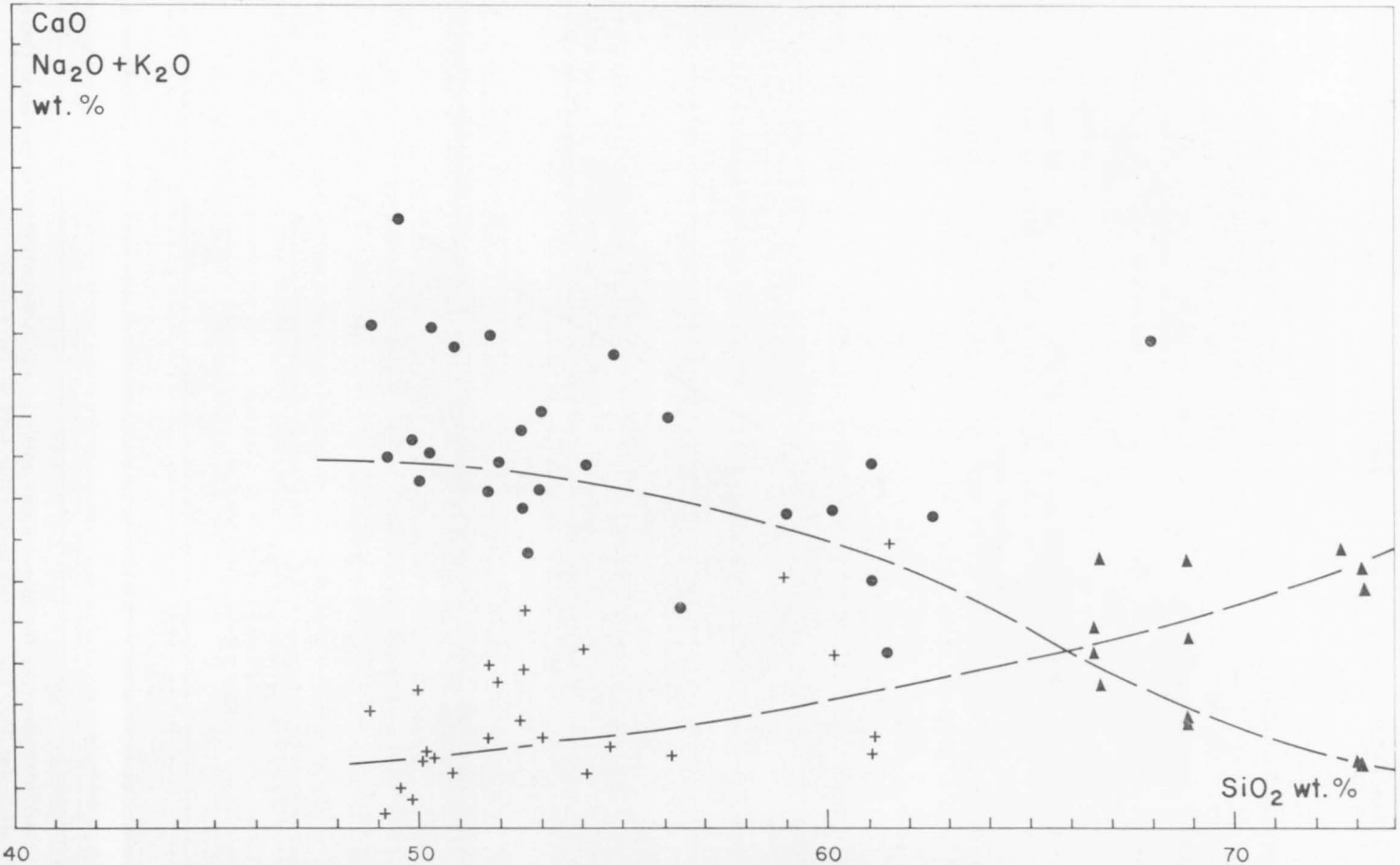


Figure 15. Peacock's calc-alkali diagram. Solid circles—lime content of ophiolites of the Kalgoorlie-Coolgardie area; crosses—alkali content of ophiolites of the Kalgoorlie-Coolgardie area; solid triangles—lime content of sodic metaporphyries; open triangles—alkali content of sodic metaporphyries; numbered open circles——lime content of average igneous rocks (Nockolds, 1954). (1) Average pyroxenite, (2) central basalt, (3) normal alkali basalt, (4) normal tholeiitic basalt, (5) average andesite, (6) average tholeiitic andesite, (7) average dacite.

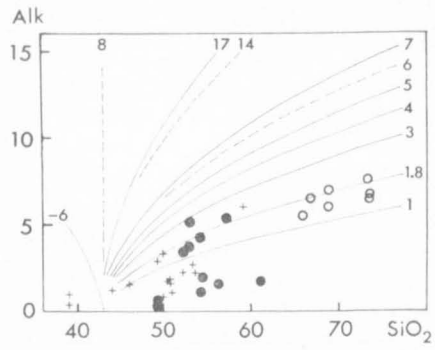


Figure 16. Relations between alkalies and silica in volcanic rock suites. Curves represent the values of the function $-\sigma = (Na_2O+K_2O)^2/SiO_2-43$. The value ranges correspond to chemical affinities as follows: Less than 1, extreme calc-alkaline; 1-1.8, strong calc-alkaline; 1.8-3, average calc-alkaline; 3-4, weak calc-alkaline; above 4, alkaline. Solid circles —ophiolites associated with the Mungari Beds; crosses—Coolgardie and Kalgoorlie ophiolites cited from Joplin (1963); open circles—sodic metaporphyries.

into groups defined as 'extreme', 'strong', 'average', and 'weak'. The sigma indices can be conveniently defined and compared by means of plots on Figure 17, in which the boundaries between the various groups are represented by curves. Plots of chemical values of the ophiolites and sodic metaporphyries on this diagram indicate that these rocks correspond to the 'average', 'strong', and 'extreme' groups of the Pacific (calc-alkaline) suite.

METAMORPHISM OF THE OPHIOLITES

Metamorphism of the Dolerites

Because of their relatively coarse grain-size, which results in a reduced intergranular contact and a consequent low susceptibility to metamorphic reconstitution, metadolerites are convenient media for tracing metamorphic reconstitution processes. Clouding of the plagioclase is probably one of the earliest alteration processes which affect the metadolerites. According to Poldervaart & Gilkey (1954), the clouding was initiated by the incipient rise of temperature, and proceeded through ionic diffusion along concentration gradients in the rock. Reactions of these ions with the feldspar would result in the crystallization of clouding products, such as biotite, amphibole, epidote, and chlorite. The most important product of incipient alteration of calcic plagioclase, however, is saussurite, the formation of which is not necessarily associated with the introduction of foreign ions, except for the addition of water.

The alumina released by the feldspar may contribute to the formation of uralitic coronae around pyroxene, or affect the conversion of actinolite into hornblende. The occurrence of zoned amphibole crystals, showing cores of actinolite and rims of acicular hornblende, has been described earlier, and could have taken place by means of one of the following processes:

(1) Late magmatic or hydrothermal marginal replacement of primary pyroxene by hornblende (uralitization), and subsequent synmetamorphic replacement of the remnant pyroxene cores by actinolite.

(2) Synmetamorphic replacement of the primary pyroxene by actinolite, and a partial replacement of the actinolite by hornblende with rising metamorphic grade.

The lime and silica released by the uralitization reaction are represented by calcite and quartz, respectively, both phases being common minor constituents of the basic meta-igneous rocks. The alumina necessary for the uralitization reaction was mainly derived from disintegration of the anorthite molecule upon the partial recrystallization of the plagioclase. Replacement of actinolite by hornblende, implied by the alternative interpretation, was favoured by Shido & Miyashiro (1959) in connexion with zoned amphiboles from the Abukuma Plateau (Japan). These authors based the boundary between the greenschist facies and the amphibolite facies partly on the transition from actinolite into hornblende.

The applicability of the second mode of development of hornblende to the basic meta-igneous rocks of the Coolgardie-Kurrawang area is supported by the observed preferential association of labradorites with actinolites (Fig. 9). It appears that the conversion of actinolite to hornblende is associated with the breakdown of the anorthite molecule, and the consequent recrystallization of the plagioclase into more sodic varieties. The accessory chlorite present in some metadolerites could have originated by the interaction of hornblende and anorthite, which also accounts for the release of silica and lime (Hutton, 1940). The released lime may combine with carbon-dioxide as calcite, or enter into reaction with ilmenite to form sphene and exsolved iron ores, both common accessories in amphibolites.

Some basic meta-igneous rocks carry subsidiary amounts of biotite, which is usually developed at the expense of amphibole. This feature may be suggestive of a minor introduction of potash from the adjacent metasediments. Because accessory quartz is common in basic meta-igneous assemblages, these rocks are commonly referred to by workers in the Kalgoorlie area as quartz dolerites, quartz basalts, etc. According to the above considerations, however, the quartz may have been formed through metamorphic reactions, and does not in itself necessarily imply primary tholeiitic affinities.

Metamorphism of the Volcanic Rocks

Because of their fine grain-size, the basalts and andesites underwent more complete metamorphic reconstitution than their coarser-grained equivalents. The types of mineralogical transformations associated with metamorphism of the basalts differed little from those associated with metamorphism of the dolerites. In some cases, however, the volcanic formations, particularly the pillowed rocks, display alteration features which have been rarely observed in the metadolerites. In spite of the generally thorough recrystallization of the fine-grained meta-igneous rocks, in some cases phenocrysts of calcic plagioclase have evaded metamorphic reconstitution. Contrary to the often perfect retention of microlites of calcic plagioclase in metabasalts investigated by Bekker (1963) at Norseman, the microlitic plagioclase of the metabasalts observed in the present study is usually recrystallized.

It is not clear whether some amphiboles of the meta-andesites of the Red Lake Ophiolites can be considered as primary non-recrystallized constituents. The acicular habit of most of the amphibole does not seem to support this possibility. The equant phenocrysts of amphibole developed in some porphyritic meta-andesites at Red Lake, on the other hand, may well constitute primary amphiboles.

Pseudomorphs of chlorite after euhedral phenocrysts of amphibole abound in the meta-andesites of the White Flag metavolcanic unit, developed on the eastern flank of the Kurrawang Syncline (Burt, 1962). The amphiboles of meta-andesites of the Red Lake ophiolites often display conspicuous porphyroblastic and cumuloblastic crystallization habits, characteristically confined to pillow cores. No compatible crystallization habit has been observed in the metadolerites.

The rock types least susceptible to metamorphic reconstitution processes are the sodic metaporphyries, many of which are considered extrusive in origin. The principal changes involved in metamorphism of these rocks are the sericitization of the sodic feldspar and the partial recrystallization of this mineral into relatively more sodic varieties. The partial recrystallization is often confined to the margins of the phenocrysts. The various ferromagnesian constituents of the sodic metaporphyries have presumably recrystallized from primary equivalents, and in some cases may represent the primary phases themselves. No unequivocal criteria are at hand for the distinction of primary from metamorphic chlorites, biotites, and amphiboles, incorporated in the groundmass of the sodic metaporphyries.

Metamorphism of the Ultrabasic Rocks

Because of the low stability of olivine, pyroxene, and calcic plagioclase under low-grade metamorphism, ultrabasic rocks are more susceptible to metamorphic reconstitution than other igneous rock types. While the metapyroxenites observed in the present study have been mostly altered to chlorite-tremolite, talc-tremolite, and talc-chlorite-tremolite assemblages, the occurrences of relict olivine and pyroxene reported by various authors from other parts of the Kalgoorlie-Norseman area demonstrate local variations in the effects of regional metamorphism (Blockley, 1956; Hudson, 1966; Williams, 1967).

Assuming that the primary pyroxene of the metapyroxenites was of magnesian composition, the formation of the chlorite-tremolite assemblages can be formulated as follows:

$$\text{pyroxene} + \text{anorthite} + \text{water} = \text{tremolite} + \text{chlorite}$$

As mentioned earlier, pseudomorphs after pyroxene mainly consist of tremolite, whereas the interstitial matrix consists of chlorite and tremolite. These relationships can be understood in terms of the restriction of most of the plagioclase of the primary pyroxenites to interstitial positions, as is the case with normal cumulates. Thus, the chloritic composition of the interstitial matrix indicates that little migration of alumina has taken place during metamorphism.

The relatively intense shearing characteristic of the meta-ultrabasic rocks is mainly the result of the mechanical weakness and the high plasticity of chlorite, serpentinite, and tremolite. The shearing planes facilitated the migration of volatiles, which accounted for the steatitization reaction:

$$\text{tremolite} + \text{carbon dioxide} + \text{water} = \text{talc} + \text{calcite} + \text{silica}$$

The metamorphic changes expressed by the above reactions culminate in the talc-carbonate-chlorite-tremolite assemblages common in the Kalgoorlie area. Following Bowen & Tuttle (1949), the formation of serpentine has probably pre-dated metamorphism, and is not therefore considered here. Upon metamorphism much of the serpentine has been replaced by chlorite, tremolite, talc, and carbonates.

Trends of Metamorphism of Basic Igneous Rocks

Wiseman (1934), in his classic study of Dalradian epidiorites, considered the chlorite-actinolite-epidote-albite assemblage as the typical product of chlorite-grade and biotite-grade metamorphism of basic igneous rocks. Andesine-hornblende assemblages, also present in the Scottish Highlands, were considered by Wiseman as the product of an abnormal metamorphic course. Turner (1935) pointed out that different mineral parageneses can develop in metamorphosed basic igneous rocks under varying water and carbon dioxide pressure.

Sutton & Watson (1951) indicated three possible trends of metamorphism of basic igneous rocks, which are controlled by the grade at which the metamorphic reactions were initiated, as follows:

Trend A—Chlorite-actinolite-epidote-albite assemblages are typical of basic meta-igneous rocks situated in the chlorite and biotite zones. The transition into the garnet zone is indicated by the appearance of almandine and oligoclase, and the decrease in the abundance of chlorite. This trend corresponds to Wiseman's 'normal trend', referred to above.

Trend B—The metamorphic reactions are initiated in the garnet zone, and have taken place in six stages:

(a) Development of secondary hornblende around pyroxene grains (uralitization). Original texture preserved.

(b) Replacement of pyroxene by quartz-hornblende aggregates. Original texture preserved.

(c) Recrystallization of the feldspar laths, with partial modification of the original texture.

(d) Recrystallization of the quartz-hornblende aggregates, with complete destruction of the original texture.

(e) Appearance of biotite.

(f) Development of green augite.

This trend of metamorphism has been referred to by Sutton & Watson (1951) as the 'Laxfordian type', and corresponds to Wiseman's 'abnormal trend'.

Trend C—The metamorphic reactions are initiated within the amphibolite and the granulite facies zones. The original pyroxene of the basic igneous rocks becomes enveloped by granular metamorphic pyroxene. The feldspar recrystallizes without notable changes in composition.

Sutton & Watson (1951) stressed that by no means can the above described trends be considered parts of one and the same line of metamorphic evolution. The high degree of preservation of igneous textures in rocks metamorphosed according to Trends B and C indicates that these rocks were not affected by wet low-grade metamorphism. The inertness of basic igneous rocks of certain metamorphic belts to low-grade metamorphism was interpreted by Yoder (1952) and by Poldervaart (1953) in terms of insufficient water pressures. The effects of pressure on the metamorphism of the basic igneous rocks was emphasized by Miyashiro (1958; 1961). Under low-pressure metamorphic conditions, the range of stability of calcic plagioclase increases, and that of epidote decreases. These relationships resulted in the relatively low degree of metamorphic reconstitution of basic igneous rocks metamorphosed under low-pressure conditions.

In comparing the mineral assemblages of the basic meta-igneous rocks of the Coolgardie-Kurrawang sequence with those corresponding to Sutton & Watson's (1951) various trends of metamorphism, the following features are pertinent:

(1) Relics of primary calcic plagioclases are often retained. The recrystallized plagioclase is often of a relatively calcic composition as well.

(2) The primary pyroxene of the basic igneous rocks has been invariably replaced with amphibole. The meta-ultrabasic rocks, on the other hand, occasionally retained relict primary pyroxenes and olivines.

(3) Both actinolite and hornblende may be present, with hornblende probably constituting the younger phase.

(4) There is a tendency for calcic plagioclase (labradorites and bytownites) to be associated with actinolites, rather than with hornblendes.

(5) Chlorite is usually only a minor constituent.

(6) Calcite is only a minor constituent.

(7) Quartz is a constant accessory.

(8) Primary igneous textures are often well preserved.

The last observation, and the common occupation of original pyroxene positions by the amphiboles in little-recrystallized metadolerites, indicate that the rocks have not been chloritized at a low metamorphic grade, for this process would have resulted in advanced destruction of the primary textures and in the removal of lime, which is clearly contradicted by the normal lime contents of most analyzed basic meta-igneous rocks. The minor chlorite present is usually developed at the expense of the amphibole, whereas opposite relationships are rather rare. It is therefore apparent that Sutton & Watson's (1951) first trend of metamorphism is not applicable to the basic meta-igneous rocks of the Coolgardie-Kurrawang area.

The dominant role of amphibole as the almost exclusive ferromagnesian constituent of the metabasites, the frequent retention of igneous textures, the scarcity of chlorite, and the relatively calcic composition of the recrystallized plagioclase, all suggest that the basic meta-igneous rocks of the Coolgardie-Kurrawang area have been metamorphosed according to the second trend of metamorphism of Sutton & Watson (1951). As is apparent from the description of the metadolerites and amphibolites, stages (b), (c), (d), and (e) of the second trend of metamorphism (Trend B) are all represented in the metabasites. The minor role of epidote, which is usually common in low-grade metabasites, may well indicate a low-pressure type of regional metamorphism, for according to Miyashiro (1961) the stability field of epidote is narrow under low-pressure conditions. The relative stability of calcic plagioclase points to the same conclusion. A low-pressure metamorphism would explain the apparent discrepancy on the ACF diagram (Fig. 17), which implies an abundance of epidote in the metabasites.

In accordance with earlier considerations, it is reasonable to consider that the actinolite-calcic plagioclase assemblages represent an earlier stage of metamorphic evolution than the hornblende-intermediate plagioclase assemblages. It appears that the hornblende-plagioclase assemblages attained a higher degree of equilibrium with the physical conditions which prevailed at the peak of the regional metamorphism than the actinolite-plagioclase assemblages which they replace.

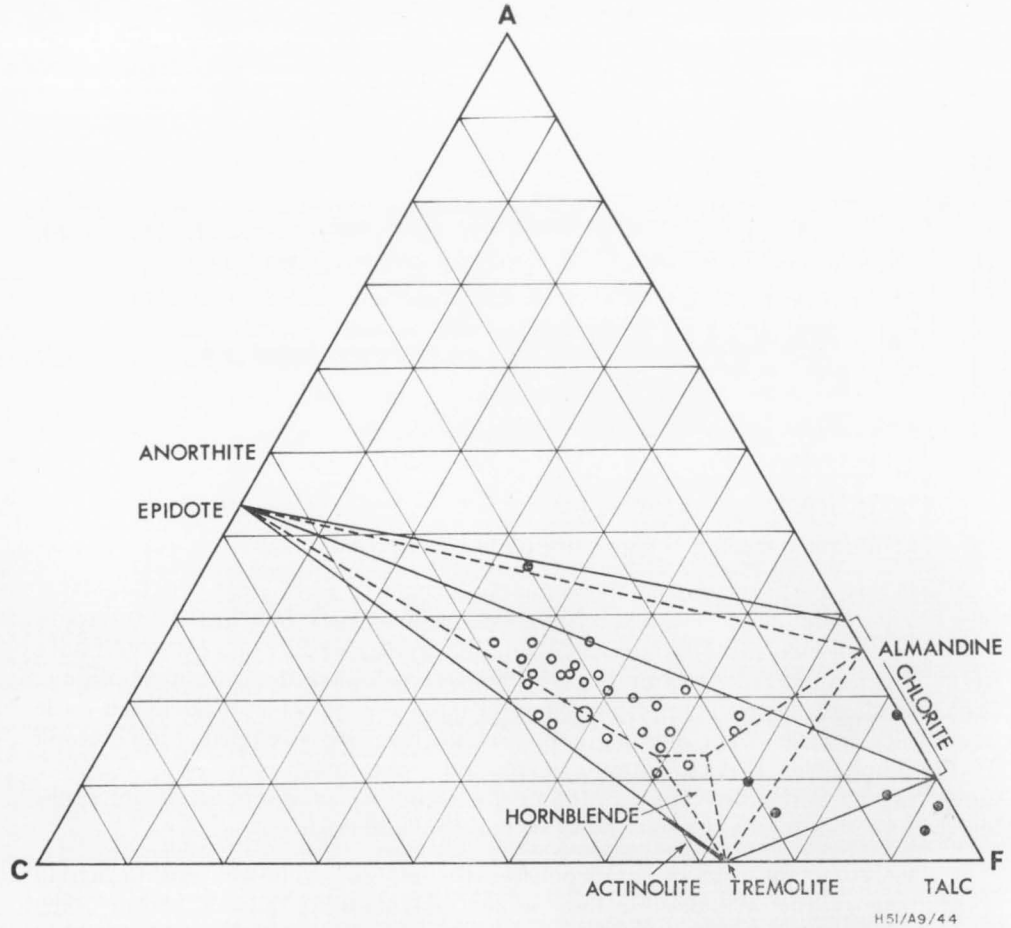


Figure 17. Plots of the chemical data of basic and ultrabasic meta-igneous rocks on the ACF diagram corresponding to the middle and the upper greenschist facies. Open circles—basic meta-igneous rocks; solid circles—ultrabasic meta-igneous rocks; continuous boundaries—middle greenschist facies phase boundaries; dashed lines—upper greenschist facies phase boundaries.

ORIGIN OF THE OPHIOLITES

Emplacement of the Ultrabasic Rocks

The origin and mode of emplacement of stratiform serpentinites is the subject of extensive debate. Most geologists regard serpentinites as altered peridotite intrusions (e.g., Hess, 1938; 1955). On the basis of studies of the MgO-SiO_2-H_2O system, Bowen & Tuttle (1949) concluded that the extremely high temperatures of peridotitic melts could not have been realized at the shallow structural levels at which serpentinites often occur. These authors envisaged the emplacement of serpentinites by means of a process of cold intrusion facilitated by the plastic properties of olivine and serpentine, as well as by the lubricating effect of interstitial vapour. This is supported by the frequently brecciated state of serpentinites, and by the lack of contact-metamorphic effects in the wall rocks of serpentinite bodies.

The problem of the origin of the meta-ultrabasic bodies incorporated in the Coolgardie ophiolites was discussed by Blockley (1956). The stratiform nature of the serpentinites, the occurrence of thin bands of magnetite and of slate intercalations, and the lack of contact-metamorphic effects, were considered by this author as evidence for a volcanic origin. The occurrence of quench spinifex-like textures in these rocks supports a volcanic origin in some cases.

While not enough is known about the composition and field relationships of serpentinites in the Kalgoorlie area, the very occurrence of these rocks is in itself significant with respect to the origin of the Kalgoorlie System. According to Hess (1955), true serpentinite belts are largely restricted to mobile orogenic belts. A distinction between Alpine serpentinites and peridotites formed through gravitative differentiation in basic sills can be made on the basis of geochemical criteria; Alpine serpentinites typically have high MgO/FeO ratios. In applying this criterion to the Coolgardie and Kalgoorlie serpentinites, their MgO/FeO ratios are considerably higher than that of the average peridotite calculated by Nockolds (1954), a difference due mainly to their lower ferrous iron content (Table 3).

Well-developed stratiform bodies of pyroxenite, with much of the original pyroxene retained, have been described from several parts of the Kalgoorlie area (e.g., Hudson, 1966; Williams, 1967). Metamorphosed pyroxenites represented by chlorite-tremolite assemblages occur within the Coolgardie ophiolites, the Mount Robinson ophiolites, and the Red Lake ophiolites. In the two latter ophiolite belts, metapyroxenite bodies are preferentially located at low stratigraphic levels. An origin of these rocks through fractional crystallization and gravitative differentiation of the overlying basic igneous rocks, however, is not warranted in view of the following considerations:

(1) The basic and intermediate meta-igneous rocks overlying the basal metapyroxenites are mostly pillowed. Since the pillows have probably formed shortly following extrusion, and before gravitative differentiation could ensue, they cannot be considered as the parent magma from which the pyroxenites have been autochthonously derived.

(2) The occurrence of slate intercalations within the basic meta-igneous rocks overlying the main bodies of metapyroxenite excludes the possibility of autochthonous gravitative differentiation.

(3) Thin sheets of metapyroxenites may occur near the top of the pillowed sequence.

The above observations indicate that the metapyroxenites have in many instances originated as independent intrusions. In the case of metapyroxenites occurring at low stratigraphic levels of stratiform metadolerites, however, an origin through gravitative differentiation of the basic magma is more likely. This is the case with a stratiform metadolerite located at the upper level of the Coolgardie ophiolites, and with which a basal meta-ultrabasic horizon is associated (Fig. 4).

Emplacement of the Dolerites

The development of subophitic textures in basic igneous rocks has been ascribed by many workers to hypabyssal conditions of crystallization. The occurrence of dolerites is not confined to hypabyssal bodies, however, as evident from

the numerous references to extrusive dolerites in the literature (e.g., Reed, 1957; Yagi, 1960). The mode of emplacemnt of the metadolerites of the Kalgoorlie system, therefore, cannot be assessed on textural criteria, and must be investigated by means of the field relationships of the bodies in question. However, because of the poor exposures, these relationships are commonly impossible to unravel in the field, and must remain a subject of indirect consideration, and of comparisons with the relatively well known metadolerite sheets in the gold mines of Kalgoorlie and Norseman.

Observation at the Golden Mile of Kalgoorlie show that the contacts of stratiform metadolerites may be locally transgressive (Woodall, 1965), and that the metadolerites may display stratigraphic zonation. Thus, the Williamstown Dolerite includes zones of quartz metadolerite and of hornblendite developed at the top and the base, respectively. Gravitative differentiation features, chilled margins, and transgressive contacts are also displayed by stratiform metadolerites at Norseman (Bekker, 1963). There can be little doubt as to the intrusive origin of these metadolerites.

Mode of Emplacement of Composite Stratiform-Ophiolites

Several ophiolite successions in the Kalgoorlie area display a preferential occurrence of meta-ultrabasics at low stratigraphic levels (Fig. 4). In the case of the Yilmia sequence, this feature applies only to individual sections believed to be separated by unconformities (Doepel, 1965). In discussing the problem of the mode of emplacement of the composite ophiolite sequences, the following features must be considered:

(1) The pillowed metavolcanics and the flow-breccias were presumably formed by means of subaqueous extrusion.

(2) The serpentinites, metapyroxenites, and metadolerites constitute both intrusive and extrusive bodies.

(3) Although individual bodies of basic and ultrabasic meta-igneous rocks may be associated with sedimentary units, there is a tendency for members of the ophiolite suite to be associated with each other in composite belts which are distinct from the main sedimentary belts.

(4) While meta-ultrabasic members may occur at various stratigraphic levels of composite ophiolite belts, there is a tendency for these rocks to occur at low stratigraphic positions.

In interpreting the spatial association of extrusive and intrusive ophiolites, and the preferential occurrence of meta-ultrabasic rocks at low stratigraphic levels, the mechanism of deep-sea eruptions envisaged by Rittmann (1962, pp. 225-226), seems a likely explanation. Considering the origin of thick stratified ultrabasic to spilitic sequences in Syria and southern Turkey, Rittmann suggested that the differentiation of the magma into various compositional fractions took place during its ascent in the volcanic fissure. The lighter differentiates were the first to be erupted on the sea bed, forming a layer of pillowed lavas. The basic magma which followed was intruded along the plane of weakness formed between the pillow lava and the underlying sediments.

Portions of the basic magma were intruded into the sedimentary sequence and the pillowed lavas, or were extruded as basalts. Basal intrusion of the ultrabasic magma followed in the same manner. Thus, according to Rittmann, ultrabasic to basic sequences originate from the contemporaneous extrusion and shallow intrusion of the products of a differentiated magma column, rather than from differentiation postdating emplacement. The main advantage of this interpretation seems to lie in the explanation it gives for the occurrence of ultrabasic to andesitic sequences, as well as for the common deviations from this pattern. These deviations, reflected by the occurrence of meta-ultrabasic rocks and metadolerites at high stratigraphic levels of sequences of pillowed meta-andesite and pillowed metabasalt, can be accounted for in terms of the intrusion into the volcanic pile of late magma fractions. If the above considerations are correct, a contemporaneous to subcontemporaneous origin of spatially associated members of the ophiolite suite is implied. The same conclusion is implied by the chemical similarity of the extrusive and intrusive basic rocks. This view differs from the previously accepted views advocating the occurrence of independent and temporally distinct phases of basic igneous volcanism and basic igneous intrusive activity, represented by 'Older Greenstones' and 'Younger Greenstones', respectively (e.g., Simpson & Gibson, 1912).

Origin of Pillowed Metavolcanic Rocks

The significance of pillow structures as indicators of the environment and mode of formation of extrusive and shallow intrusive igneous rocks has been extensively discussed in the literature (Zavaritsky, 1946; Wilson, 1960; Snyder & Fraser, 1963). Most authors assume a subaqueous origin of the pillows. Snyder & Fraser (1963) believed that the juxtaposition of a hot fluid magma and a cold fluid, generally water or muds, is necessary for pillow formation. Ellipsoidal structures developed in subaerial flows, however, have been described by several authors (Lewis, 1914; Stark, 1938). Wilson (1942) and Macdonald (1953) pointed out the basic differences between subaerially formed volcanic structures (e.g., pahoehoe) and subsequently formed lava pillows, and suggested criteria to discriminate between them.

Several workers have referred to the possibility of an intrusive origin for some pillowed igneous rocks. Snyder & Fraser (1963) investigated sheets and pods of pillowed andesite and dacite intercalated in argillites at Unalaska island, Alaska, and favoured an intrusive origin of the pillows for the following reasons:

(1) The pillows and apophyses projecting from the pillows truncate the associated sedimentary beds.

(2) Breccia and peperite are developed along contacts between the pillows and the sediments, as well as between the pillows themselves.

(3) Small pillows are developed along igneous-sedimentary contacts.

(4) Sedimentary layers overlying pillowed bodies are upwarped.

The presence or absence of the above features constitute criteria affording the discrimination of intrusive from extrusive pillows. The process of formation of extrusive and intrusive pillows, however, is still little understood. Views on the relationships between pillow formation and volcanic eruption fall into the following categories:

(1) Globulation of the lava occurs instantaneously upon the contact of the magma with the aqueous medium (Dewey & Flett, 1911; Osborn, 1949; Henderson, 1953).

(2) Pillows develop by the frothing of the lava at the fronts and margins of advancing flows (Lewis, 1914).

(3) Pillows develop subsequent to the emplacement of the flow (Foye, 1924).

Most workers favour the first view, which is supported by the occurrence of individual lava pillows embedded in pyroclastic deposits or sediments (e.g., Rittmann, 1962), as well as by the non-occurrence of interpillow conduits. On the basis of observations on pillowed rocks in the Kalgoorlie region and in the Canadian Shield, McKinstry (1939, p. 203) noted that each pillow is a distinct entity, and in a sense an individual flow which cooled within its own crust.

In considering the mode of formation of the pillowed metabasalts and meta-andesites of the Coolgardie-Kurrawang sequence, the following observations are pertinent:

(1) No sedimentary material intermixed with the pillows has been observed.

(2) Conformable horizons of slate intercalated with the pillowed bodies are not disturbed by the igneous rocks.

(3) The pillowed volcanics may be associated with flow-breccias of probable extrusive origin.

Considering the pillowed igneous rocks as extrusive in origin, and in agreement with McKinstry's view, it appears likely that each pillow constituted an independent entity, the formation of which preceded emplacement. As indicated by the tight fit of the pillows into each other, as well as by the occurrence of collapse structures at pillow tops, the pillows must have been in a plastic state upon accumulation. The occurrence of very thick sequences of pillowed lavas in Coolgardie, Norseman, and other parts of the Kalgoorlie region represent the globulation of enormous volumes of erupted magma, thereby implying a syn-extrusive disintegration of the flows and/or a deep penetration of meteoric water into the erupted lava. In both cases it could be expected that large volumes of magma would evade disintegration into pillows, a condition not recognized in the study of continuous pillowed metabasalt profiles carried out at Norseman (Bekker, 1963).

Compositional Differentiation of Pillows

Chemical variations displayed by pillowed volcanic rocks have been usually dealt with in conjunction with the spilite problem (Vuagnat, 1949; Nicholls, 1958; Vallance, 1960; 1965). The differentiation shown by pillows of the Kalgoorlie area may have originated through the following processes:

(1) Intrapillow magmatic differentiation.

(2) Deuteric autometamorphism by late-magmatic fluids.

(3) Late-magmatic alteration associated with the introduction of extra-magmatic fluids (meteoric water).

(4) Diagenetic differentiation.

(5) Metamorphic and metasomatic differentiation.

In view of the assumed rapid cooling of pillow lavas, intrapillow magmatic differentiation is not generally considered a likely mechanism for pillow differentiation. Work on fresh basaltic pillows and chilled basaltic fragments yielded little evidence for magmatic differentiation (Nicholls, 1965). On the other hand, gravitative settling of olivine crystals within pillows was reported by Yagi (1960). Many workers regarded deuteric alteration processes within pillows as the main cause of spilitization (e.g., Dewey & Flett, 1911; Sundius, 1930). Nicholls (1958) envisaged the development of two immiscible late-magmatic phases, the one rich in water, total iron, and magnesia, and the other high in silica and soda. The intrapillow separation of these phases from each other was considered responsible for the observed pillow zonation pattern. An introduction of extraneous fluids of metasomatic or meteoric origin into the cooling pillows was considered the source of soda needed for the spilitization by Beskow (1929), Gilluly (1935), and Rittmann (1958). If this view is correct, and in view of the apparent absence of spilites from the Archaean ophiolites of Australia, Canada, and South Africa, it is possible to speculate that this absence is related to the generally postulated low soda content of the primordial oceans.

The importance of diagenetic processes with respect to the differentiation of pillows has been stressed by Vallance (1960; 1965), who pointed out that post-consolidational diffusion associated with devitrification of the pillow shells would result in intrapillow as well as interpillow redistribution of the elements. In some cases pillows behave as open chemical systems, whereas in others they behave as closed chemical systems with respect to their environment (Vallance, 1965).

Because of their primary fine grain size and their structural inhomogeneity, pillowed volcanic rocks are more susceptible to metamorphic recrystallization and differentiation than coarser-grained basic igneous rocks. Porphyroblastic segregation of amphibole in pillow cores of meta-andesites has been described earlier in this paper. Pillow boundaries evidently served as conduits for metasomatic fluids, which resulted in the accentuated alteration of the rocks. The role of the metamorphic and metasomatic alteration processes, however, is difficult to distinguish from that of possible deuteric and diagenetic processes.

The high degree of retention of primary textures shown by the Coolgardie-Kurrawang pillows gives some indication as to the magmatic and late-magmatic history of these rocks. There can be little doubt that the late-magmatic amphibolitic selvedges of the pillows represent metamorphosed volcanic glass. The observed abundance of phenocrysts of calcic plagioclase and their recrystallized equivalents in pillow shells, as contrasted with their almost total absence from the cores, presents a problem. Had these phenocrysts been of an intratelluric origin, and assuming that phenocrysts have been evenly distributed in the magma from which the pillows have formed, their elimination from the cores can be accounted for by one of the following processes:

(1) Synmagmatic flotation of phenocrysts from pillow interiors to pillow margins.

(2) Differential diagenetic and/or metasomatic resorption of phenocrysts in the cores.

(3) Late-magmatic resorption of phenocrysts by residual acid fluids concentrated in the cores.

Synmagmatic flotation, although possibly of some importance, can be hardly considered responsible for the total elimination of phenocrysts from the cores. Differential dissolution of phenocrysts through diagenetic or metasomatic processes is not considered likely either, because such a process could be expected to have affected the shells as well as the cores. The possibility of a late-magmatic resorption of phenocrysts from the cores by residual acid liquids appears a likely explanation of the differential distribution of phenocrysts in the pillows, and is supported by the following evidence:

(1) As mentioned earlier in this paper, the cores have a higher silica content than the pillow margins (Fig. 12). Assuming that this feature is partly of primary origin, it could be interpreted as representative of a residual acid phase, which was also responsible for the resorption of the phenocrysts.

(2) An outward boiling of volatiles from pillow interiors is suggested by the bulbous-budding pattern displayed by varioles at the margins of meta-andesite pillows of the Red Lake ophiolites (Pl. 2). This process may indicate a gas pressure build-up within the cooling pillows; a process which could be associated with the development of a residual magmatic phase.

The pillow shells must have been in a plastic state in order to afford the penetration of gas bubbles from the cores. In describing spilitic pillows from the Ural Mountains, Zavaritsky (1946, p. 677) wrote: 'Volatile components in lavas extruded under water are retained in greater quantities than in lavas extruded subaerially. The existence of vesicular zones in the peripheries of pillow lavas shows that a boiling-up and a partial escape of gas took place, and that there is no foundation for speaking of the impermeability of glassy shells'.

A likely alternative interpretation for the occurrence of phenocrysts at pillow margins is a higher rate of nucleation and crystal growth in the shells. Bekker (1963) ascribed the relatively coarses grain-size of the plagioclase in pillow margins at Norseman to the relatively high rate of diffusion of ions in the water-saturated shells upon cooling. Yagi (1960) also advocated late crystallization of pillow shells due to high water content.

The possible role of late-magmatic intrapillow differentiation does not belittle the possibility of post-consolidational diagenetic, metamorphic, and metasomatic alteration processes. As pointed out by Vallance (pers. comm.), the variations between pillow cores and pillow shells are often too extreme to be accounted for by magmatic or late-magmatic differentiation alone. In the following, features attributable to metasomatic and diagenetic processes are discussed. Hornblende-chlorite aggregates associated with pillow meta-andesites at Red Lake may occur as interpillow mesostases, as veins emplaced along fracture planes, or as the matrix in brecciated meta-andesite.

The occurrence of the veins along the north-northwest-striking fracture system, which is parallel to the regional schistosity, defines the origin of the hornblende-chlorite aggregates to syntectonic or post-tectonic stages. The development of hornblende at the expense of chlorite indicates that the veins originally consisted of

chlorite, and that the growth of the amphibole was a later phenomenon probably associated with metamorphism. It is reasonable to assume that at least a part of the iron and magnesia incorporated in the ultramafic mesostasis was derived from the amphibole-poor pillow margins (Pl. 3).

Chloritic pillow shells charged to varying degrees by amphibole, epidote, zoisite, plagioclase, pyrite, and sphene have been described from Norseman by Bekker (1963), who noted the following relationships:

(1) Chloritic pillow margins are mainly characteristic of metabasalts located within the mineralized zones, whereas pillows located further away from the auriferous shoots are characterized by carbonate-rich chlorite-poor margins.

(2) Chloritic aggregates identical with those prevailing at pillow rims may occur as lenses or veins within the pillows.

The introduction of the chloritic veins was probably associated with a high fluid pressure, and may have accounted for the autobrecciation of the pillowed meta-andesites at Red Lake. If this interpretation is correct, these rocks can be appropriately designated as metasomatic breccias. The pre-metamorphic origin of the breccia is indicated by the development of porphyroblasts of garnet at the expense of both the meta-andesite fragments and the interfragmental matrix.

Veins of carbonate, prehnite, epidote, clinozoisite, quartz, biotite-quartz, albite, and tourmaline are commonly associated with the pillowed metavolcanic rocks, both in the Coolgardie-Kurrawang area and in other parts of the Kalgoorlie-Norseman area. The varied composition of these veins implies the migration of all the chemical elements in the rocks. The common truncation of pillow boundaries by these veins shows that in many instances the pillows behaved as open chemical systems. No rigid schemes of metasomatic alteration can be suggested for the pillowed metavolcanic rocks. Thus, the behaviour of carbonate differs markedly in various instances; in the Red Lake area calcite is mainly concentrated at pillow cores, as well as in veins, whereas at Norseman, it predominates at pillow margins (Bekker, 1963). Siliceous veins are commonly located at boundaries between pillows, but are not absent from the cores. Quartz-biotite veins occurring both at interpillow positions and as discordant veins at Norseman have been considered by Bekker (1963) as genetically associated with sodic porphyries, and possibly with the gold mineralization.

Origin of the Red Lake Flow-Breccia

A comparison between the fragments of the flow breccia and the various rock types incorporated in the Red Lake ophiolites indicates that the fragments of the breccia could not have been exclusively derived from the associated igneous rocks. Thus, the ophiolites underlying the flow-breccia comprise pillowed meta-andesites with porphyritic-variolitic margins, which are not represented in the flow-breccia. Likewise, no fragments of ultrabasic rocks, which are common in the Red Lake ophiolites, were encountered in the flow-breccia. It appears, therefore, that the flow-breccia originated independently of the associated pillowed volcanics.

Some small angular fragments incorporated in the finely comminuted matrix of the flow-breccia exhibit the development of dichotomic and comb-like aggregates composed of chains of microcrystalline amphibole. Similar textures have been observed by Doepel (1965) in metabasaltic tuffs at Yilmia (Lake Lefroy). These growth patterns can be correlated with panicled dichotomic aggregates of chainlets of microcrystalline to crypotocrystalline pyroxene developed in basaltic pillows in the Ural Mountains (Zavaritsky, 1946), and it can be inferred that the amphibole chainlets, constituting a growth pattern unknown from any other basic meta-igneous rocks, are pseudomorphic after aggregates of pyroxene similar with those described by Zavaritsky.

The movement of the flow-breccia must have been facilitated by the lubricating effect of the eutaxitic flows associated with the finely comminuted interfragmental matrix. The composition of the metatachylyte corresponds to quartz basalt according to Rittman's classification (Table 4). The flow-breccia probably formed through the extrusion of silica-saturated basaltic magma highly charged by fragments derived from the wall rocks of the volcanic vent. In view of the relatively small proportion of metatachylyte in the flow-breccia, the flow must have chilled rapidly.

As represented by the paucity of fragments of metatachylyte, little movement took place subsequent to the solidification of the flow. Although the glassy tongues and flames characteristic of the flow-breccia are not dissimilar to 'fiamme', their occurrence as selvedges around fragments is peculiar to the Red Lake flow-breccia. The chilled basalt fragments are another little-understood element of the flow-breccia. Basalt fragments with chilled selvedges have been dredged from the Mid-Atlantic Ridge, and were described by Nicholls (1965). Brecciated pillowed basalts associated with aquagene tuffs were described by Henderson (1953) and Carlisle (1963). Carlisle described basalt fragments partly coated by sideromelane vitrophyre, embedded in a groundmass composed of glass shards. No eutaxitic flows, however, have been detected.

Petrogenesis of the Sodic Porphyries

The metasomatic origin of some granites has long been advocated by the school of the 'transformationists' (Turner & Verhoogen, 1960, pp. 375-388). A metasomatic origin has also been suggested for relatively small bodies of acid porphyry (e.g., Bradley, 1957). Most arguments brought forward in favour of a metasomatic origin of granites and porphyries are based on textural and structural criteria. Thus, transitions from incipient feldspar crystals into fully developed euhedral phenocrysts, imperceptibly merged phenocryst-matrix boundaries, inclusions of matrix within phenocrysts, etc., were considered by Bradley (1957), Goodspeed (1933), and Misch (1949) as evidence for the metasomatic growth of the feldspar phenocrysts. Bekker (1963, pp. 164-166) gave the following arguments in favour of a metasomatic origin of the porphyries at Norseman:

(1) The boundaries between porphyries and greenstones are of an embayed nature.

(2) Isolated blebs of porphyry may occur within the greenstones.

(3) No contact-metamorphic effects have been detected along the boundaries of porphyry bodies.

Interpreting the origin of porphyry pebbles incorporated in the metaconglomerate of the Merougil Creek area, Lake Lefroy, Braybrooke & Middleton (1964) considered the possibility that the growth of the phenocrysts of feldspar and quartz was metasomatic. They pointed out textural similarities between the porphyry pebbles and the supposedly metasomatic feldspar and quartz growth described by Goodspeed (1933), Misch (1949), and Bradley (1957). The possibility of a metasomatic origin for porphyries showing palimpsest conglomeratic and brecciated structures has been studied by O'Beirne (1968), who considered these rocks to be recrystallized and homogenized sediments, the phenoclasts of which were originally derived from porphyritic source rocks. Little ion-exchange between porphyries and their wall rocks is believed to have taken place. Trendall (1964) regarded the porphyries as distinctly igneous, as indicated by the occurrence of oscillatory zonation in the feldspar, and by their general similarity to true volcanic rocks. In considering the origin of the porphyries of the Coolgardie-Kurrawang sequence, the following arguments are pertinent:

(1) The boundaries of the porphyries appear to be sharp.

(2) No palimpsest sedimentary textures or structures were observed in the porphyries.

(3) No penetration of pebble-matrix boundaries by phenocrysts has been observed in metaconglomerates with porphyry pebbles.

(4) Had the porphyries been metasomatic in origin, soda enrichment of adjacent metasediments would be likely. Analyses of metasediments adjacent to porphyry outcrops, however, do not reflect such a trend.

It appears, therefore, that the porphyries of the area studied are consistent in most respects with igneous porphyries, and that no criteria favouring metasomatic origin are at hand.

One striking feature of the sodic metaporphyries is the complete lack of structures and textures diagnostic of extrusive origin. This absence, coupled by the observations of intrusive porphyry contacts made in the gold mines (e.g., the Golden Mile, Binduli, Coolgardie, Norseman), account for the fact that most workers have regarded the sodic metaporphyries as intrusive. In recent years, however, references to extrusive porphyries have been made by several authors. Horwitz & Sofoulis (1965) described some stratiform porphyries in the Kalgoorlie-Norseman areas as 'acid-flows'. Trendall (1964) noted the occurrence of spherulitic and perlitic textures in some porphyries, thereby considered as volcanic flows. O'Beirne (1968) demonstrated the occurrence of flow-structures in some porphyries. In the present study, considerations bearing on the mode of emplacement of the porphyries are based on the composition of the metasediments associated with the porphyries, as well as on the shape and stratigraphic position of the porphyry bodies, as follows:

(1) The composition of the associated metagreywackes suggests that sodic porphyries were the major source rocks (Glikson, 1968). The extensive exposure of porphyries in the source area, implied by this conclusion, is much more likely to have constituted a widespread volcanic terrain than a terrain of exposed hypabyssal porphyries.

(2) Some porphyry bodies are laterally replaced by porphyry metaconglomerates. Similar relationships were observed by Trendall (1964).

Considering the pebbles as autochthonous derivatives of the porphyries, an exposure of the porphyries within the depositional basin is implied, and is best interpreted in terms of their subaqueous volcanic origin.

(3) Assuming an extrusive origin of the major porphyry bodies, their location at high stratigraphical levels of ophiolite belts can be interpreted in terms of an increasing acidity of igneous rocks with time.

Amphibole may constitute a minor or an essential component of sodic metaporphyries adjacent to ultrabasic and basic meta-igneous rocks. Enrichment in amphibole could be explained in terms of one of the following processes:

(1) Marginal contamination of the porphyritic magma by iron, magnesia, and lime, derived from adjacent basic igneous wall rocks.

(2) Synmetamorphic diffusion of iron, magnesia, and lime from the basic igneous wall rocks into the porphyries.

One difficulty involved in the first interpretation is the apparent lack of basic enclaves within the porphyries. The uniform distribution of the amphibole in some marginally contaminated porphyries suggests that the introduction of the above elements took place through uniform diffusion, rather than through irregular contamination. The alternative explanation therefore appears more likely. In other cases, however, it appears that the porphyry magma was originally rich in iron and magnesia. Thus, extensive bodies of amphibole sodic metaporphyry, showing no apparent relationships with ophiolite bodies, occur within the Mount Robinson ophiolites. In view of the size of these bodies, their origin through metasomatic addition of iron, magnesia, and lime would imply a long-range ionic diffusion. Another difficulty involved in the metasomatic interpretation is the restriction of the amphibole to the groundmass of the amphibole sodic metaporphyries, for, had the introduction of iron, magnesia, and lime been a secondary process, the amphibole could be expected to develop at the expense of both the matrix and the feldspar phenocrysts. It appears likely, therefore, that the elements necessary for the crystallization of the amphibole were primarily present in the porphyry magma. The non-occurrence of quartz phenocrysts in the amphibole sodic metaporphyries, as contrasted with their frequent occurrence in sodic metaporphyries, indicates that the first group cannot be considered as the contaminated equivalent of the latter group. The possible significance of these rocks with respect to the relationships between the sodic metaporphyries and the ophiolites is considered below.

Porphyry-Ophiolite Relationships

The origin of sodic metaporphyries and the relationships between these rocks and greenstones have been discussed by many authors, particularly in connexion with the gold mines of Kalgoorlie. Stillwell (1928), on the basis of indirect evidence, considered the albite porphyries as magmatically related to and younger than the greenstones. Co-magmatic relationships between the porphyries and the greenstones were also suggested by Thomson (1913). As pointed out by Prider (1940), the conclusions made by these authors were based on observations made on rocks displaying varying degrees of metasomatism, and therefore unsuitable for the study of primary origin. A comparison between the chemical compositions of a quartz dolerite, a basic porphyrite, and an albite porphyry with similar CO_2

contents (about 6 to 8 percent) suggested that these rocks are members of a continuous differentiation series. This was indicated by both the systematic changes in the chemical compositions of these rocks and their field relationships (Prider, 1940). On the basis of studies of the Norseman gold mines, Bekker (1963) suggested that the porphyries were the product of metasomatism affected by acid emanations separated from basic magmas. Bekker also ascribed the deposition of sulphides, tellurides, and gold to the same emanations.

Assuming an extrusive origin for some thick porphyries present in the Coolgardie-Kurrawang sequence, the preferential occurrence of these bodies at high stratigraphic levels of ophiolite belts indicates that the main episodes of acid igneous activity closely followed periods of basic volcanism. The frequent association of small lenses of sodic metaporphyry with ophiolite-metasediment contacts observed in the Coolgardie-Kurrawang area has also been recorded in other parts of the Kalgoorlie region. Bekker (1963, p. 165) wrote that 'Porphyries are known to occur in the greenstones on either side of the meta-sediments of the Lake Dundas Group. However, porphyry dykes were not seen cutting across the meta-sediments'.

Assuming that many of the small porphyry bodies are intrusive, their emplacement along ophiolite-metasediment contacts may well have resulted from the mechanical weakness of these planes. It appears, therefore, that the spatial association of porphyries with ophiolites in the Coolgardie-Kurrawang area issues from two independent factors, namely, the temporal relationships between the basic and the acid igneous activity, and the mechanical weakness of ophiolite-metasediment contacts. Significantly enough, both basic and igneous rocks are completely unknown from the Kurrawang Beds, which constitute the stratigraphically highest unit in the Kalgoorlie region. The simultaneous termination of both basic and acid igneous activity in the area points further to genetic relationships between these rocks.

In comparing the compositions of sodic metaporphyries and the basic to intermediate meta-igneous rocks, the following similarities are apparent:

(1) Both the metaporphyries and the metabasites are characterized by extremely low potash contents.

(2) The metaporphyries, metabasalts, and metadolerites have average lime/magnesia ratios higher than those of the corresponding average igneous rocks of Nockolds (1954).

(3) The sodic metaporphyries and the metabasites display calc-alkaline to calcic chemical affinities (Fig. 15).

A textural link between the metabasalts and the sodic metaporphyries is provided by the porphyritic meta-andesites and the amphibole-rich sodic metaporphyries. It is apparent that these rocks grade into each other with respect to their compositional, mineralogical, and textural characteristics. In conclusion, the evidence furnished by the field relationships, and by the petrographic and geochemical criteria suggests genetic relationships between the sodic metaporphyries and the ophiolites. Further investigations of the distribution of trace elements in the ophiolites in relation to the porphyries are needed, however, in order to confirm this suggestion.

CONCLUSIONS

When the stratigraphic variations shown by the metavolcanic rocks of the Coolgardie-Kurrawang sequence are considered, a cyclic evolution from basic and ultrabasic igneous rocks to intermediate and acid igneous rocks becomes apparent. An increase in the abundance of intermediate and acid igneous rocks with time is also represented by the succession exposed on the eastern flank of the Kurrawang Syncline (Fig. 4). The lowermost metavolcanic rocks exposed on this flank are the metabasalts of the Golden Mile of Kalgoorlie (Woodall, 1965). The overlying Black Flag unit consists of tuffs and agglomerates representing intermediate and acid volcanic activity. The peak of intermediate and acid volcanism is manifested by the lavas, breccias, and tuffs of the White Flag unit (Burt, 1962) and the Binduli porphyry belt. These volcanic formations represent the termination of the geosynclinal igneous cycle, for the overlying Kurrawang Beds are devoid of either extrusive or intrusive rocks.

There seems to be ample evidence in favour of a co-magmatic origin of the various meta-igneous members of the Coolgardie-Kurrawang sequence. The main arguments supporting this suggestion are as follows:

(1) The potash contents of the metapyroxenites, metabasalts, metadolerites, meta-andesites, and sodic metaporphyries are extremely low in comparison with those of the correspondnig average igneous rocks (Tables 4-9).

(2) According to Niggli's magma-type classification, the metapyroxenites, metabasalts, metadolerites, and meta-andesites are alkali-poor (except for the sodic metadolerites), and lime-normal to lime-rich. A comparison of the average sodic metaporphyry with the average calc-alkali rhyolite (Table 9), shows that the alkali content of the metaporphyry is lower than that of the average ryholite. The lime content of the average metaporphyry is higher than that of the average calc-alkali rhyolite. These relationships are consistent with those shown by the basic and intermediate meta-igneous rocks.

(3) The entire range of meta-igneous rocks displays calc-alkaline to calcic affinities.

(4) The progressive evolution from basic igneous activity to intermediate and acid igneous activity represents increasing generation of intermediate and acid melts, and probably reflects progressive magmatic differentiation, and/or cyclic decrease in the degrees of partial melting.

The frequent alternation of basic and intermediate meta-igneous rocks with sodic metaporphyries which takes place in the Mungari Beds may suggest that basic and acid magmas existed simultaneously in depth. Such an interpretation was given by Wilson (1965) in connexion with interbedded andesites and albite rhyolites of the Abitibi Group in the Canadian Shield. Alternatively, marked fluctuations in the degree of partial melting of the underlying basic crust and upper mantle are implied.

The ophiolites of the Eastern Goldfields of Western Australia represent major phases of eugeosynclinal subaqueous volcanic activity, intimately associated in time and space with the intrusion of basic and ultrabasic magmas. The occurrence of ultrabasic to basic and acid cycles, the thickness of the meta-igneous

successions, the abundance of serpentinites and pillow lavas, and the nature of the associated sediments all point to the similarity between the greenstones and typical Alpine ophiolites. The mechanism of deep-sea eruption envisaged by Rittmann (1962) appears to be applicable to the Archaean ophiolites. Recent evidence brought forward by South African geologists suggests that some ultrabasics characterized by high lime and low alumina contents may be of extrusive origin. The predominance of oceanic tholeiitic basalts implies that the ophiolites constituted part of the Archaean oceanic crust (e.g., Engel, 1966).

The ophiolites display remarkable similarities to Archaean greenstone sequences described from South Africa (Viljoen & Viljoen, 1967; Anhaeusser et al., 1967) and Canada (Wilson et al., 1965; Goodwin, 1968; Baragar, 1966; 1968). This comparison is dealt with elsewhere (Glikson, 1970).

Deformation and regional metamorphism of the ophiolites obliterated much of their primary characteristics. However, thanks to the low metamorphic grade, the low pressure, low volatile pressures, and the commonly minor role of metasomatism, many of the rocks retained original textural and compositional characteristics. Little metamorphosed ultrabasic rocks described from Western Australia (Hudson, 1966; Williams, 1967) and South Africa (Anhaeusser, pers. comm.), appear to represent an extreme retardation of the metamorphic reactions. These characteristics render further studies of the Archaean greenstones invaluable for the elucidation of the earliest chapters of the evolution of the earth.

REFERENCES

ANHAEUSSER, C. R., ROERING, C., VILJOEN, M. J., and VILJOEN, R. P., 1967—The Barberton Mountainland: A model of the elements and evolution of an Archaean fold belt. *Inf. Circ. No.* 38, *Econ. Geol. Res. Unit,* Univ. Witwatersrand, Johannesburg.

AUBOUIN, J., 1965—GEOSYNCLINES. *(Elsevier: Amsterdam.)*

BARAGAR, W. R. A., 1966—Geochemistry of the Yellowknife volcanic rocks. *Can. J. Earth Sci.,* 3, 9-30.

BARAGAR, W. R. A., 1968—Major elements geochemistry of the Noranda volcanic belt. Quebec-Ontario. *Can. J. Earth Sci.,* 4, 773-90.

BEKKER, C., 1963—The 'greenstones' of the Norseman District. *M.Sc. Thesis, Univ. W. Aust.* (Unpubl.).

BESKOW, G., 1929—Södra storfjället im Südlichen Lappland. Eine petrographische und geologische studie im zentralen teil des Skandinavischen Hochgebirges. *Sver. Geol. Undersoek,* Arsbok, 21 (1927), 5, 335 pp.

BICKLEY, J., 1956—The petrology of the Bayley's group of leases. *B.Sc. (Hons.) Thesis, Univ. W. Aust.* (Unpubl.).

BOWEN, N. L., and TUTTLE, O. F., 1949—The system MgO-SiO_2-H_2O. *Bull. geol. Soc. Amer.,* 60, 439-60.

BRADLEY, J., 1957—Geology of the west coast of Tasmania, part III. *Proc. Roy. Soc. Tas.,* 91, 163-90.

BRAYBROOKE, J. C., and MIDDLETON, D. D., 1964—The geology of the Merougil Creek area, northwest corner of Lake Lefroy, Western Australia. *B.Sc. (Hons.) Thesis, Univ. W. Aust.* (Unpubl.).

BROWN, W. L., 1962—Peristerite unmixing in the plagioclases, and metamorphic facies series. *Norsk Geol. Tidsskr.,* 42, 354-82.

BURRI, C., 1964—PETROCHEMICAL CALCULATIONS. *(Israel Program for Scientific Translations: Jerusalem.)*

BURT, D. R. L., 1962—The geology of the northwestern extension of the White Flag Lake, near Kalgoorlie, Western Australia. *B.Sc. (Hons.) Thesis, Univ. W. Aust.* (Unpubl.).

CARLISLE, D., 1963—Pillow breccias and their aquagene tuffs, Quadra Island, British Columbia. *J. Geol.,* 71, 49-71.

DEER, W. A., HOWIE, R. A., and ZUSSMAN, J., 1963—ROCK-FORMING MINERALS. *(Longmans: London.)*

DEWEY, H., and FLETT, J. S., 1911—On some British pillow lavas and rocks associated with them. *Geol. Mag.,* 8, 2029, 241-48.

DOEPEL, J. J. G., 1965—The geology of the Yilmia area, west of Lake Lefroy, Western Australia. *B.Sc. (Hons.) Thesis, Univ. W. Aust.* (Unpubl.).

ENGEL, A. E. J., ENGEL, C. G., and HAVENS, R. G., 1965—Chemical characteristics of oceanic basalts and the upper mantle. *Bull. geol. Soc. Amer.,* 76, 719-34.

ENGEL, A. E. J., 1966—The Barberton Mountainland: Clues to the differentiation of the Earth. *Inf. Circ. No.* 27, *Econ. Geol. Res. Unit,* Univ. Witwatersrand, Johannesburg.

FOYE, W. G., 1924—Pillow structures in the Triassic basalts of Connecticut. *Bull. geol. Soc. Amer.,* 35, 329-46.

GILLULY, J., 1935—Keratophyres of eastern Oregon and the spilite problem. *Amer. J. Sci.,* 29, 225-52.

GLAESSNER, M. F., and TEICHERT, C., 1947—Geosynclines—a fundamental concept in geology. *Amer. J. Sci.,* 245, 465-82, 571-91.

GLIKSON, A. Y., 1968—The Archaean geosynclinal succession between Coolgardie and Kurrawang, near Kalgoorlie. Western Australia. *Ph.D. Thesis, Univ. W. Aust.* (Unpubl.).

GLIKSON, A. Y., 1970—Geosynclinal evolution and geochemical affinities of Early Precambrian systems. *Tectonophysics,* 9, 397-433.

GOODSPEED, G. E., 1933—Development of albite porphyroblasts. *Am. Miner.,* 22, 133.

GOODWIN, A. M., 1968—Archaean protocontinental growth and early crustal history of the Canadian Shield. Proc. *23rd Int. geol. Congr., Prague,* 1, 69-89.

HAMILTON, W., 1965—Origin of volcanic rocks of eugeosynclines and island arcs, *in* CONTINENTAL MARGINS AND ISLAND ARCS—A SYMPOSIUM. *Geol. Surv. Canada Pap.,* 66-15, 348-55.

HENDERSON, J. F., 1953—On the formation of pillow lavas and breccias. *Roy. Soc. Canada Trans.,* 47, 23-32.

HESS, H. H., 1938—A primary peridotitic magma. *Amer. J. Sci.*, 35, 321-44.

HESS, H. H., 1955—Serpentines, orogeny and epeirogeny, *in* POLDERVAART, A. (Ed.), CRUST OF THE EARTH—A SYMPOSIUM. *Geol. Soc. Amer. Spec. Paper*, 62, 391-408.

HEY, M. H., 1954—A new review of the chlorites. *Min. Mag.*, 30, 277.

HONMAN, C. S., 1914—The geology of the country between Kalgoorlie and Coolgardie. *Geol. Surv. W. Aust. Bull.*, 56.

HORWITZ, R. C., and SOFOULIS, J., 1965—Igneous activity and sedimentation in the Precambrian between Kalgoorlie and Norseman, Western Australia. *Proc. Aust. Inst. Min. Metall.*, 214, 45-59.

HOWELL, J. V., 1960—GLOSSARY OF GEOLOGY AND RELATED SCIENCES. 2nd ed. *(Amer. Geol. Inst.: Washington.)*

HUDSON, G. R., 1966—The geology of part of the Norseman succession, west of the mining area, Norseman, Western Australia. *B.Sc. (Hons.) Thesis, Univ. W. Aust.* (Unpubl.).

HUTTON, C. O., 1940—Metamorphism in the Lake Wakatipu region, western Otago, New Zealand. *Geol. Surv. New Zealand Mem. No. 5.*

JOPLIN, G. A., 1963—Chemical analyses of Australian rocks. Part 1: Igneous and metamorphic. *Bur. Min. Resour. Aust. Bull.*, 65.

KAY, M., 1951—North American geosynclines. *Geol. Soc. Amer. Mem.*, 48.

LEAKE, B. E., 1965—The relationships between the composition of calciferous amphiboles and the grade of metamorphism. *in* PITCHER, W. S., and FLINN, G. W. (Eds), CONTROLS OF METAMORPHISM—A SYMPOSIUM, 299-316. *(Oliver and Boyd: Edinburgh.)*

LEWIS, J. V., 1914—Origin of pillow lavas. *Bull. Geol. Soc. Amer.*, 25, 591-654.

MACDONALD, G. A., 1953—Pahoehoe, aa, and block-lava. *Amer. J. Sci.*, 251.

MANSON, V., 1967—Geochemistry of basaltic rocks; major elements, *in* HESS, H. H., and POLDERVAART, A. (Eds), BASALTS. *(Interscience Publishers: New York.)*

MAZZUCHELLI, R., 1962—The geology of Mt Pleasant, Broad Arrow Goldfield, Western Australia. *B.Sc. (Hons.) Thesis, Univ. W. Aust.* (Unpubl.).

MCCALL, G. J. H., BRAYBROOKE, J. C., MIDDLETON, D. D., and MUHLING, P. C., 1967—Sedimentology of some eugeosynclinal rocks of the Early Precambrian Kalgoorlie System, Western Australia. *Proc. 7th Int. Sedimentol. Cong., Edinburgh.*

MCKINSTRY, H. E., 1939—Discussion: Pillow lavas of Borabora, Society Islands. *J. Geol.*, 47, 202-4.

MISCH, P., 1949—Metasomatic granitisation of batholitic dimensions. *Amer. J. Sci.*, 247, 743.

MIYASHIRO, A., 1957—Chlorite of crystalline schists. *J. geol. Soc. Japan*, 63, 1.

MIYASHIRO, A., 1958—Regional metamorphism of the Gosaisyo-Takunuki District in the Central Abukuma Plateau. *J. Fac. Sci. Univ. Tokyo*, XI, 219-72.

MIYASHIRO, A., 1961—Evolution of metamorphic belts. *J. Petrol.*, 2, 277-311.

MÜHLING, P. C., 1965—The geology of the Bayley's working area, west of Lake Lefroy, Western Australia. *B.Sc. (Hons.) Thesis, Univ. W. Aust.* (Unpubl.).

NICHOLLS, G. D., 1958—Autometasomatism in the lower spilites of the Builth Volcanic Series. *Quart. J. Geol. Soc. London*, 114, 137-62.

NICHOLLS, G. D., 1965—Basalts from the deep ocean floor. *Min. Mag.*, 34, 373-88.

NOCKOLDS, S. R., 1954—Average chemical compositions of some igneous rocks. *Bull. Geol. Soc. Amer.*, 65, 1007-32.

O'BEIRNE, W. R., 1968—The porphyries of the Kalgoorlie area, Western Australia. *Ph.D. Thesis, Univ. W. Aust.* (Unpubl.).

OSBORN, E. F., 1949—Cellular structures in glass as related to structures in lava. *J. Geol.*, 57, 738.

PEACOCK, M. A., 1931—Classification of igneous rocks. *J. Geol.*, 39, 54-67.

POLDERVAART, A., 1953—Review of the metamorphism of the basaltic rocks. *Bull. Geol. Soc. Amer.*, 64, 259-74.

POLDERVAART, A., and HESS, H. H., 1951—Pyroxenes in the crystallisation of basaltic magma. *J. Geol.*, 59, 472.

POLDERVAART, A., and GLIKEY, A. K., 1954—On clouded plagioclase. *Am. Miner.*, 39, 75.

PRIDER, R. T., 1940—A note on the age relations of the basic porphyrites and albite porphyries of the Golden Mile, Kalgoorlie, Western Australia. *J. Roy. Soc. W. Aust.*, 26, 99-101.

PRIDER, R. T., 1961—The 'greenstones' of south-western Australia. *J. Roy. Soc. W. Aust.*, 44, 1-9.

PRIDER, R. T., 1965—Geology and mineralisation of the Western Australian Shield, *in* MCANDREW, J. (Ed.), GEOLOGY OF AUSTRALIAN ORE DEPOSITS, 56-65. *(Aust. Inst. Min. Metall., Melbourne.)*

REED, J. J., 1957—Petrology of the Lower Mesozoic rocks of the Wellington District. *N.Z. Geol. Surv. Bull.*, 57.

RITTMANN, A., 1952—Nomenclature of volcanic rocks. *Bull. Volcanology*, 12, 75-102.

RITTMANN, A., 1958—Geosynclinal volcanism, ophiolites and Barramiya rocks. *Egypt. J. Geol.*, 2, 61-65.

RITTMANN, A., 1962—VOLCANOES AND THEIR ACTIVITY. *(Wiley: New York.)*

SHIDO, F., and MIYASHIRO, A., 1959—Hornblendes of basic metamorphic rocks. *J. Fac. Sci. Univ. Tokyo,* XII, 85-102.

SIMPSON, E. S., and GIBSON, C. G., 1912—Contribution to the study of the geology and ore deposits of Kalgoorlie, East Coolgardie Goldfield. *Geol. Surv. W. Aust. Bull.*, 42.

SNYDER, G. L., and FRASER, G. D., 1963—Pillowed lavas. I. Intrusive layered lava pods and pillowed lavas, Unalaska Island, Alaska. *U.S. Geol. Surv. Prof. Pap.*, 454-B. II. A review of selected literature. *U.S. Geol. Surv. Prof. Pap.*, 454-C.

SOFOULIS, J., 1966—Widgiemooltha, Western Australia—1:250,000 geological map with explanatory notes. *Geol. Surv. W. Aust.*

STARK, J. T., 1938—Vesicular dykes and subaerial pillow lavas of Borabora, Society Islands. *J. Geol.*, 46, 225-38.

STILLWELL, F. L., 1928—Geology and ore deposits of the Boulder belt, Kalgoorlie. *Bull. Geol. Surv. W. Aust.*, 94.

SUNDIUS, N., 1930—On the spilitic rocks. *Geol. Mag.*, 67, 1-17.

SUTTON, J., and WATSON, J., 1951—Varying trends in the metamorphism of dolerites. *Geol. Mag.*, 88, 25-35.

THOMSON, J. A., 1913—The petrology of the Kalgoorlie Goldfield. *Quart. J. Geol. Soc. London,* 69, 621-77.

TRENDALL, A., 1964—Notes on the nomenclature and the significance of 'porphyry' and 'porphyrite' in Western Australia. *Geol. Surv. W. Aust. Ann. Rep.* for 1963, 96-100.

TUREK, A., 1966—Geochronology of the Kalgoorlie area. *Ph.D. Thesis, Australian National Univ.* (Unpubl.).

TURNER, F. J., 1935—Contribution to the interpretation of mineral facies in metamorphic rocks. *Amer. J. Sci.*, 29, 409-21.

TURNER, F. J., and VERHOOGEN, J., 1960—IGNEOUS AND METAMORPHIC PETROLOGY. (2nd ed.) *(McGraw-Hill: New York.)*

VALLANCE, T. G., 1960—Concerning spilites. *Proc. Linn. Soc. N.S.W.*, IXXXV (p. 1), 8-52.

VALLANCE, T. G., 1965—On the chemistry of pillow lavas and the origin of spilites. *Min. Mag.*, 34 (Tilley Volume), 471-81.

VILJOEN, M. J., and VILJOEN, R. P., 1967—A reassessment of the Onverwacht Series in the Komati River Valley. *Inf. Circ. No.* 36, *Econ. Geol. Res. Unit,* Univ. Witwatersrand, Johannesburg.

VUAGNAT, M., 1949—Variolites et spilites; comparison entre quelques pillow lavas britanniques et alpines. *Archives des Sciences.*, 2, f. 2, 223-36.

WILLIAMS, C., 1967—Geology of the Ora Banda norite. *B.Sc. (Hons.) Thesis, Univ. W. Aust.* (Unpubl.).

WILSON, A. F., COMPSTON, W., JEFFERY, P. M., and RILEY, G. H., 1960—Radioactive ages from the Precambrian rocks in Australia. *J. Geol. Soc. Aust.*, 6, 179-96.

WILSON, H. D. B., ANDREWS, P., MOXHAM, R. L., and RAMLAL, K., 1965—Archaean volcanism in the Canadian Shield. *Can. J. Earth Sci.*, 2, 161-75.

WILSON, M. E., 1942—Structural features of the Keewatin volcanic rocks of western Quebec. *Bull. Geol. Soc. Amer.*, 53, 53-69.

WILSON, M. E., 1960—Origin of pillow structures in Early Precambrian lavas of western Quebec. *J. Geol.*, 68, 97-102.

WILSON, M. E., 1965—The Precambrian of Canada: The Canadian Shield, *in* RANKAMA, K. (Ed.). THE PRECAMBRIAN. *(Interscience Publishers: New York.)*

WISEMAN, J. D. H., 1934—The central and south-west Highlands epidiorites. *Quart. J. Geol. Soc. London,* 90, 354-417.

WOODALL, R. W., 1965—Structure of the Kalgoorlie Goldfield, *in* MCANDREW, J. (Ed.), GEOLOGY OF AUSTRALIAN ORE DEPOSITS, 719. *(Aust. Inst. Min. Metall.: Melbourne.)*

ZAVARITSKY, V. A., 1946—The spilite-keratophyre formation in the region of the Blyara deposit in the Ural Mountains. *Int. Geol. Rev.*, 1960, 2, 551-76. (English translation.)

YAGI, K., 1960—Alkali rocks of Nemure Peninsula, with special reference to their pillow lavas. *Int. Geol. Rev.*, 2, 912-20.

YODER, H. S., JR., 1955—Role of water in metamorphism, *in* POLDERVAART, A. (Ed.), CRUST OF THE EARTH. *Geol. Soc. Amer. Spec. Pap.*, 62, 505-24.

NOTE IN PROOF

Since the manuscript of this paper was submitted (November 1969), rapid progress has taken place in the study of Archaean greenstones, particularly in Western Australia and South Africa. Hallberg (1970) completed a detailed geochemical investigation in the Norseman-Lake Lefroy-Coolgardie belt and indicated a high degree of compositional uniformity of the basic igneous rocks and an absence of andesites. Hallberg's results confirm the commonly isochemical metamorphism suggested above, the low Al_2O_3, K_2O and Fe_2O_3/FeO, and the high CaO and Na_2O/K_2O of the metabasites. A correlation of the basalts with oceanic tholeiites is thus further substantiated. The lack of intermediate igneous rock, on the other hand, suggests that at least some of the chemically defined meta-andesites of this paper may represent silica-enriched, iron- and magnesia-depleted metabasalts. That intermediate rocks are not entirely absent in the Kalgoorlie System, however, is apparent from the occurrence of dacite porphyries (O'Beirne, 1968) and hornblende meta-andesites (Burt, 1962), although chemical analyses of the latter are not available.

A study of the Archaean Onverwacht Series in eastern Transvaal (Viljoen & Viljoen, 1969) shows that this sequence, which consists of a wide range of extrusive and intrusive basic and ultrabasic rocks, represents a well exposed analogue of the Coolgardie ophiolites. The extrusive origin of some stratiform meta-pyroxenites and metaperidotites is shown by the occurrence of pillows and quench textures in these rocks. In a recently submitted paper, which deals with the significance of major and trace element data in relation to the Archaean geotectonic pattern (Glikson, 1971), further reasons are given showing that these ultrabasic-basic sequences represent relicts of an Archaean oceanic crust.

REFERENCES

GLIKSON, A. Y., 1971—Primitive Archaean element distribution patterns: Chemical evidence and geotectonic significance. *Earth Planet. Sci. Lett.*, 12, 309-320.

HALLBERG, J. A., 1970—Petrology and geochemistry of metamorphosed Archaean basic volcanic rocks between Coolgardie and Norseman, Western Australia. *Ph.D. Thesis, Univ. W. Aust.* (unpubl.).

VILJOEN, R. P., and VILJOEN, M. J., 1969—Papers published in: *The Upper Mantle Project, Geol. S. Africa spec. Publ. No.* 2, 9-304.

Page 190 is blank.

PLATE 16

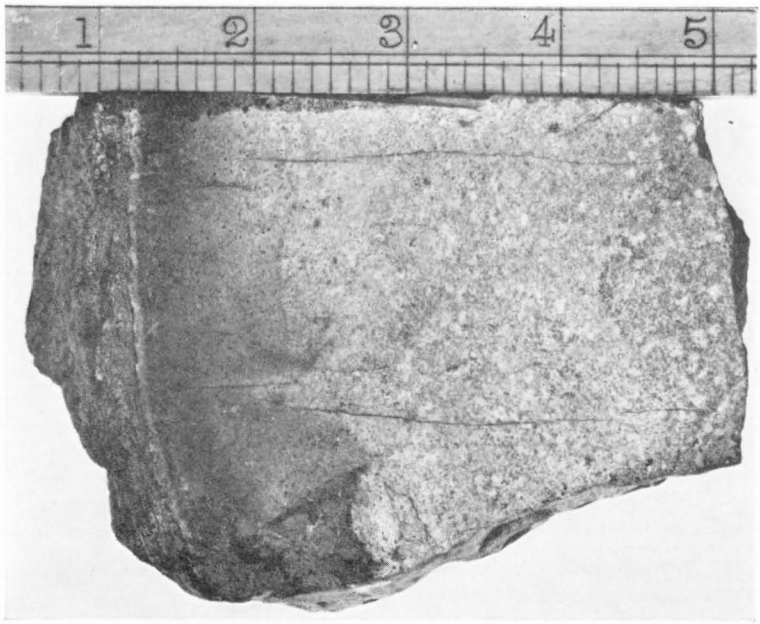


Figure 1. Section across a metabasalt pillow from the Coolgardie ophiolites, showing (from right to left): (1) pillow interior, consisting of fine-grained amphibole, and plagioclase-quartz lenses; (2) core-shell transition zones, finely spotted by opaques, and including recrystallized plagioclase phenocrysts; (3) pillow shell, composed of microcrystalline amphibole. Scale in inches.

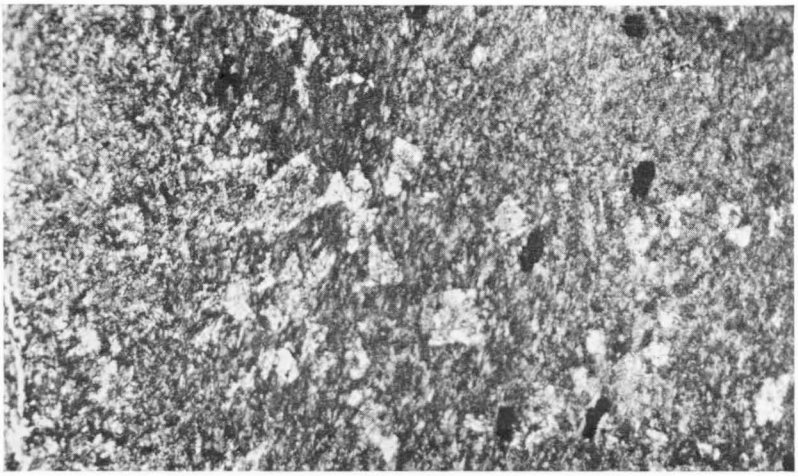


Figure 2. Photomicrograph of the margin of a metabasalt pillow, showing recrystallized phenocrysts of plagioclase. ×10; plane polarized light.

PLATE 17

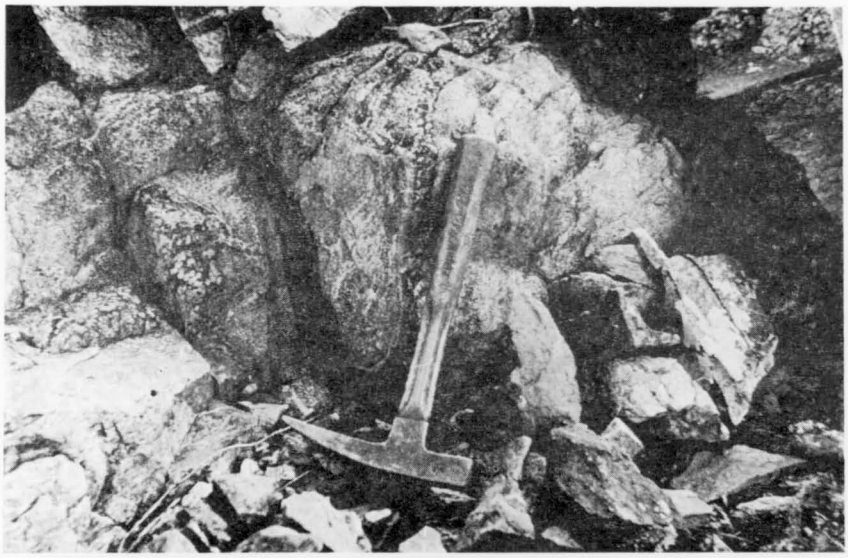


Figure 1. Pillowed meta-andesites of the Red Lake ophiolites, showing variolitic-porphyritic margins.

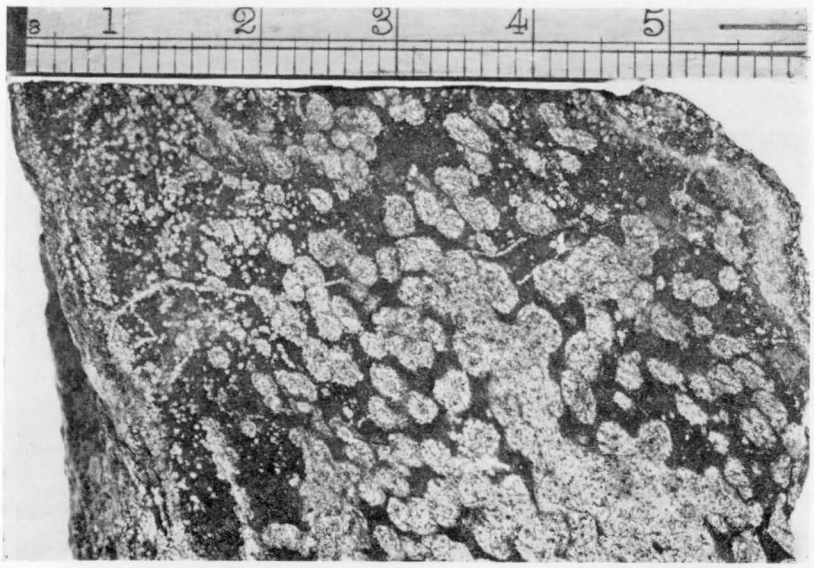


Figure 2. Variolitic-porphyritic shell of a meta-andesite pillow. The leucocratic lenses and the fine white spots represent recrystallized variolites and phenocrysts of calcic plagioclase, respectively. The phenocrysts are concentrated near the pillow boundary, on the left. Scale in inches.

PLATE 18

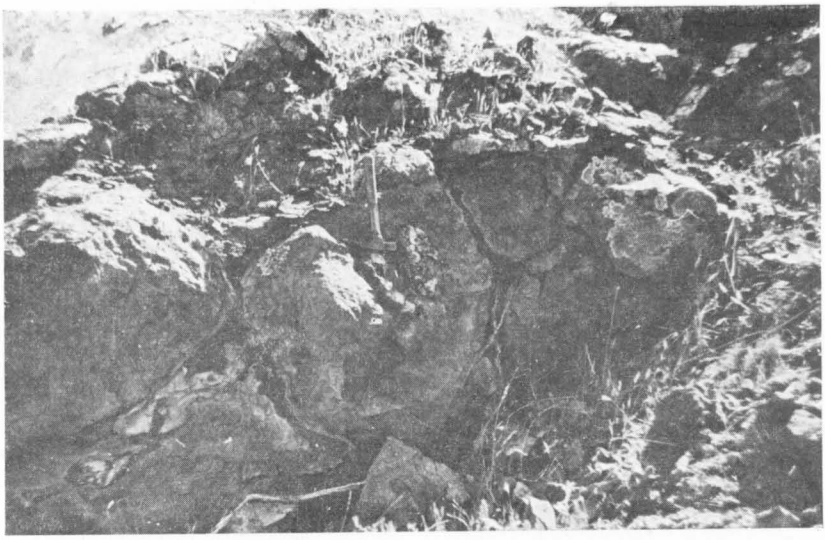


Figure 1. Pillowed porphyroblastic meta-andesites of the Red Lake ophiolites. Note the black mesostasis, which consists of chlorite-hornblende aggregates.

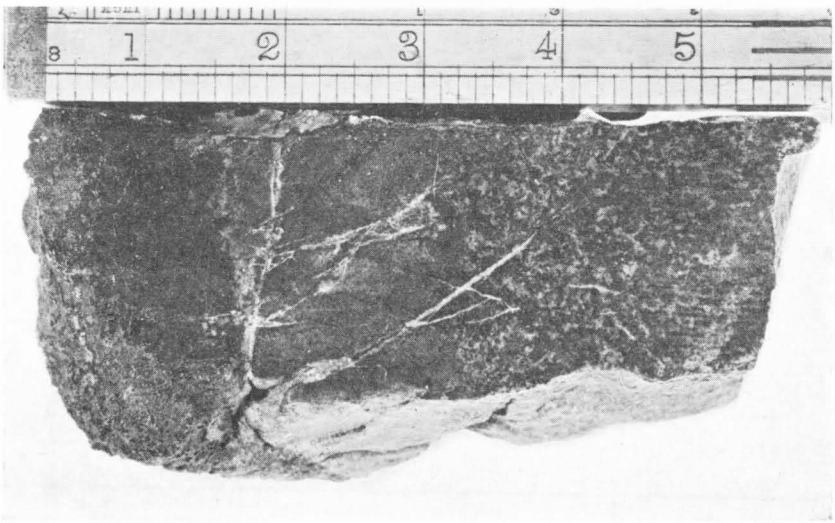


Figure 2. Section across a meta-andesite pillow, showing (from right to left): (1) porphyroblastic pillow interior, consisting of coarse-grained amphiboles set in carbonate-quartz-plagioclase matrix; (2) pillow shell, characterized by a fine-grained texture, and a higher plagioclase-amphibole ratio; (3) ultramafic mesostasis, composed of hornblende developed at the expense of ferroan chlorite. Scale in inches.

PLATE 19



Figure 1. Outcrop of basic flow-breccia at Red Lake.

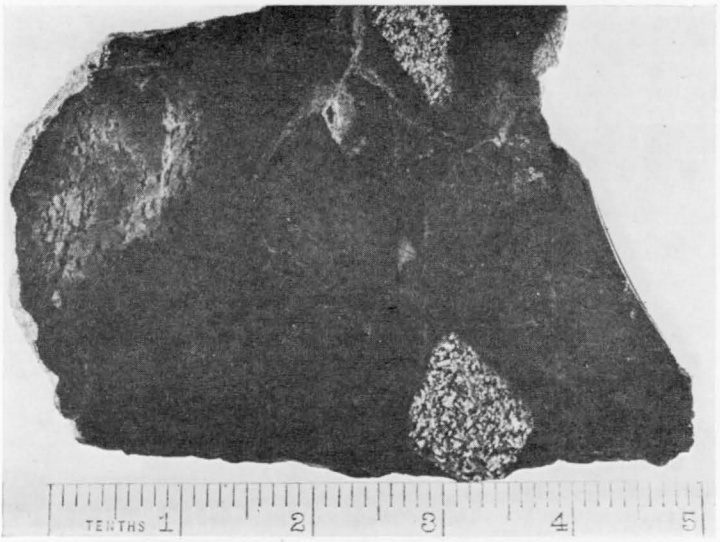


Figure 2. Polished slab of basic flow-breccia, showing metadolerite fragments (top and bottom of slab), an acid volcanic fragment (upper left), and metabasalt fragments (weakly defined at the centre of the slab). Scale in inches.

PLATE 20

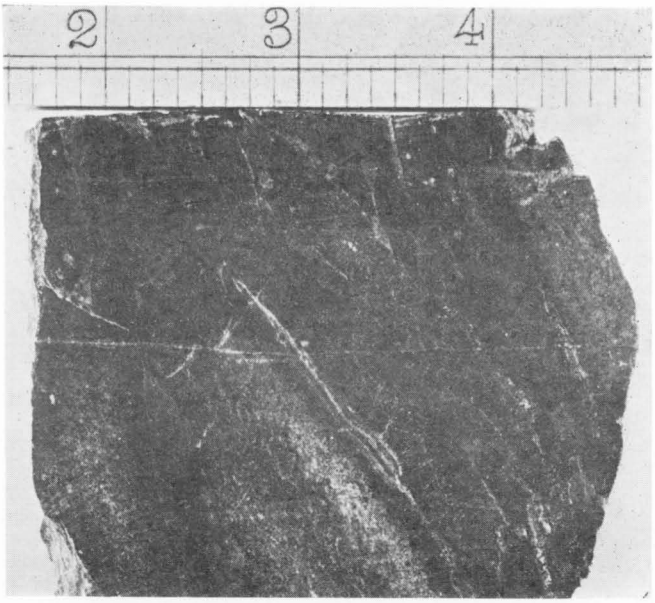


Figure 1. Polished slab of basic flow-breccia, showing: (1) chilled meta-andesite fragments, with crystallized cores and metatachylyte selvedges; (2) eutaxitic tongues and flows of metatachylyte; (3) angular fragments of metatachylyte; (4) fragmental matrix (the dark grey interstitial material). Scale in inches.



Figure 2. Photomicrograph of the basic flow-breccia, showing (from left to right): (1) a ropy aggregate of amphibole, representing a small-scale flow of volcanic glass (metatachylyte); (2) finely comminuted interfragmental matrix; (3) a microlitic metabasalt fragment, including recrystallized phenocrysts of plagioclase. ×10; plane polarized light.

PLATE 21

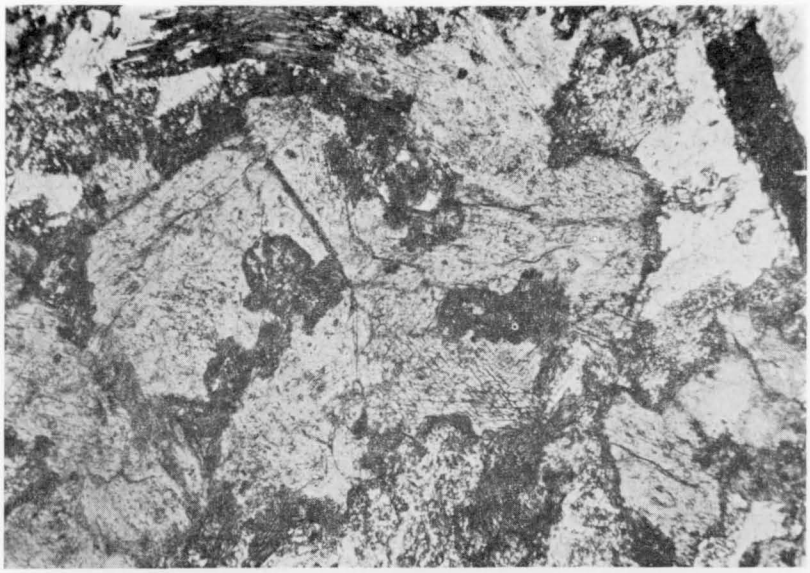


Figure 1. Photomicrograph of a labradorite-hornblende-actinolite subophitic metadolerite, showing saussuritized prisms of plagioclase enclosed by zoned crystals of amphibole. ×25; plane polarized light.

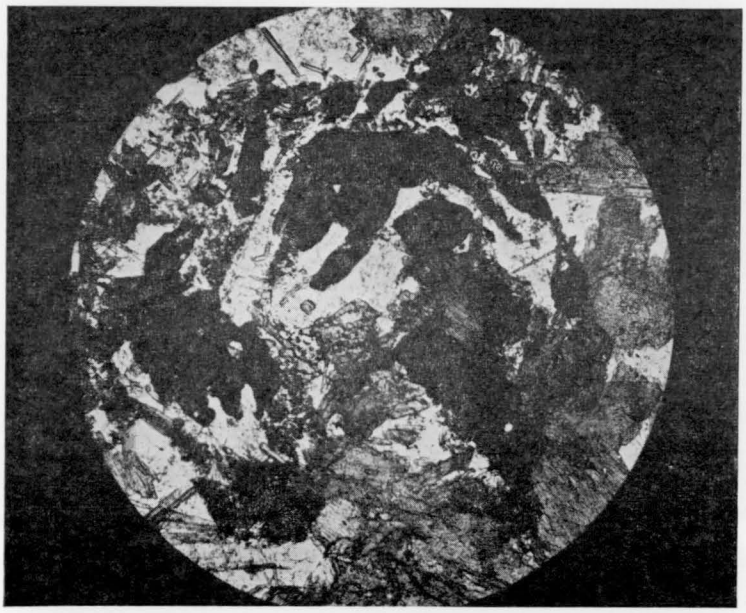


Figure 2. Photomicrograph of a skeletal phenocryst of ilmenite set in aggregates of recrystallized plagioclase and amphibole in a metadolerite. ×63; plane polarized light.

PLATE 22

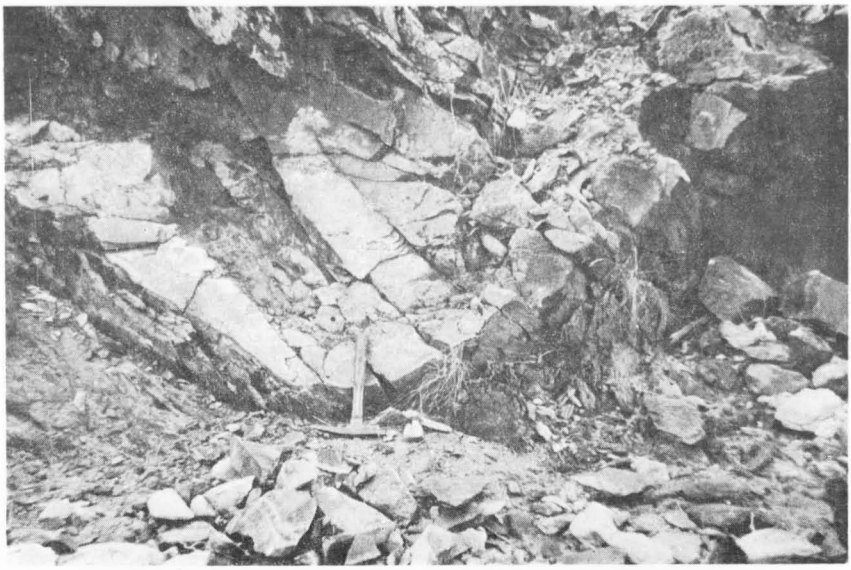


Figure 1. Folded sill of quartz-albite metaporphyry emplaced in sheared chlorite-tremolite metapyroxenites (dark band behind hammer) of the Red Lake ophiolites.

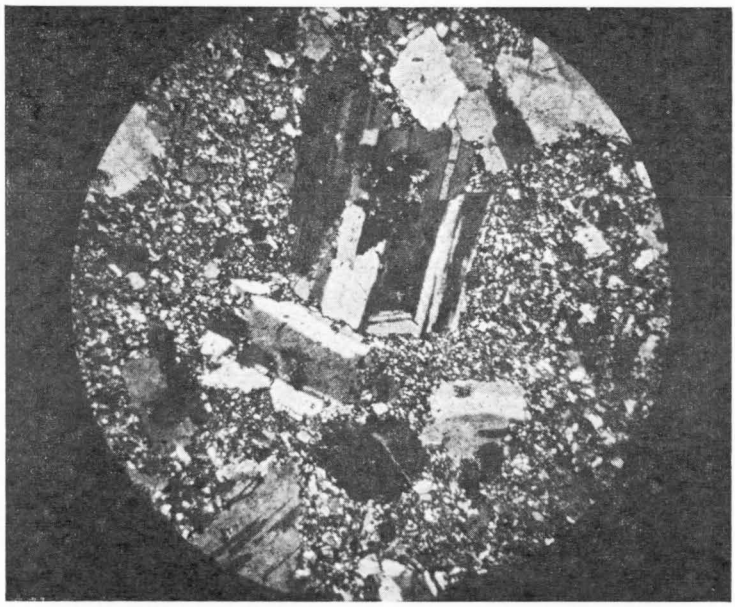


Figure 2. Photomicrograph of a biotite-quartz-albite metaporphyry, showing twinned phenocrysts of plagioclase set in a microcrystalline quartzo-feldspathic groundmass. ×25; crossed nicols.

PLATE 23

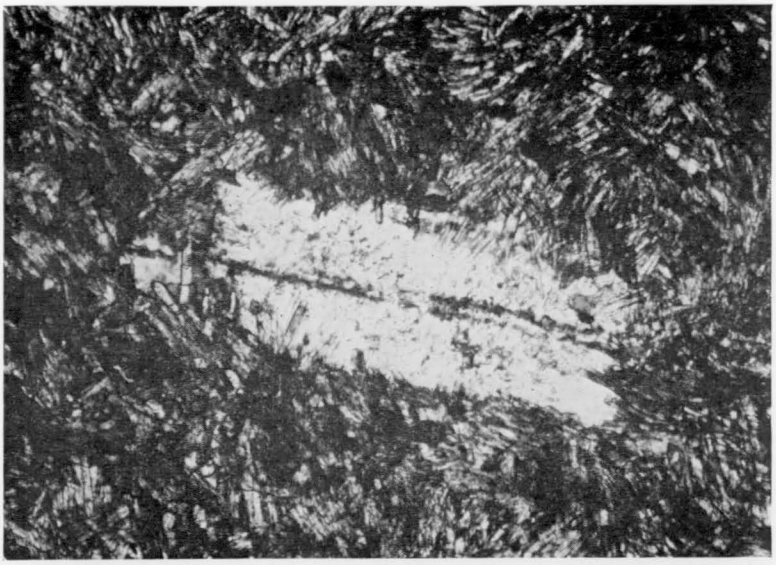


Figure 1. Photomicrograph of a metabasalt pillow shell, showing a relict igneous phenocryst of plagioclase (andesine, An 47), set in a matted aggregate of plagioclase. ×117; crossed nicols.

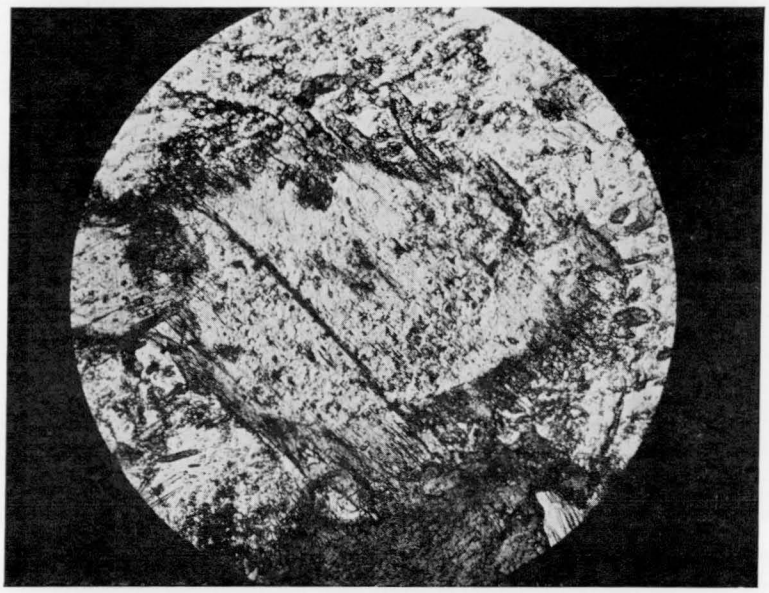


Figure 2. Photomicrograph of a metadolerite, showing a zoned crystal of amphibole, with a core of actinolite and a rim of hornblende. The amphiboles are separated by a sharp boundary, and are in optical continuity with one another. ×63; plane polarized light.

PROBLEMS OF PROVENANCE OF THE YAMPI IRON ORES, WEST KIMBERLEY REGION, WESTERN AUSTRALIA

by

D. C. Gellatly

SUMMARY

The Precambrian hematite iron ores of Yampi Sound in the Kimberley region, Western Australia, are fossil ironsand deposits. Regional geological mapping of the Yampi area indicates that they are part of the Kimberley Basin sedimentary sequence, and lie at the base of the Yampi Member of the Pentecost Sandstone. Their occurrence is related to reversal of the dominant palaeocurrent directions, and to minor unconformities in the sequence. Study of heavy mineral abundances suggests that the ores have formed through concentration of detrital iron minerals by reworking and winnowing on an ancient beach or sand-bar. Composition of the hematite suggests primary derivation from jaspilite source rocks. Deposition took place in two stages. Initially deposits of iron-bearing sandstone were laid down. These were subsequently eroded and the iron minerals concentrated to form the Yampi iron ores which locally contain pebbles and cobbles of the pre-existing iron-bearing sandstone.

INTRODUCTION

The Precambrian iron ore deposits of Yampi Sound are situated on Koolan and Cockatoo Islands of northern Western Australia. They have been known since about 1890 when they were discovered by the crews of pearling luggers and utilized for ballast. Early geological accounts were given by Campbell (1909) and Montgomery (1920). They were described comprehensively by Canavan & Edwards (1938) and Finucane (1939), and by Reid (1958) who described in detail the geology of Cockatoo Island. The ores have been mined since 1948 when shipments commenced from Cockatoo Island, and both Koolan and Cockatoo Islands are currently being worked.

Apart from the detailed work on Cockatoo and Koolan Islands, and on nearby Irvine and Bathurst Islands where thin hematite beds are present, the only previous geological work in the area was a reconnaissance survey of the adjacent mainland by Harms (1959). The field work on which this paper is based was carried out by a joint Bureau of Mineral Resources and Geological Survey of Western Australia field party in 1966 and 1967 as part of a programme of regional mapping of the Precambrian rocks of the Kimberley region. A full account of the geology of the

Yampi area will be included in a Bulletin on the geology of the West Kimberley area (Gellatly, Sofoulis, & Derrick, in prep.). The principal objects of this paper are to relate the ore beds to the stratigraphy and palaeocurrent systems of the area and to suggest possible source areas and parent rock types.

The Yampi Iron Ores

Since detailed descriptions of the Yampi iron ores have been given by Canavan & Edwards (1938) and Reid (1958), only a short summary, based partly on the earlier work, is given here as a background to the present results.

The Yampi iron ores consist of fine- to medium-grained hematite rock, hematite-rich quartz sandstone, and hematite-rich phyllite and schist. The ores and associated sediments show all gradations from pure quartzite to pure hematite. They occur as steeply dipping locally overturned beds that are conformable with the (stratigraphically) overlying quartz sandstone, schist, and phyllite, and the underlying quartz sandstone and hematitic sandstone. Cross-bedding, with 2- to 3-inch-thick foreset units and foreset laminae grading from a hematite-rich lower part to a quartz-rich top, has been noted in the ores. In places localized conglomerate is present in the ores and contains either pebbles and cobbles of quartzite and hematite quartzite or has cavities where the pebbles have been leached out (Pl. 24). Similarly, leaching of interstitial silica from silica-cemented hematite ores has produced 'powder' hematite ores consisting of uncemented sand-size hematite grains.

Minor accessory detrital minerals present in the ores and associated beds are characteristic of sedimentary deposits. They include tourmaline, zircon, rutile, anatase, garnet, plagioclase, and possible monazite. The hematite grains have octahedral form and commonly contain relict cores of magnetite suggesting that all the hematite was previously magnetite.

Origin of the ores as clastic sediments with possible enrichment by leaching out of silica has been suggested by Reid (1958; 1965). While this interpretation is considered to be the only one consistent with established geologic facts, the earlier work leaves several problems unsolved; namely—

(1) The stratigraphic position of the ores and their lateral relationship to other sediments of equivalent stratigraphic level in the area.
(2) Nature of the iron.
(3) Mechanism of concentration.
(4) Direction of transport.

The following sections are directed towards the solution of these problems.

SUMMARY OF GEOLOGY

The Precambrian of the West Kimberley region consists of a complex of ?Archaean schists (Halls Creek Group), and Lower Proterozoic acid volcanics, granites, and basic intrusives (Lamboo Complex), overlain uncomformably by Carpentarian (Middle Proterozoic) sediments and basic volcanics of the Speewah and Kimberley Groups* which together make up the greater part of the Kimberley Basin succession (*see* Table 1 and Fig. 1). The Yampi iron ores are considered to occur at the base of the Yampi Member of the Pentecost Sandstone, the topmost

* The Kimberley Group has been dated at about 1800 m.y. by the Rb-Sr isochron method (Bofinger, 1967). According to subdivisions of the Precambrian used by the Bureau of Mineral Resources, the Kimberley Group is considered to be near the base of the Carpentarian. According to the subdivision of the Precambrian adopted by the Geological Survey of Western Australia it is considered to belong to the upper part of the Lower Proterozoic.

formation of the Kimberley Group (*see* section on Stratigraphic Position of the Ore Beds).

The Yampi Member of the Pentecost Sandstone, originally named the 'Yampi Beds' by Harms (1959), is essentially a ferruginous sequence of quartz sandstone, hematite sandstone, feldspathic sandstone, arkose, siltstone, and minor pebble and cobble conglomerate. In the vicinity of Yampi Sound it has undergone low-grade metamorphism. On Koolan and Cockatoo Islands the main part of the Yampi Member consists of alternating beds of phyllite or schist, hematite-bearing quartzite, and hematite rock, forming cyclic sedimentation units that show reversed graded bedding (Reid, 1958). In the east the Yampi Member consists mainly of arkose. These lithologies contrast markedly with the uniform sequence of white quartz sandstone that makes up the rest of the Pentecost Sandstone.

STRATIGRAPHIC POSITION OF THE ORE BEDS

Over most of the Kimberley region the Kimberley and Speewah Groups are flat-lying or only gently folded, but in the Yampi area they are intensely folded and faulted. Intense folding including overfolding is common on the islands of Yampi Sound and on adjacent parts of the mainland, and faulting including reverse faulting is found on the mainland. Despite these structural complexities and the presence of areas obscured by sea it has been possible to trace the known stratigraphy of the mainland across to Koolan Island by way of a syncline of Warton Sandstone to the southeast (Fig. 1). The closure of the syncline is not complete but lithological correlation can be made with reasonable confidence across the gaps.

Evidence for correlation across the gaps in this structural closure depends (1) on distinguishing the Pentecost Sandstone, which in the vicinity of the closure contains thin siltstone beds and has a conspicuously bedded appearance on air photographs, from the Warton Sandstone which is the only relatively thick, clean-washed, poorly bedded quartz sandstone in the area; and on tracing the Warton Sandstone around the syncline and across to Koolan Island; and (2) on distinguishing the Elgee Siltstone which is the only relatively thick (30 to 100 m) dominantly siltstone sequence in the vicinity. The Elgee Siltstone, which is present on the mainland opposite Koolan Island, can be traced part of the way round the synclinal closure and is correlated with the lithologically similar 'Hanging Wall Schist' of Koolan Island.

On the basis of this tentative tracing of the Warton Sandstone from the mainland to Koolan Island, the stratigraphy of Koolan Island may be correlated with that of the adjacent parts of the mainland (Fig. 2). The principal difficulty of this correlation is that it suggests stratigraphic equivalence of dissimilar sequences of Pentecost Sandstone, in that the Yampi Member of Koolan Island appears on this correlation to be a lateral equivalent of the basal beds of the Pentecost Sandstone of the mainland, whereas farther east (Fig. 3) the Yampi Member forms the upper part of the formation.

The differences in the lower part of the sections compared in Figure 2 are possibly due to the presence of unconformities, one at the base of the Elgee Siltstone and one at the base of the Yampi Member. That at the base of the Elgee Siltstone is prominent about 50 km to the southeast, but on the mainland near Koolan Island its presence can be inferred only from the absence of the upper sandstone member of the Warton Sandstone and from a thin discontinuous pebble conglomerate at the base of the Elgee Siltstone.

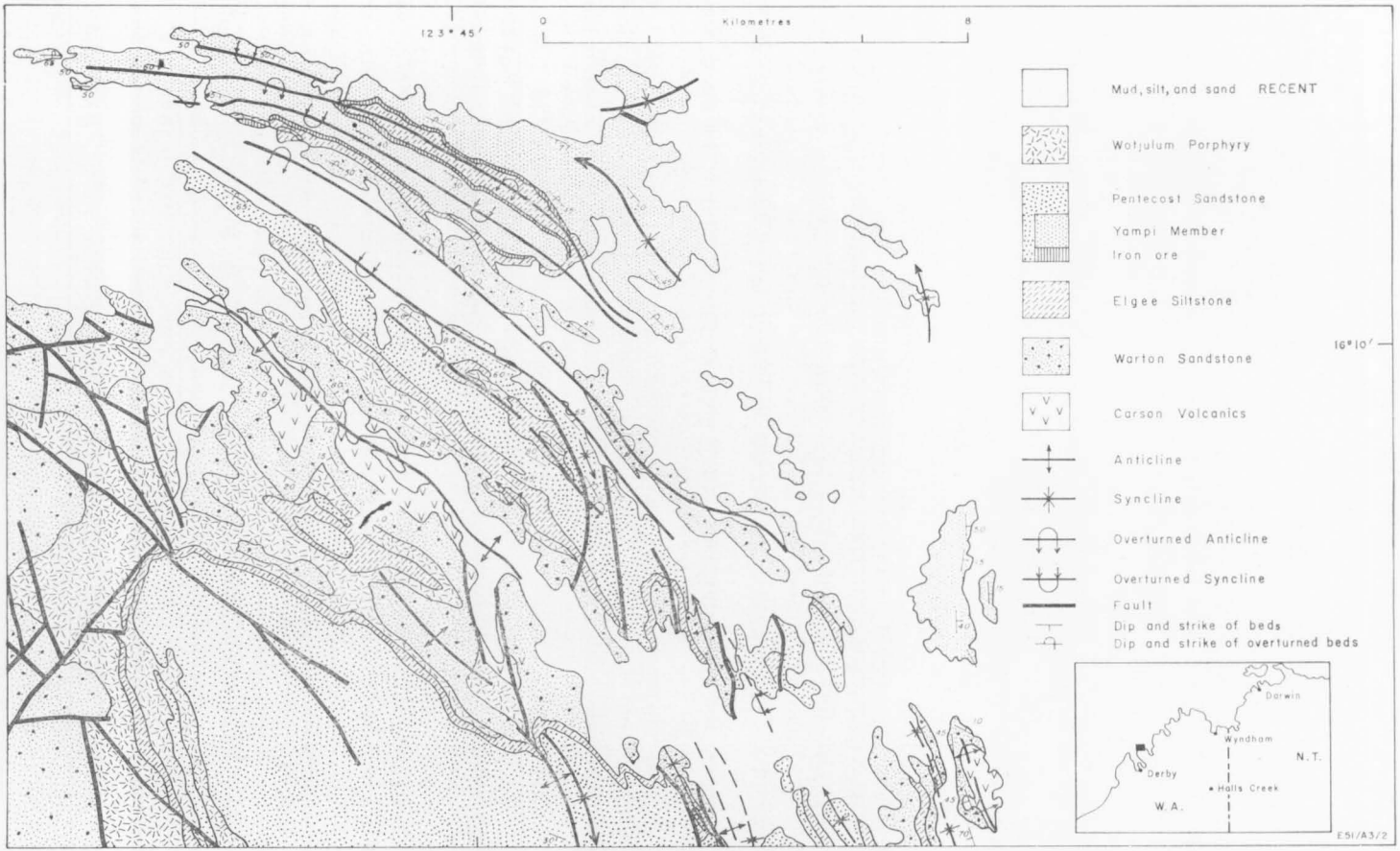


Figure 1. Geological map of Koolan Island and adjacent parts of Yampi Peninsula, Western Australia.

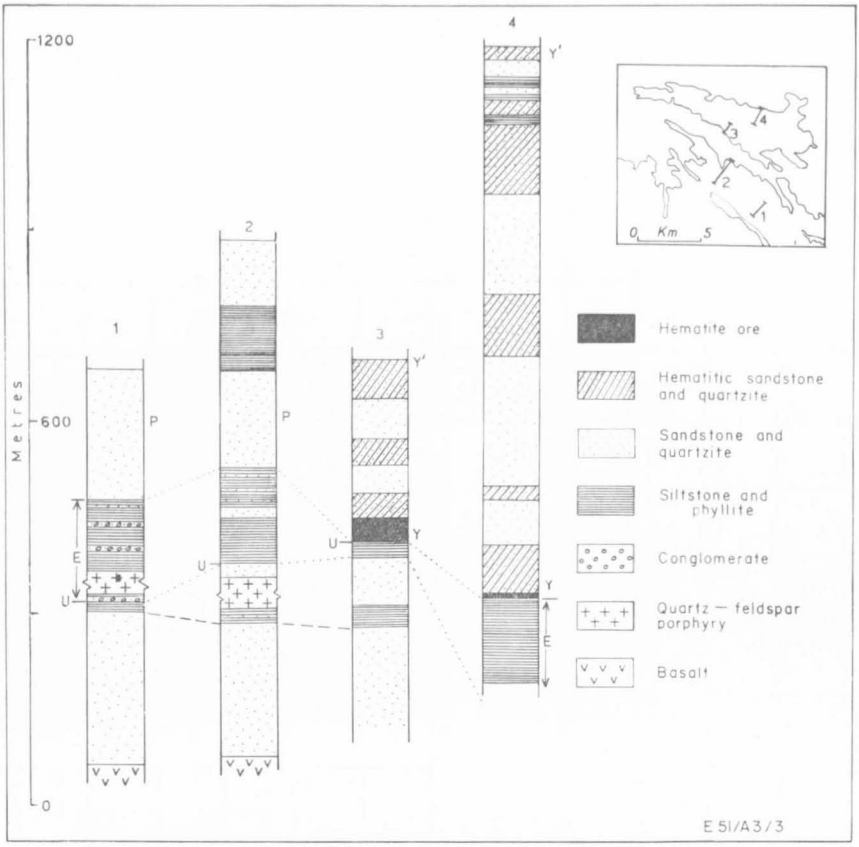


Figure 2. Comparison of stratigraphy of Koolan Island and Yampi Peninsula. P—Pentecost Sandstone; Y—Y′—Younger Member; E—Elgee Siltstone; W—Warton Sandstone; U—possible unconformities. Data from Sofoulis et al. (in prep.) and Finucane (1939).

The relationship of the Yampi Member to the rest of the Pentecost Sandstone is uncertain. In the east of the Yampi Sheet area it appears to be a facies equivalent of the middle part of the Pentecost Sandstone of the Kimberley Plateau, but in the west lies directly on the Elgee Siltstone and must either lie unconformably on it or must be a facies equivalent of the lower part of the Pentecost Sandstone. Figure 3 illustrates the problems of correlation. Correlation of these sections may be based on two lithological features—on the presence of hematite or of glauconite-bearing beds.

Throughout the central and eastern parts of the Kimberley Basin a conspicuous glauconite-bearing bed, generally overlain by a thin siltstone sequence, is found at levels varying from 140 to 400 m from the base of the sequence (Gellatly, Derrick, & Plumb, 1965; Gellatly & Sofoulis, 1966). A ferruginous glauconite bed at about 500 to 750 m above the base of the formation in the eastern part of the Yampi Sheet area is probably a lateral equivalent of this bed. A glauconitic bed in the Yampi Member of Cockatoo Island could be correlative of this or could be equivalent to glauconitic beds at the top of the Yampi Member around Collier Bay. The latter correlation appears more likely.

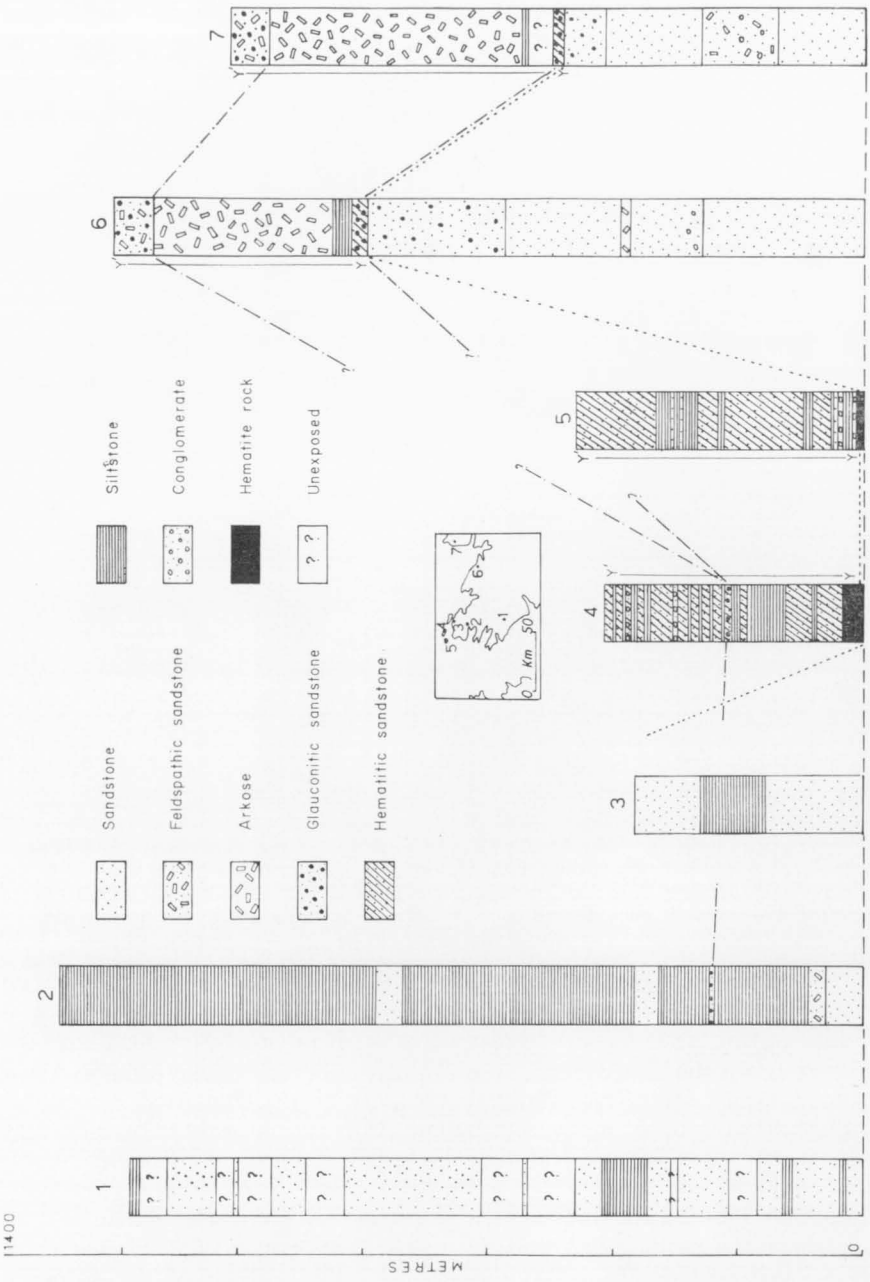


Figure 3. Stratigraphy and correlations of the Pentecost Sandstone Yampi Sheet area. Column 4 from Reid (1958); others from Sofoulis et al. (in prep.). Dashed line corresponds with top of Elgee Siltstone; dotted line shows correlations based on hematite. Other correlations based on glauconite occurrences.

Correlation on the presence of hematite is indicated on Figure 3. On this basis an unconformity is inferred at the base of the Yampi Member which would presumably be transgressive to the northwest over progressively lower beds on the Pentecost Sandstone to Koolan and Cockatoo Islands where it overlies the Elgee Siltstone. The area where this suggested transgression takes place is

obscured by sea. This correlation agrees with the second of the two possible correlations based on glauconite beds.

This interpretation of the stratigraphic position of the ores necessitates re-interpretation of the structure of the Yampi Sound area presented by Canavan & Edwards (1938). The two cross sections are compared in Figure 4. Canavan

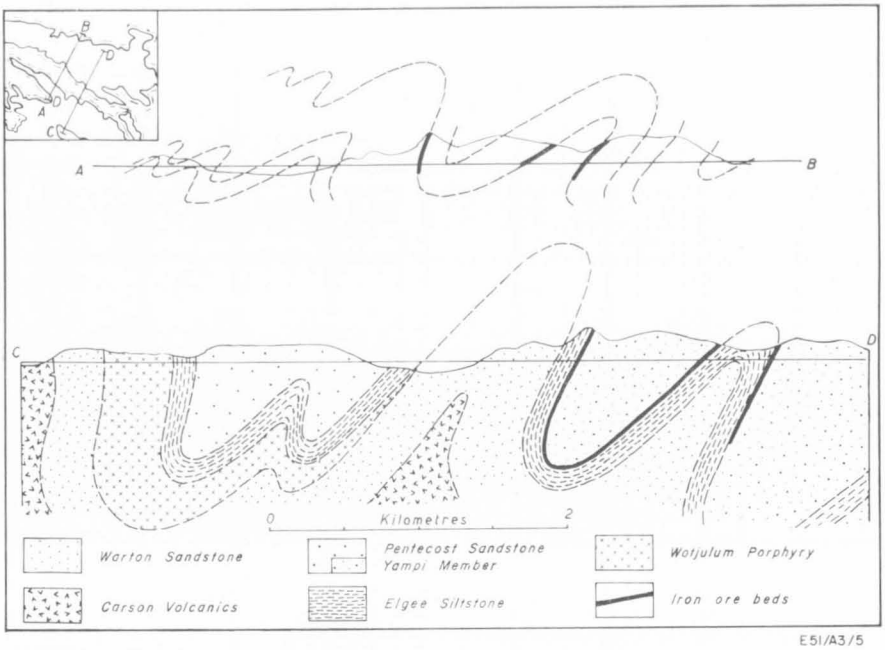


Figure 4. Geological cross sections of Koolan Island and Yampi Peninsula. A-B from Canavan and Edwards; C-D this work.

and Edwards interpret the ores as belonging to beds about 2500 feet above the Elgee Siltstone, and thus infer that the absence of hematite on the mainland is due to erosion after the main period of folding. According to this interpretation, the quartzite (which is here correlated with the Warton Sandstone) underlying the ore beds and 'Hanging Wall Schist' of Koolan Island would be equivalent to the siltstones in the upper part of the Pentecost Sandstone in the mainland area.

In the interpretation put forward here the absence of ores on the adjacent parts of the mainland could be due either to erosion or to nondeposition. The absence of the lower (nonferruginous) beds of the Pentecost Sandstone is attributed to their erosion from Koolan Island (*see* Figs 2, 3) prior to deposition of the Yampi Member. It may be necessary to postulate gradual facies changes across strike to explain the absence of hematitic beds about 15 to 24 km south of Koolan Island where a greater thickness of the Pentecost Sandstone is preserved (Fig. 3, column 2) than on the peninsula immediately opposite Koolan Island. Evidence for such facies changes across strike is provided by the ore beds themselves. Although they extend along strike for 30 km they show a rapid thinning across strike; e.g. on Koolan Island they thin northwards from 30 m to 6 m over a distance (after removal of the effects of folding) of 3 km.

NATURE OF THE ORIGINAL IRON

The physical state of the iron mineral at the time of deposition is important in considering the probable mechanism of concentration. Its chemical composition may reflect the type of source rock.

The iron mineral is now almost entirely hematite but small amounts of magnetite are found locally as relict cores enclosed by lamellae of secondary hematite developed along octahedral cleavages (*see* Canavan & Edwards, 1938, figs 19, 20). Octahedral magnetite crystal forms, common in both the ores and the hematite quartzites, are unabraded and thus the iron must have been recrystallized to form the magnetite octahedra after deposition. Conversion to hematite represents a second period of post-depositional recrystallization. Because of the two processes of recrystallization after deposition the identity of the iron mineral at the time of deposition remains unknown, but was probably either magnetite or hematite.

The close association of the hematite with detrital quartz, zircon, rutile, and tourmaline, and the sensitivity to variation in the relative percentages of quartz and hematite (e.g. as in graded foreset laminae), suggest that the original iron mineral had similar hydraulic characteristics to the quartz, and that it was probably present as detrital grains.

The possibility that the iron was deposited directly as a chemical or biochemical precipitate is unlikely in view of the obviously clastic nature of the associated sediments and the absence of chert and jaspilite normally associated with precipitate-type iron deposits. Although the conglomerate clasts, which consist of hematite-bearing quartzite, indicate that the immediately preceding source rocks were hematite-bearing clastic sediments similar to those associated with ores, they provide no direct evidence of the primary source rocks.

Iron oxide minerals may show considerable variation in minor element contents depending on host-rock composition, and spectrographic determinations of Cu, Co, Ni, Mn, and Ti* have been carried out on hematite from the Yampi iron ores and associated sediments from a number of rock types from the West Kimberley area in order to obtain an indication of possible source rocks for the ores.

Hematites from the following rock types were analyzed: jaspilites from the Halls Creek Group near Louisa Downs, Mount Ramsay Sheet area; phyllite and hornfels from the Elgee Siltstone and Warton Sandstone of the Yampi area; vein hematite from the Elgee Siltstone, Warton Sandstone, and Carson Volcanics; hematitic chert from the Warton Sandstone of the Yampi area and from the Carson Volcanics in the Drysdale 1:250,000 Sheet area; agglomerate and phyllitic tuff from the Carson Volcanics of the Yampi area (*see* Fig. 5).

The compositions of these hematites fall almost entirely outside the compositional range of hematites from the Yampi iron ores and other hematitic sediments from the Yampi Member, and most of the geologically possible source rocks must be excluded on chemical grounds. The only rocks of the Yampi iron ores are the jaspilites. Although hematite from the chert in the Warton Sandstone differs in composition from that in the ores, hematitic sandstone from this formation (no specimen available for analysis) remains a possible intermediate source rock for the ores.

* Cr was determined also but results were rejected because of contamination during crushing.

Figure 5. Minor element variations in the Yampi iron ores and possible source rocks. Analyses by optical emission spectography (unpublished BMR data).

Other possible source rocks, such as granite or pelitic metamorphics, which could possibly have provided hematite or magnetite of suitable composition, are considered unlikely on the grounds of relative heavy mineral abundances. The only detrital mineral of probable metamorphic origin identified is garnet, and this is extremely rare. Granite commonly contains minor amounts of magnetite, but derivation of the ores from such a source would imply extreme concentration not only of the magnetite, but also of other heavy minerals such as zircon, rutile, and monazite, in which case these three minerals should increase considerably with

increasing iron content. No such increase in zircon, rutile, and monazite has been found (*see* below) and this eliminates the possibility of a granitic source for the ores.

MECHANISM OF CONCENTRATION

To provide evidence of the mechanism of concentration, the heavy mineral suites of the Yampi iron ores and of sandstones of other formations in the Kimberley Group have been studied. The heavy mineral fraction was first separated using bromoform, and the hematite dissolved with HCl. A portion of the resultant insoluble heavy-mineral fraction was mounted on a graticule microscope slide and the grains counted. Identification of the mineral species present was confirmed by X-ray diffraction powder photographs. Appropriate weight percentages of the principal constituents were calculated (Fig. 6). Distribution of the dominant heavy minerals is shown in Figure 7.

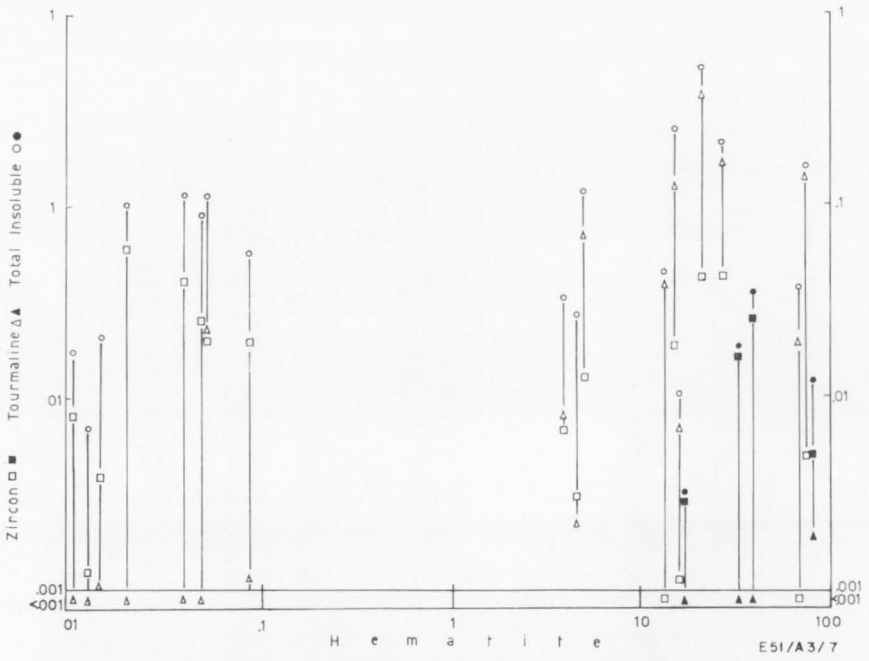


Figure 6. Relative percentages of heavy minerals in Kimberley Group sediments. Solid symbols, Yampi iron ores; open symbols, other formations. K—King Leopold Sandstone; W—Warton Sandstone; E—Elgee Siltstone; P—Pentecost Sandstone; Y—Yampi Member.

The principal insoluble heavy minerals present are tourmaline, zircon, rutile, and anatase; minor monazite and garnet were also identified. Zircons are well rounded. Rutile grains are rounded in general outline but have minor marginal euhedral overgrowths. Tourmaline grains are generally angular but have rounded cores. Anatase is highly angular and has presumably been derived *in situ* from a pre-existing detrital titanium mineral. Thus the principal heavy minerals present apparently reflect the original detrital heavy-mineral content of the sediments.

The principal feature of the heavy-mineral variations (Fig. 6) are that tourmaline is the dominant insoluble heavy mineral in the Yampi Member (except for the ore beds where zircon is the more abundant), whereas zircon, rutile, and anatase predominates in other formations. The only specimen from non-ferruginous beds of the Pentecost Sandstone contained dominant zircon suggesting that the dominance of tourmaline is a feature peculiar to the Yampi Member and a few other beds, notably hematite-bearing sandstone from both the Warton Sandstone and the Elgee Siltstone.

If concentration of detrital iron-bearing sediments to produce the ores occurred through sorting during transport, or by current winnowing at the site of deposition, such concentration would have depended principally on the grain size and/or specific gravity of the minerals concerned, namely; quartz, 2.65; tourmaline, 3.1; rutile, 4.2; zircon, 4.7; hematite, 4.9 to 5.3; and magnetite 5.2. There is little variation in grain size apparent in the ores and hematitic sandstones and the more important factor appears to have been specific gravity.

Removal of quartz through differential transport or winnowing should be accompanied initially by an increase in the content of all the other minerals mentioned and subsequently, with stronger current action, by a reduction in the amount of lighter heavy minerals, especially of tourmaline.

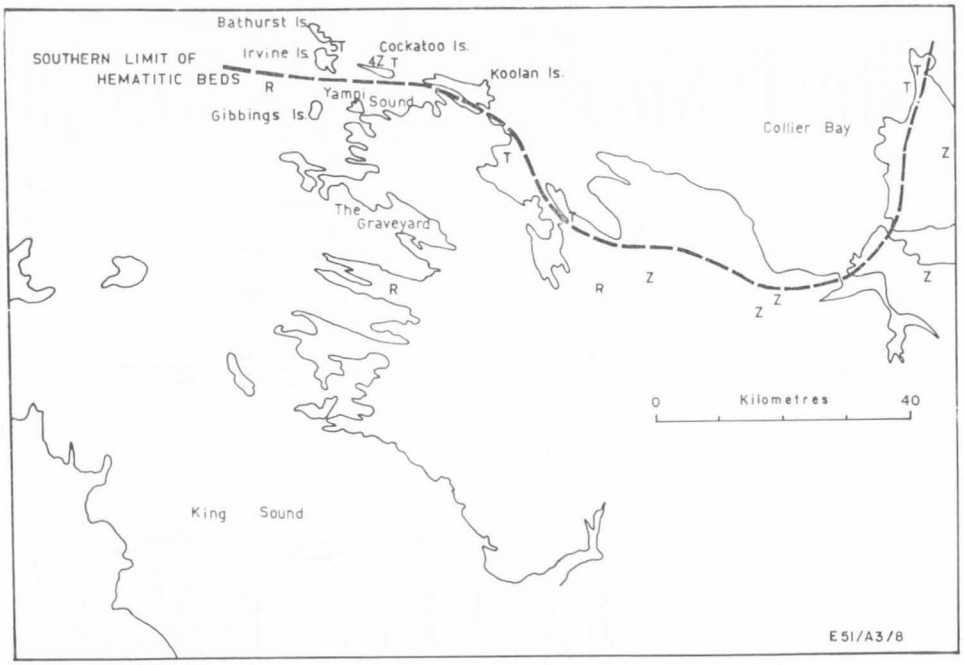


Figure 7. Distribution of dominant heavy minerals in the Yampi Sheet area. A—anatase; R—rutile; T—tourmaline; Z—zircon. Letter symbols indicate one specimen from each locality except where otherwise indicated by numbers.

Figure 6 shows that there is little general increase in the total insoluble heavy mineral content with increasing iron content and that such increase as is present is due mainly to an increase in tourmaline; and also that the hematite

ores are greatly impoverished in tourmaline relative to specimens of equivalent hematite content from higher iron beds of the Pentecost Sandstone. It should be noted that, despite the concentration of hematite in the ores through removal of quartz, there is no corresponding increase in zircon content with increasing hematite. This infers partial removal of zircon in addition to the almost complete removal of quartz and tourmaline, and illustrates the close parallel between the proportion of a mineral removed and its specific gravity.

These variations in heavy minerals imply that there has been strong concentration, probably due to winnowing, in the ores but to a lesser degree in the rest of the iron-rich succession. Extreme winnowing and reworking could account for the thick development of the hematite forming the ore beds, in contrast to the rapid alteration of quartzite, hematite-quartzite, hematite, and schist in the overlying beds of the Pentecost Sandstone.

The evidence of concentration of the heavier minerals, probably by winnowing and reworking, and removal of the lighter ones provides a ready explanation for the reversed graded bedding noted by Reid (1958). In repetitive graded units around 10 m thick there is an increase upwards in both grain size and in hematite content (Fig. 8). This type of gradation, the opposite to that more commonly found in sediments, infers gradually increasing current velocities, and consequently increasing reworking and winnowing, from the bottom to top of each unit.

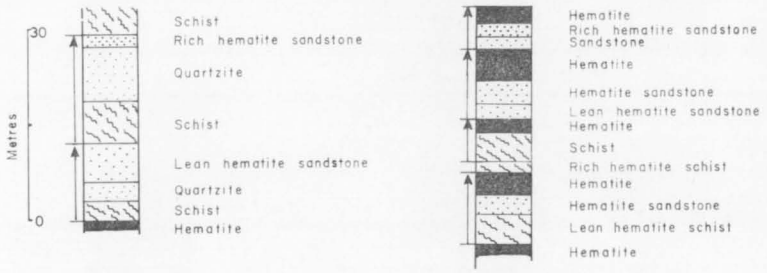


Figure 8. Cyclic sedimentation units in the Yampi Member, Cockatoo Island. After Reid (1958).

Direction of Transport

A study of palaeocurrent directions deduced from cross-bed orientations has been made of the whole Kimberley Basin (Gellatly, Derrick, & Plumb, in press). Over most of the basin the dominant current direction is from north-northwest; minor reversals from the southeast are associated with conglomerate beds. The weight of evidence suggests that the current direction indicated by the cross-beds was the primary transport direction.

In the Yampi area as in the rest of the Kimberley Basin, currents from north-northwest predominate. Current reversals associated with conglomerates are found in the Elgee Siltstone and in the iron ores, but elsewhere in the Pentecost Sandstone directions are predominantly from the north-northwest (Fig. 9). Directions in the northeastern part of the Yampi area are from the east; the significance of this is not known. With minor exceptions it may be said that the cross-bed directions in the Yampi Member are from the south-southeast, those from the

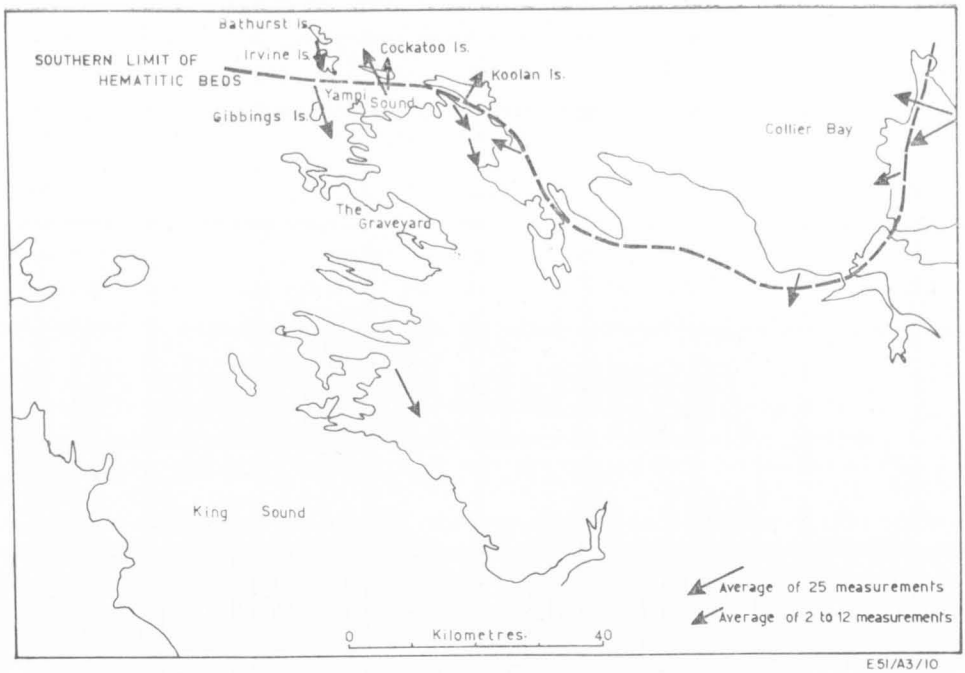


Figure 9. Palaeocurrent directions in the Pentecost Sandstone, Yampi Sheet area.

rest of the Pentecost Sandstone are from the north-northwest, and that the dividing line between the two coincides with the southern limit of hematite in the sediments.

However, it cannot be established that the current directions from the south in the iron ores reflect the primary transport direction. Such a direction would infer iron-rich sandstones to the south, whereas only minor hematitic sandstone (in the Warton Sandstone) is present in the south. Also, the cross-beds on Cockatoo and Koolan Islands, which indicate transport from the south, are very thin (5 to 8 cm) and lensing, whereas most of those elsewhere in the Kimberley Group are thicker (15 to 60 cm), are more persistent laterally, and have steeper dips relative to bedding. It is thus possible that those beds indicating currents from the southeast are related to reworking currents and do not indicate the primary direction of transport as the others probably do. The general transport direction for most of the Kimberley Basin sediments appears to have been from the north; this may also be true of the Yampi iron ores.

CONCLUSIONS

Evidence presented above suggests that the Yampi iron ores have had a complex and at least two-stage depositional history. They have apparently been derived from an initial iron-rich source, possibly from Archaean or Lower Proterozoic jaspilites. Erosion of these and transport southwards was followed by deposition in sands of the Warton Sandstone. Erosion of some of the latter possibly accompanied by additional derivation from the original source rocks (abundant feldspar in the Yampi Member in the eastern part of the Yampi area suggests that some of the detrital material was derived directly from crystalline source rocks) took place in the Yampi Sound area.

Two probable unconformities associated with conglomerates and current direction reversals in the overlying beds have been noted in the Yampi Sound area. The Yampi iron ores occur in the sequence immediately overlying one of these unconformities.

The conglomerates in the ores suggest that deposition took place probably near a shoreline, and that the ores represent heavy-mineral concentrations on a beach or on a nearshore bar. The distribution of the ores in an elongate west-northwest-trending belt suggests that the inferred shoreline was also of this trend.

Concentration probably took place by reworking over a long period during which quartz and the less dense heavy minerals, especially tourmaline, were progressively removed, leaving a deposit consisting essentially of hematite or magnetite sand.

ACKNOWLEDGEMENTS

The assistance of Dampier Mining Company in providing facilities at Koolan Island during field investigations, and of Mr I. W. Reid of Broken Hill Proprietary Ltd for arranging a visit to the more important localities on Koolan and Cockatoo Islands is gratefully acknowledged. The writer also acknowledges the assistance of his colleagues, G. M. Derrick and C. M. Morgan (BMR) and J. Sofoulis and R. A. Farbridge (G.S.W.A.) who contributed to the mapping of the Yampi Sheet area.

REFERENCES

BOFINGER, V. M., 1967—Geochronology in the East Kimberley Region, Western Australia. *Aust. N.Z. Assoc. Adv. Sci., Abstract. Vol.,* 110-111.

CAMPBELL, W. D., 1909—Yampi Sound iron ore deposits. *Geol. Surv. W. Aust., Ann. Prog. Rep.* (for 1908), 13-14.

CANAVAN, F., and EDWARDS, A. B., 1938—The iron ores of Yampi Sound, Western Australia. *Aust. Inst. Min. Metall. Proc.* No. 110, 59-101.

FINUCANE, K. J., 1939—The iron deposits of Yampi Sound, Western Australia. *Aer. Geol. Geophys. Surv. N. Aust., W. Aust. Rep.,* 50.

GELLATLY, D. C., and SOFOULIS, J., 1966—The geology of the Drysdale-Londonderry 1:250,000 Sheet area SD. 52-9 and 5, Western Australia. *Bur. Miner. Resour. Aust. Rec.* 1966/55 (Unpubl.).

GELLATLY, D. C., DERRICK, G. M., and PLUMB, K. A., 1965—The geology of the Landsdowne 1:250,000 Sheet area SE. 52-5, Western Australia. *Bur. Miner. Resour. Aust. Rec.* 1965/210 (Unpubl.).

GELLATLY, D. C., DERRICK, G. M., and PLUMB. K. A., *in press*—Proterozoic palaeocurrent directions in the Kimberley region, northwestern Australia. *Geol. Mag.*

GELLATLY, D. C., SOFOULIS, J., and DERRICK, G. M., in prep.—The Precambrian geology of the Kimberley region, Western Australia: The West Kimberley. *Bur. Miner. Resour. Aust. Bull.*

HARMS, J. E., 1959—The geology of the Kimberley Division, Western Australia and of an adjacent area of the Northern Territory. *M.Sc. Thesis, Univ. Adelaide* (Unpubl.).

MONTGOMERY, A., 1920—Report on the iron ore deposits of Yampi Sound. *Dep. Mines W. Aust.*

REID, I. W., 1958—The geology of Cockatoo Island, Yampi Sound, Western Australia. *Aust. Inst. Min. Metall., Stillwell Anniversary Volume,* 213-39.

REID, I. W., 1965—Iron ore deposits of Yampi Sound. *In* THE GEOLOGY OF AUSTRALIAN ORE DEPOSITS, pp. 126-31. *8th Commonw. Min. Metall. Congr., Melbourne, 1965.*

SOFOULIS, J., GELLATLY, D. C., DERRICK, G. M., FAIRBRIDGE, R. A., and MORGAN, C. M., 1970—The geology of the Yampi 1:250,000 Sheet area SE. 51-3, Western Australia. *Bur. Miner. Resour. Aust. Rec.* (Unpubl.).

TABLE 1. SUMMARY OF PRECAMBRIAN STRATIGRAPHY OF THE YAMPI AREA.
(Summarized from Sofoulis et al., in prep.)

CARPENTARIAN	INTRUSIVE INTO KIMBERLEY GROUP	
	Wotjulum Porphyry	Grey quartz-feldspar porphyry
	Hart Dolerite	Dark grey and grey-green tholeiitic dolerite
	KIMBERLEY GROUP	
	Pentecost Sandstone	White quartz sandstone; buff feldspathic sandstone, grey siltstone
	Yampi Member	Hematitic sandstone and hematite rock, feldspathic sandstone, arkose, siltstone; minor conglomerate and glauconitic sandstone
	Elgee Siltstone	Grey and red-brown siltstone; red-brown quartz sandstone and feldspathic sandstone; pebble to boulder conglomerate
	Warton Sandstone	White and buff quartz sandstone and feldspathic sandstone; grey siltstone; minor hematitic sandstone and siltstone, chert and andalusite granofels
	Carson Volcanics	Grey and grey-green tholeiitic basalt and spilite; minor tuff, feldspathic sandstone and siltstone
	King Leopold Sandstone	White and pale buff quartz sandstone
	SPEEWAH GROUP	Quartz sandstone, micaceous quartzite; minor phyllite and pebble conglomerate
	UNCONFORMITY	
LOWER PROTEROZOIC		
	LAMBOO COMPLEX	Porphyritic ashflow tuff, granite and granodiorite, amphibolitized dolerite
?ARCHAEAN		
	HALLS CREEK GROUP	Phyllite and mica schist

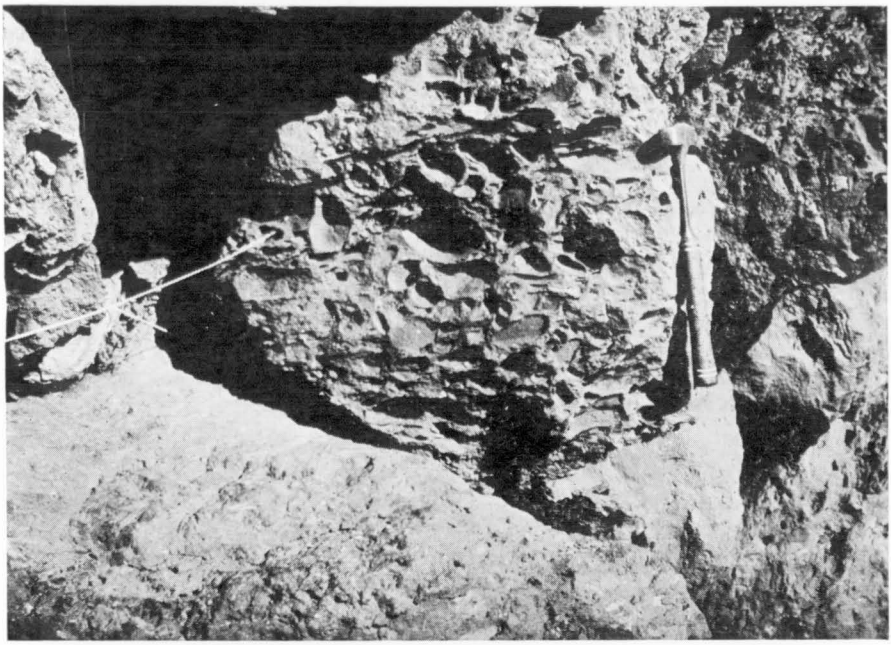


Figure 1. Leached hematite conglomerate ore, Koolan Island quarry. The ore consists of finely granular hematite with cavities where siliceous pebbles have been leached out.

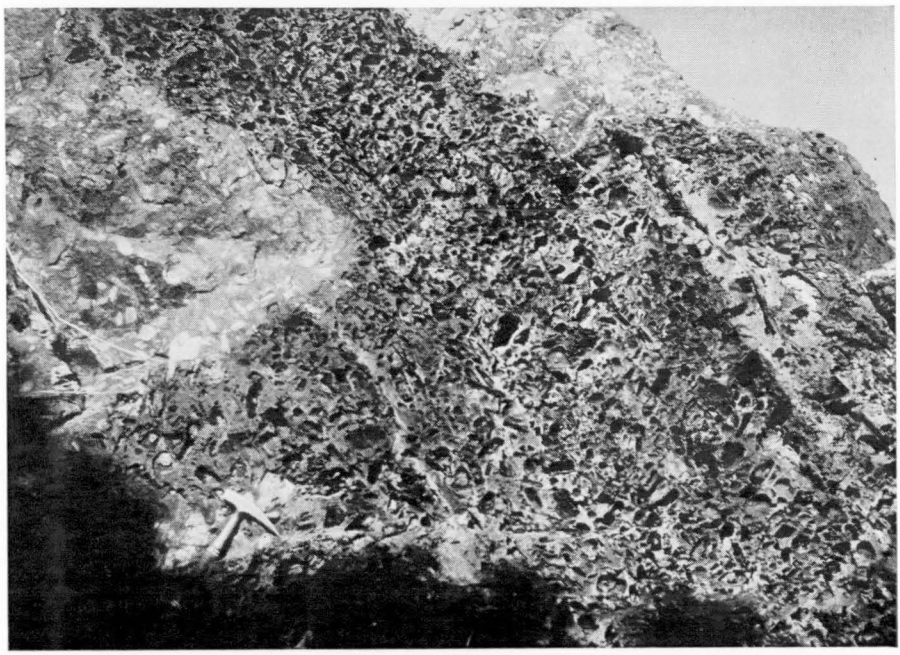


Figure 2. Hematite conglomerate, west end of main ore body, Koolan Island. Pebbles and cobbles of hematite-bearing quartzite are enclosed by a granular hematite matrix. The leaching zone consists almost entirely of hematite.